

# **Making WALRUS applicable for large catchments: a case study in the Reusel catchment**

**MSc Thesis**

**Raymond Loos**

**September 2014 – March 2015**



# **Making WALRUS applicable for large catchments: a case study in the Reusel catchment**

**MSc Thesis**

**Raymond Loos**

Registration number: 910830528010

Hydrology and Quantitative Water Management Group

Wageningen University

September 2014 – March 2015



# Preface

This report is the final result of around six months of thesis work at the Hydrology and Quantitative Water Management Group (HWM) of the Wageningen University. I would like to thank my supervisors Claudia Brauer, Paul Torfs and Ryan Teuling for their help and useful feedback. I look back on a pleasant cooperation. I also like to thank Esther Vermue (Water board 'De Dommel') for providing most data on the Reusel catchment and her interest in my results. I thank Jeroen Tempelaars (Water board 'De Dommel') for providing data of the Wageningen Model. Furthermore, I would like thank Wil Kraayvanger and Niels Entzinger (both from Water board 'De Dommel') for giving me lots of information during the field visit day and showing me all relevant weirs and places. Unfortunately, there was not enough time to use all data and information, for instance the data of a special wet nature area (De Utrecht Noord) where Niels set up some discharge measurements. Finally, I would like to thank all friends who helped me through this six months of computer work and often provided me some relaxation moments during lunch/coffee breaks and after working hours.

Raymond Loos  
March, 2015



# Abstract

The Wageningen Lowland Runoff Simulator (WALRUS) is a lumped rainfall-runoff model, which only needs five calibrated parameters. In previous studies, it has already been tested on relatively small catchments ( $<10 \text{ km}^2$ ). The objective is to investigate if WALRUS is able to simulate discharges correctly in a larger catchment, since the five parameters are representing local catchment characteristics. The Reusel catchment ( $145 \text{ km}^2$ ) in the Netherlands is used as research area for this study. First the WALRUS parameters were calibrated for the entire catchment. After validation, an average Nash-Sutcliffe efficiency of 0.79 was found. WALRUS was also applied to three subcatchments, each with its own parameter set. An average Nash-Sutcliffe efficiency of 0.53 was the result of validation. A nonlinear reservoir model was used to investigate if routing of discharge time series from the subcatchments (observed or simulated) could improve simulation results for the entire catchment. Results of two (only available) hydrological years were contradictory, probably caused by observational errors. Another focus was on the coupling of subcatchments in WALRUS by using (observed or simulated) discharge of one subcatchment as input for the next subcatchment downstream. Testing this coupling on two hydrological years leads to acceptable results. Finally, WALRUS results were compared to already existing simulation data of the Wageningen Model for the entire catchment and one subcatchment. It was found that WALRUS is performing better, especially when focusing on peak discharges. In terms of Nash-Sutcliffe efficiency, average values of 0.70 (WALRUS) and 0.53 (Wageningen Model) were found for the entire catchment and 0.44 (WALRUS) and  $-0.67$  (Wageningen Model) for the subcatchment. It can be concluded that WALRUS is able to simulate discharges in larger catchments, but more research can be done on hydrological routing and coupling of subcatchments.



# Contents

|                     |   |           |
|---------------------|---|-----------|
| <b>1</b>            | <b>Introduction</b>                         | <b>1</b>  |
| 1.1                 | Hydrological models                         | 1         |
| 1.2                 | Complexity of models                        | 1         |
| 1.3                 | Flow routing                                | 2         |
| 1.4                 | WALRUS: Wageningen Lowland Runoff Simulator | 2         |
| 1.5                 | Objective and research questions            | 2         |
| <b>2</b>            | <b>Reusel catchment</b>                     | <b>5</b>  |
| 2.1                 | Surface water system                        | 5         |
| 2.2                 | Geology and soils                           | 6         |
| 2.3                 | Land use                                    | 6         |
| 2.4                 | Climatology and hydrology                   | 7         |
| 2.5                 | Waste water treatment plant                 | 7         |
| <b>3</b>            | <b>Data</b>                                 | <b>9</b>  |
| 3.1                 | Subcatchments                               | 9         |
| 3.2                 | Precipitation                               | 10        |
| 3.3                 | Evapotranspiration                          | 10        |
| 3.4                 | Discharge                                   | 10        |
| 3.5                 | Groundwater flow                            | 11        |
| 3.6                 | Waste water treatment plant                 | 11        |
| 3.7                 | Water balance                               | 11        |
| <b>4</b>            | <b>Methods</b>                              | <b>15</b> |
| 4.1                 | WALRUS: Wageningen Lowland Runoff Simulator | 15        |
| 4.2                 | Calibration and validation                  | 16        |
| 4.3                 | Reservoir routing                           | 17        |
| 4.4                 | Coupling of subcatchments                   | 20        |
| 4.5                 | WALRUS versus Wageningen Model              | 20        |
| <b>5</b>            | <b>Results</b>                              | <b>23</b> |
| 5.1                 | Calibration and validation                  | 23        |
| 5.2                 | Reservoir routing                           | 27        |
| 5.3                 | Coupling of subcatchments                   | 32        |
| 5.4                 | WALRUS versus Wageningen Model              | 36        |
| <b>6</b>            | <b>Discussion</b>                           | <b>39</b> |
| <b>7</b>            | <b>Conclusions &amp; recommendations</b>    | <b>41</b> |
| <b>Bibliography</b> |   | <b>43</b> |
| <b>A</b>            | <b>Calibration conditions</b>               | <b>i</b>  |

|   |               |
|---|---------------|
| <b>B Validation plots</b>               | <b>iii</b>    |
| B.1 Validation catchment 0024           | iii           |
| B.2 Validation catchment 0072           | xxi           |
| B.3 Validation catchment 0098           | xxiv          |
| B.4 Validation catchment 0099           | xxxi          |
| <b>C Reservoir routing plots</b>        | <b>xxxvii</b> |
| <b>D WALRUS versus Wageningen Model</b> | <b>lv</b>     |

# 1 | Introduction

Understanding relations between hydrological time series (e.g. storage, precipitation and discharge) in catchments is becoming more and more important. Climate is changing and therefore more extreme conditions are likely to occur. Good models are needed in order to predict how a catchment is reacting to expected (extreme) weather conditions. Another reason why good models are necessary, is because of the lack of hydrological measurements. Models are needed to extrapolate current measurements in space and time (Beven, 2011). A distinction can be made between hydrological models, which account for the hydrological processes in catchments (Section 1.1), and hydraulic models that focus on the movement of water through the channel (Section 1.3).

## 1.1 Hydrological models

Hydrologic models can be classified according to the description of physical processes (black box, conceptual and physically-based models) or according to the spatial description of catchment processes (distributed and lumped models) (Refsgaard, 1997). Models which do not use any physics are the so-called black box models. These models relate input variables to output variables, without considering the processes inside a catchment (Beven, 2011). Physically-based models are describing a catchment using basic mathematical representations of the flow of mass (Refsgaard, 1996). Conceptual models are more basin-oriented than physically based models, e.g. there is a great variability of physical processes in space and the parameters of the conceptual model represent an average of this variability. These models have a limited data demand and are therefore applicable in catchments where less data is available (Bergström, 1991).

Distributed hydrological models are structured to account for the spatial variation in catchment characteristics (Refsgaard, 1997), while lumped models regard a catchment as one unit. Variables and parameters are representing average values for the whole catchment.

Usually a combination of models as described above is used. Physically-based models normally have to be fully distributed and are also called white box models (Refsgaard, 1996). Conceptual models, also called parametric models or grey box models, are usually used as a lumped-type model. Parametric rainfall-runoff models consist of a number of reservoirs and flowroutes (Wagener et al., 2004). Examples of parametric models are HBV (Bergström and Forsman, 1973), Sacramento Model (Burnash et al., 1995), SWAT (Arnold et al., 1998) and WALRUS (Brauer et al., 2014a). WALRUS will be used in this research project.

## 1.2 Complexity of models

Nowadays, water managers in the Netherlands often use very complex hydrological models, for instance SOBEK (Deltares, 2013). Complex models include many parameters that require calibration. An advantage of complex models is a very detailed simulation output, but there is also a risk of over-parameterization (Kirchner, 2006).

Perrin et al. (2001) demonstrated that very simple models can achieve a level of performance as high as models with more parameters, but because more complex models are subject to over-parameterization, the number of free parameters should be restricted between three and five for lumped rainfall-runoff models.

In order to reduce parameter uncertainty in complex models, some additional information could be added. Lamb et al. (1998) used some groundwater measurements as additional output variables to reduce the parameter uncertainty in TOPMODEL, a parametric rainfall-runoff model for mountainous catchments, developed by Beven and Kirkby

(1979). Wagener et al. (2001) stated that adding too many observations locations (more than 100) lead to an increase in parameter uncertainty.

### 1.3 Flow routing

Conceptual models are mostly used in a lumped-type (e.g. assuming the catchment as one single unit). Since the model parameters have a quite strong relation with the (local) catchment characteristics and variations in precipitation input, taking one parameter set for a larger area may introduce uncertainties.

The use of flow routing techniques could help to obtain more accurate runoff simulations. Flow routing is often used to predict the spatial and temporal variations of a hydrograph between different points in a catchment (e.g. inlet, outlet). When a flood wave is moving through a network of channels, attenuation in the peak flow occurs due to friction and storage in the surface water reservoir. Implementing a flow routing technique in a hydrological model is important in order to obtain more accurate simulations, especially in larger catchments.

In general, there are two flow routing techniques available: hydraulic flow routing and hydrological flow routing. Hydraulic flow routing is fully based on the St. Venant equations, while hydrological flow routing is based on the storage-continuity equation (e.g. Ten Broek, 2014). Hydraulic flow routing techniques are much more accurate than hydrological flow routing techniques, but they require much more input data, initial conditions and boundary conditions. Hydrological flow routing techniques are more simple in data input and very useful when preliminary estimates of the time and shape of a flood curve are needed (O'Sullivan et al., 2012).

There are different methods that are using the hydrological flow routing approach. The Muskingum flow routing method is the most popular and used in many projects (e.g. Gill, 1978; O'Sullivan et al., 2012; Kim and Lee, 2010). A detailed description of the Muskingum method can be found in the engineers manual for flood-runoff analysis of the US Army Corps of Engineers (USACE, 1994).

### 1.4 WALRUS: Wageningen Lowland Runoff Simulator

The model used for this research is WALRUS (Wageningen Lowland Runoff Simulator) and is developed by Brauer et al. (2014a). This lumped rainfall-runoff model is suitable for lowland catchments with shallow groundwater and there are only five parameters that need to be calibrated, which makes the model not too complex. To run WALRUS, time series of precipitation, potential evapotranspiration and discharge are required as input. Additional information (e.g. surface water supply or extraction, seepage or groundwater extraction) can be added. A complete model description can be found in Chapter 4.1.

WALRUS is tested on the Hupsel Brook catchment ( $6.5 \text{ km}^2$ ) and Cabauw polder ( $0.5 \text{ km}^2$ ), both in the Netherlands (Brauer et al., 2014b). After calibration on one year of discharge observations, Nash-Sutcliffe efficiencies of 0.87 for the Hupsel Brook catchment and 0.83 for the Cabauw catchment were found. After calibration, the model was validated for two periods on another year in order to see if the model simulates observed discharge quite well. Nash-Sutcliffe efficiencies of 0.74 (Hupsel Brook) and 0.76 (Cabauw) were found, which indicates that WALRUS works quite well in these catchments.

### 1.5 Objective and research questions

Since WALRUS is tested in two relatively small catchments (see Section 1.4), the objective of this research project is to see if WALRUS is also applicable to larger catchments. When WALRUS can accurately simulate discharges (compared to observed discharges), the model is more widely applicable by for instance water boards. Therefore,

a larger catchment should be divided in several subcatchments that have their own WALRUS and corresponding parameter sets, which are representative for that area.

In order to reach the objective, the following research questions are formulated:

- How does WALRUS simulate discharges in a larger catchment without modifications?
- What are the effects on discharge simulations when using WALRUS in combination with a flow routing technique?
- In which ways can subcatchments be coupled in WALRUS?
- What are the differences in output comparing WALRUS to previous used models?

Chapter 2 will give a short introduction to the Reusel catchment, describing the surface water system, geology and soils, land use, climatology and hydrology. Chapter 3 will give an overview of the data used for this research. The methods are described in Chapter 4 and afterwards the results are shown in Chapter 5. Some topics will be discussed in Chapter 6 and the conclusions and recommendations are presented in Chapter 7.



## 2 | Reusel catchment

The Reusel catchment is a lowland catchment located in the south of the Netherlands, roughly between the Belgian border and the cities of Tilburg and Eindhoven (Figure 2.1). The total area is 145 km<sup>2</sup> and the catchment is part of the management area of Water board 'De Dommel'. This chapter describes several environmental aspects of the Reusel catchment.

### 2.1 Surface water system

The Reusel is a tributary of the lower river Meuse basin. The stream is south-north oriented and consists of many branches. The Reusel starts as a small stream between the Belgian border and the village Reusel. The total length to the outlet of the catchment is about 31 kilometers. The elevation varies between 38 meter (m a.s.l.) upstream in the catchment and 7 meter (m a.s.l.) near the outlet of the catchment. After passing the outlet near the village of Oisterwijk, the Reusel is merging with another stream (Voorste Stroom), the name changes into Achterste Stroom and later on into Essche Stroom, which ends up in the river Dommel.

The Reusel catchment can be divided in several subcatchments which are maintained by Water board 'De Dommel'. Discharge is measured at the outlet of several subcatchments (named with numbers 0072, 0098 and 0099). More information about the available data and subcatchments can be found in Chapter 3.

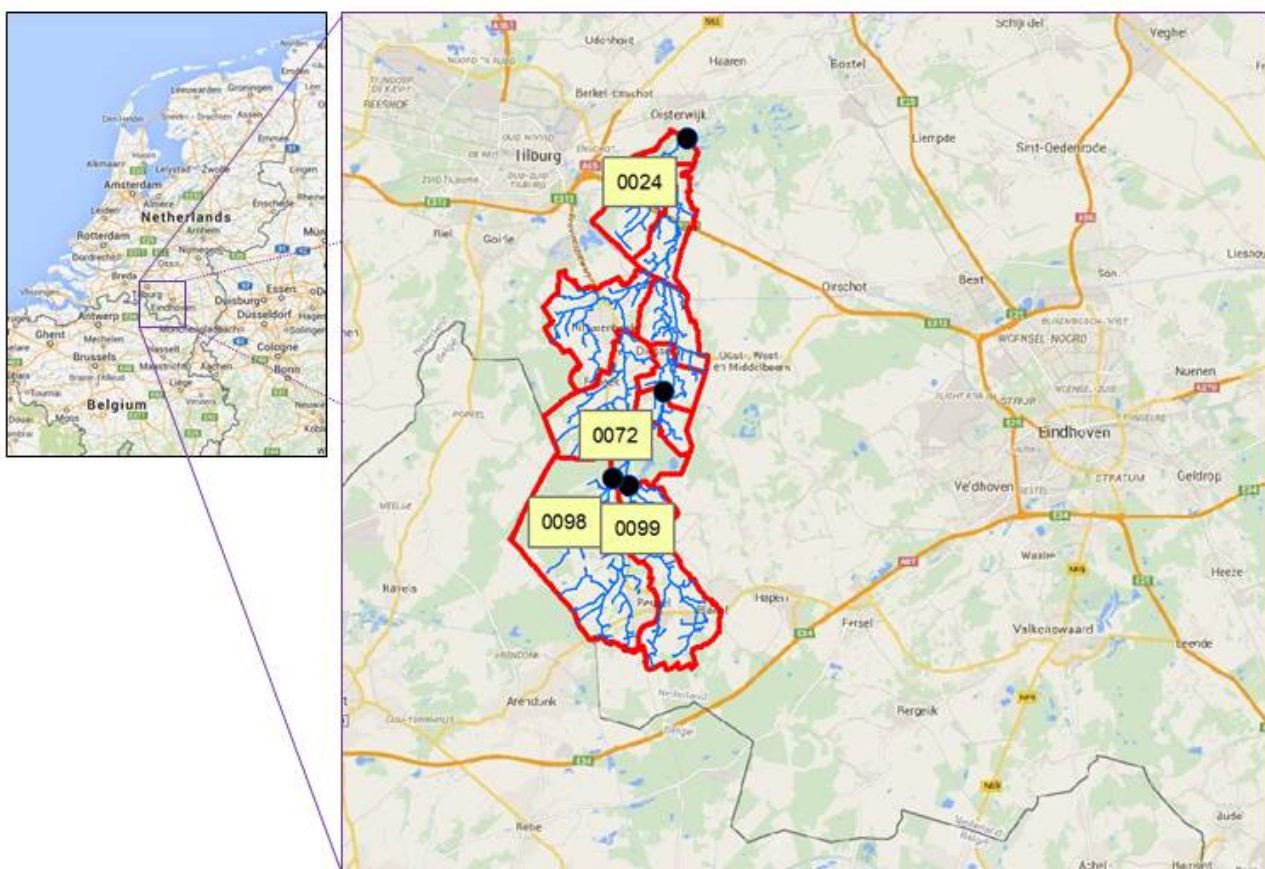


Figure 2.1: The Reusel catchment in The Netherlands, including streams (blue) and boundaries of subcatchments (red). Discharge measurements of (sub)catchments 0024, 0072, 0098 and 0099 are only used (see Chapter 3).

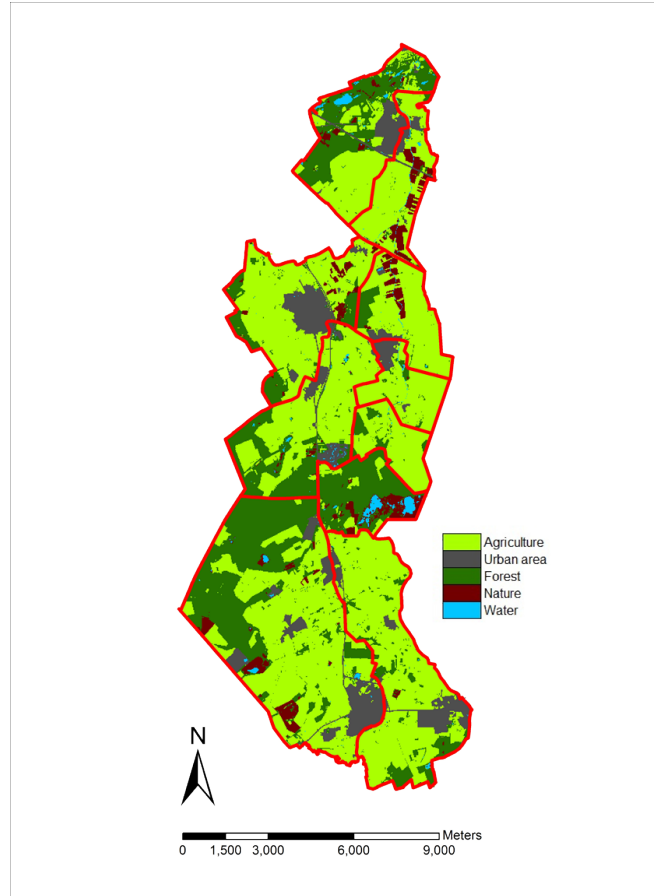


Figure 2.2: Land use map of the Reusel catchment.

## 2.2 Geology and soils

The geomorphology of this lowland valley varied throughout history, due to climate changes and geomorphological processes (Van Huissteden et al., 1986). In the Early Pleniglacial, a braided river system was developed due to the presence of permafrost. This changed into a meandering system during the Middle Pleniglacial and in the Upper Pleniglacial permafrost occurred again and the system changed back. At the end of the Pleniglacial, the valley was filled with cover sand. During the late Glacial the conditions changed, which caused sharp incisions. Parts of the new incised valley were filled with dune sands in the Early Dryas. Filling of the Reusel valley continued during the Holocene. Nowadays, soils in the Reusel catchment consist mainly of coarse sand material, deposited by the Meuse river system (Van Huissteden et al., 1986).

## 2.3 Land use

Figure 2.2 shows the land use map, from which percentages of certain land use classes are derived. Table 2.1 shows the results for the entire Reusel catchment (named with number 0024) and for several subcatchments (which will be further introduced in Section 3.1). Agriculture is the most common land use in the catchment, but also forests make up a large part of the area.

Table 2.1: Overview of the total area of the Reusel catchment (0024) and some subcatchments (0072, 0098, 0099) and the land use based on the LGN6 monitoring files. See Section 3.1 for the descriptions of the subcatchments.

|                         | 0024 | 0072 | 0098 | 0099 |
|-------------------------|------|------|------|------|
| Area (km <sup>2</sup> ) | 145  | 74   | 39   | 22   |
| Agriculture (%)         | 60.3 | 57.4 | 52.0 | 77.3 |
| Urban area (%)          | 9.3  | 8.5  | 10.1 | 10.5 |
| Forest (%)              | 25.4 | 29.5 | 34.2 | 11.7 |
| Nature (%)              | 3.9  | 3.5  | 3.3  | 0.3  |
| Water (%)               | 1.1  | 1.0  | 0.4  | 0.2  |

## 2.4 Climatology and hydrology

Climatological values for precipitation and potential evapotranspiration in the Reusel catchment (upstream of 0024) do not much deviate from the Dutch climatology. Based on the period 1987–2012, the yearly precipitation is on average 850 mm. Potential evapotranspiration values are on average 583 mm/y. The catchment average discharge is 326 mm/y. A maximum discharge of 20 m<sup>3</sup>/s has been observed, while the average discharge is 1.5 m<sup>3</sup>/s. Figure 2.3 shows a graphical overview of the annual precipitation, potential evapotranspiration, discharge and rest term.

## 2.5 Waste water treatment plant

One waste water treatment plant (WWTP) is present in the Reusel catchment. This installation removes contaminants from sewage water and precipitation which entered the sewage system. After cleaning the water, it is pumped into the Reusel (Waterschap De Dommel, 2015). The installation has a capacity of 2850 m<sup>3</sup>/h and discharge was measured (Section 3.6). Since the WWTP is located halfway between discharge station 0072 and 0024 (Figure 2.1, it only influences the discharge at the outlet of the Reusel catchment (station 0024).

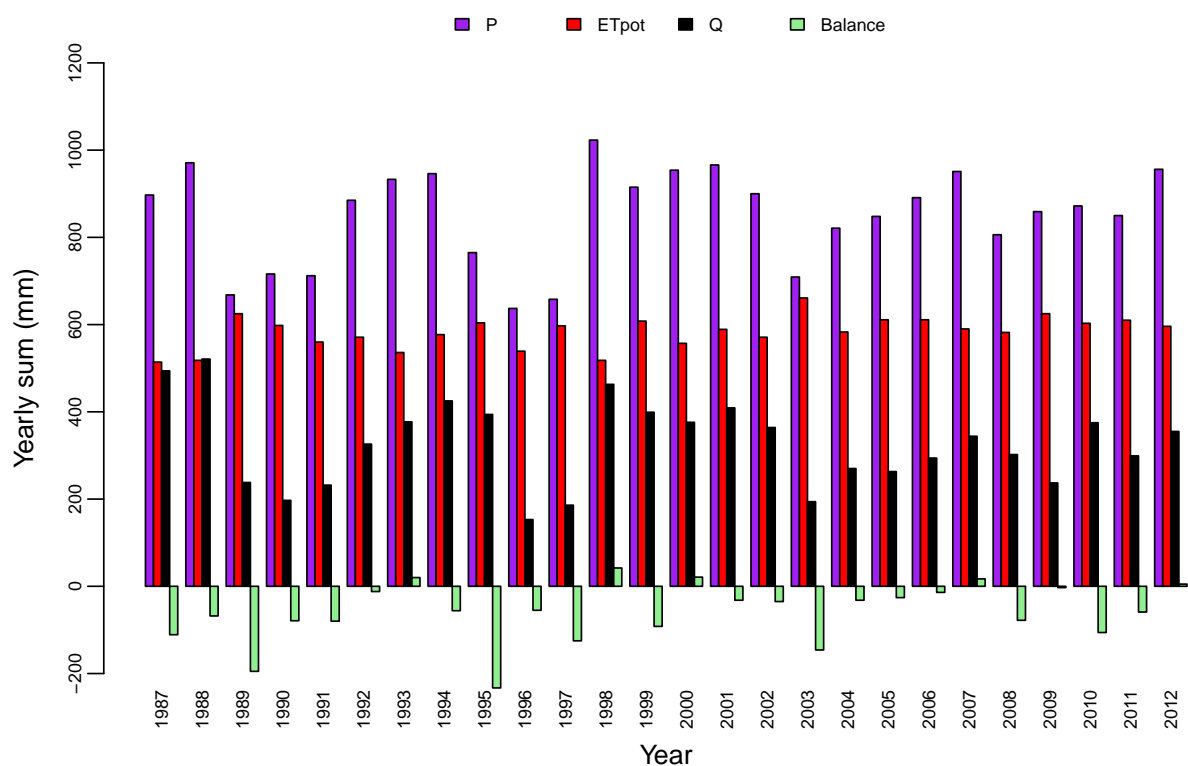


Figure 2.3: Plot of the annual precipitation ( $P$ ), potential evapotranspiration ( $ET_{pot}$ ), discharge ( $Q$ ) and the overall balance of these terms ( $P-ET_{pot}-Q$ ) in Reusel catchment (upstream of station 0024) in the period 1987–2012.

# 3 | Data

This chapter describes the data used for this research. Every subcatchment has its own dataset, since each catchment has a specific average catchment precipitation and observed discharge. Considering the size of the catchment, WALRUS has to run on a hourly time scale. Otherwise discharge peaks could be missed by the model. Availability and preprocessing of the required input data are described in the following sections, but first a short introduction to the subcatchments will be given.

## 3.1 Subcatchments

The Reusel catchment is divided by the Water board into different subcatchments (Figure 3.1). Discharge is measured at the weirs at the outlet of most subcatchments. Each discharge station has a number which will be used as name of the subcatchment (e.g. area upstream of that discharge measurement location) in this research. The number of the station which measures the discharge of the entire Reusel catchment is 0024. Subcatchments (that are used for this research) are numbered with 0072, 0098 and 0099. Figure 3.1 shows the location of the subcatchments and also the measurement locations of precipitation and discharge which are used for this research. The area of the subcatchments and information on land use is obtained by GIS maps. This information is already given in Table 2.1. Detailed information on the geometry of the streams was also available and used in Section 4.3.

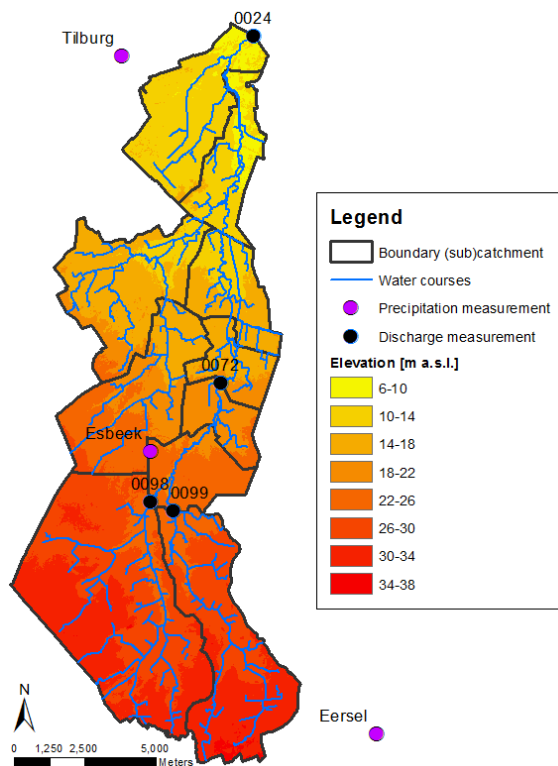


Figure 3.1: Elevation map of the Reusel catchment, including boundaries of subcatchments and streams. Measurement locations of precipitation and discharge which are used in this research are also pointed out.

## 3.2 Precipitation

The KNMI (Royal Netherlands Meteorological Institute) has a network of 325 volunteers who observe precipitation amounts and snow height every morning. Daily time series of these observations are available (for free) on the website of the KNMI (KNMI, 2014). Time series of locations Esbeek, Eersel and Tilburg are used (see Figure 3.1).

Since hourly data are needed as input for WALRUS, the daily precipitation data are compared to hourly precipitation data from an automatic KNMI weather station in Eindhoven. Daily precipitation amounts are (in proportion) divided over the hours with rainfall observed in Eindhoven. When no rainfall is observed in Eindhoven on a certain day, but only at (one) of the three daily measurement stations, the amount of observed precipitation is equally divided over the 24 hours of that specific day.

Because precipitation data are obtained from point observations, the catchment average precipitation is derived by using Thiessen polygons. With this method the importance of each of the three measurement stations for a specific subcatchment is determined, by assigning land to the nearest rain gauge. The fraction of land in a subcatchment that belongs to one of the three measurement is determined (see Table 3.1). Catchment average precipitation time series are created with use of these fractions.

Table 3.1: Percentage of precipitation data of a measurement station (Esbeek, Eersel, Tilburg) that is used to create the (sub)catchment average precipitation time series.

| Catchment | Esbeek | Eersel | Tilburg |
|-----------|--------|--------|---------|
| 0024      | 68.3   | 12.9   | 18.8    |
| 0072      | 74.8   | 25.2   | 0.0     |
| 0098      | 85.6   | 14.4   | 0.0     |
| 0099      | 40.8   | 59.2   | 0.0     |

## 3.3 Evapotranspiration

There are no evapotranspiration measurements in the Reusel catchment. Therefor, daily potential evapotranspiration data are obtained from a KNMI measurement station in Eindhoven (KNMI, 2014). These data are estimated with use of the method of Makkink (Makkink, 1957), temperature and global radiation data.

The evapotranspiration data need to be converted to hourly time scales. In order to create this time series, the same method as for the hourly precipitation time series is applied. The assumption is made that during one day, evapotranspiration is proportional to observed global radiation. The daily evapotranspiration is divided (in proportion) over the hours, using hourly global radiation observations.

Potential evapotranspiration data are not corrected for land use (with for instance crop factors), since land use can change throughout the years and crop factors can vary throughout the seasons. Because detailed information on those variabilities is missing, one single time series of potential evapotranspiration is used for the entire catchment (and subcatchments).

## 3.4 Discharge

Hourly time series of discharge are provided by Water board 'De Dommel'. There are several weirs in the catchment where discharge is measured. Water levels upstream and downstream of the weir, as well as the level of the weir itself are measured on a hourly scale. Discharge is calculated with use of a weir-specific stage-discharge relation.

Table 3.2: Availability of discharge time series (hydrological years) and the percentages of missing observations of stations 0024, 0072, 0098 and 0099.

| Station | Period 1  | Period 2  | Period 3 | Missing |
|---------|-----------|-----------|----------|---------|
| 0024    | 1987–2012 | -         | -        | 3.8%    |
| 0072    | 2009–2012 | -         | -        | 5.4%    |
| 0098    | 1999–2003 | 2006–2012 | -        | 6.9%    |
| 0099    | 1999–2002 | 2006–2009 | 2012     | 5.0%    |

This relation is not valid when the water level downstream equals or exceeds the level of the weir (e.g. the weir is submerged). In these situations, a special 'submergence relation' will be applied to calculate the discharge.

Weir levels at station 0024 and 0072 can vary; they can be regulated automatically or manually (Figures 3.2(a) and 3.2(b)). The weirs at station 0098 and 0099 are permanent weirs, with a fixed level, which can only be changed by adding or removing flash boards (Figures 3.2(c) and 3.2(d)). Table 3.2 shows the available discharge time series for these four measurement locations. The percentages of missing data within the available periods are also displayed. Gaps between two observations in the time series are filled by using linear interpolation.

The discharge time series are investigated. Sometimes the observed discharge fluctuates in an unnatural way, caused by the settings of the automatically operated weir. When the water level drops below a certain threshold, the weir is raised a little, water level rises above the threshold and the weir is lowered again, causing very quick fluctuations in the discharge. Because the model cannot simulate these unnatural fluctuations, all discharge time series are smoothed using a moving average of 24 hours. This "quick fix" removed the unnatural fluctuations, but sharp discharge peaks are slightly dampened and low (or zero) discharges are slightly increased. The sum of discharges does not change. Figure 3.3 shows an example of an original time series and the same time series filtered by using a moving average.

### 3.5 Groundwater flow

Regional groundwater flow and seepage are difficult to measure in the field, since there is much variation throughout the catchment. Van Walsum et al. (2002) found that upward seepage in the Reusel catchment occurs around the ditches in the little valleys. Downward seepage is more likely to occur in the higher parts of the catchment. Since there are no seepage measurements available for this research and because seepage is expected to occur within the catchment boundaries, seepage is not considered to occur on the water balance for the whole catchment. Although, the impact of seepage is investigated in some subcatchments.

### 3.6 Waste water treatment plant

Measurements of discharge from the WWTP 'Biest-Houtakker' are available for the period 2004–2012. The WWTP discharge varies between 29–34 mm/y, with an average of 32 mm/y. Since this is about 10% of average annual discharge of the entire catchment, this flux needs to be included in this study (e.g. as a surface water supply flux in the model).

### 3.7 Water balance

A simple water balance is made as a first check to see if the data are reliable and to identify striking years. Because no data are available on seepage, the water balance is based on observed precipitation (catchment averaged), potential



Figure 3.2: The weirs at four discharge measurement stations in the Reusel catchment.

evapotranspiration and observed discharge:

$$\frac{dS}{dt} = P - ET_{\text{pot}} - Q, \quad (3.1)$$

where  $dS/dt$  is the change in storage, expressed as an average change in water depth over a certain period (in this case mm/y).  $P$  is the amount of precipitation and  $ET_{\text{pot}}$  the amount of potential evapotranspiration, both in mm/h.  $Q$  is the observed discharge at the outlet of the catchment and is converted from  $\text{m}^3/\text{s}$  (according to the stage-discharge relation) to mm/h, with use of the size (in  $\text{m}^2$ ) of the catchment.

Table 3.3 shows the water balance for the entire catchment, based on Equation 3.1 and summed over hydrological years (1 April – 31 March). Using Equation 3.1, the average balance is  $-62$  mm, which means that more water is leaving the catchment than entering the catchment. This can be due to errors in the observations of  $P$ ,  $ET_{\text{pot}}$  ( $ET_{\text{pot}}$  can be higher than  $ET_{\text{act}}$ ) and  $Q$ , but also due to missing information on seepage. A second balance is added for the hydrological years 2004–2012, including the available information on the discharge ( $f_{xs}$ ) of the WWTP. The average of the second balance (including  $f_{xs}$ ) is  $-15.4$  mm. Note that 2007 and 2008 do not cover a complete hydrological year (see Table 3.3), since discharge observations are missing for a longer period. Those two years are not included in the average water balances as mentioned above.

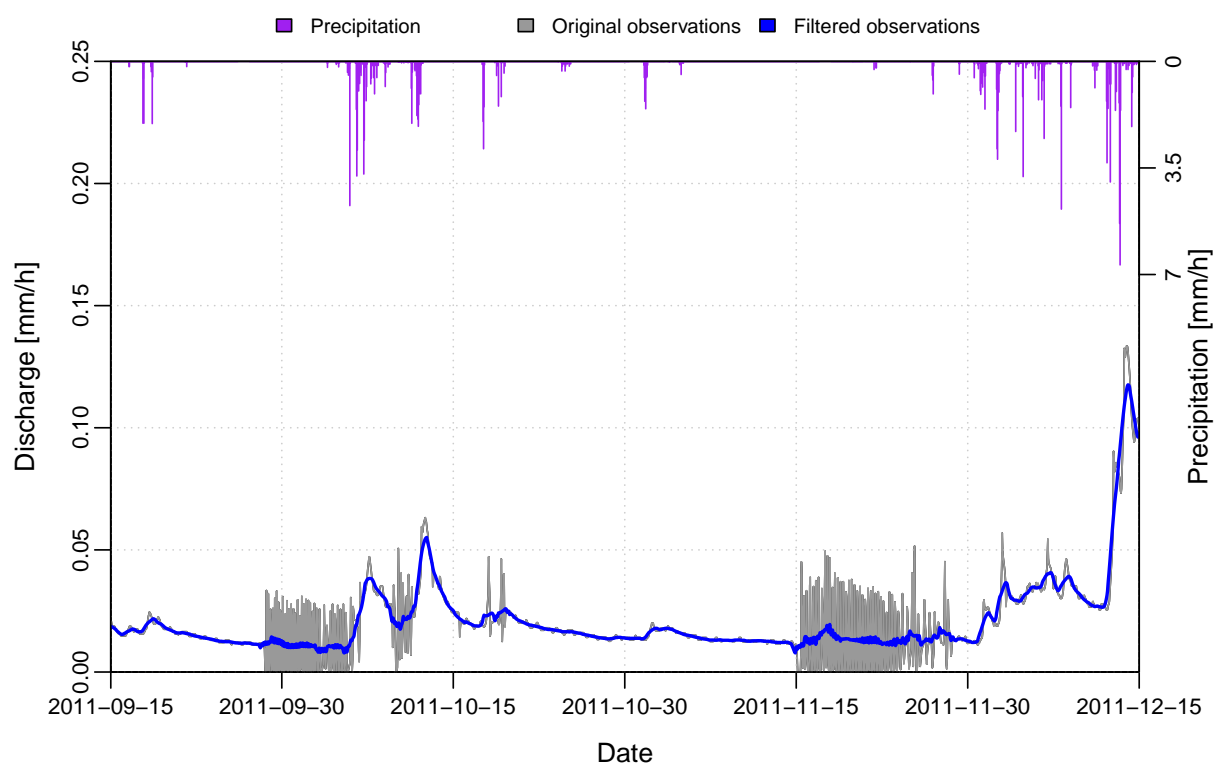


Figure 3.3: Plot of the original discharge time series (grey) of discharge station 0024 and the filtered time series (blue), by using a moving average of 24 hours.

Table 3.3: Water balance for the available hydrological years of station 0024 (entire catchment). A second balance is added for the hydrological years 2004–2012 and includes the surface water supply ( $f_{XS}$ ) of the WWTP. Note that some start and end dates differ from the standard hydrological year (1 April - 31 March), because discharge observations are missing for a longer period, for example in 2007 and 2008. The balances of these two years are not representative. Deviating dates are shown in italics.

| Year | Start date      | End date        | Days | Missing<br>[d] | P<br>[mm] | $ET_{pot}$<br>[mm] | Q<br>[mm] | Balance<br>[mm] | $f_{XS}$<br>[mm] | Balance<br>[mm] |
|------|-----------------|-----------------|------|----------------|-----------|--------------------|-----------|-----------------|------------------|-----------------|
| 1987 | 19870401        | 19880331        | 366  | 0              | 1047      | 511                | 590       | -54             | -                | -               |
| 1988 | 19880401        | 19890331        | 365  | 13             | 800       | 534                | 377       | -111            | -                | -               |
| 1989 | 19890401        | <i>19900330</i> | 364  | 6              | 675       | 624                | 203       | -152            | -                | -               |
| 1990 | <i>19900408</i> | 19910331        | 358  | 2              | 646       | 581                | 191       | -126            | -                | -               |
| 1991 | 19910401        | 19920331        | 366  | 0              | 717       | 547                | 215       | -45             | -                | -               |
| 1992 | 19920401        | 19930331        | 365  | 2              | 871       | 582                | 350       | -61             | -                | -               |
| 1993 | 19930401        | 19940331        | 365  | 0              | 1055      | 528                | 484       | 43              | -                | -               |
| 1994 | 19940401        | 19950331        | 365  | 0              | 1042      | 586                | 480       | -24             | -                | -               |
| 1995 | 19950401        | 19960331        | 366  | 0              | 507       | 591                | 166       | -250            | -                | -               |
| 1996 | 19960401        | 19970331        | 365  | 3              | 678       | 547                | 187       | -56             | -                | -               |
| 1997 | 19970401        | 19980331        | 365  | 0              | 720       | 596                | 218       | -94             | -                | -               |
| 1998 | 19980401        | 19990331        | 365  | 0              | 1109      | 520                | 600       | -11             | -                | -               |
| 1999 | 19990401        | 20000331        | 366  | 0              | 869       | 601                | 301       | -33             | -                | -               |
| 2000 | 20000401        | 20010331        | 365  | 2              | 980       | 552                | 407       | 21              | -                | -               |
| 2001 | 20010401        | 20020331        | 365  | 2              | 997       | 609                | 453       | -65             | -                | -               |
| 2002 | 20020401        | 20030331        | 365  | 0              | 755       | 584                | 264       | -93             | -                | -               |
| 2003 | 20030401        | 20040331        | 366  | 0              | 785       | 642                | 189       | -46             | -                | -               |
| 2004 | 20040401        | 20050331        | 365  | 45             | 825       | 584                | 287       | -46             | 31               | -15             |
| 2005 | 20050401        | 20060331        | 365  | 3              | 822       | 604                | 248       | -30             | 33               | 3               |
| 2006 | 20060401        | 20070331        | 365  | 9              | 974       | 618                | 361       | -5              | 36               | 31              |
| 2007 | 20070401        | <i>20071114</i> | 228  | 1              | 581       | 515                | 111       | -45             | 19               | -26             |
| 2008 | <i>20080821</i> | 20090331        | 223  | 7              | 445       | 178                | 166       | 101             | 17               | 118             |
| 2009 | 20090401        | 20100331        | 365  | 0              | 843       | 626                | 308       | -91             | 30               | -61             |
| 2010 | 20100401        | 20110331        | 365  | 1              | 867       | 611                | 363       | -107            | 33               | -74             |
| 2011 | 20110401        | 20120331        | 366  | 1              | 825       | 610                | 273       | -58             | 31               | -27             |
| 2012 | 20120401        | 20130331        | 365  | 1              | 947       | 582                | 362       | 3               | 32               | 35              |

# 4 | Methods

This chapter describes the methods and assumptions made in this research. The model used in this research will be introduced in Section 4.1. Section 4.2 will discuss the calibration methods that were used. The methods used for reservoir routing will be described in Section 4.3 and the coupling of different subcatchments will be introduced in Section 4.4 and Finally, the output of WALRUS will be compared to the output of WALRUS in Section 4.5.

## 4.1 WALRUS: Wageningen Lowland Runoff Simulator

The Wageningen Lowland Runoff Simulator (WALRUS) is a lumped rainfall-runoff model, developed by Brauer et al. (2014a). It is a model that is suitable for lowland catchments with shallow groundwater and there are only five parameters that need to be calibrated. It is also possible to calibrate on channel depth and initial groundwater level. The model is programmed in R, an open source programming environment for statistical computing and graphics. Figure 4.1 shows a schematic overview of WALRUS. A complete description can be found in (Brauer et al., 2014a). The next sections will give a brief introduction.

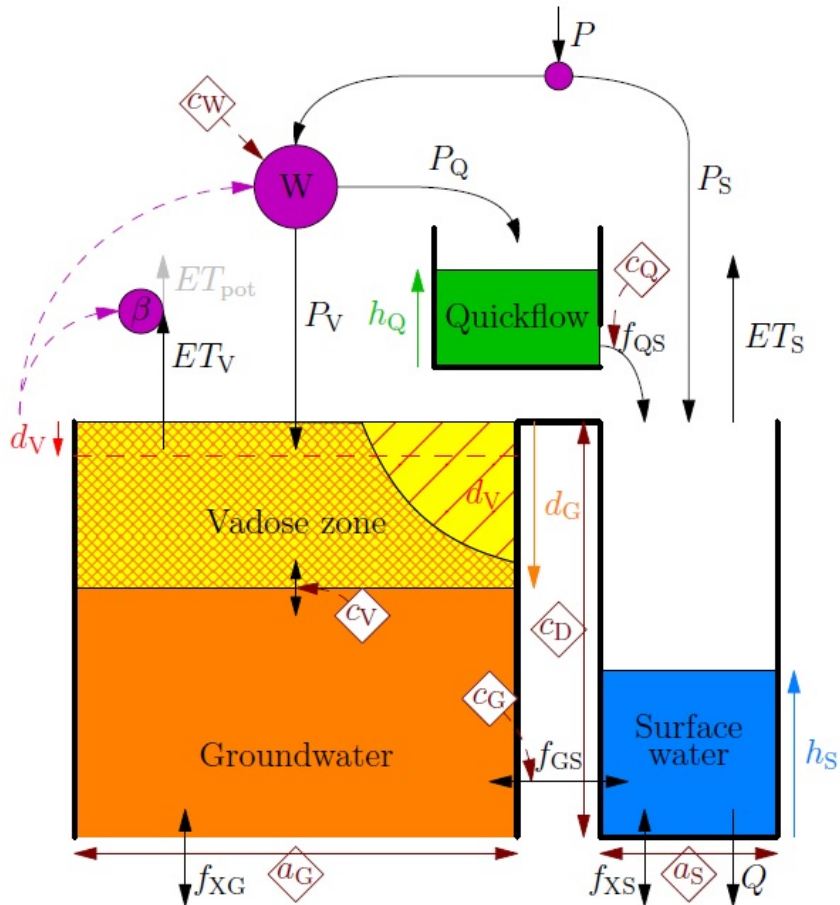


Figure 4.1: Schematic overview of WALRUS with all internal and external fluxes, states and parameters (Brauer et al., 2014a). A short explanation is given in the text.

The model consists of five compartments: land surface, vadose zone, groundwater zone, quickflow reservoir and surface water reservoir (see Figure 4.1). Precipitation ( $P$ ) enters the model in the land surface compartment. A

certain amount is directly falling on the surface water reservoir ( $P_S$ ). The soil wetness index ( $W$ ) determines which part of the remaining amount of precipitation is going to the vadose zone ( $P_V$ ) and which part is going directly to the quickflow reservoir ( $P_Q$ ). The vadose zone is, together with the groundwater zone, part of soil reservoir (slow reservoir). The quickflow reservoir represents overland flow and flow through drainage pipes and soil cracks. The wetness index ( $W$ ) ranges between 0 (all water to the soil reservoir) and 1 (all water to the quickflow reservoir) and is a function of storage deficit ( $d_V$ ). The storage deficit is expressed as the volume of empty soil pores per unit area, e.g. the depth of water needed to reach saturation. This storage deficit also controls the reduction of evapotranspiration ( $\beta$ ). There is a coupling between the vadose zone and the groundwater table and between the surface water reservoir and groundwater zone. There can be a flux from the quickflow reservoir into the surface water reservoir ( $f_{QS}$ ), but not the other way around. Internal fluxes such as surface water infiltration and drainage of groundwater ( $f_{GS}$ ) are depending on groundwater depth ( $d_G$ ) and surface water level ( $h_S$ ). External fluxes are upward/downward seepage ( $f_{xG}$ ), surface water supply/extraction ( $f_{xs}$ ) and discharge ( $Q$ ). Discharge is determined from the surface water level ( $h_S$ ) with use of a default stage-discharge relation. This stage-discharge relation can be changed by the user. The change of water level in the quickflow reservoir ( $h_Q$ ) is determined by the difference between the water that is flowing into the quickflow reservoir ( $P_Q$ ) and the water that is leaving the reservoir ( $f_{QS}$ ) divided by the groundwater reservoir area fraction ( $a_G$ ).

WALRUS needs as input a dataset with time series of precipitation ( $P$ ), potential evapotranspiration ( $ET_{pot}$ ) and observed discharge ( $Q$ ). When time series of seepage or groundwater extraction ( $f_{xG}$ ) or surface water supply/extraction ( $f_{xs}$ ) are applicable, those can be added to the dataset.

For the simulation, values for channel depth, initial groundwater level (which can be calibrated), soil type and the fraction of surface water need to be given. The initial surface water level is determined with use of the first discharge observation and the stage-discharge relation. Depending on the parameter set, WALRUS gives a simulation of the discharge as output, of which the performance is quantified by the Nash-Sutcliffe efficiency (Nash and Sutcliffe, 1970). The actual evapotranspiration, wetness index, storage deficit, groundwater depth, and the external fluxes are stored for each time step in a text file, as well as in a figure. Selected parameters and initial conditions are stored in an another file. Another file contains the terms of the water balance, which is computed as:

$$\Sigma P - \Sigma ET_{act} - \Sigma Q + \Sigma f_{xG} + \Sigma f_{xs} = -\Delta d_V \cdot a_G + \Delta h_Q \cdot a_G + \Delta h_S \cdot a_S. \quad (4.1)$$

The water balance should always close, but sometimes small deviations from zero are caused by rounding errors.

There are five parameters which require calibration: the wetness index parameter ( $c_W$ ), vadose zone relaxation time ( $c_V$ ), groundwater reservoir constant ( $c_G$ ), the quickflow reservoir constant ( $c_Q$ ) and the bankfull discharge ( $c_S$ ; only when the default stage-discharge relationship is used). These parameters are representative for the catchment characteristics. The next section describes the calibration methods.

## 4.2 Calibration and validation

Calibration is done with use of two calibration methods: HydroPSO and Levenberg-Marquardt. HydroPSO is a stochastic optimization software developed by Zambrano-Bigiarini and Rojas (2013). A swarm of a chosen number of particles is trying to find the optimal parameter values (between given boundaries) by searching for the lowest sum of residuals in the model outcome. The more particles are chosen, the bigger the chance that the best parameter set can be found. HydroPSO is the standard calibration method which is implemented in the WALRUS example scripts. Brauer et al. (2014b) state that equally good model results (e.g. Nash-Sutcliffe efficiencies) can be found by using

Table 4.1: Initial and boundary values for calibration of the five parameters using HydroPSO.

|                | $c_W$ | $c_V$ | $c_G$             | $c_Q$ | $c_S$ |
|----------------|-------|-------|-------------------|-------|-------|
| Lower boundary | 100   | 0.1   | $0.1 \times 10^6$ | 1     | 0.1   |
| Upper boundary | 400   | 100   | $100 \times 10^6$ | 200   | 20    |
| Initial value  | 200   | 4     | $0.5 \times 10^6$ | 10    | 4     |

Table 4.2: Initial and boundary values for calibration of the five parameters using Levenberg-Marquardt.

| Boundary | $c_W$ | $c_V$ | $c_G$              | $c_Q$ | $c_S$ |
|----------|-------|-------|--------------------|-------|-------|
| Lower    | 100   | 0.1   | $0.1 \times 10^6$  | 1     | 0.1   |
| Upper    | 400   | 100   | $100 \times 10^6$  | 200   | 10    |
| Set 1    | 110   | 95    | $50 \times 10^6$   | 25    | 9.50  |
| Set 2    | 250   | 70    | $97.5 \times 10^6$ | 10    | 6.25  |
| Set 3    | 200   | 1     | $25 \times 10^6$   | 125   | 3.75  |
| Set 4    | 275   | 30    | $87.5 \times 10^6$ | 175   | 7.50  |
| Set 5    | 300   | 20    | $62.5 \times 10^6$ | 75    | 0.50  |
| Set 6    | 150   | 40    | $12.5 \times 10^6$ | 190   | 1.25  |
| Set 7    | 225   | 50    | $37.5 \times 10^6$ | 150   | 5.00  |
| Set 8    | 350   | 80    | $75.0 \times 10^6$ | 50    | 8.75  |
| Set 9    | 390   | 60    | $0.15 \times 10^6$ | 100   | 2.50  |

different combinations of parameters. In order to find the best parameter set for each catchment, another calibration technique is also applied: the Levenberg-Marquardt algorithm (Moré, 1977). The Levenberg-Marquardt calibration always results in the same parameter set when calibrating with the same start values for the parameters.

Because there is enough data available for the different (sub)catchments and the fact that calibration results can vary, due to different hydrological circumstances, the two calibration methods are applied to several hydrological years. For each subcatchment, WALRUS was calibrated on a dry, an average and a wet hydrological year, based on the annual amount of precipitation.

Table 4.1 shows the initial and boundary values for the parameters when using the HydroPSO calibration method. The Levenberg-Marquardt calibration approach differs a little bit. It can happen that the wrong parameters are chosen, because the Levenberg-Marquardt calibration gets stuck in a local minimum of the sum of residuals. To avoid that situation and to check whether the found parameter set is the right one, nine random sets of initial parameter values are made (see Table 4.2). After calibration, those nine sets should give the same parameter sets. It can be compared to the particle swarm in the HydroPSO method (e.g. each set represents a particle which is moving between the boundaries, starting in another place).

Parameters are calibrated for each catchment several times, under different conditions (by manually changing the channel depth, initial groundwater depth, presence of seepage and implementation of the specific stage-discharge relation). The best calibration results are determined with use of the Nash-Sutcliffe efficiency and by evaluating the simulation with own experience, since models can give the right answers for the wrong reasons (Kirchner, 2006). The conditions with the best calibration results are chosen during the validation. Table A.1 in Appendix A gives an overview of all calibration conditions.

### 4.3 Reservoir routing

Since routing of surface water is not directly included in the model, WALRUS is also used in combination with a flow routing technique, which accounts for the attenuation and dampening of peak flows between two points. In this

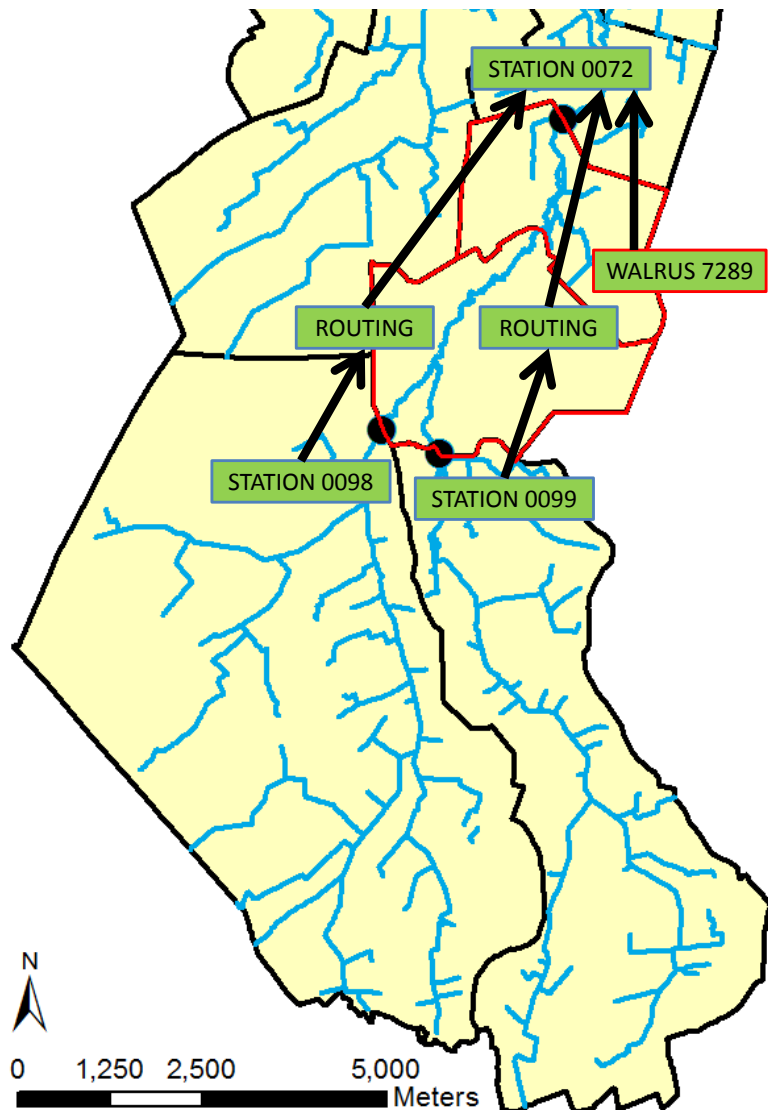


Figure 4.2: Schematic overview of the routing method. The total routed discharge at station 0072 consists of a routed discharge time series of 0098 and 0099, as well as a WALRUS output of subcatchment 7289 (area between red borders).

case, the trajectory between discharge stations 0098/0099 and 0072 is investigated. The model output of WALRUS of the hydrological years 2009–2010 and 2012–2013 is used since for these years observations of all three discharge stations were available.

The total routed discharge at station 0072 consists of three components:

1. A routed discharge time series of station 0098.
2. A routed discharge time series of station 0099.
3. The WALRUS output of subcatchment 7289.

Figure 4.2 gives an overview of the components that are considered. Subcatchment 7289 is an extra subcatchment (see the red borders in Figure 4.2). Since subcatchment 0072 consists of the complete area upstream of measurement

station 0072 (e.g. including subcatchment 0098 and 0099), the area of subcatchments 0098 and 0099 is subtracted from subcatchment 0072. The remaining area is called subcatchment 7289. This subcatchment has its own catchment averaged precipitation time series and the observed discharge is determined by taking the observed discharge at station 0072 and subtracting the discharge measured at the same time at stations 0098 and 0099. WALRUS simulates the discharge by using the same parameters as subcatchment 0072.

Routing is performed using a nonlinear reservoir model. The trajectory is considered to be one big reservoir, with a total storage  $S$ . This model only uses the mass balance and is described by:

$$\frac{dS}{dt}(t) = Q_{\text{in}}(t) - Q_{\text{out}}(t), \quad (4.2)$$

which can be discretized as:

$$S(t+1) = S(t) + \Delta t(Q_{\text{in}}(t) - Q_{\text{out}}(t)), \quad (4.3)$$

where  $S$  is the total storage in the reservoir (in  $\text{m}^3$ ) at a certain time  $t$  (in seconds),  $Q_{\text{in}}$  is the volume of water that is entering the reservoir (in  $\text{m}^3/\text{s}$ ) and  $Q_{\text{out}}$  is the volume of water that is leaving the reservoir (in  $\text{m}^3/\text{s}$ ).  $\Delta t$  is the time between two measurements (in this case 3600 seconds).

The storage in the river reach can be determined by creating a backwater curve. A backwater curve is computed for a stationary situation ( $Q_{\text{in}}$  equals  $Q_{\text{out}}$ ). Water levels at the location of the weir are calculated for the complete range of observed discharges at station 0072 (0.001–3.2  $\text{m}^3/\text{s}$ ), using the stage-discharge relation. The backwater curves (representing the water levels upstream) are calculated with use of a differential equation (Equation 4.4) and the Manning equation (Equation 4.5):

$$\frac{da}{dx} = \frac{S_o - S_f}{1 - Fr^2}, \quad (4.4)$$

$$Q = \frac{\sqrt{S_o}}{n} \cdot A \cdot R^{\frac{2}{3}}, \quad (4.5)$$

where  $da/dx$  is the change in water level over a certain distance,  $S_o$  is the average slope of the trajectory (-),  $S_f$  is the friction slope,  $Fr$  is the Freude number,  $Q$  is the discharge ( $\text{m}^3/\text{s}$ ),  $n$  is the Manning coefficient (-),  $A$  is the area of the cross section ( $\text{m}^2$ ) and  $R$  is the hydraulic radius (m).

To convert the water level for a specific discharge into a volume, the integral of water height over distance is calculated (area under the backwater curve). Since water levels are not equally distributed (higher water levels close to the weir), the area is divided by the total length of the river reach to get the average water level. Actual cross sections of the stream were available by the water board and are inspected at 25 locations on the trajectory. The average cross section of the stream is multiplied with the average water level to obtain the storage belonging to a specific discharge at the outlet.

Then, a storage-discharge relation is determined by plotting the storage against the discharge and fitting a regression line through the data points. The relation between storage and discharge is:

$$Q = a \cdot S^b. \quad (4.6)$$

When the storage and discharge are plotted on a log-log scale,  $\log(a)$  is the intercept and  $b$  is the slope of the regression line.

Going back to Equation 4.3,  $Q_{\text{in}}$  is a time series of the WALRUS output of station 0098 or 0099.  $Q_{\text{out}}$  can be determined with use of the current storage in the reservoir (and the relationship in Equation 4.6). This is done separately for the trajectories 0072–0098 and 0072–0099. For each time step, calculated discharges are summed together with the output of WALRUS for subcatchment 7289. In the end, the total routed discharge is compared to the discharge observations at station 0072.

#### 4.4 Coupling of subcatchments

It was supposed that WALRUS is not really able to simulate discharges in a larger catchment, since the five parameters are not representative for the local catchment characteristics anymore, but more as an average of the whole catchment. Therefor it is investigated if coupling of subcatchments leads to better simulation results. The same subcatchments as described before are used (0072, 0098 and 0099). The parameters of WALRUS are calibrated on the discharge observations of each subcatchment. Afterwards, a convincing parameter set is chosen for the validation. The only common hydrological years are 2009–2010 and 2012–2013, so the coupling is performed for those years. The observed discharges of subcatchments 0098 and 0099 are summed for each time step, creating a new time series which is implemented in the time series of subcatchment 0072 as an external surface water supply flux ( $f_{\text{xs}}$ ). This is also done for WALRUS output of 0098 and 0099. Precipitation data of the subcatchment is replaced with the precipitation time series of catchment 7289 (see Section 4.3). The new dataset is calibrated and validated again. The results can be found in Chapter 5.3.

#### 4.5 WALRUS versus Wageningen Model

WALRUS results are compared to results of the Wageningen Model, which is already used in the Reusel catchment. This rainfall-runoff model is developed by Stricker and Warmerdam (1982) in the seventies and consists of a soil moisture reservoir, a groundwater reservoir and two other reservoirs which represent the slow and fast discharge components (see Figure 4.3).

The amount of soil moisture ( $SM$ ) is calculated with the water balance of the soil moisture reservoir, which includes precipitation ( $P$ ) and evapotranspiration ( $ET_a$ ). When the amount of soil moisture ( $SM$ ) does not exceed the field capacity ( $FC$ ), capillary rise from the groundwater reservoir ( $CAP$ ) is calculated. When the amount of soil moisture exceeds the field capacity ( $FC$ ), effective precipitation ( $PEF$ ) is calculated. This effective precipitation ( $PEF$ ) is divided ( $DIV$ ) over two reservoirs: one reservoir which accounts for the slow discharge component (base flow) and one reservoir for the fast discharge component (overland flow and drainpipes). The slow reservoir is described by the  $j$ -model (Kraijenhoff van de Leur, 1958) and the fast reservoir is described by the convection-diffusion ( $CD$ ) model (Dooge and Harley, 1967).

There are six parameters that need to be calibrated:  $J$ ,  $E$ ,  $F$ ,  $CR$ ,  $REPA$  and  $FOS$ . Parameter  $J$  is coupled to the  $j$ -model, and parameters  $E$  and  $F$  are connected to the  $CD$ -model.  $CR$  is an empirical parameter which describes the relation between the divider ( $DIV$ ) and the groundwater storage ( $G_{\text{store}}$ ). Parameter  $REPA$  controls the rate at which the effective precipitation flows out of the soil moisture reservoir. Parameter  $FOS$  controls the rate at which capillary rise occurs.

This model is already used by the water board and time series of discharge simulations are available. These time series are plotted, together with the results of WALRUS and the observed discharges. This is done for the whole

catchment (weir 0024) and for subcatchment 0098. Nash-Sutcliffe efficiencies will be computed in order to quantify which model performs better.

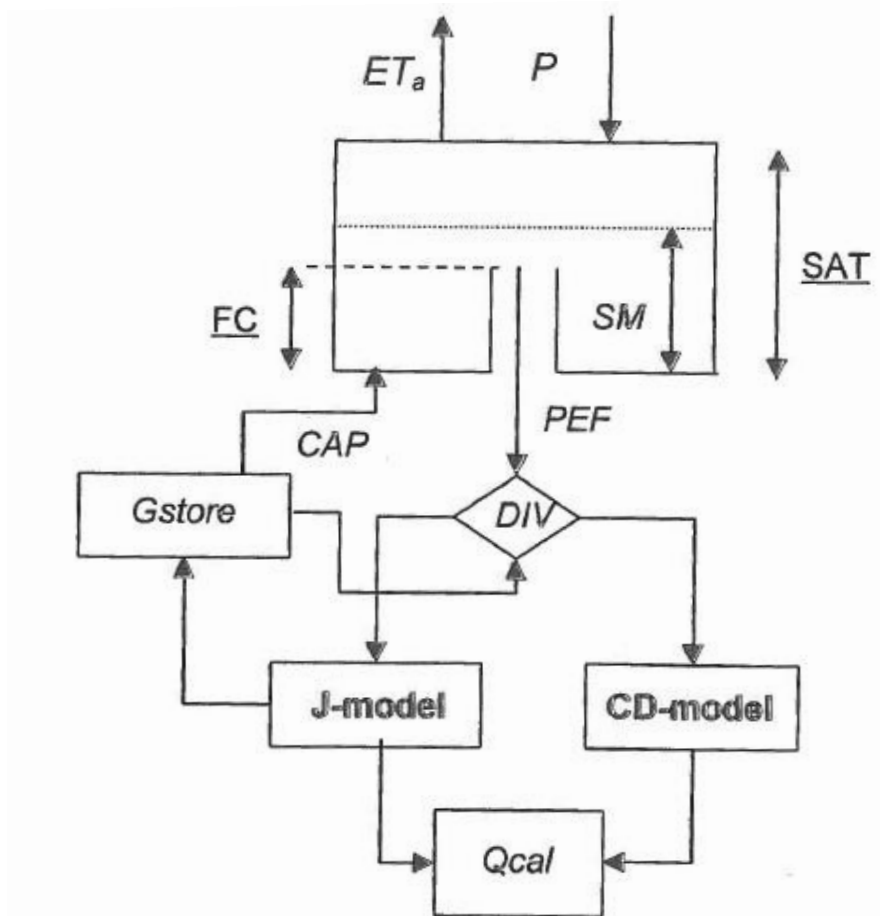


Figure 4.3: Schematic overview of the Wageningen Model (Warmerdam and Kole, 2008). A short description can be found in Section 4.5.



# 5 | Results

This chapter shows all results, starting with the calibration and validation results in Section 5.1. Afterwards, the results of reservoir routing are shown in 5.2. Then the results of coupling different subcatchments to each other are presented in Section 5.3 and finally the results of the comparison of WALRUS with the Wageningen Model are given in Section 5.4.

## 5.1 Calibration and validation

Calibration runs are executed under different setups (see Appendix A). Table 5.1 gives an overview of the selected hydrological years (dry, average, wet), based on the amount of precipitation. Catchment 0072 is only calibrated on two hydrological years, because of a limited amount of available data. Since the water balance is not closed, it can be concluded that there are errors in the observations or other hydrological processes are influencing the water balance, for instance seepage (see Section 3.5). Therefor, some calibration runs are executed with a seepage flux. Seepage rates are estimated by deriving the water balance between two time steps where the groundwater levels are the same (e.g. storage is the same). The amount of water that is missing (negative balance), is divided over the number of hours in that period, resulting in a seepage flux of 0.01 or 0.02 mm/h.

Table 5.1: Selected hydrological years for calibration of the five WALRUS parameters. Deviating dates are shown in italics.

| Catchment | Condition | Year | Start date      | End date        | Days<br>[d] | P<br>[mm] | ET <sub>pot</sub><br>[mm] | Q<br>[mm] | Balance<br>[mm] |
|-----------|-----------|------|-----------------|-----------------|-------------|-----------|---------------------------|-----------|-----------------|
| 0024      | dry       | 1995 | 19950401        | 19960331        | 366         | 507       | 591                       | 166       | -250            |
| 0024      | avg       | 2011 | 20110401        | 20120331        | 366         | 825       | 610                       | 273       | -58             |
| 0024      | wet       | 1998 | 19980401        | 19990331        | 365         | 1109      | 520                       | 600       | -11             |
| 0072      | -         | 2010 | 20100401        | <i>20110328</i> | 362         | 854       | 607                       | 208       | 39              |
| 0072      | -         | 2011 | <i>20110412</i> | 20120331        | 354         | 815       | 583                       | 156       | 76              |
| 0098      | dry       | 2002 | 20020401        | 20030331        | 365         | 751       | 584                       | 188       | -21             |
| 0098      | avg       | 2011 | 20110401        | 20120331        | 365         | 823       | 608                       | 185       | 30              |
| 0098      | wet       | 2007 | 20070401        | 20080331        | 366         | 930       | 590                       | 266       | 74              |
| 0099      | dry       | 1999 | 19990401        | <i>19990930</i> | 183         | 383       | 500                       | 49        | -166            |
| 0099      | avg       | 2009 | 20090401        | 20100331        | 365         | 815       | 626                       | 225       | -36             |
| 0099      | wet       | 2000 | 20000401        | 20010331        | 365         | 944       | 552                       | 371       | 21              |

Calibration runs for HydroPSO and Levenberg–Marquardt did not result in unique parameter sets. Therefor, the best parameter sets are obtained by adjusting a good set of parameters by hand, trying to increase the Nash–Sutcliffe efficiency and to improve the fit of the simulation (e.g. peaks, shape of recession, base flow). Table 5.2 shows the selected parameters for each (sub)catchment. Since the default stage-discharge relation is chosen for all (sub)catchments, parameter  $c_S$  is also calibrated.

A second parameter set is selected for catchment 0024, where the dataset included the available time series of the WWTP as a surface water supply flux ( $f_{xs}$ ). The following parameters are found:  $c_W=255$  mm,  $c_V=100$  h,  $c_G=75 \times 10^6$  mm h,  $c_Q=175$  h and  $c_S=7$  mm/h.

After calibration, the selected parameter sets (Table 5.2) are validated on the available hydrological years (Table 3.2). Figure 5.1 shows one of the results of WALRUS for the complete catchment (0024). It is a very good simulation ( $NS=0.89$ ). Timing and the amount of peak discharge is well simulated most of the times. WALRUS is able to simulate the first peak discharge (in September) after a longer period of almost no discharge. Only base flow is too

Table 5.2: Selected parameter sets and conditions for each (sub)catchment.

|          | 0024             | 0072            | 0098            | 0099             | Unit |
|----------|------------------|-----------------|-----------------|------------------|------|
| $c_W$    | 249              | 287             | 294             | 283              | mm   |
| $c_V$    | 70.0             | 100.0           | 3.6             | 63.6             | h    |
| $c_G$    | $56 \times 10^6$ | $5 \times 10^6$ | $5 \times 10^6$ | $44 \times 10^6$ | mm h |
| $c_Q$    | 72.0             | 80.0            | 4.6             | 81.7             | h    |
| $c_S$    | 5.00             | 0.15            | 0.10            | 10.00            | mm/h |
| $d_{G0}$ | 1200             | 1200            | 1200            | 1200             | mm   |
| $c_D$    | 1500             | 1000            | 1500            | 1000             | mm   |
| $f_{XG}$ | 0.00             | 0.00            | 0.00            | 0.01             | mm/h |
| $f_{XS}$ | 0.00             | 0.00            | 0.00            | 0.00             | mm/h |
| $a_G$    | 0.99             | 0.99            | 0.99            | 0.99             | -    |
| $a_S$    | 0.01             | 0.01            | 0.01            | 0.01             | -    |
| $st$     | sand             | sand            | sand            | sand             | -    |
| $Q-h$    | default          | default         | default         | default          | -    |

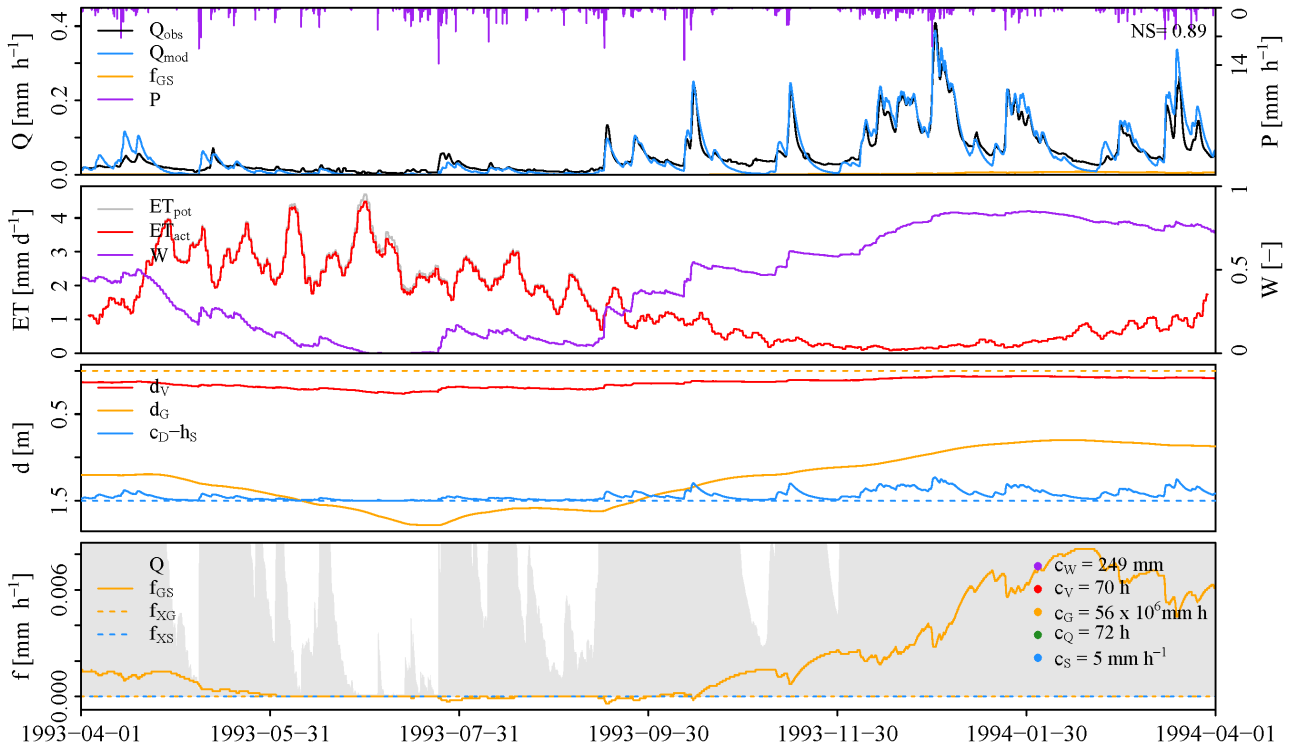


Figure 5.1: Validation of the selected parameter set for catchment 0024 on the hydrological year 1993–1994.

low, which can be noticed by the fact that the recession curve is decreasing too much. This can be caused by the surface water supply of the WWTP, of which the data are missing for this year. Figure 5.2 compares two simulations of the same hydrological year, one without the WWTP data and one including the WWTP data as a surface water supply flux. The influence of the WWTP is clearly visible. Simulations improve when adding this data as a surface water supply flux to the model.

All validations results can be found in Appendix B. Table 5.3 summarizes the results by showing the average Nash-Sutcliffe efficiencies over the available validation years. Because most parameters are a little bit adjusted by hand, the calibration years are also included in the validation and in the average Nash-Sutcliffe efficiencies.

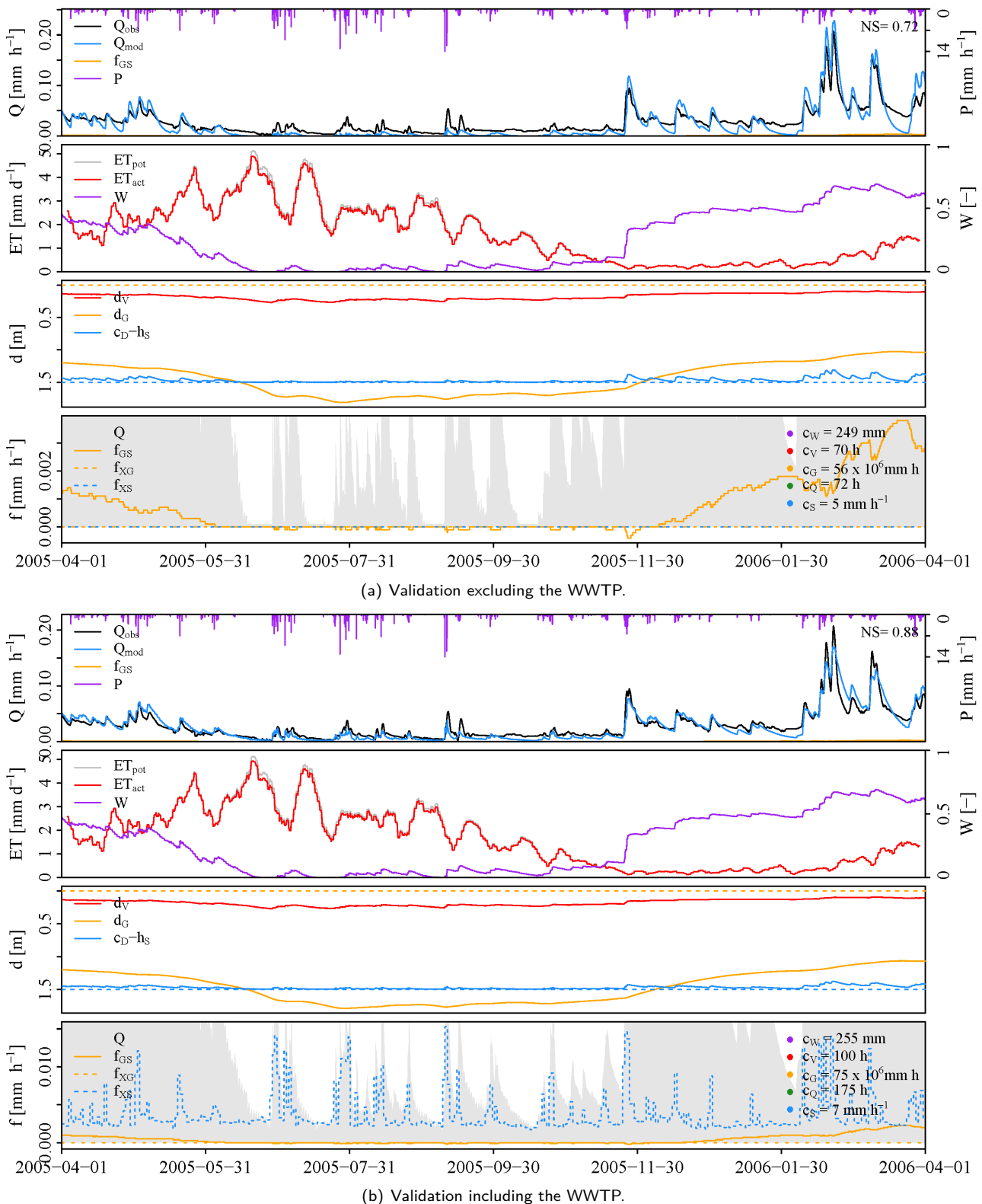


Figure 5.2: Validation of the selected parameter set for catchment 0024 on the hydrological year 2005–2006, by excluding and including the WWTP time series. Note the different parameter sets, since the dataset which includes the WWTP is calibrated separately.

Table 5.3: Average Nash-Sutcliffe efficiencies found for the validation of the selected parameter sets. The column 'years' show the number of years that is validated and used for deriving the average Nash-Sutcliffe. The last two columns show the number of years with a specific Nash-Sutcliffe efficiency, since the average value can give a wrong impression of the reality.

| Catchment             | NS   | Years | NS>0.50 | NS>0.75 |
|-----------------------|------|-------|---------|---------|
| 0024                  | 0.73 | 24    | 22      | 10      |
| 0024 (including WWTP) | 0.79 | 7     | 7       | 5       |
| 0072                  | 0.64 | 4     | 4       | 0       |
| 0098                  | 0.54 | 12    | 11      | 0       |
| 0099                  | 0.40 | 9     | 6       | 1       |

## 5.2 Reservoir routing

Following the method in Section 4.3, backwater curves are computed for both trajectories (0098–0072 and 0099–0072). Figure 5.3 shows the backwater curves for trajectory 0099–0072. Minimum discharge ( $Q$ ) was  $0.001 \text{ m}^3/\text{s}$  and maximum discharge was  $3.2 \text{ m}^3/\text{s}$ . As can be seen in the figure, the weir can influence water levels up to 1250 meter upstream, due to the small gradient in the lowland stream.

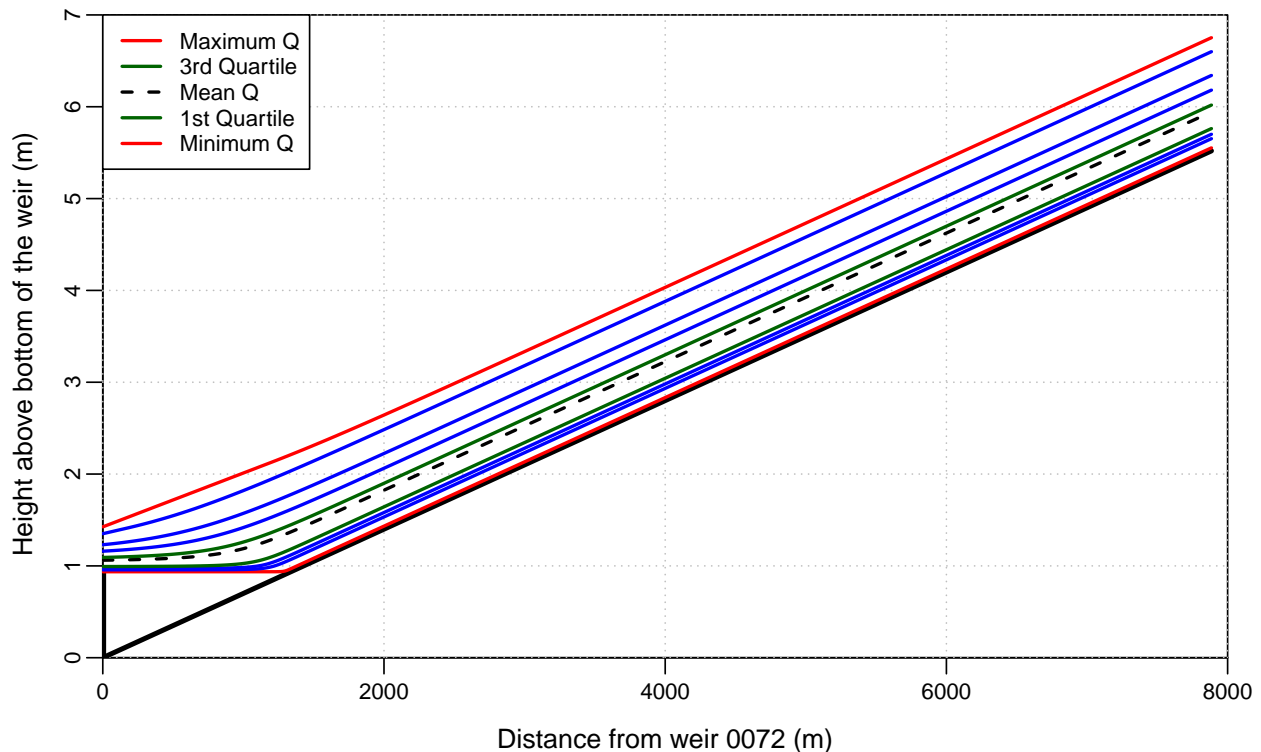


Figure 5.3: Backwater curve of the river reach between measurement location 0099 and 0072.

After calculating the storage for each discharge at the outlet, a storage-discharge relation is determined (Equation 4.6). Table 5.4 shows the values of  $a$  and  $b$  for the storage-discharge relations of both trajectories, as well as the length of the trajectory ( $L$ ), the Manning coefficient ( $n$ ) and the average slope ( $S_o$ ).

With use of the specific storage-discharge relation and Equation 4.3,  $Q_{\text{out}}$  is derived for each time step. First this is done with simulated discharges from station 0098 and 0099 (separately, representing component 1 and 2 as mentioned in Section 4.3). These two components are summed, together with the WALRUS output of subcatchment

Table 5.4: Values of parameters and variables used by applying the reservoir routing technique (Equation 4.5 and 4.6).

|       | 0098–0072              | 0099–0072              |
|-------|------------------------|------------------------|
| $a$   | $2.712 \times 10^{-9}$ | $2.658 \times 10^{-9}$ |
| $b$   | 1.957527               | 1.955417               |
| $L$   | 7620                   | 7885                   |
| $n$   | 0.04                   | 0.04                   |
| $S_o$ | 0.0007                 | 0.0007                 |

Table 5.5: Nash-Sutcliffe efficiencies for the WALRUS simulation of subcatchment 0072 (no routing), the total routed discharge at location 0072 by using WALRUS simulations of 0098 and 0099 (routing QW) and the total routed discharge at location 0072 by using discharge observations of subcatchments 0098 and 0099 (routing QD).

|      | no routing<br>WALRUS | routing QW<br>WALRUS | routing QD<br>observations |
|------|----------------------|----------------------|----------------------------|
| 2009 | 0.73                 | 0.77                 | 0.88                       |
| 2012 | 0.59                 | 0.40                 | 0.34                       |

7289 (component 3). The results are shown in Figure 5.4. Figure 5.6(a) shows the same results, but then zoomed in on a random period of 18 days of the specific hydrological year. Appendix C contains more zoomed plots.

The most striking result of routing with WALRUS discharges (Figure 5.4) is the fact that the routed discharge peaks are often too high. The shape of the routed discharge curve (orange line) is often better than the discharge curve of the WALRUS output of station 0072 (blue line). The timing of the routed discharge is also more accurate, but sometimes slightly too early. This is the case for both hydrological years. When comparing the results in terms of Nash-Sutcliffe efficiency (see Table 5.5), it can be concluded that the two hydrological years are somewhat contradictory.

As a second approach, the same steps are performed but component 1 and 2 are replaced by the observed discharges of stations 0098 and 0099. These results are shown in Figure 5.5, 5.6(b) and Table 5.5. The green line shows the routed discharge (QD). For 2009–2010, the result is much better than when using simulated discharges of WALRUS (Figure 5.4(a)); only in the second half of the period, peak discharge are a little bit overestimated. For 2012–2013, the results are not as good as those from the WALRUS routing (Figure 5.4(a)). Again the peaks are overestimated most of the time. The mass balance reveals that more water is entering the catchment (sum of the observations of stations 0098 and 0099), than leaving the catchment (observed at station 0072). A possible explanation is given in Section 5.3.

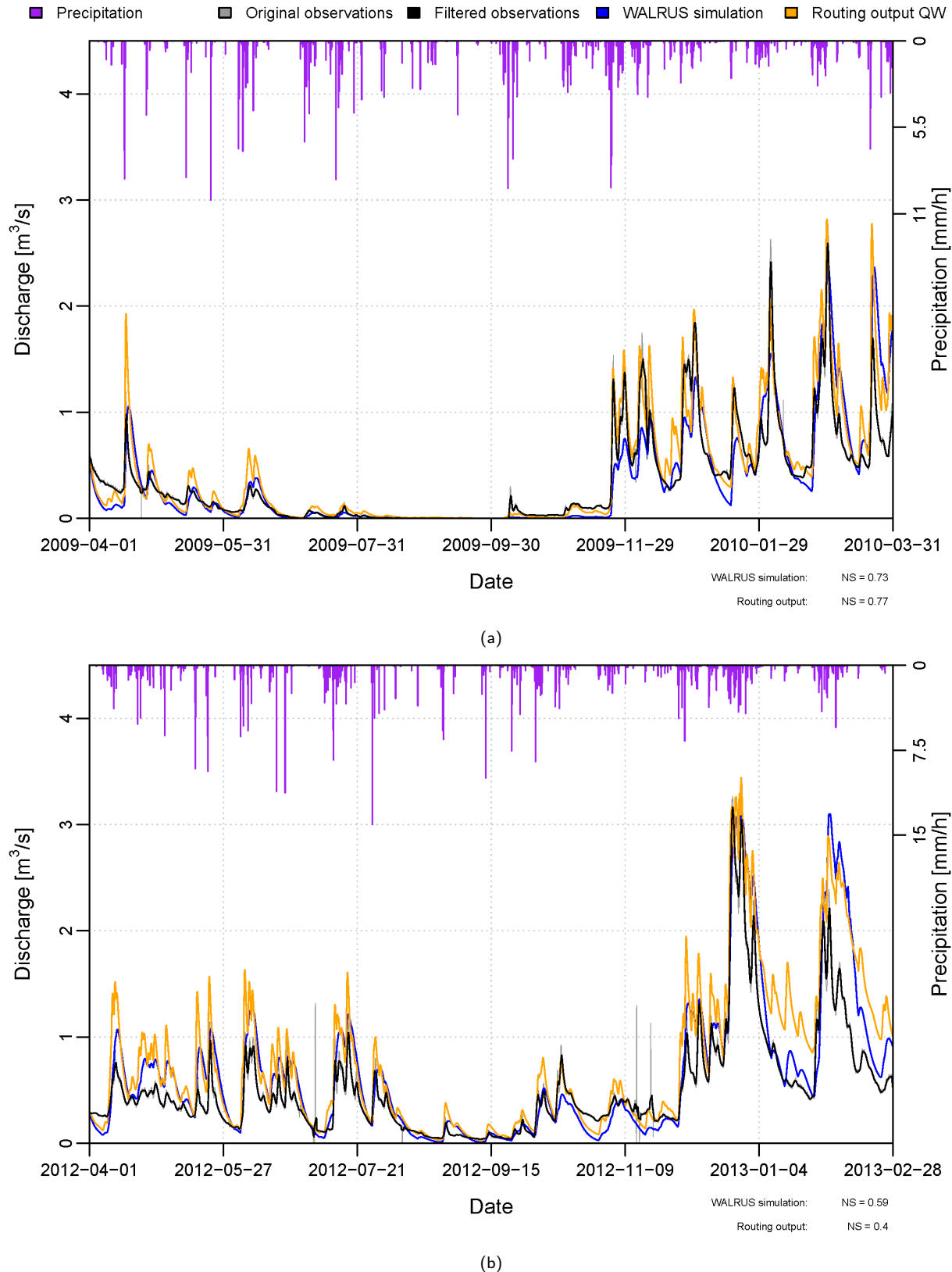


Figure 5.4: Results of the routing technique that is applied to simulate the discharge at station 0072, using WALRUS output (QW) of stations 0098 and 0099 for the hydrological years 2009–2010 (a) and 2012–2013 (b).

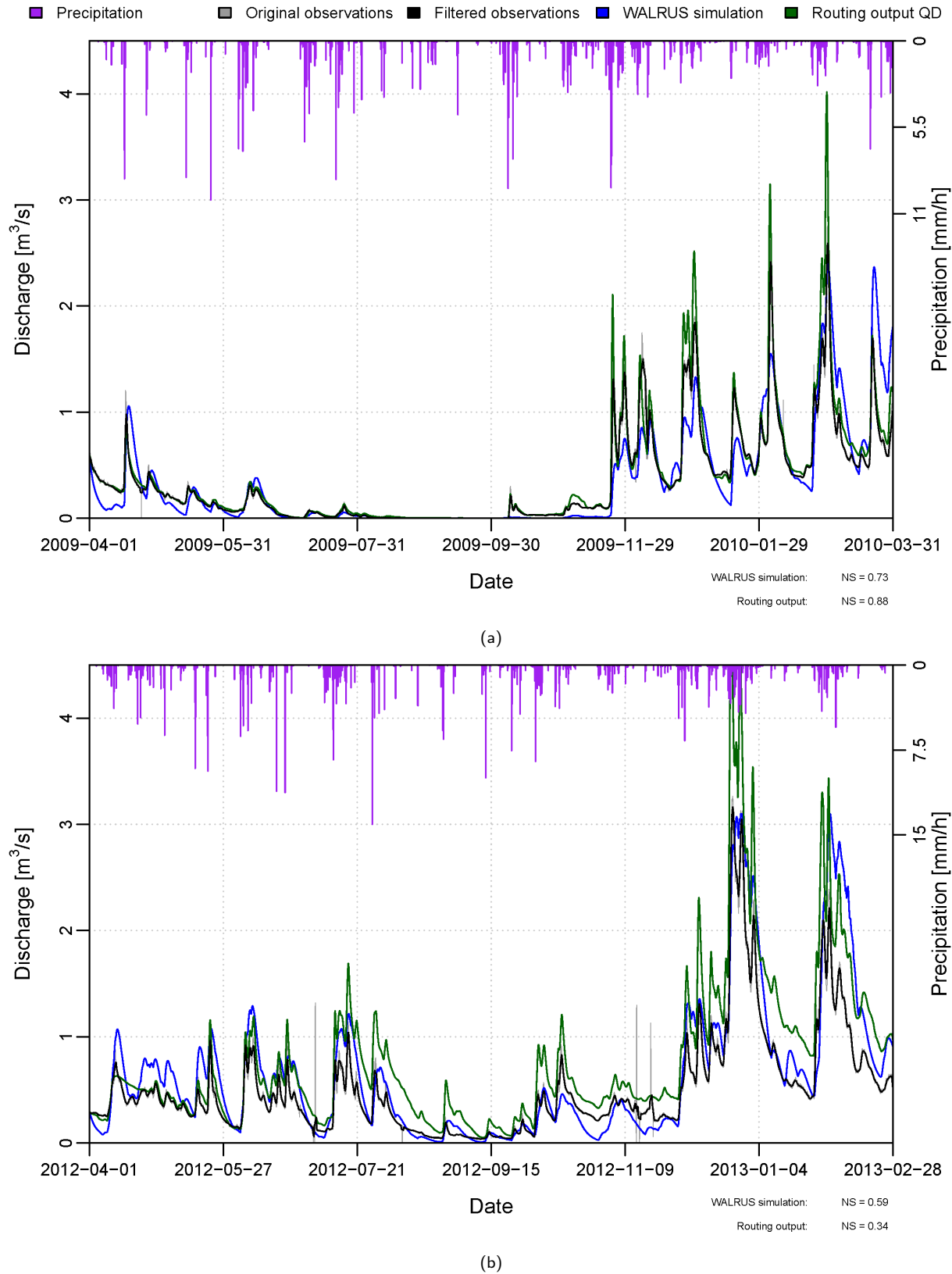


Figure 5.5: Results of the routing technique that is applied to simulate the discharge at station 0072, using observed discharges (QD) of stations 0098 and 0099 for the hydrological years 2009–2010 (a) and 2012–2013 (b).

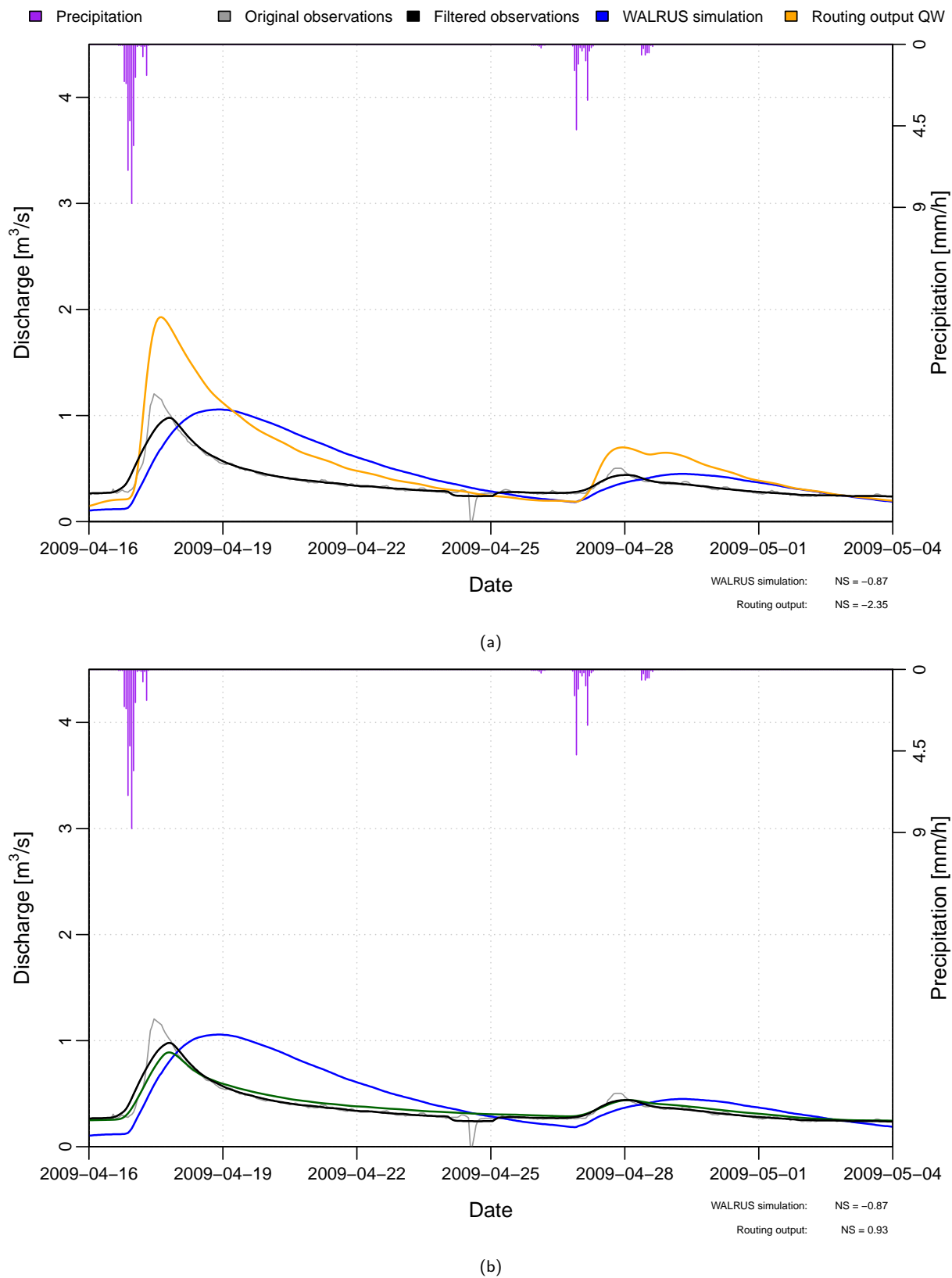


Figure 5.6: Same results as Figures 5.4(a) and 5.5(a), but now zoomed in on a period of 18 days.

### 5.3 Coupling of subcatchments

A new dataset for subcatchment 7289 was created (see Section 4.4). Calibration resulted in the following parameters:  $c_W=100$  mm,  $c_V=0.1$  h,  $c_G=53 \times 10^6$  mm h,  $c_Q=200$  h and  $c_S=1$  mm/h. After validating, Nash-Sutcliffe efficiencies of 0.78 (2009–2010) and 0.11 (2012–2013) were found for the coupling of observed discharges of subcatchments 0098 and 0099 to subcatchment 7289 (Figure 5.7). The coupling of WALRUS output of subcatchments 0098 and 0099 to subcatchment 7289 resulted in Nash-Sutcliffe efficiencies of 0.73 (2009–2010) and 0.87 (2012–2013), see Figure 5.8.

WALRUS is able to simulate the discharge at station 0072 very well for 2009–2010, using observations of station 0098 and 0099 (Figure 5.7(a)). Again, after a dry period in the summer of 2009, the first discharge peak is simulated very accurately. The shapes of the recession curves are also in agreement with the observations. The bottom panel shows the simulated discharge (grey area) and the surface water supply flux of catchments 0098 and 0099 (blue dashed). It can be noticed that the incoming water of the subcatchments is not directly discharged, but with a certain delay. It seems that WALRUS is already routing that water through the catchment. The routing technique is hidden in the parameter set and model set-up.

The simulation of catchment 7289, using the WALRUS output of subcatchments 0098 and 0099 is less good for 2009–2010 (Figure 5.8(a)). This can be explained by the fact that simulations are almost never as good as the observations, so when using simulation results with the coupling of the catchments, the error can increase. Figure 5.8(b) shows contradictory results again (compared to 2009–2010).

The result of 2012–2013 are less good when using the observations of station 0098 and 0099 (Figure 5.7(b)). Almost the entire year, WALRUS is overestimating the discharge at station 0072. This can be explained by the observed discharge at the stations. For 2009–2010, the input of subcatchment 0098 and 0099 ( $f_{xs}$ ) was in total 853 mm, the observed discharge ( $Q_{obs}$ ) at station 0072 was 852 mm. These are reasonable numbers, since measurements of seepage are unknown. For 2012–2013,  $f_{xs}$  was 1506 mm, while the observed discharge downstream was only 1133 mm. It means that around 373 mm (around 33%) is removed from the system by an unknown flux. This is not realistic, so probably other problems play a role, for instance the accuracy of the observations.

To investigate the observed discharges, discharges are summed per day and days with less than 24 observations (due to missing data) are removed. Daily discharges are calculated to avoid the effects of peak discharges (a peak at 0098 or 0099 does not directly cause a peak discharge at station 0072, but the peak is delayed). When plotting the observed discharges of stations 0098 and 0099 against observed discharge at station 0072, it seemed that discharge is structurally overestimated at 0098 and 0099 or that discharge is underestimated at station 0072 (Figure 5.9), especially in 2012–2013. Figure 5.10 shows the cumulative discharges of subcatchments 0098 and 0099 plotted against the cumulative discharge of subcatchment 0072. Subcatchment 0099 is about 40% smaller than subcatchment 0098 (see Table 2.1), so less discharge (in terms of total volume) is expected. Figure 5.10(b) shows an almost unique cumulative discharge pattern of subcatchment 0098 and 0099, so based on this figure, it can be concluded that station 0099 overestimates the discharge in 2012–2013. This results in an overestimation of discharge by WALRUS for that year (1806 mm in total). In the end of December, the bankfull discharge is even reached, which means that surface water levels are as high as the land surface, causing inundation (in the modeled situation).

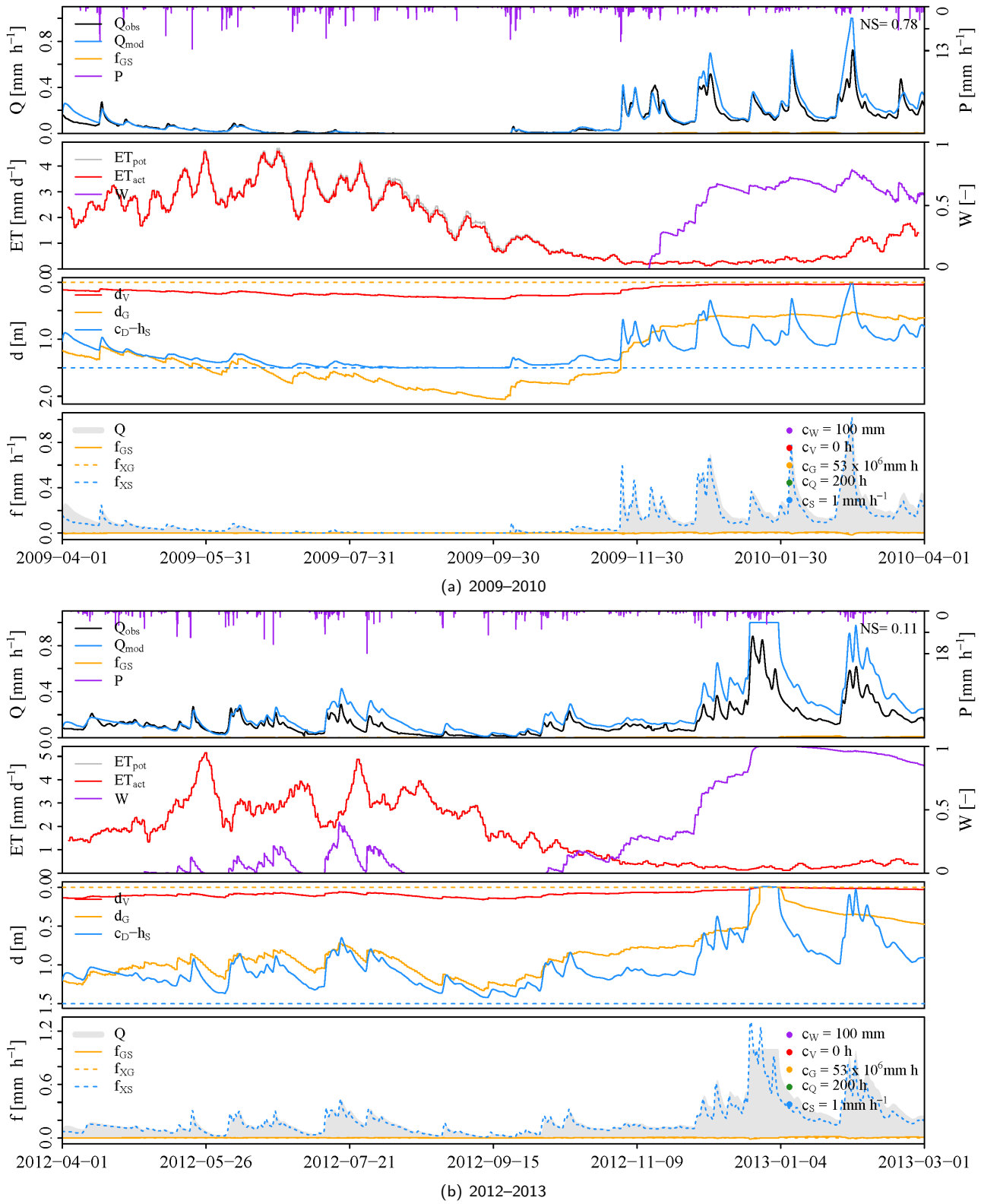


Figure 5.7: Validation of the selected parameter set for the coupling of the observed discharges of subcatchments 0098 and 0099 to subcatchment 7289.

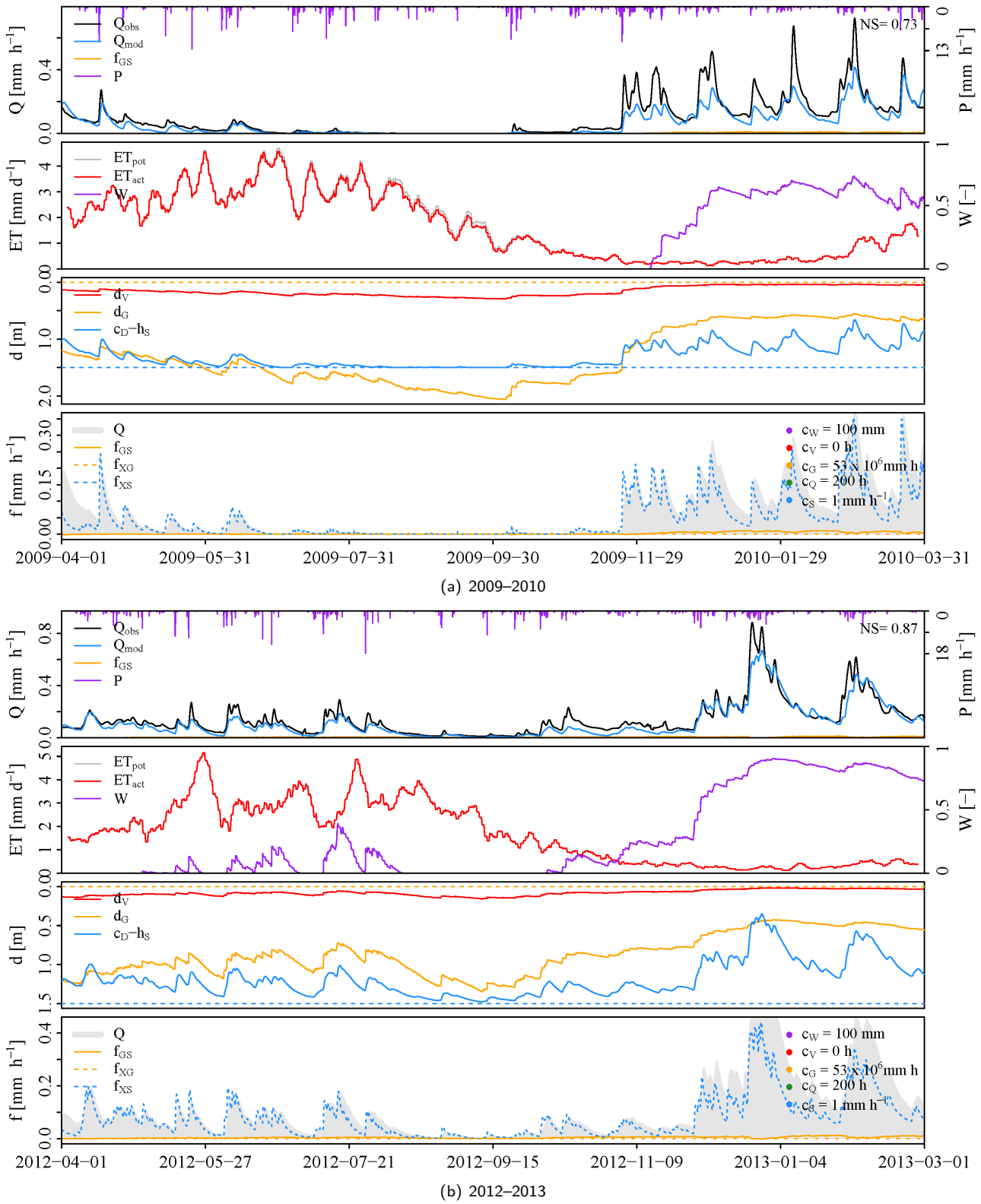


Figure 5.8: Validation of the selected parameter set for the coupling of the WALRUS output of subcatchments 0098 and 0099 to subcatchment 7289.

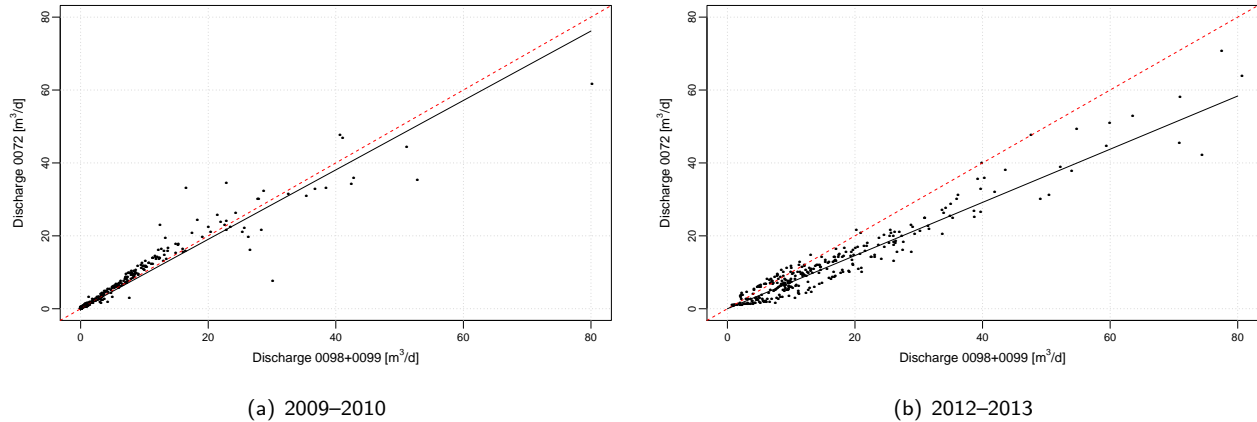


Figure 5.9: Plot of the daily observed discharge of subcatchment 0098 and 0099 against the observed daily discharge of subcatchment 0072.

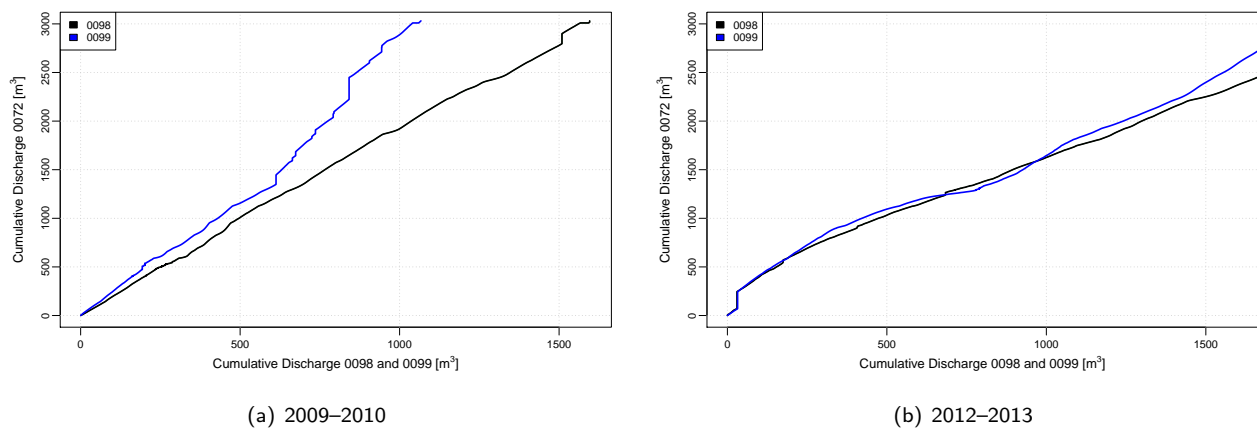


Figure 5.10: Plot of the cumulative discharge of subcatchment 0098 and 0099 plotted against the cumulative discharge of subcatchment 0072.

## 5.4 WALRUS versus Wageningen Model

The Wageningen Model is already used by the water board. Time series of simulated discharge were available for the entire catchment (measurements from station 0024) and subcatchment 0098. Table 5.6 gives an overview of the used parameters for the Wageningen Model. The parameter set of WALRUS is the same as found for the calibration without the WWTP (see Section 5.1).

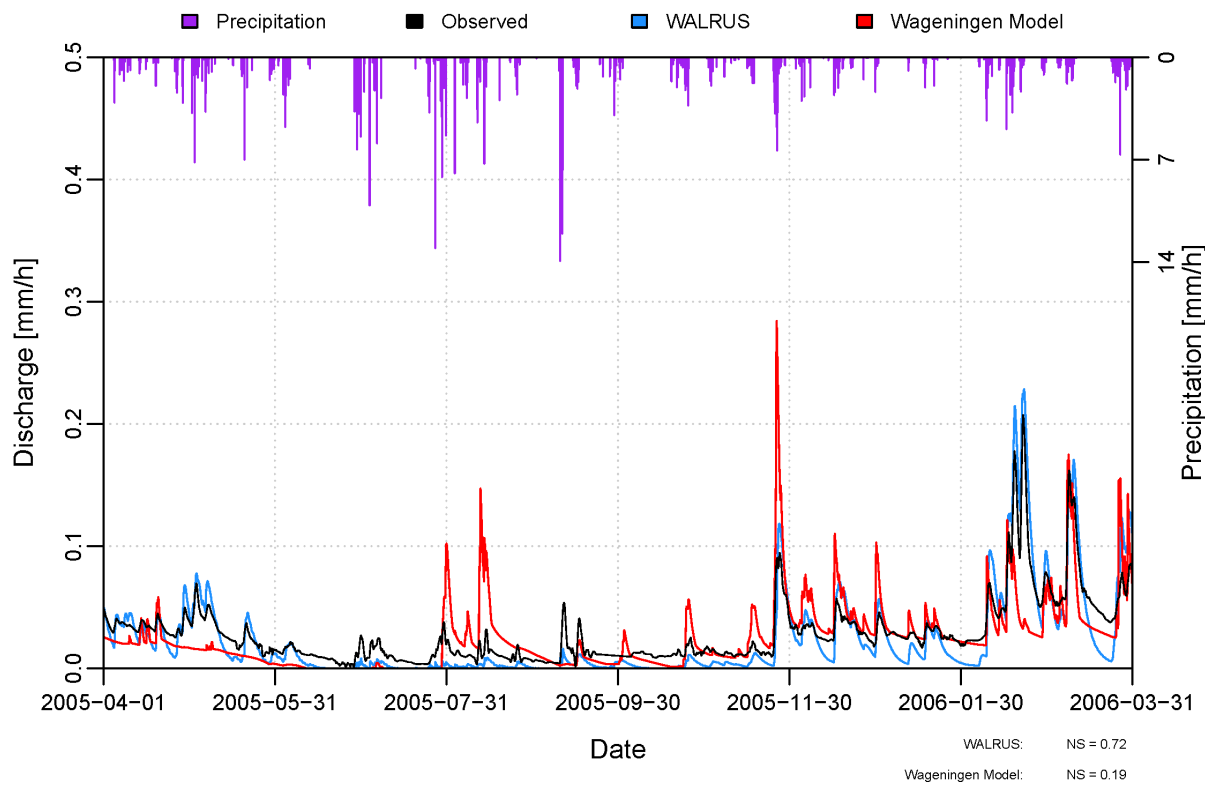
Table 5.6: Parameters of the Wageningen Model for catchments 0024 and 0098.

| Parameter | 0024 | 0098 |
|-----------|------|------|
| $J$       | 3464 | 3464 |
| $E$       | 2.05 | 2.05 |
| $F$       | 1.42 | 1.42 |
| $CR$      | 2.69 | 2.69 |
| $REPA$    | 0.09 | 0.12 |
| $FOS$     | 0.22 | 0.12 |

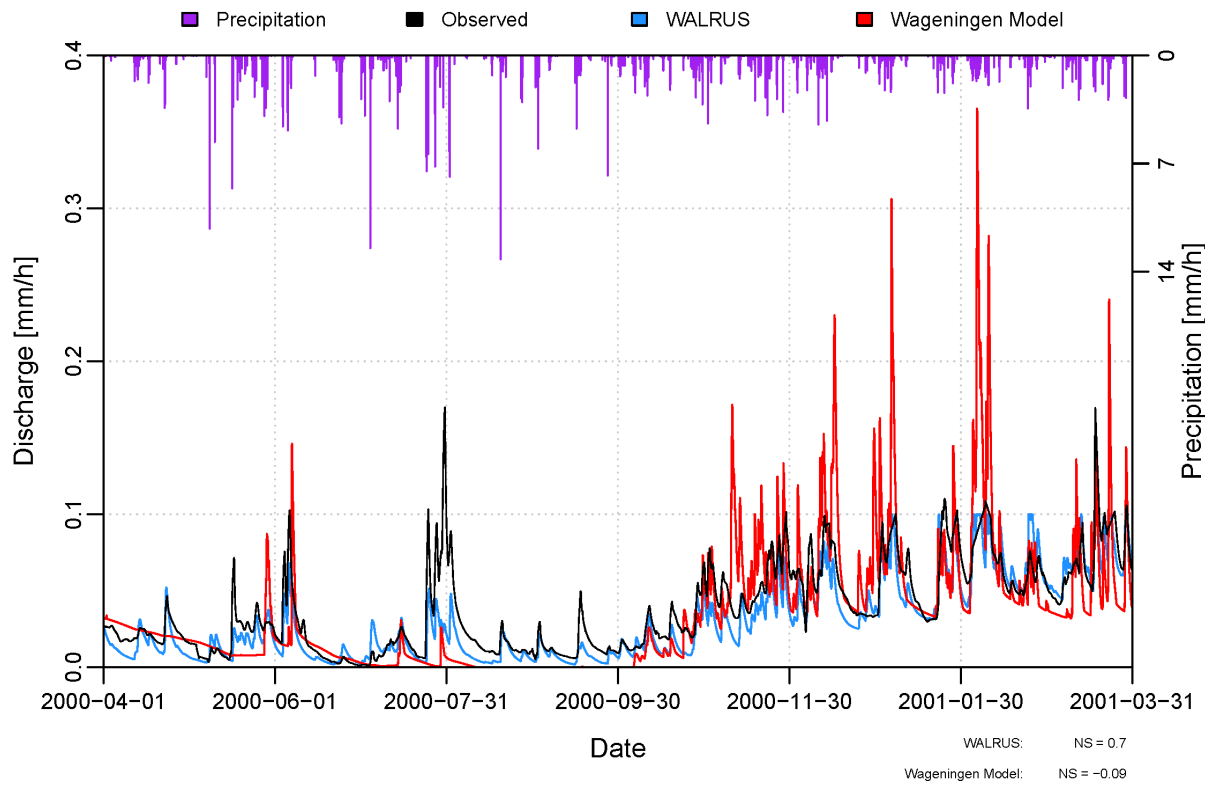
The results of WALRUS and the Wageningen Model are plotted together with the observed discharge. For the whole catchment, this is done for 11 hydrological years. Six hydrological years are used for subcatchment 0098. Figure 5.11 shows for each (sub)catchment the results of one hydrological year. All plots can be found in Appendix D.

The Wageningen Model overestimates the discharge peaks most of the times. These peaks are very sharp and after a strong decrease, the base flow is almost a straight line, instead of a curve visible in most other hydrographs. It must be stated that WALRUS shows a more natural recession curve, but most times this curve drops below the observed discharge. In summer periods, WALRUS is able to simulate the small discharge peaks, while the Wageningen Model is simulating zero discharge.

Nash-Sutcliffe efficiencies are determined to quantify the results. For catchment 0024, average Nash-Sutcliffe efficiencies of 0.70 for WALRUS and 0.53 for the Wageningen Model were found. For the selected hydrological years of subcatchment 0098, the average Nash-Sutcliffe efficiency was 0.44 for WALRUS and -0.67 for the Wageningen Model. The low Nash-Sutcliffe efficiencies for the Wageningen Model are mainly caused by the overestimation of discharge peaks. Two tables in Appendix D show all numbers and include also a simple water balance, based on precipitation, potential evapotranspiration and simulated discharge.



(a) One plot of the results of WALRUS and the Wageningen Model, plotted together with the observed discharge of the whole catchment 0024.



(b) One plot of the results of WALRUS and the Wageningen Model, plotted together with the observed discharge in subcatchment 0098.

Figure 5.11: Plots of the comparison of WALRUS and the Wageningen Model.



# 6 | Discussion

This chapter contains some discussion points, starting with the calibration results, the quality of data and finally about the comparison of WALRUS with the Wageningen Model.

## Calibration results

Two calibration methods are used during this research: HydroPSO and Levenberg-Marquardt. It was found that these two methods did not result in one unique parameter set for a specific calibration year. It is expected that calibration of one specific dataset should always lead to one unique parameter set. The Levenberg-Marquardt calibration always results in the same parameter set when calibrating with the same start values for the parameters. To check if the founded parameter set is the optimal one, nine different sets of initial parameter values (between the same boundary values) were calibrating on the same dataset (see Table 4.2). After doing the calibration, not every set ended up at the same parameter values, which means that by calibrating, some parameters end up in local minima of sum of residuals (at the boundary for instance). It often happened that for four out of five parameters, boundary values were presented as best parameter values (see Table 6.1). That is not likely to be the case, so one can ask the question how reliable the calibration results are. Sometimes, better calibration results (based on own interpretation of the simulated discharge) were found when calibrated parameters were adjusted by hand. This should not be possible, because the calibration method should do the work and find the optimal parameter set.

Table 6.1: An example of calibration results for subcatchment 0072 (using the Levenberg-Marquardt method) where four out of five parameters are boundary values ( $c_W=100\text{--}400 \text{ mm}$ ,  $c_V=0.1\text{--}100 \text{ h}$ ,  $c_G=0.1 \times 10^6\text{--}100 \times 10^6 \text{ mm h}$ ,  $c_Q=1\text{--}200 \text{ h}$ ,  $c_S=0.1\text{--}10 \text{ mm/h}$ ). For all simulations:  $aS=0.01$ ,  $st=\text{sand}$ ,  $c_D=1000$ ,  $d_{G0}=1200$ , no  $f_{XS}$  and  $f_{XG}$ .

| Year | Set | NS<br>[-] | Observations |                    |           | Simulations        |           | Parameters    |              |                   |              |                 |
|------|-----|-----------|--------------|--------------------|-----------|--------------------|-----------|---------------|--------------|-------------------|--------------|-----------------|
|      |     |           | P<br>[mm]    | $ET_{pot}$<br>[mm] | Q<br>[mm] | $ET_{act}$<br>[mm] | Q<br>[mm] | $c_W$<br>[mm] | $c_V$<br>[h] | $c_G$<br>[mm h]   | $c_Q$<br>[h] | $c_S$<br>[mm/h] |
| 2010 | 1   | 0.41      | 854          | 607                | 208       | 558                | 291       | 287           | 100.0        | $100 \times 10^6$ | 200.0        | 10.0            |
| 2010 | 2   | 0.41      | 854          | 607                | 208       | 558                | 291       | 286           | 100.0        | $100 \times 10^6$ | 200.0        | 10.0            |
| 2010 | 3   | 0.42      | 854          | 607                | 208       | 558                | 291       | 288           | 100.0        | $100 \times 10^6$ | 200.0        | 3.5             |
| 2010 | 4   | 0.42      | 854          | 607                | 208       | 558                | 291       | 288           | 100.0        | $100 \times 10^6$ | 200.0        | 3.5             |
| 2010 | 5   | 0.74      | 854          | 607                | 208       | 565                | 210       | 400           | 0.1          | $5 \times 10^6$   | 58.7         | 0.1             |
| 2010 | 6   | 0.42      | 854          | 607                | 208       | 558                | 291       | 288           | 100.0        | $100 \times 10^6$ | 200.0        | 3.5             |
| 2010 | 7   | 0.42      | 854          | 607                | 208       | 558                | 291       | 288           | 100.0        | $100 \times 10^6$ | 200.0        | 3.5             |
| 2010 | 8   | 0.43      | 854          | 607                | 208       | 555                | 304       | 400           | 100.0        | $0.6 \times 10^6$ | 200.0        | 10.0            |
| 2010 | 9   | 0.60      | 854          | 607                | 208       | 567                | 235       | 400           | 0.1          | $2 \times 10^6$   | 200.0        | 0.2             |
| 2011 | 1   | -0.55     | 815          | 583                | 156       | 565                | 193       | 100           | 100.0        | $100 \times 10^6$ | 200.0        | 5.9             |
| 2011 | 2   | 0.08      | 815          | 583                | 156       | 563                | 253       | 400           | 100.0        | $0.4 \times 10^6$ | 200.0        | 10.0            |
| 2011 | 3   | 0.26      | 815          | 583                | 156       | 566                | 225       | 277           | 100.0        | $100 \times 10^6$ | 200.0        | 0.1             |
| 2011 | 4   | 0.62      | 815          | 583                | 156       | 566                | 172       | 231           | 100.0        | $100 \times 10^6$ | 8.9          | 0.1             |
| 2011 | 5   | 0.84      | 815          | 583                | 156       | 565                | 174       | 400           | 100.0        | $5 \times 10^6$   | 80.8         | 0.1             |
| 2011 | 6   | 0.26      | 815          | 583                | 156       | 566                | 225       | 277           | 100.0        | $100 \times 10^6$ | 200.0        | 0.1             |
| 2011 | 7   | 0.26      | 815          | 583                | 156       | 565                | 228       | 284           | 100.0        | $100 \times 10^6$ | 200.0        | 0.1             |
| 2011 | 8   | 0.84      | 815          | 583                | 156       | 565                | 174       | 400           | 100.0        | $5 \times 10^6$   | 80.2         | 0.1             |
| 2011 | 9   | 0.76      | 815          | 583                | 156       | 566                | 185       | 400           | 0.1          | $5 \times 10^6$   | 60.1         | 0.1             |

Parameters can change due to changes in climate or land use (Merz et al., 2011), or to errors in the model. Therefor, parameter sets should always be up to date and not based on a time series from a few decades ago or a previous version of the model. Difference in parameter sets can also be caused by the chosen hydrological year. It was found that WALRUS performs better when precipitation input is high (wet years). There is a positive correlation

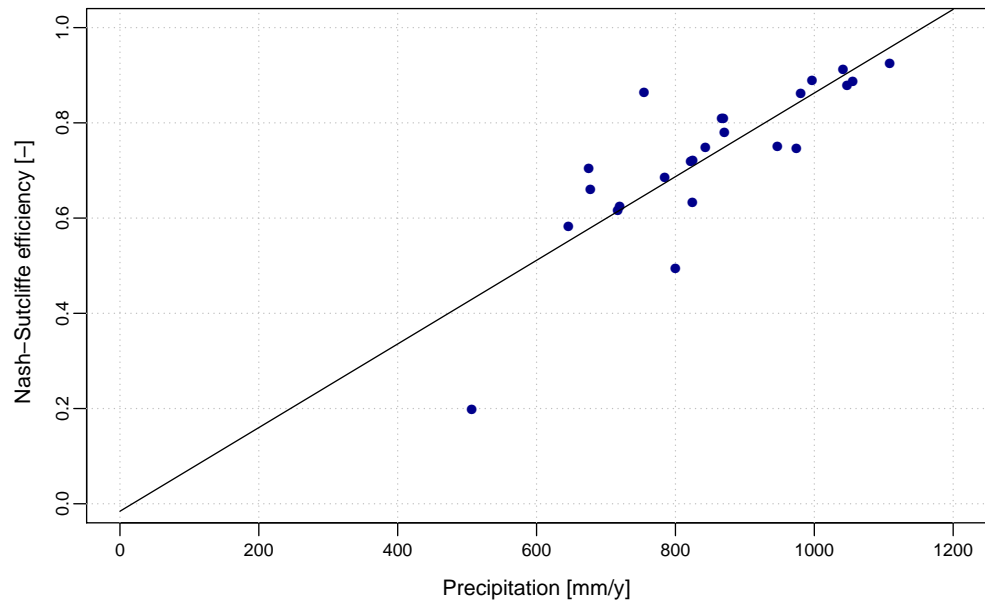


Figure 6.1: Correlation between annual amount of precipitation and Nash-Sutcliffe efficiencies found for the validation of catchment 0024.

between the amount of precipitation and the Nash-Sutcliffe efficiency of the simulation of that year (see Figure 6.1). Therefor, parameter sets can also be related to the hydrological conditions (season-dependent) instead of one parameter set which covers all hydrological conditions (wet and dry years).

## Quality of data

It is observed that there is a structural overestimation of the discharge measurements of subcatchment 0099 (see Figure 5.10). Therefor, the routing and coupling of subcatchments could not be further investigated, since errors will increase. This may explain why higher Nash-Sutcliffe efficiencies were found for the entire catchment (with more accurate observations) than for smaller subcatchments. Also precipitation time series could differ from the reality, since several point measurements are used to calculate the catchment average precipitation intensities. Including information on actual evapotranspiration and seepage can also improve the modeling results. Besides a good model structure which covers all relevant hydrological processes, good observations are important. More attention should be paid on the errors in measurements (Beven and Westerberg, 2011).

## Comparison WALRUS with Wageningen Model

Two conceptual models were compared in this study. Time series of simulated discharge were provided by the water board, as well as some information on selected parameters. However, it is not entirely clear which precipitation and evapotranspiration time series were used. These could be slightly different from the time series used as input for WALRUS. Also parameter uncertainties and other assumptions (e.g. initial groundwater level and surface water level, soil type, use of specific stage-discharge relation) can cause different results for instance. It could be interesting to do another intercomparison study with other lumped (as in Kloosterman (2012)) or distributed models (as in Reed et al. (2004)).

# 7 | Conclusions & recommendations

Conclusions of this thesis are drawn with use of the research questions mentioned in Section 1.5. Afterwards, some recommendations for further research are given.

## Conclusions

### How does WALRUS simulate discharges in a larger catchment without modifications?

In previous studies, WALRUS has only been tested on a relatively small catchments (Brauer et al., 2014a). It runs with only four calibrated parameters and those parameters are representing the local catchment characteristics. On forehand, it was supposed that WALRUS was not able to simulate correct discharges in larger catchments, since the local catchment characteristics were averaged out, resulting in a parameter set which is not good enough to simulate discharges. Calibrating discharge data of the entire catchment, resulted in a surprisingly high Nash-Sutcliffe efficiency. After adding available time series of surface water supply by a waste water treatment plant (WWTP), discharge simulations were even more accurate. It can be concluded that it is very important to implement these kind of water sources into a rainfall-runoff model, since these sources do influence simulation results. The results from the simulation of the entire catchment are on average better than those of the studied subcatchments. There is positive correlation between the Nash-Sutcliffe efficiency and the amount of precipitation of the simulation period. WALRUS performs better under wetter conditions. Another conclusion is that WALRUS can simulate the first peak discharge after a longer period of low discharge very well (end-of-summer peak).

### What are the effects on discharge simulations when using WALRUS in combination with a flow routing technique?

The trajectory between the outlet of two subcatchments and the outlet of the adjacent subcatchment downstream of these two subcatchments was used as a test case for this research question. The total routed discharge consisted of three components: two routed discharge time series of each of the two subcatchments (by using a nonlinear reservoir model and a storage-discharge relation based on computed backwater curves belonging to stationary flows) and a time series of discharge in the downstream subcatchment (simulated by WALRUS). In the end, the total routed discharge was compared to the observations and WALRUS simulation of the discharge of the downstream subcatchment (which includes all three subcatchments). This was done for two hydrological years. The total routed discharge was overestimated during peak discharges, but the timing and shape of the peaks were better, compared to the WALRUS simulation. In terms of Nash-Sutcliffe efficiency, the two years show opposite results, probably caused by errors in the observations.

### In which ways can subcatchments be coupled in WALRUS?

It is investigated if it is possible to couple subcatchments to each other by implementing the observed discharge of certain subcatchment to another subcatchment downstream. In this case, two subcatchments were coupled to an adjacent subcatchment downstream. A new time series, consisting of the sum of discharges of the two subcatchments is implemented as a surface water supply flux ( $f_{xs}$ ) in the WALRUS of the downstream subcatchment. For the hydrological year 2009–2010, this resulted in a NS of 0.78, compared to a NS of 0.72 for the output of WALRUS of the original subcatchment (which included the discharge and area of all three subcatchments upstream of the outlet).

For the hydrological year 2012–2013, the results were again contradictory, since a NS of 0.11 was found (compared to a NS of 0.60 for the WALRUS simulation of the original subcatchment).

### **What are the differences in output comparing WALRUS to previous used models?**

WALRUS was compared to the output of the Wageningen Model, of which time series were available of the entire catchment and one subcatchment. WALRUS is better able to simulate the right shape of the recession curve (compared to the observations), but sometimes with a structural difference (too little or to much discharge). This can be due to missing information on seepage or the waste water treatment plant. Average Nash-Sutcliffe values of 0.70 (WALRUS) and 0.53 (Wageningen Model) were found for the entire catchment and for the subcatchment, average Nash-Sutcliffe values were 0.44 for WALRUS and –0.67 for the Wageningen Model. Based on the Nash-Sutcliffe efficiencies, the conclusion can be made that WALRUS performs better.

Overall, it is clear that WALRUS can simulate discharge in such large catchments, given that accurate observations are available. If that is not the case, it is better to have a good calibration method ensuring good simulation of discharge peaks rather than having a reliable routing method for instance.

## **Recommendations**

During this thesis, it became clear that (when comparing the discharge of several stations) some discharge measurements were not as accurate as they seemed. Normally, it is not logical that the sum of two discharge stations is structurally higher than one discharge station around 8 km downstream. Good management of weirs and measurement equipment is important, because without accurate observations, models can not correctly be calibrated. The testing of a routing technique stopped after applying a nonlinear reservoir method. Further research can be done on applying other techniques (like for instance the Muskingum method) or implementing WALRUS in other hydraulic models.

Another very important recommendation is the calibration technique. HydroPSO and Levenberg-Marquardt did result in a unique set of parameters. During calibration, parameters got stuck in local minima of the sum of residuals or against the boundaries given for each parameter. More research is needed in order to avoid this problem. The sensitivity of parameters should also be investigated. Then, better parameter sets can be found, which can result in better discharge simulations.

# Bibliography

- Arnold, J. G., Srinivasan, R., Muttiah, R. S., Williams, J. R., 1998. Large area hydrologic modeling and assessment part I: Model development. *JAWRA Journal of the American Water Resources Association* 34, 73–89.
- Bergström, S., 1991. Principles and confidence in hydrological modelling. *Nordic Hydrology* 22, 123–136.
- Bergström, S., Forsman, A., 1973. Development of a conceptual deterministic rainfall-runoff model. *Meddelanden / Sveriges meteorologiska och hydrologiska institut: Serie D. Centraltryckeriet*.
- Beven, K., Westerberg, I., 2011. On red herrings and real herrings: disinformation and information in hydrological inference. *Hydrological Processes* 25, 1676–1680.
- Beven, K. J., 2011. Rainfall-runoff modelling: The primer, 2nd Edition. John Wiley & Sons, LTD, Chichester, UK.
- Beven, K. J., Kirkby, M. J., 1979. A physically based, variable contributing area model of basin hydrology. *Hydrological Sciences Bulletin* 24, 43–69.
- Brauer, C. C., Teuling, A. J., Torfs, P. J. J. F., Uijlenhoet, R., 2014a. The Wageningen Lowland Runoff Simulator (WALRUS): a lumped rainfall-runoff model for catchments with shallow groundwater. *Geoscientific Model Development Discussions* 7, 2313–2332.
- Brauer, C. C., Torfs, P. J. J. F., Teuling, A. J., Uijlenhoet, R., 2014b. The Wageningen Lowland Runoff Simulator (WALRUS): application to the Hupsel Brook catchment and Cabauw polder. *Hydrology and Earth System Sciences Discussions* 18, 4007–4028.
- Burnash, R. J. C., Singh, V. P., et al., 1995. The NWS river forecast system-catchment modeling. *Computer models of watershed hydrology*, 311–366.
- Deltires, last visited on: 11 September 2014 2013. Deltires: SOBEK, 1D/2D modelling suite for integral water solutions. Tech. rep., Deltires.  
URL [www.deltaressystems.com/hydro/product/108282/sobek-suite](http://www.deltaressystems.com/hydro/product/108282/sobek-suite)
- Dooge, J., Harley, B., 6–8 September 1967. Linear routing in uniform open channels. *Int. Hydrol. Symp.* 8, 57–63.
- Gill, M. A., 1978. Flood routing by the Muskingum method. *Journal of Hydrology* 36, 353–363.
- Kim, N. W., Lee, J., 2010. Enhancement of the channel routing module in SWAT. *Hydrological Processes* 24, 96–107.
- Kirchner, J. W., 2006. Getting the right answers for the right reasons: Linking measurements, analyses, and models to advance the science of hydrology. *Water Resources Research* 42.
- Kloosterman, P., 2012. A comparison of the performance of lumped hydrological models in modelling a flash flood in the hupsel brook catchment. Master's thesis, Wageningen University.
- KNMI, last visited on: 6 Oktober 2014. Klimatologie.  
URL <http://www.knmi.nl/klimatologie/>
- Kraijenhoff van de Leur, D., 1958. A study of non-steady ground-water flow with special reference to the reservoir-coefficient. *De Ingenieur* 19, 87–94.

- Lamb, R., Beven, K., Myrabo, S., 1998. Use of spatially distributed water table observations to constrain uncertainty in a rainfall-runoff model. *Advances in Water Resources* 22, 305–317.
- Makkink, G., 1957. Testing the penman formula by means of lysimeters. *J. Inst. Water Eng* 11, 277–288.
- Merz, R., Parajka, J., Bloschl, G., 2011. Time stability of catchment model parameters: Implications for climate impact analyses. *Water Resources Research* 47.
- Moré, J., 1977. Levenberg–Marquardt algorithm: implementation and theory.
- Nash, J., Sutcliffe, J., 1970. River flow forecasting through conceptual models part I: A discussion of principles. *Journal of Hydrology* 10, 282–290.
- O'Sullivan, J. J., Ahilan, S., Bruen, M., 2012. A modified Muskingum routing approach for floodplain flows: Theory and practice. *Journal of Hydrology* 470–471, 239–254.
- Perrin, C., Michel, C., Andréassian, V., 2001. Does a large number of parameters enhance model performance? Comparative assessment of common catchment model structures on 429 catchments. *Journal of Hydrology* 242, 275–301.
- Reed, S., Koren, V., Smith, M., Zhang, Z., Moreda, F., Seo, D.-J., 2004. Overall distributed model intercomparison project results. *Journal of Hydrology* 298, 27–60.
- Refsgaard, J. C., 1996. Terminology, modelling protocol and classification of hydrological model codes. *Distributed Hydrological Modelling* 22, 17–39.
- Refsgaard, J. C., 1997. Parameterisation, calibration and validation of distributed hydrological models. *Journal of Hydrology* 198, 69–97.
- Stricker, J. N. M., Warmerdam, P. M. M., 1982. Estimation of the water balance in the Hupselse Beek basin over a period of three years and a first effort to simulate the rainfall-runoff process for a complete year. In: Proceedings of the International symposium on hydrological research basins and their use in water resources planning. Bern, Switzerland. pp. 379–388.
- Ten Broek, J., 2014. Coupling WALRUS to SOBEK. Master's thesis, Hydrology and Quantitative Water Management Group, Wageningen University, internship report.
- USACE, August 1994. Flood-runoff analysis. Department of the Army, DC 20314-1000, em 1110-2-1417 Edition.
- Van Huissteden, J., Van Der Valk, L., Vandenberghe, J., 1986. Geomorphological evolution of a lowland valley system during the Weichselian. *Earth Surface Processes and Landforms* 11, 207–216.
- Van Walsum, P., Helming, J., Schouwenberg, E., Stuyt, L., Groenendijk, P., Bont, C. d., Vereijken, P., Kwakernaak, C., Bakel, P. v., Staalduin, L. v., Ypma, K., 2002. Waterwijs: plannen met water op regionale schaal. Vol. Alterra-rapport 433. Alterra, Research Instituut voor de Groene Ruimte.
- Wagener, T., Boyle, D. P., Lees, M. J., Wheater, H. S., Gupta, H. V., Sorooshian, S., 2001. A framework for development and application of hydrological models. *Hydrology and Earth System Sciences* 5, 13–26.
- Wagener, T., Wheater, H., Gupta, H., 2004. Rainfall-runoff Modelling in Gauged and Ungauged Catchments. Imperial College Press.

- Warmerdam, P. M. M., Kole, J., 2008. Practicum Stroomgebiedshydrologie. Wageningen Universiteit, Wageningen, instructie en oefeningen Neerslag Afvoer modellering.
- Waterschap De Dommel, last visited on: 14 February 2015. Biest-Houtakker.  
URL <http://www.dommel.nl/algemeen-glm/rioolwater/biest-houtakker.html>
- Zambrano-Bigiarini, M., Rojas, R., 2013. A model-independent particle swarm optimisation software for model calibration. Environmental Modelling & Software 43, 5–25.



# A | Calibration conditions

Table A.1: All different sets of calibrations that has been done in order to find the best parameter set for each (sub)catchment. Each set has different initial conditions of  $d_{G0}$ ,  $c_D$ ,  $f_{XG}$ ,  $f_{XS}$ ; the presence of a weir-specific stage-discharge relation during the calibration is also investigated.

|      | Dataset  | $d_{G0}$<br>[mm] | $c_D$<br>[mm] | $f_{XG}$<br>[mm/h] | $f_{XS}$<br>[mm/h] | Q-h<br>relation | Calibration technique          |
|------|----------|------------------|---------------|--------------------|--------------------|-----------------|--------------------------------|
| 0024 | original | 1200             | 1500          | 0.00               | 0.00               | no              | HydroPSO                       |
| 0024 | filtered | 1200             | 1500          | 0.00               | 0.00               | no              | HydroPSO                       |
| 0024 | filtered | 1200             | 1500          | 0.00               | RWZI <sup>1</sup>  | no              | HydroPSO & Levenberg-Marquardt |
| 0072 | filtered | 1200             | 1500          | 0.00               | 0.00               | no              | HydroPSO                       |
| 0072 | filtered | 1200             | 1500          | 0.00               | 0.00               | no              | Levenberg-Marquardt            |
| 0072 | filtered | 1200             | 1000          | 0.00               | 0.00               | no              | Levenberg-Marquardt            |
| 0072 | filtered | 1200             | 1500          | 0.00               | 0.00               | yes             | Levenberg-Marquardt            |
| 0072 | filtered | 450              | 1500          | 0.00               | 0.00               | yes             | Levenberg-Marquardt            |
| 0072 | filtered | -                | 1500          | 0.00               | 0.00               | yes             | Levenberg-Marquardt            |
| 0072 | filtered | 1200             | 1500          | 0.01               | 0.00               | no              | Levenberg-Marquardt            |
| 0072 | filtered | 1200             | 1000          | 0.01               | 0.00               | no              | Levenberg-Marquardt            |
| 0072 | filtered | 1200             | 1500          | 0.01               | 0.00               | yes             | Levenberg-Marquardt            |
| 0072 | filtered | 450              | 1500          | 0.01               | 0.00               | yes             | Levenberg-Marquardt            |
| 0072 | filtered | -                | 1500          | 0.01               | 0.00               | yes             | Levenberg-Marquardt            |
| 0098 | original | 1200             | 1500          | 0.00               | 0.00               | no              | HydroPSO                       |
| 0098 | filtered | 1200             | 1500          | 0.00               | 0.00               | no              | HydroPSO & Levenberg-Marquardt |
| 0098 | filtered | 1200             | 1500          | 0.01               | 0.00               | no              | HydroPSO & Levenberg-Marquardt |
| 0098 | filtered | 1200             | 1000          | 0.01               | 0.00               | no              | HydroPSO & Levenberg-Marquardt |
| 0098 | filtered | 1200             | 1500          | 0.01               | 0.00               | yes             | HydroPSO & Levenberg-Marquardt |
| 0099 | original | 1200             | 1500          | 0.00               | 0.00               | no              | HydroPSO                       |
| 0099 | filtered | 1200             | 1500          | 0.00               | 0.00               | no              | HydroPSO & Levenberg-Marquardt |
| 0099 | filtered | 1200             | 1500          | 0.01               | 0.00               | no              | HydroPSO & Levenberg-Marquardt |
| 0099 | filtered | 1200             | 1500          | 0.02               | 0.00               | no              | HydroPSO                       |
| 0099 | filtered | 1200             | 1000          | 0.01               | 0.00               | no              | HydroPSO & Levenberg-Marquardt |
| 0099 | filtered | 1500             | 1000          | 0.01               | 0.00               | no              | HydroPSO                       |
| 0099 | filtered | 1200             | 1500          | 0.01               | 0.00               | yes             | HydroPSO & Levenberg-Marquardt |
| 0099 | filtered | 800              | 1500          | 0.01               | 0.00               | yes             | HydroPSO & Levenberg-Marquardt |
| 0099 | filtered | -                | 1500          | 0.01               | 0.00               | yes             | HydroPSO & Levenberg-Marquardt |

<sup>1</sup>Time series of surface water supply by the waste water treatment plant (RWZI) are used instead of a fixed flux.



# B | Validation plots

## B.1 Validation catchment 0024

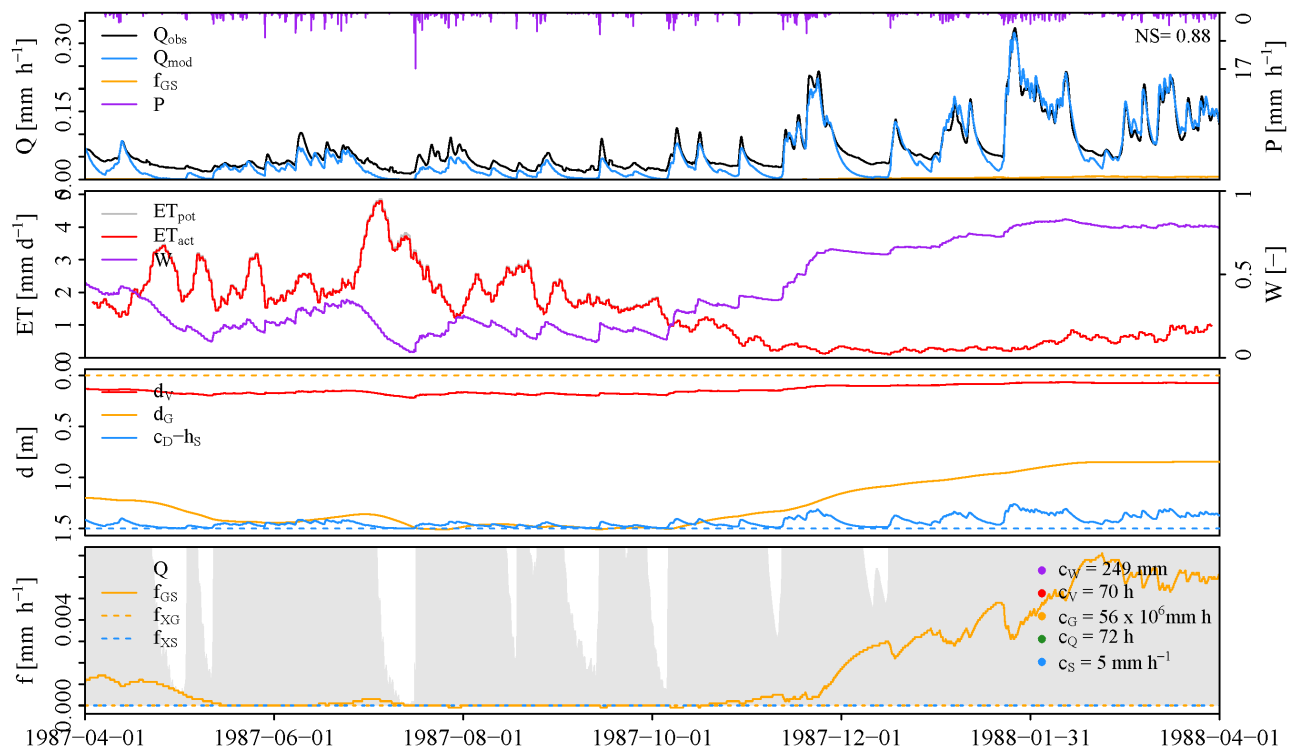


Figure B.1: Validation of the selected parameter set for catchment 0024 on the hydrological year 1987–1988.

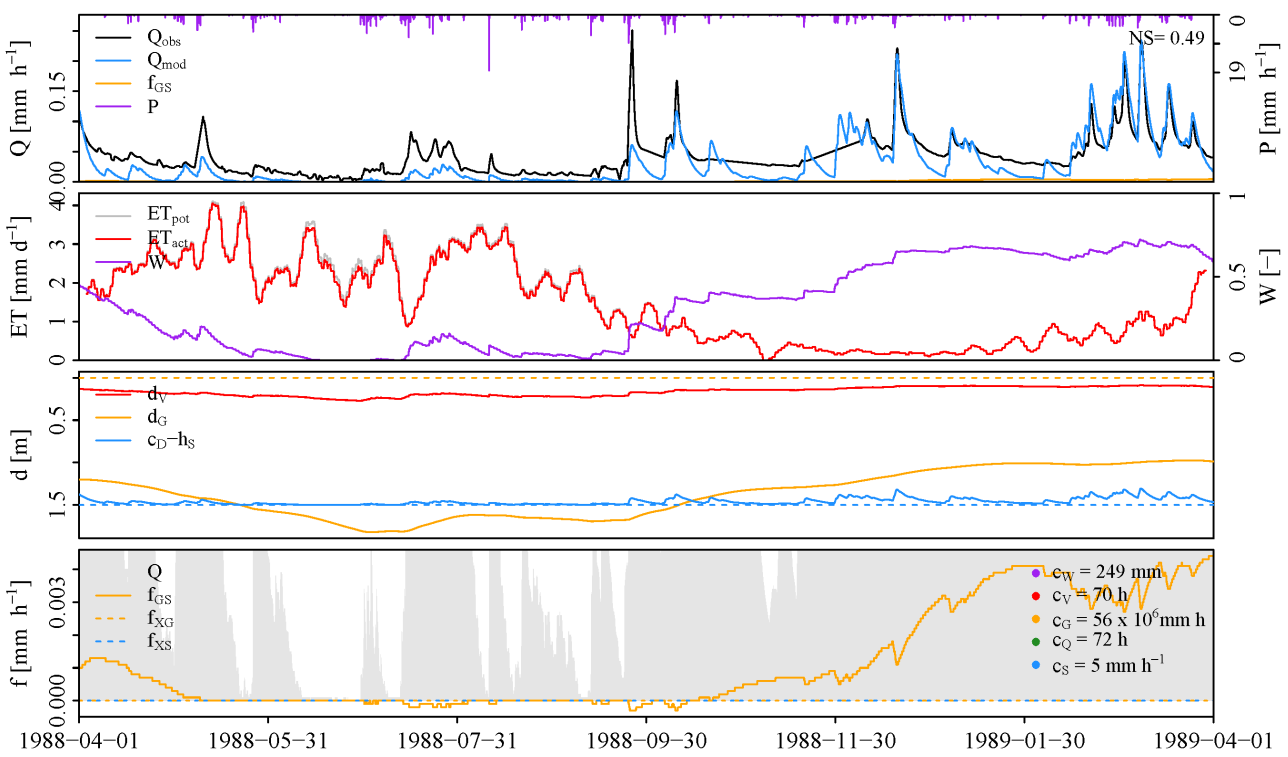


Figure B.2: Validation of the selected parameter set for catchment 0024 on the hydrological year 1988–1989.

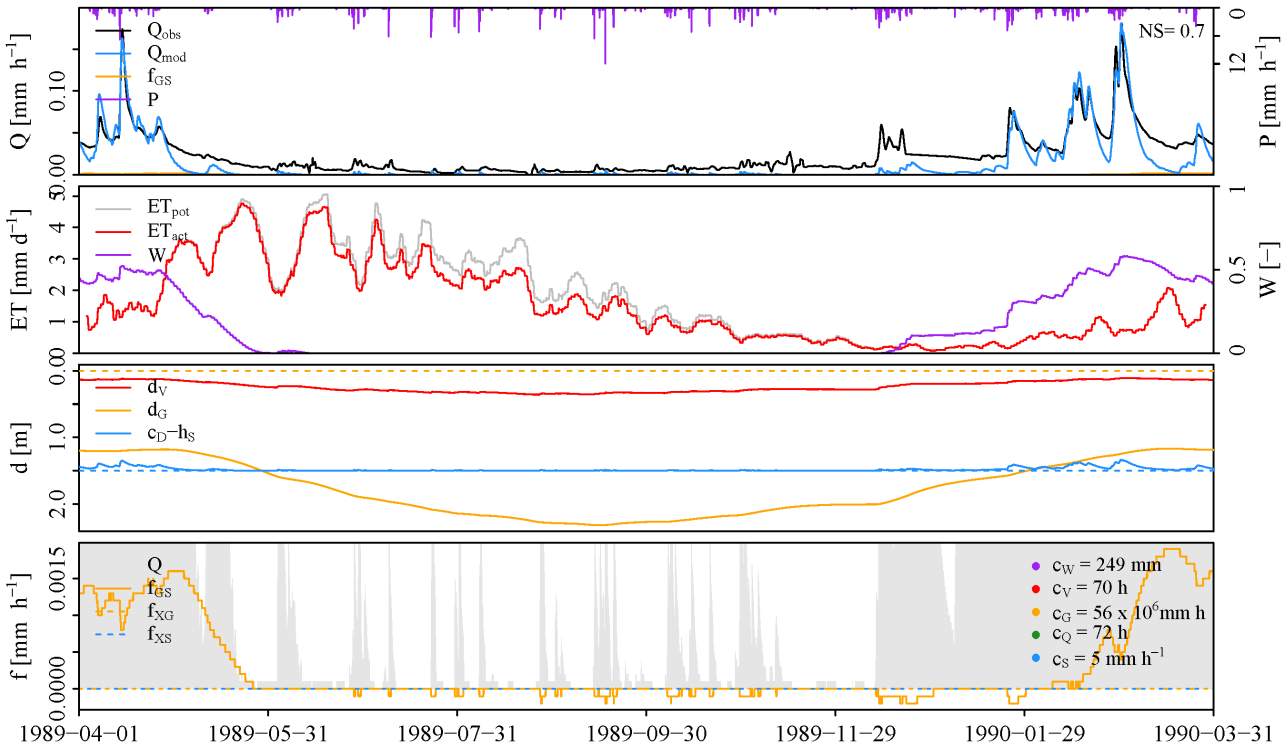


Figure B.3: Validation of the selected parameter set for catchment 0024 on the hydrological year 1989–1990.

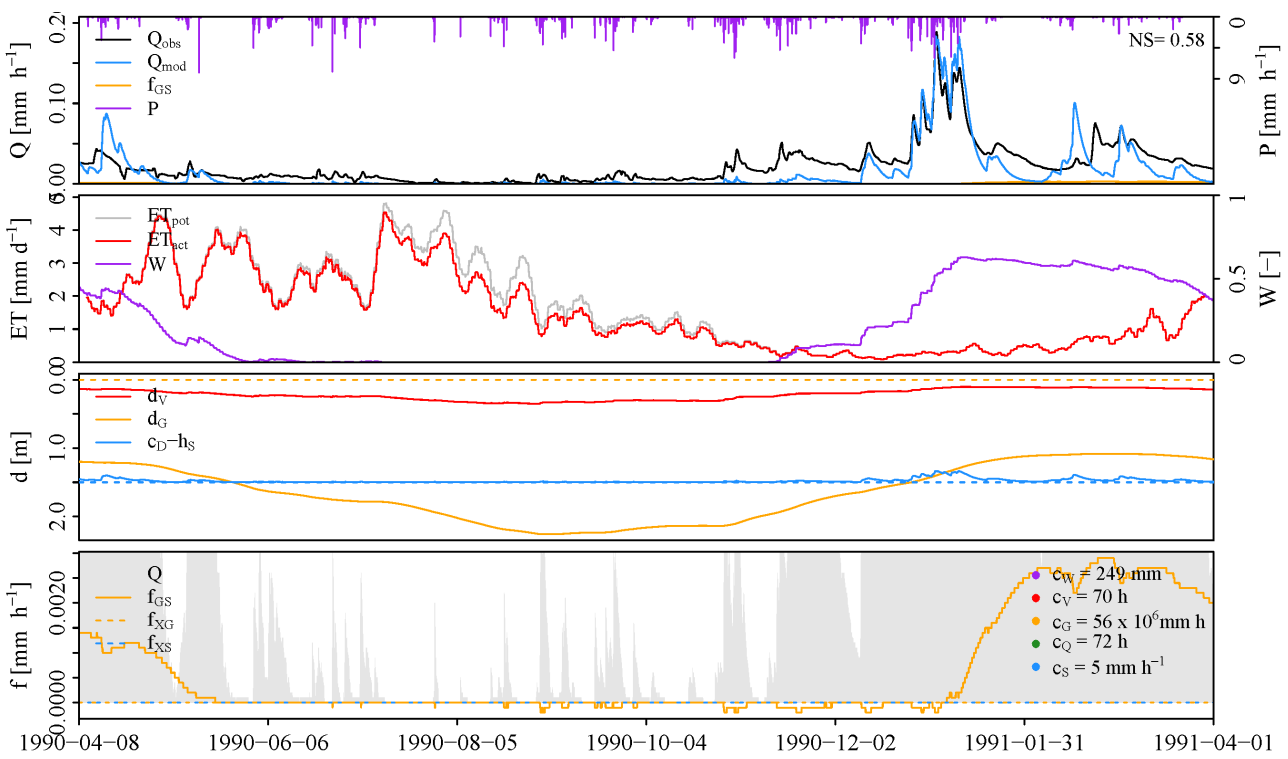


Figure B.4: Validation of the selected parameter set for catchment 0024 on the hydrological year 1990–1991.

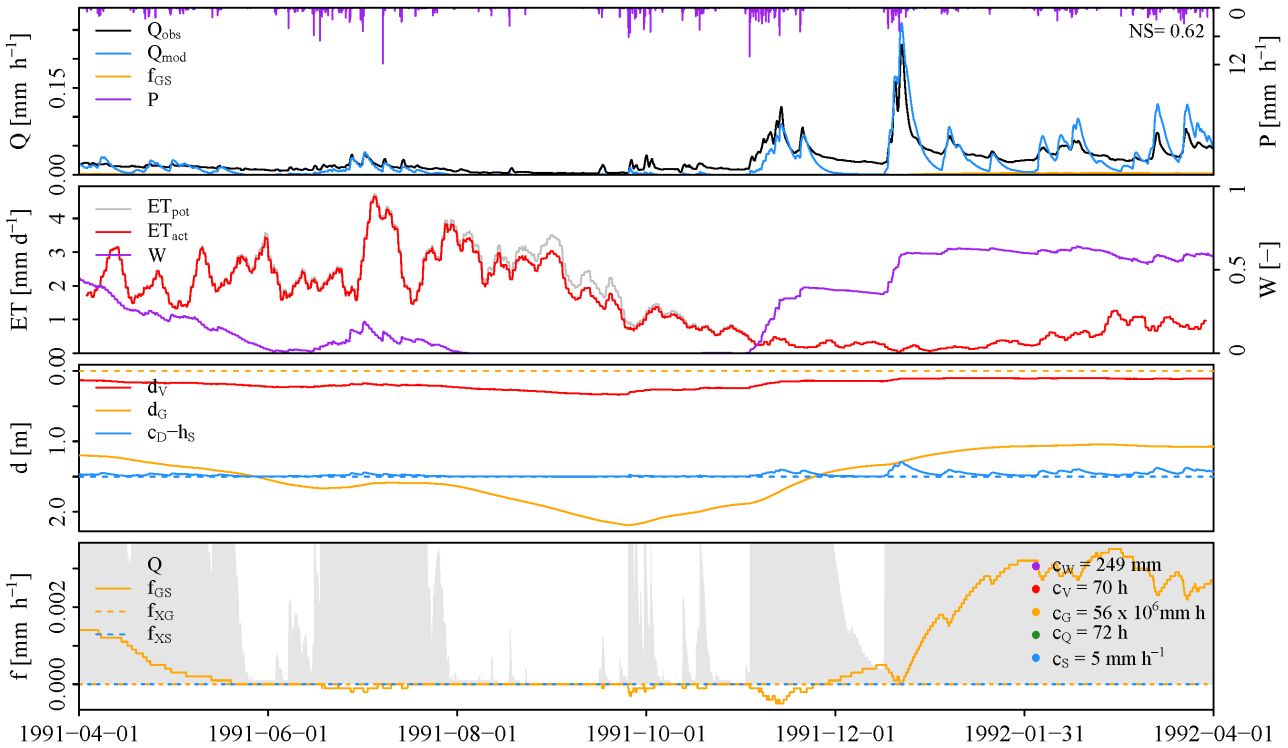


Figure B.5: Validation of the selected parameter set for catchment 0024 on the hydrological year 1991–1992.

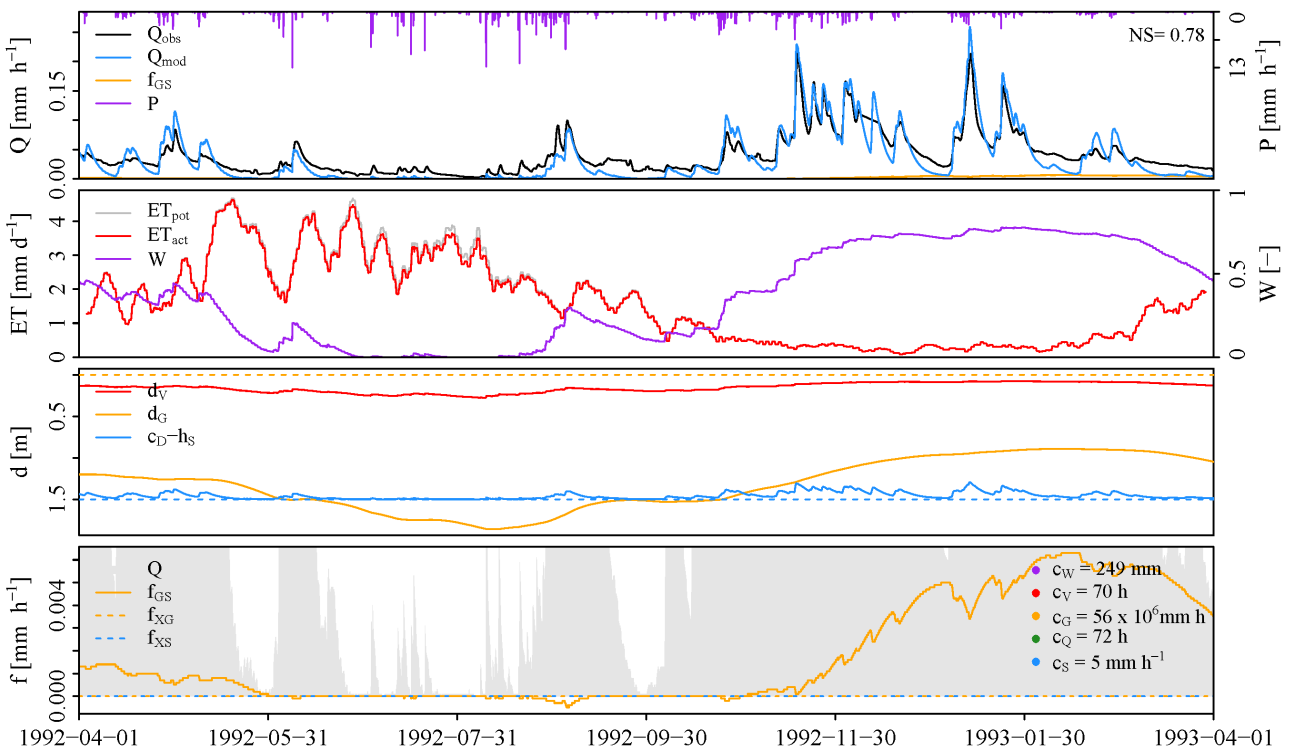


Figure B.6: Validation of the selected parameter set for catchment 0024 on the hydrological year 1992–1993.

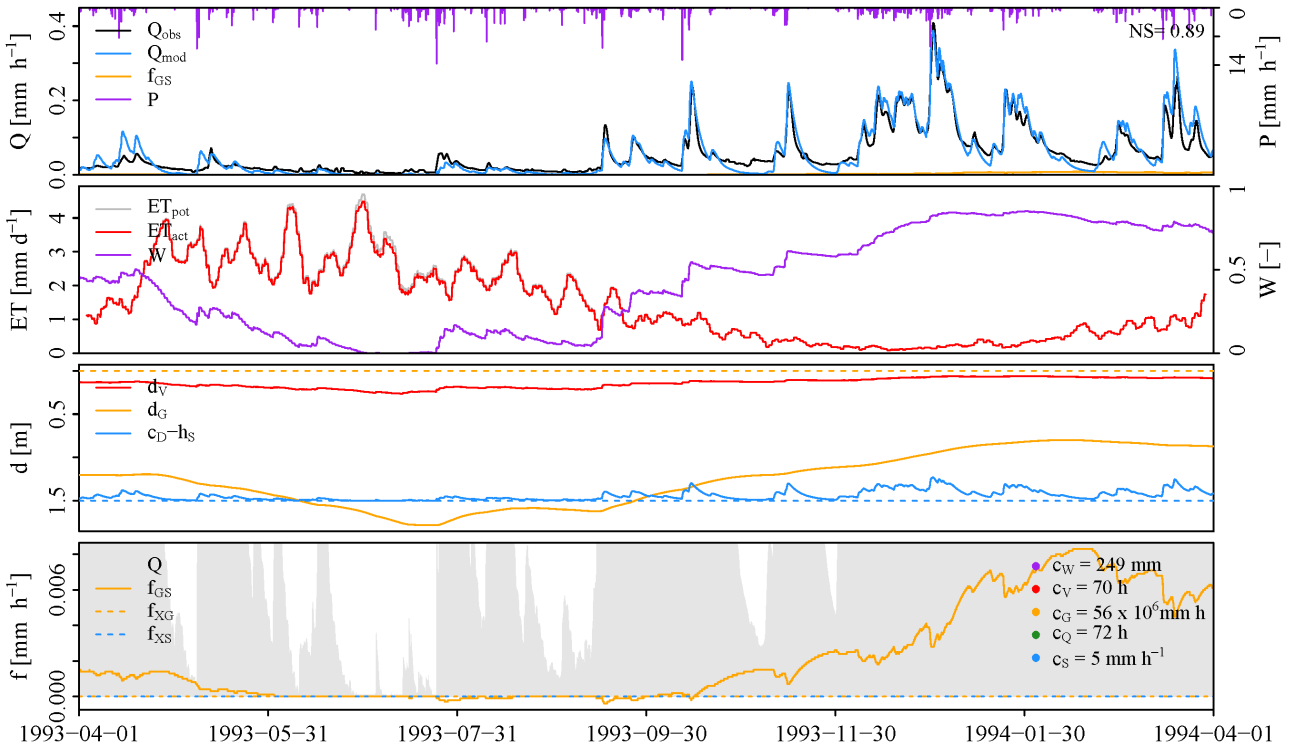


Figure B.7: Validation of the selected parameter set for catchment 0024 on the hydrological year 1993–1994.

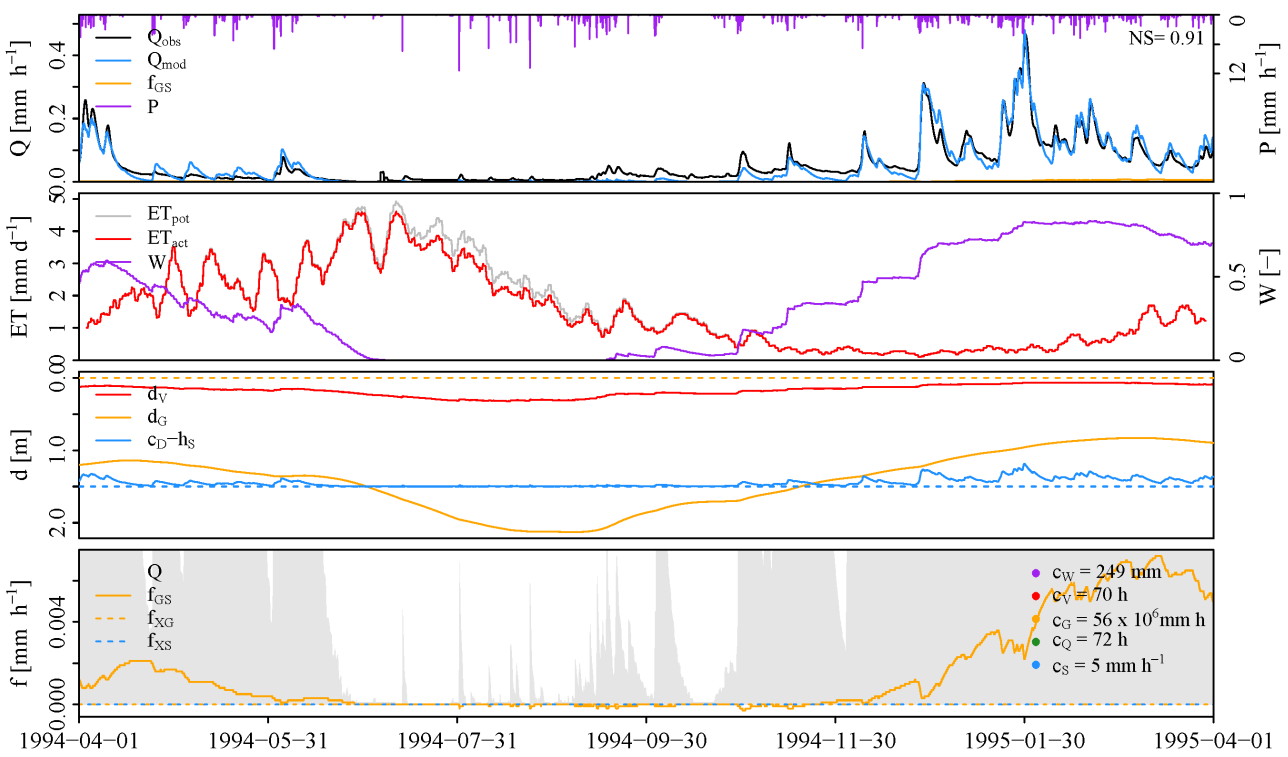


Figure B.8: Validation of the selected parameter set for catchment 0024 on the hydrological year 1994–1995.

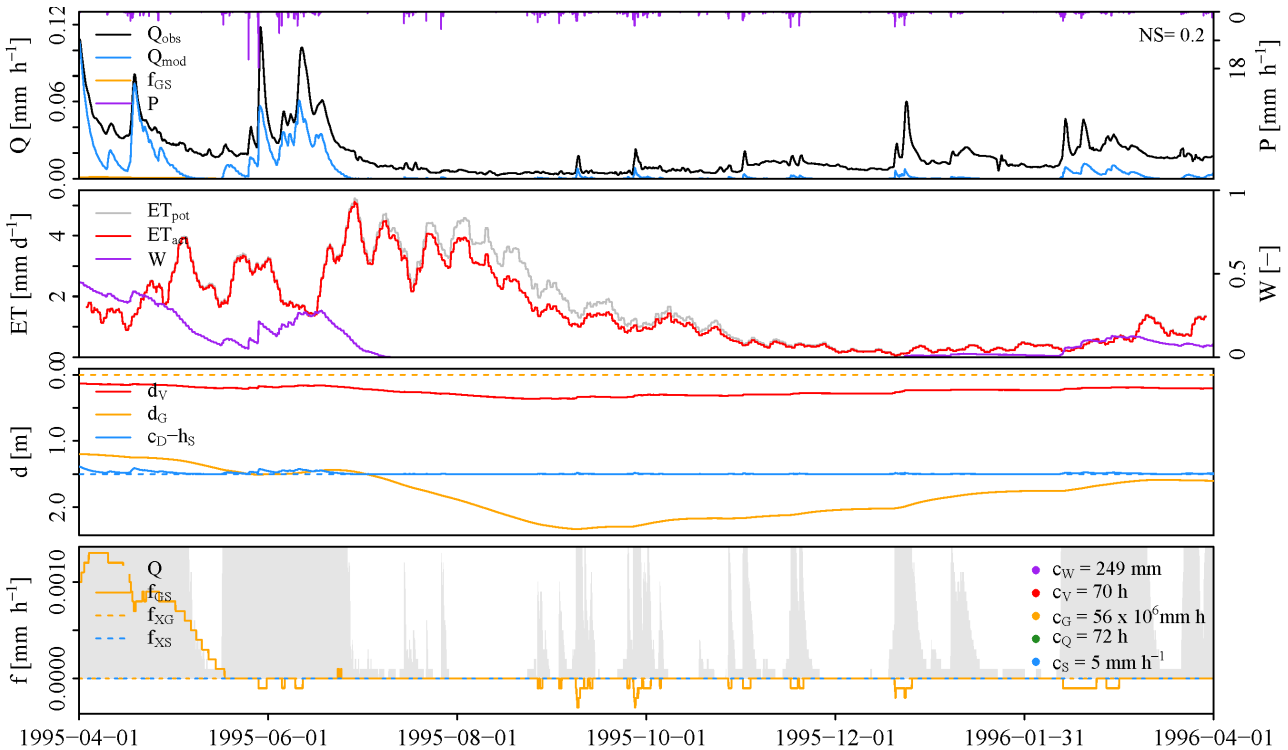


Figure B.9: Validation of the selected parameter set for catchment 0024 on the hydrological year 1995–1996.

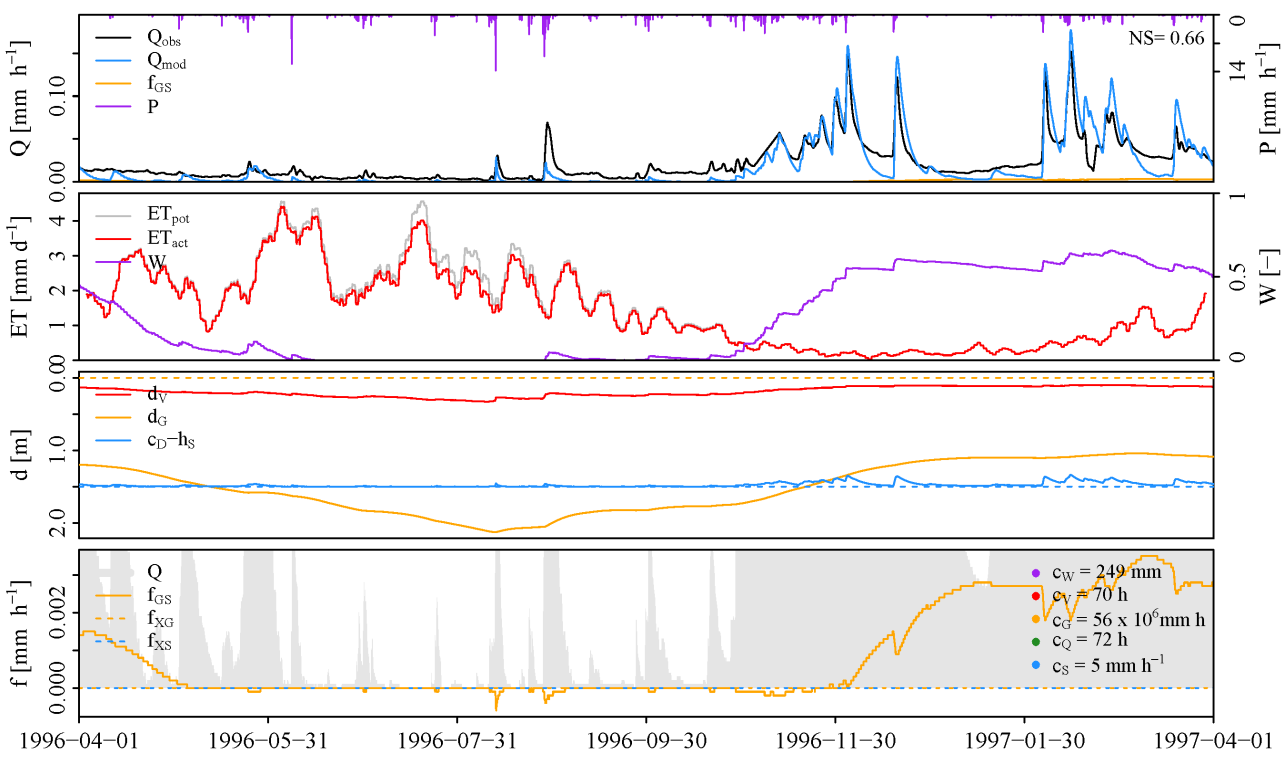


Figure B.10: Validation of the selected parameter set for catchment 0024 on the hydrological year 1996–1997.

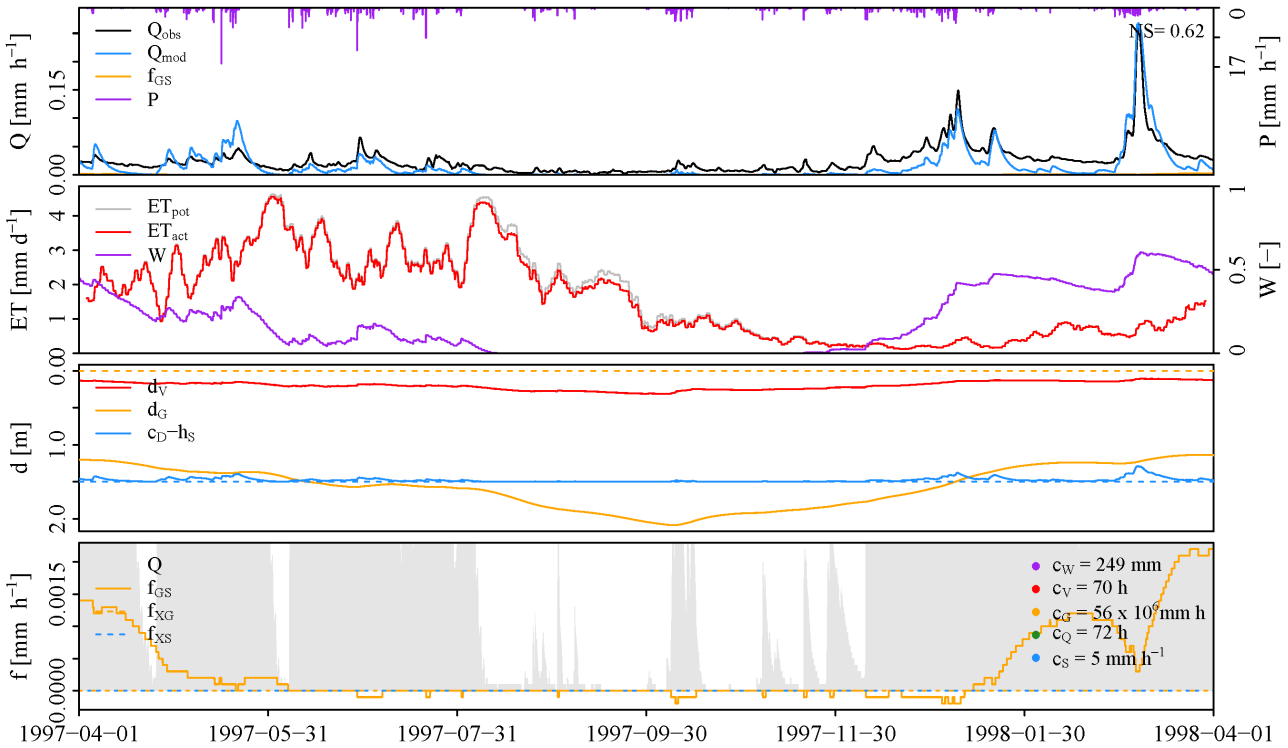


Figure B.11: Validation of the selected parameter set for catchment 0024 on the hydrological year 1997–1998.

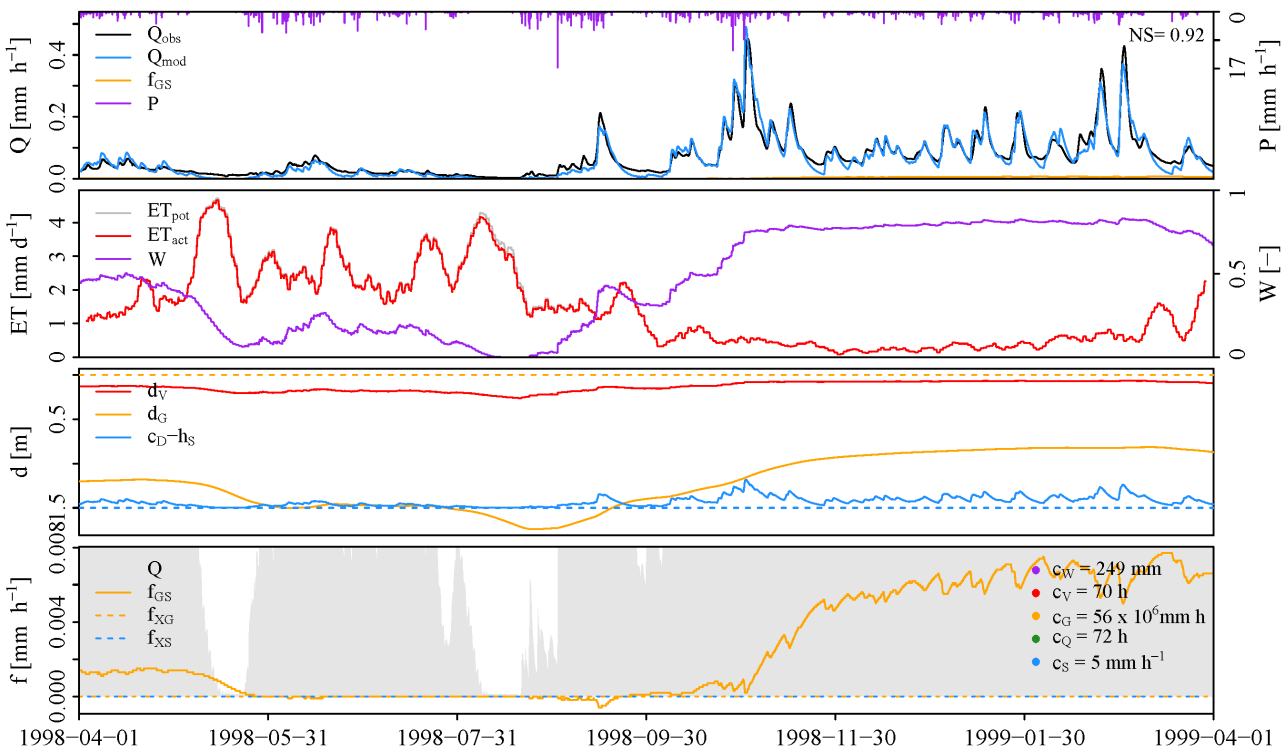


Figure B.12: Validation of the selected parameter set for catchment 0024 on the hydrological year 1998–1999.

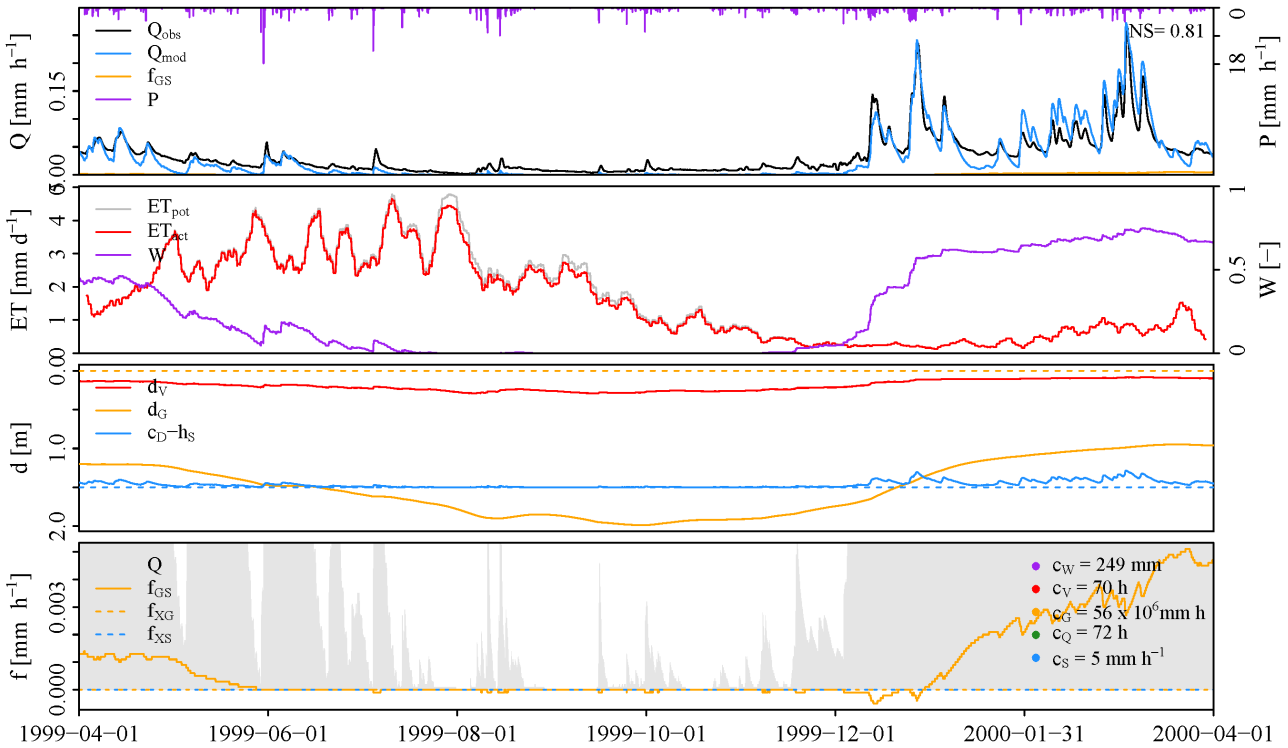


Figure B.13: Validation of the selected parameter set for catchment 0024 on the hydrological year 1999–2000.

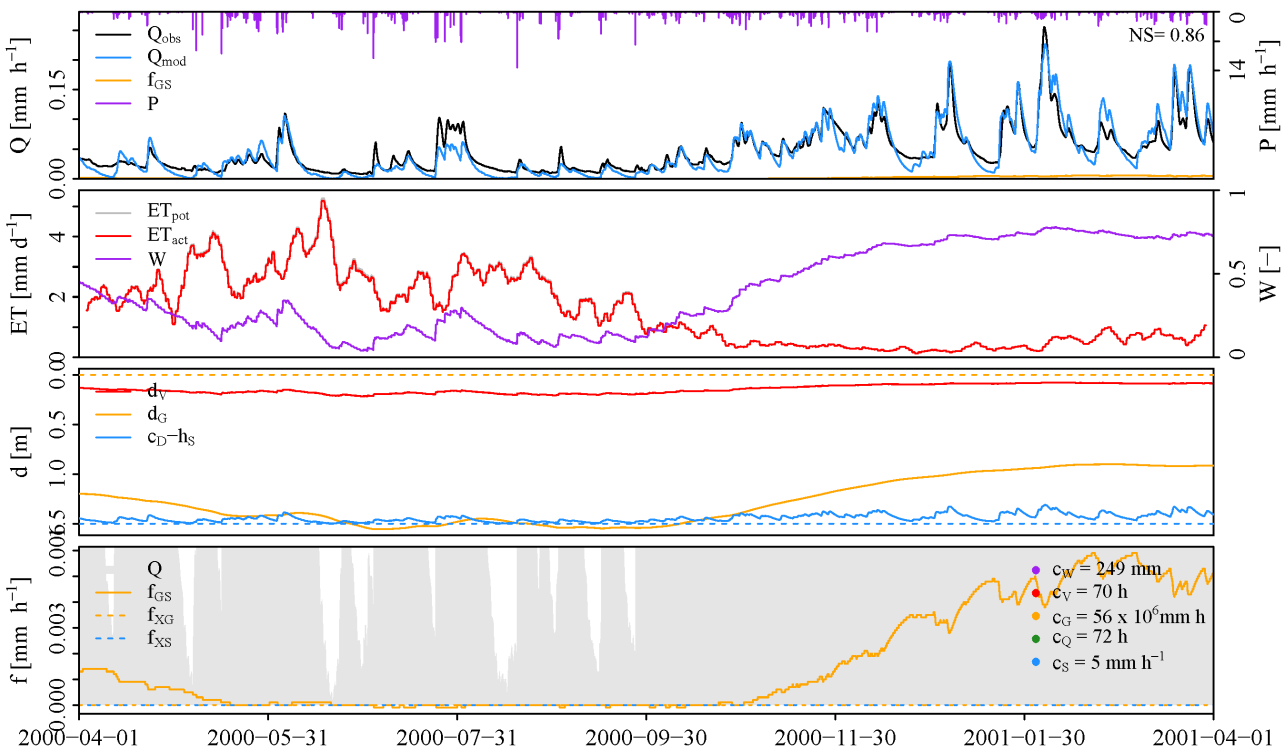


Figure B.14: Validation of the selected parameter set for catchment 0024 on the hydrological year 2000–2001.

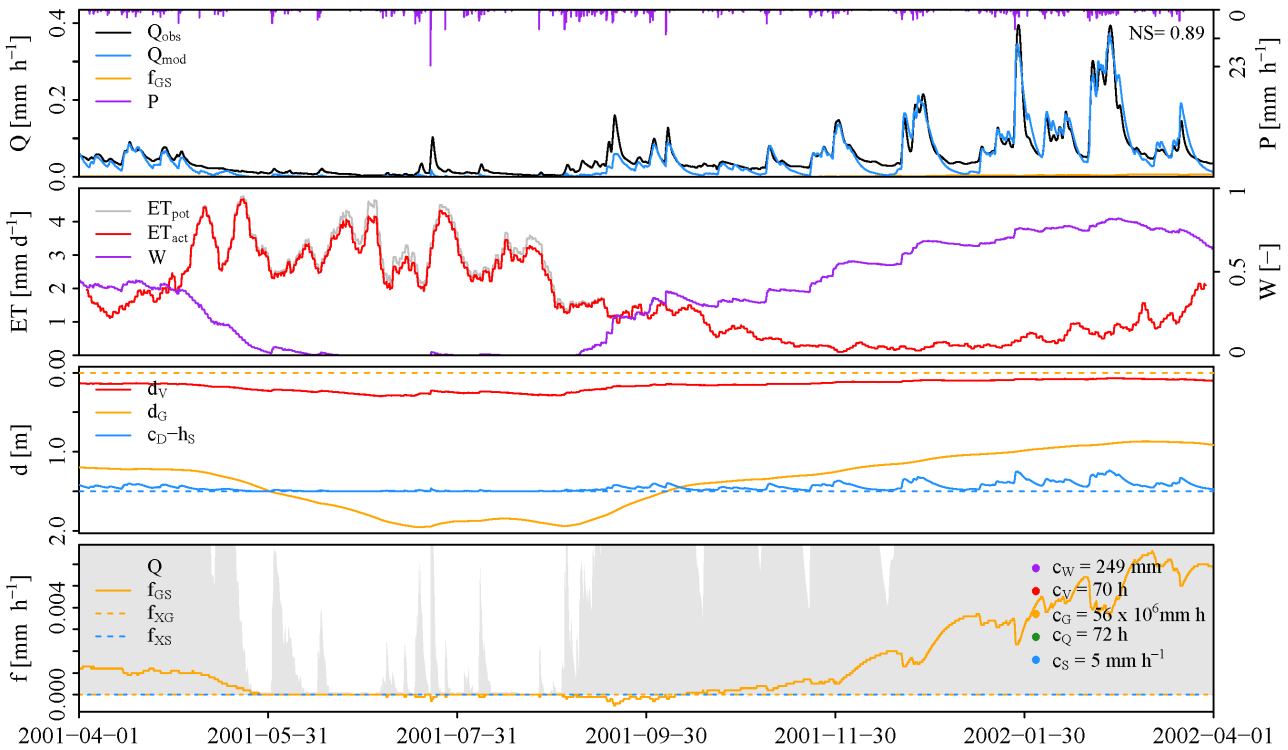


Figure B.15: Validation of the selected parameter set for catchment 0024 on the hydrological year 2001–2002.

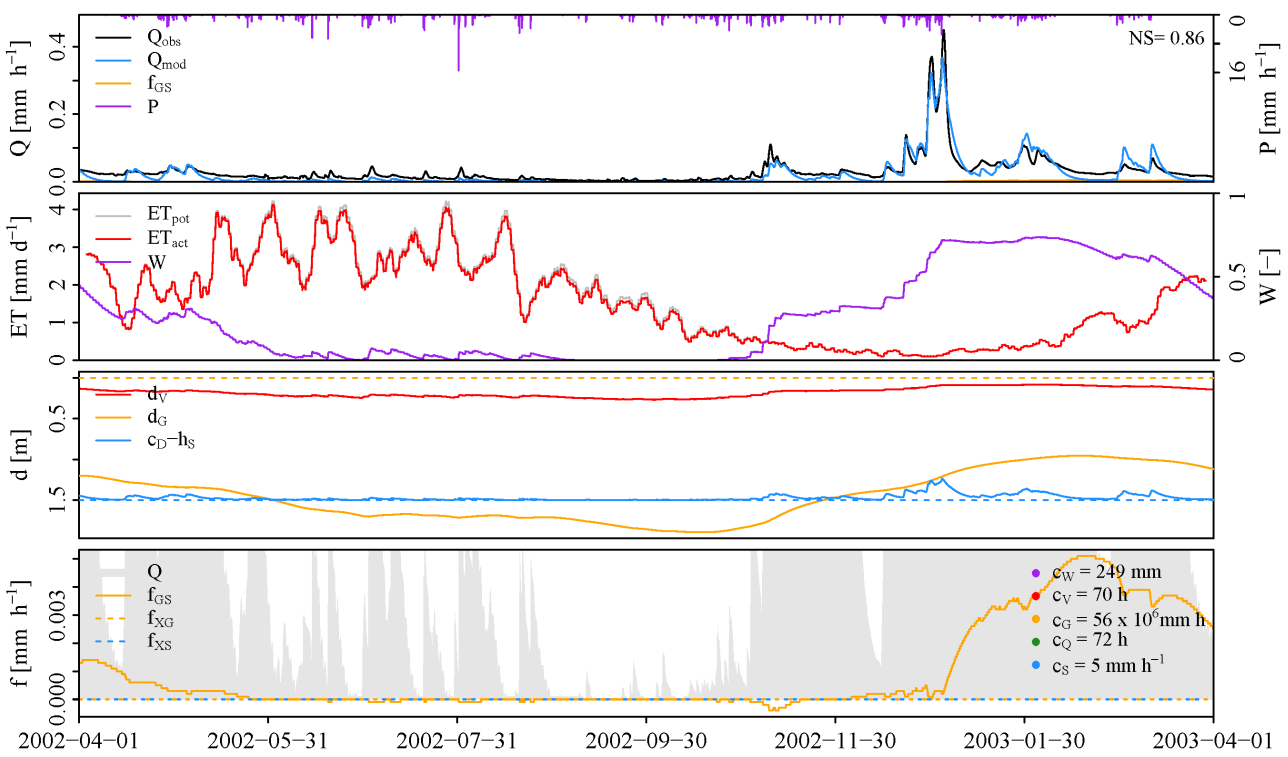


Figure B.16: Validation of the selected parameter set for catchment 0024 on the hydrological year 2002–2003.

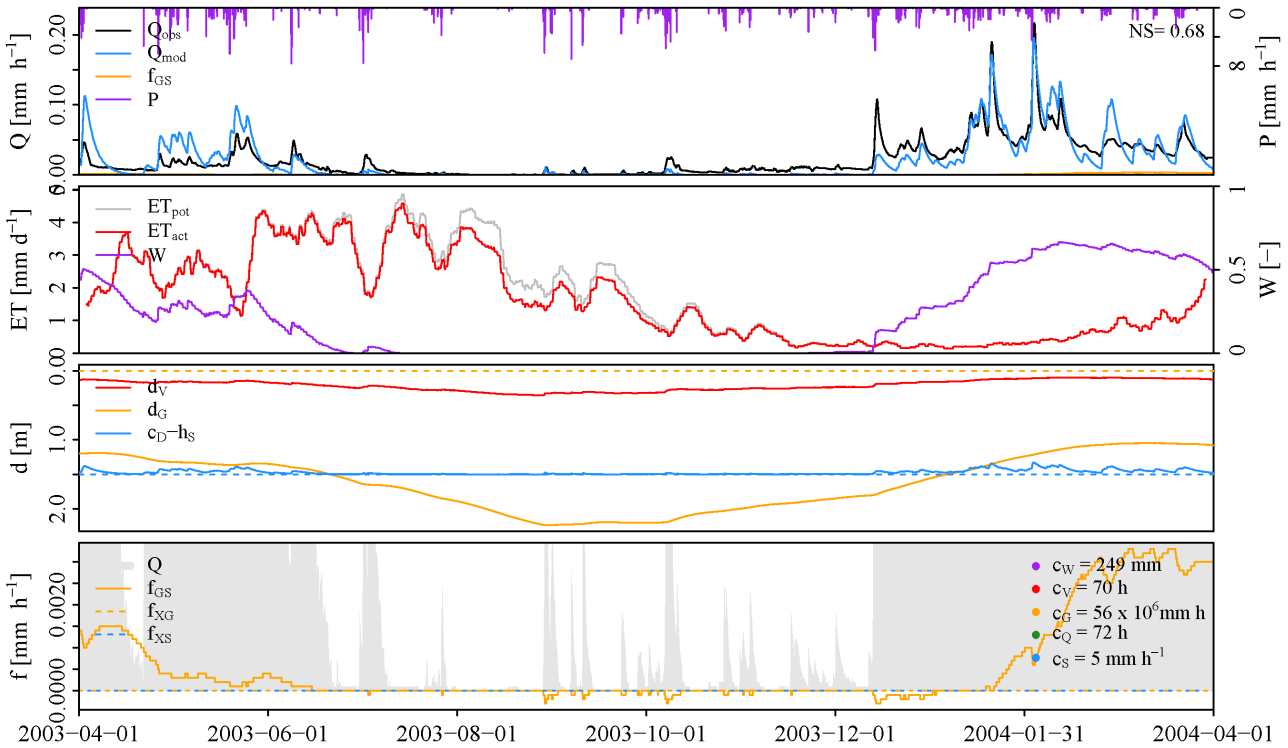


Figure B.17: Validation of the selected parameter set for catchment 0024 on the hydrological year 2003–2004.

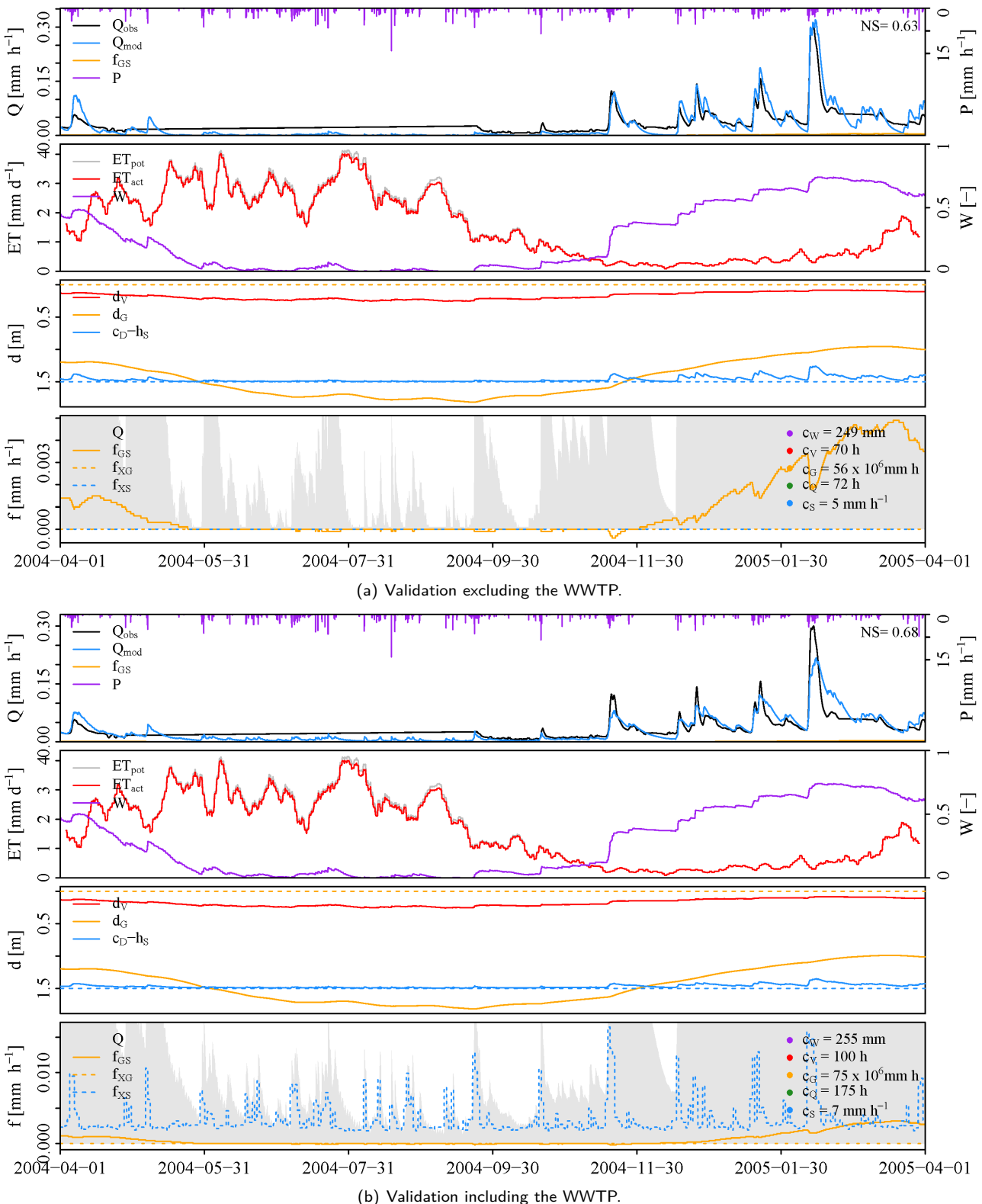


Figure B.18: Validation of the selected parameter set for catchment 0024 on the hydrological year 2004–2005.

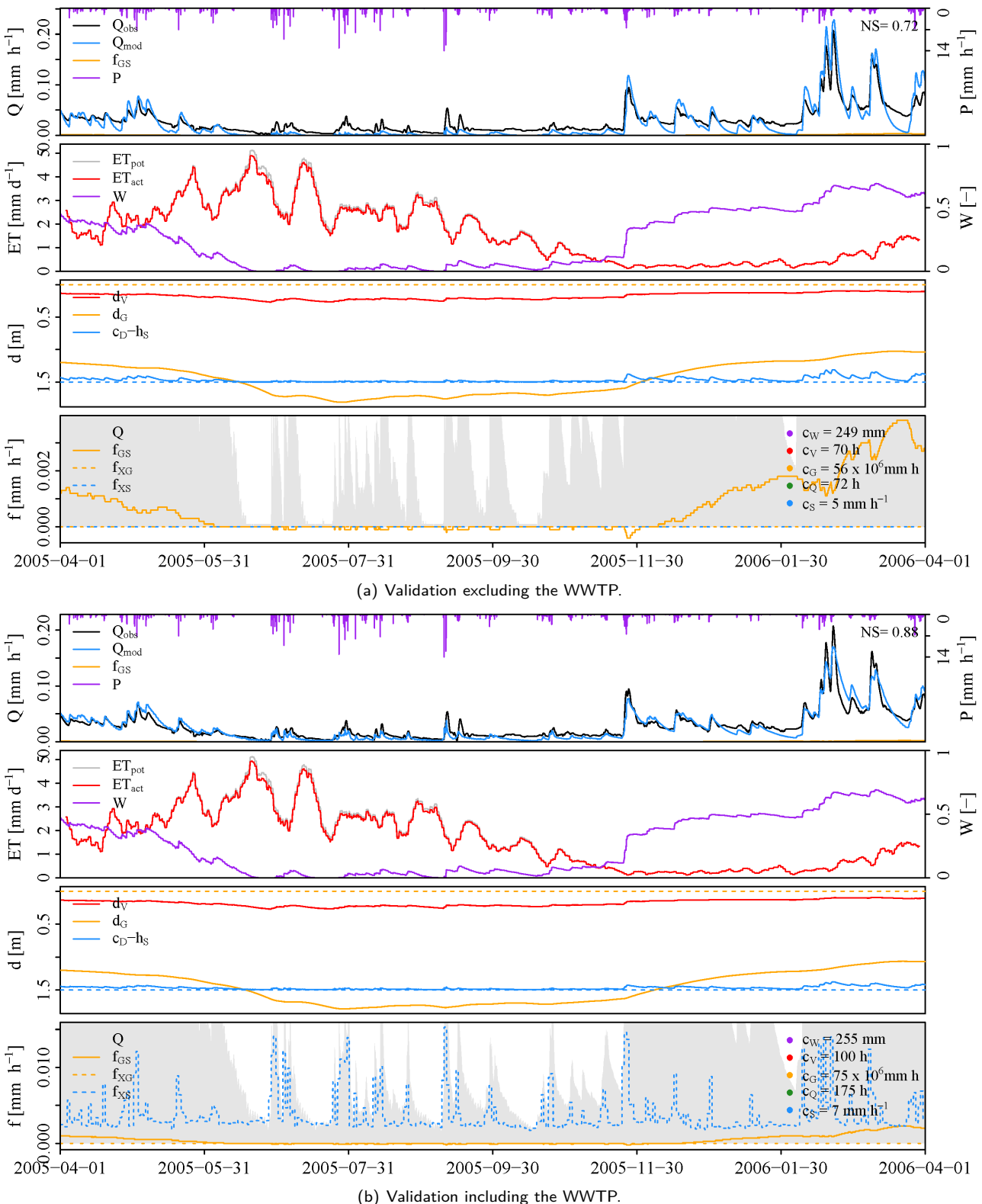


Figure B.19: Validation of the selected parameter set for catchment 0024 on the hydrological year 2005–2006.

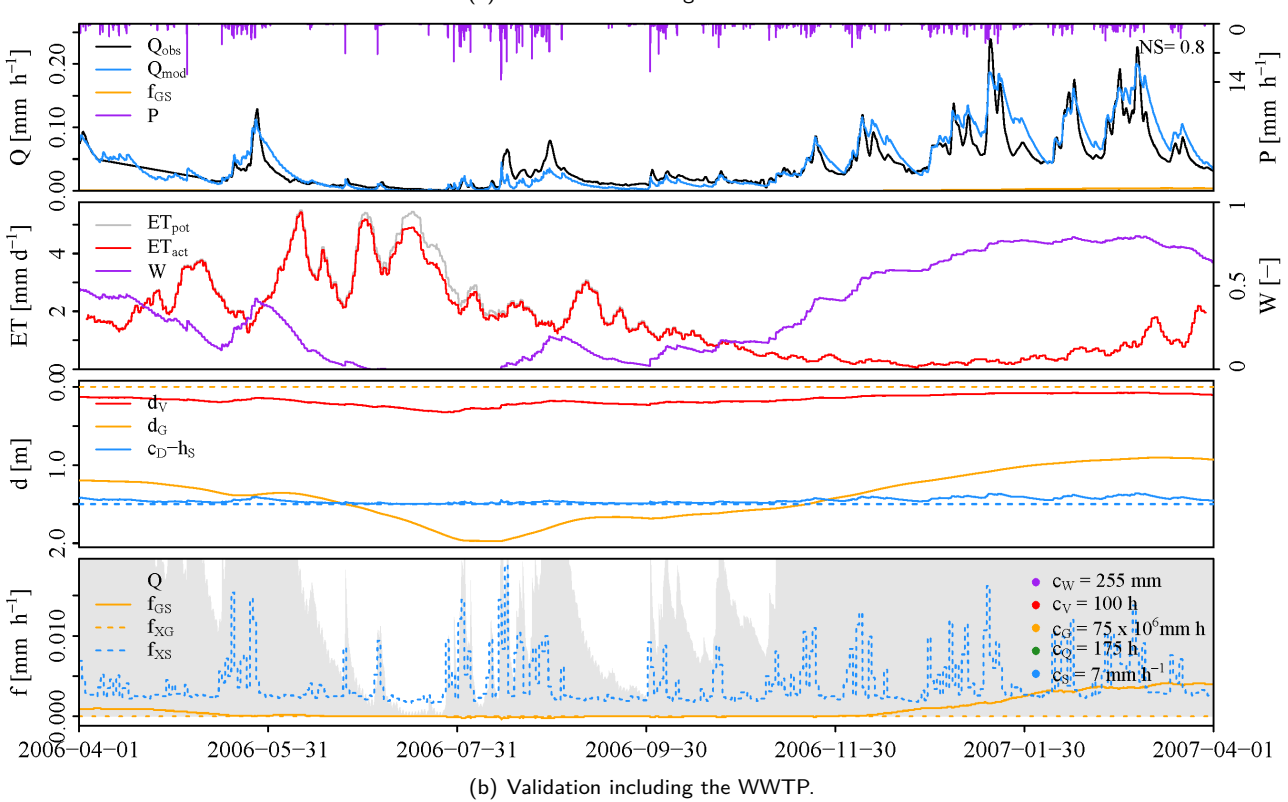
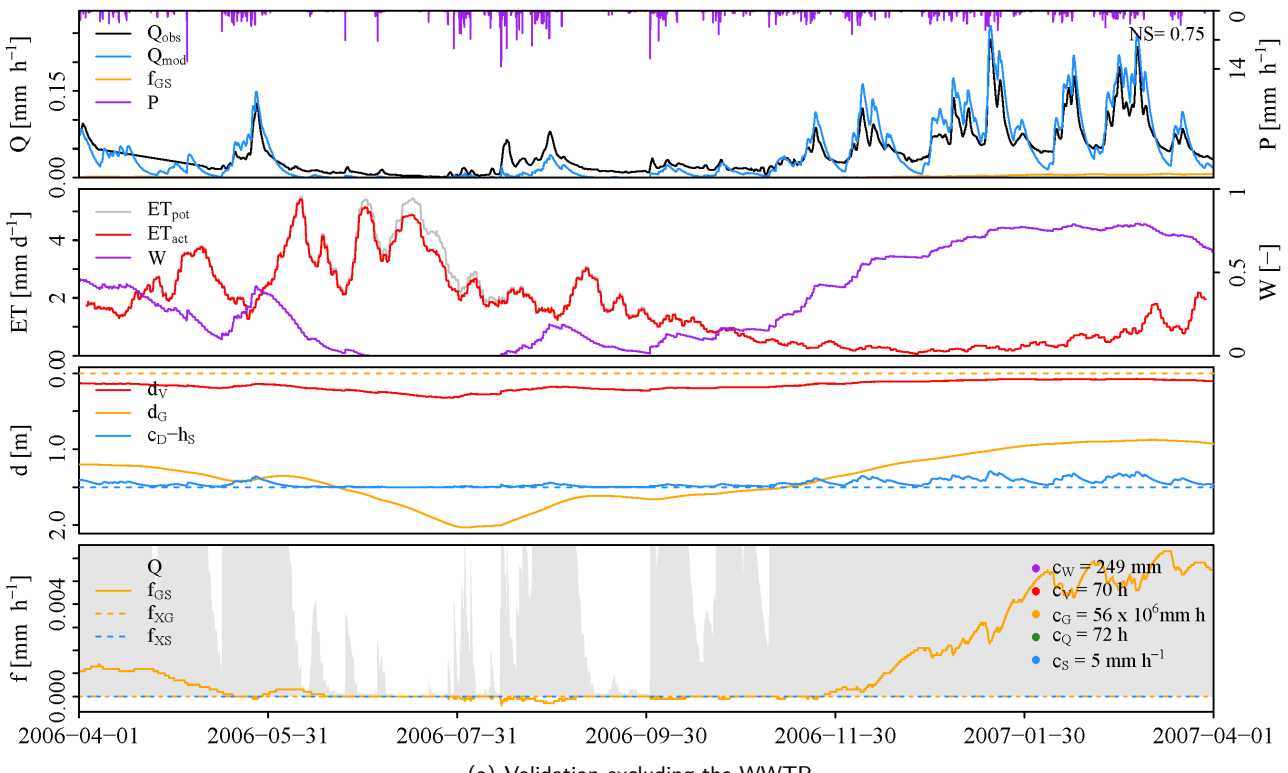
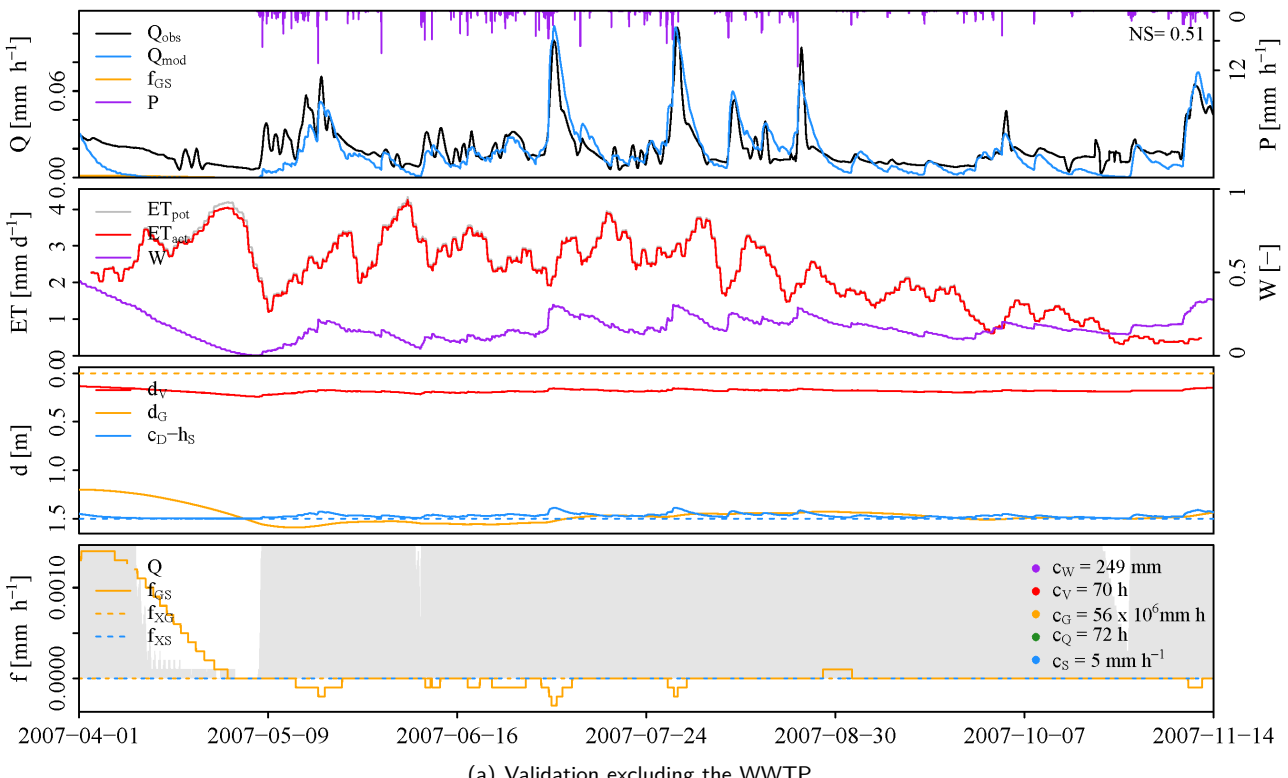
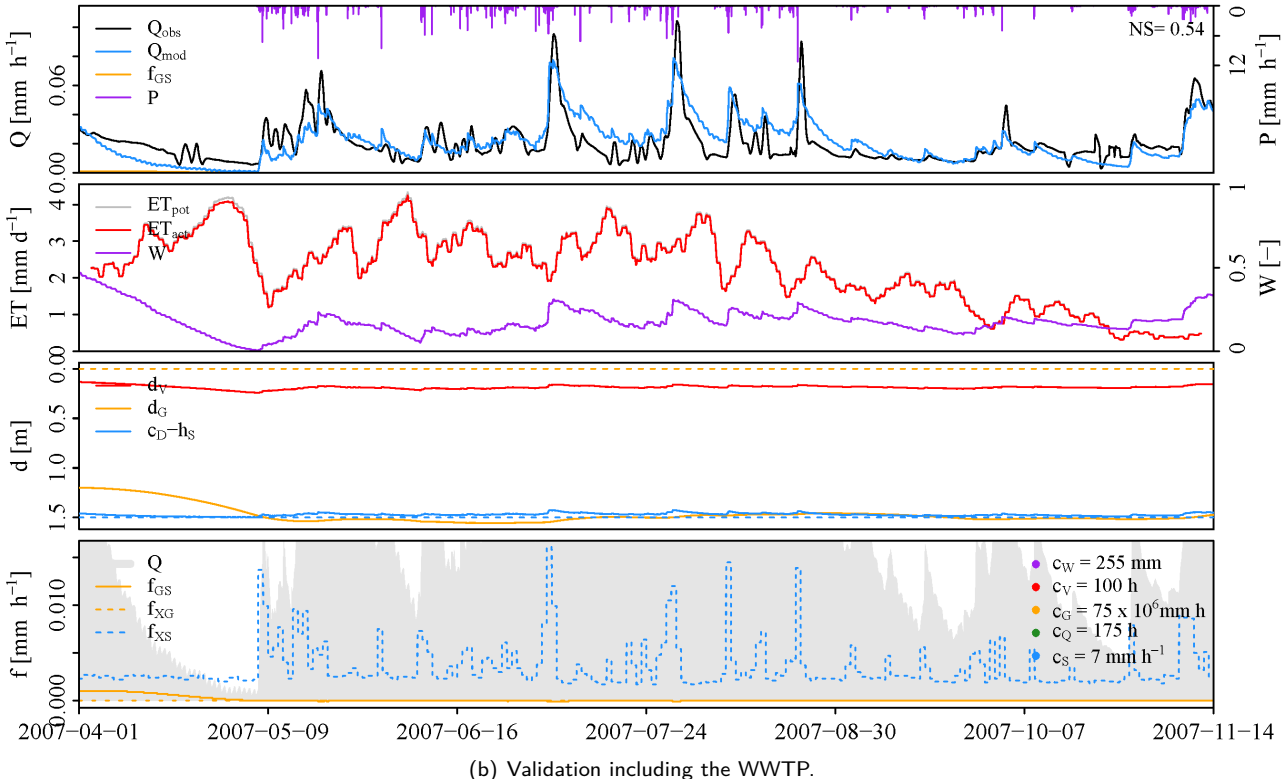


Figure B.20: Validation of the selected parameter set for catchment 0024 on the hydrological year 2006–2007.



(a) Validation excluding the WWTP.



(b) Validation including the WWTP.

Figure B.21: Validation of the selected parameter set for catchment 0024 on the hydrological year 2007–2008.

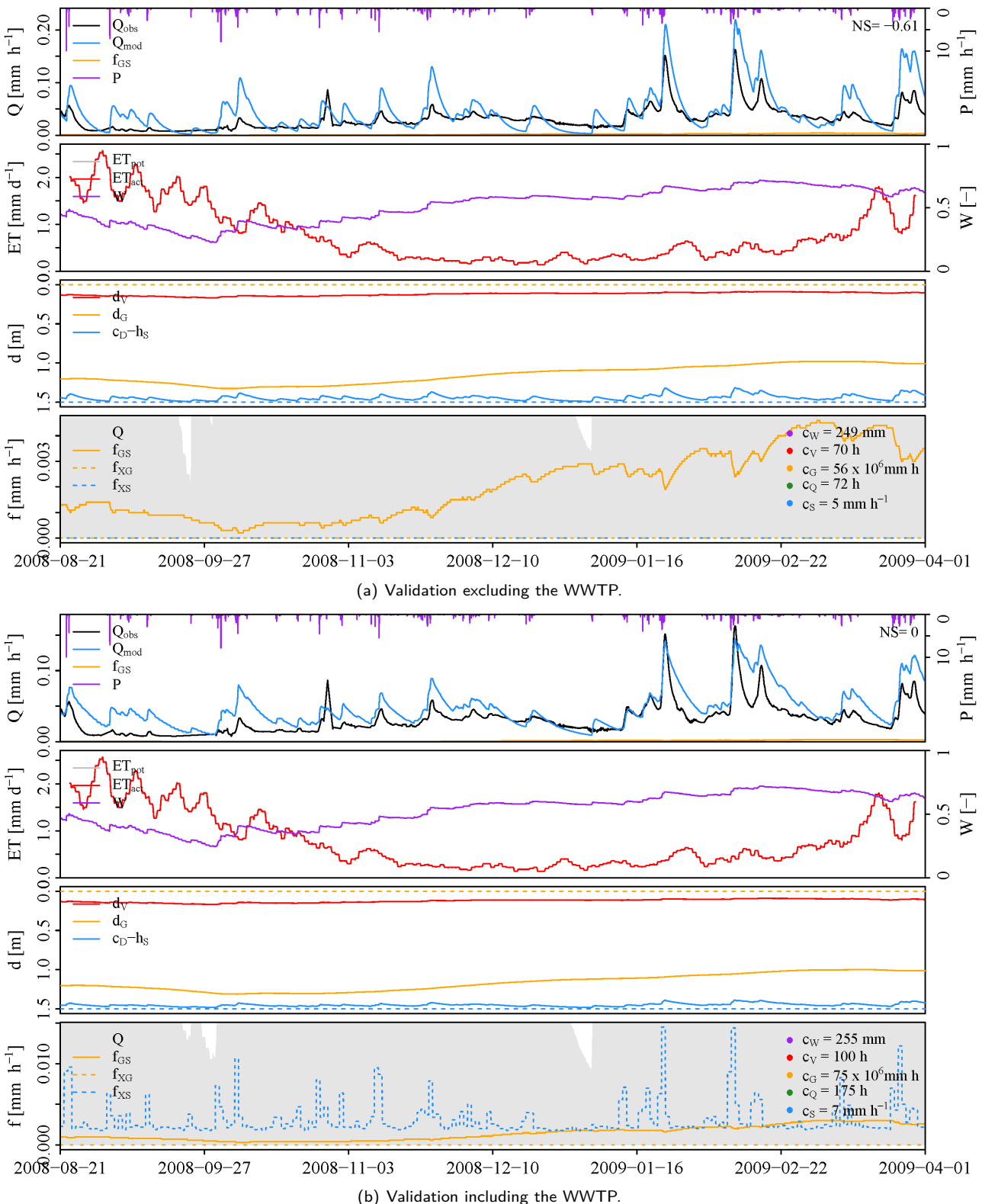


Figure B.22: Validation of the selected parameter set for catchment 0024 on the hydrological year 2008–2009.

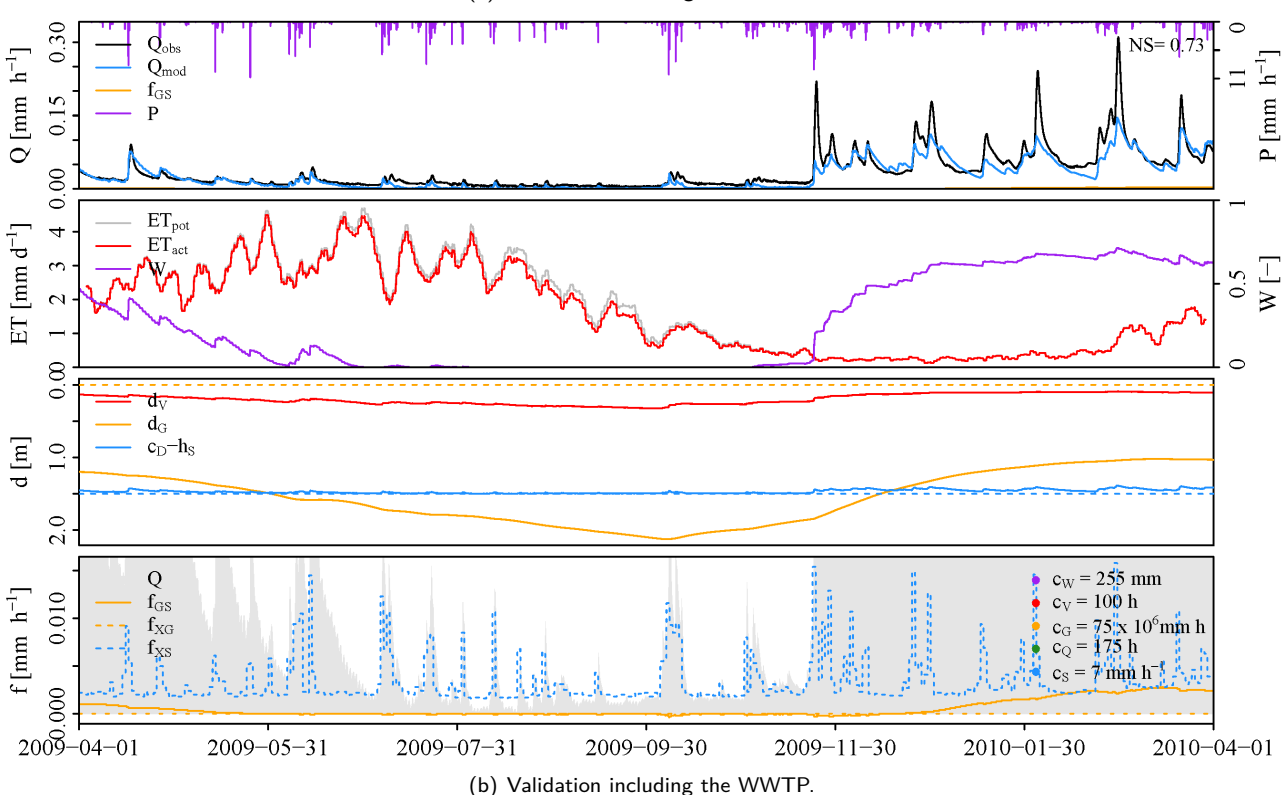
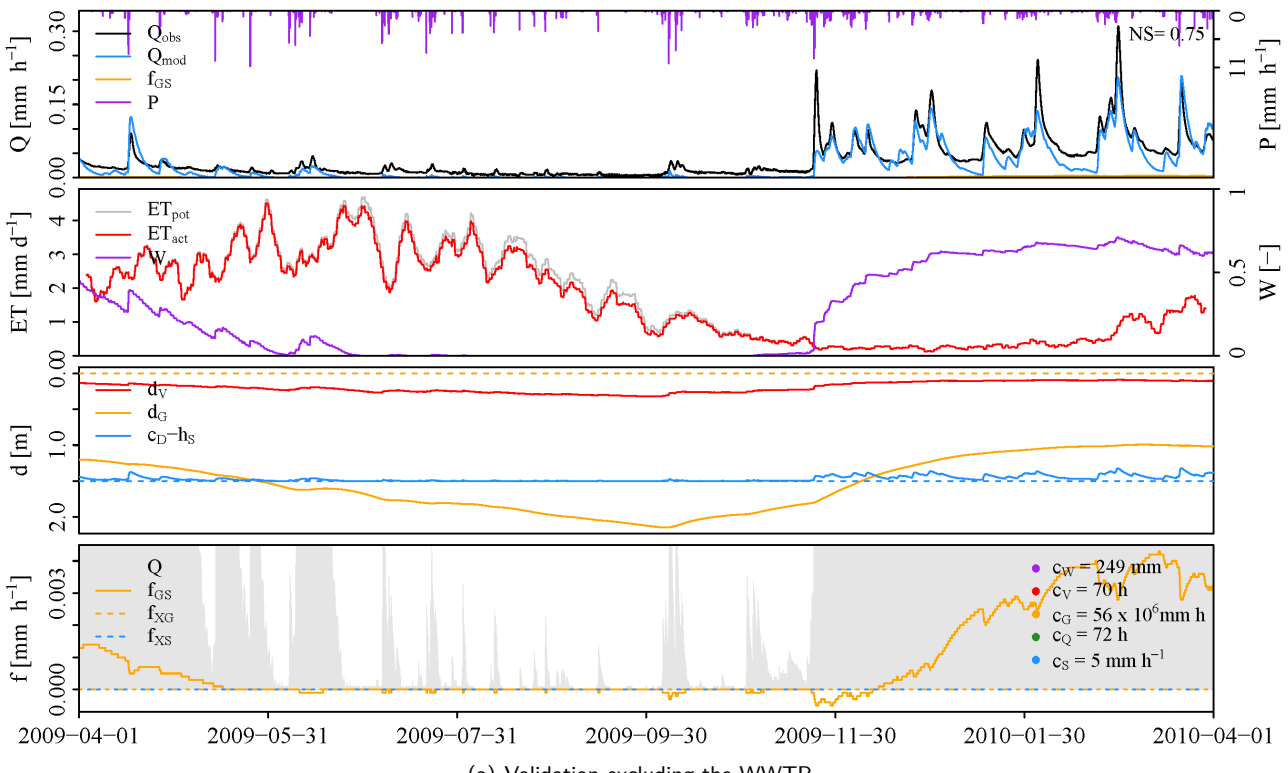


Figure B.23: Validation of the selected parameter set for catchment 0024 on the hydrological year 2009–2010.

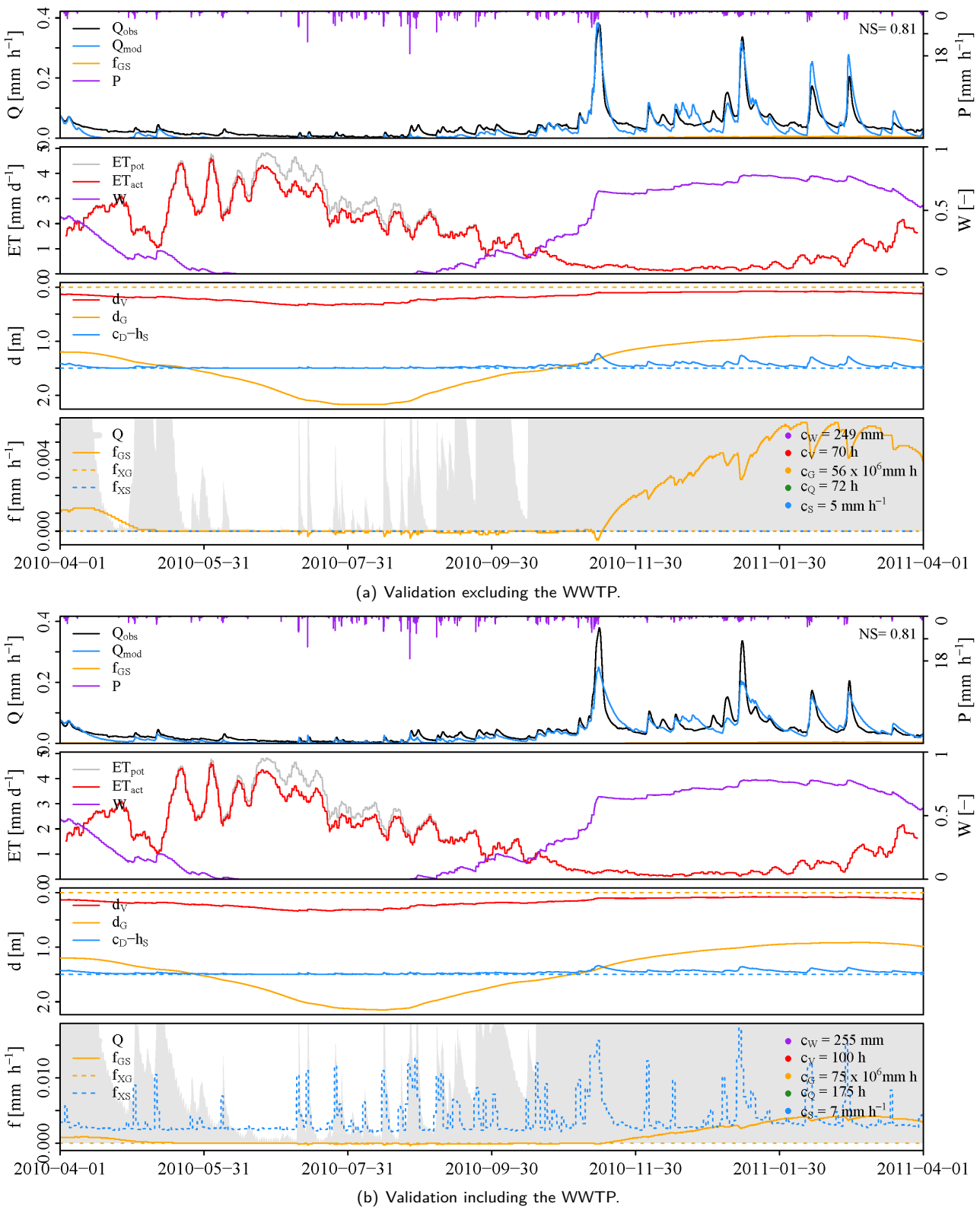


Figure B.24: Validation of the selected parameter set for catchment 0024 on the hydrological year 2010–2011.

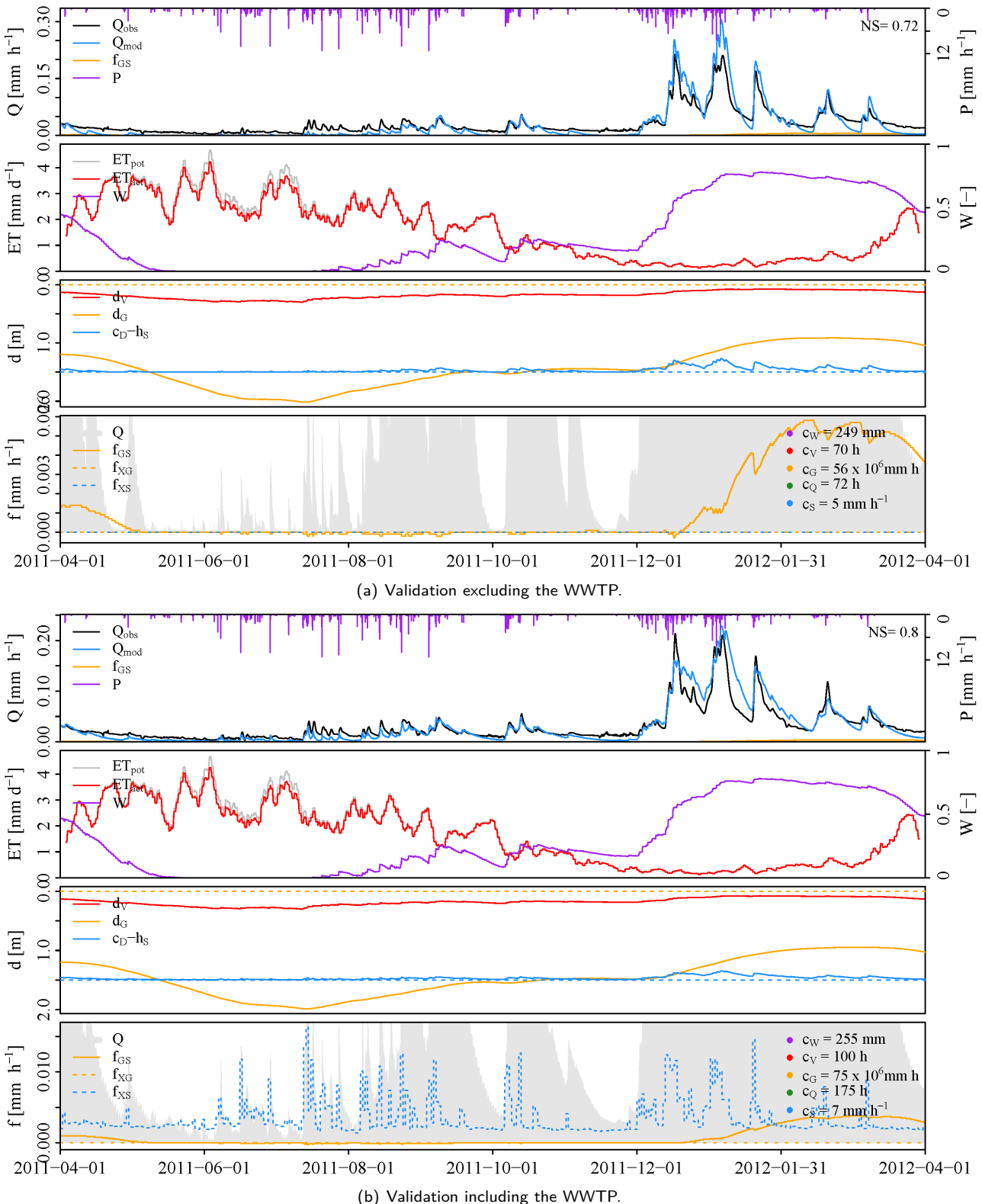


Figure B.25: Validation of the selected parameter set for catchment 0024 on the hydrological year 2011–2012.

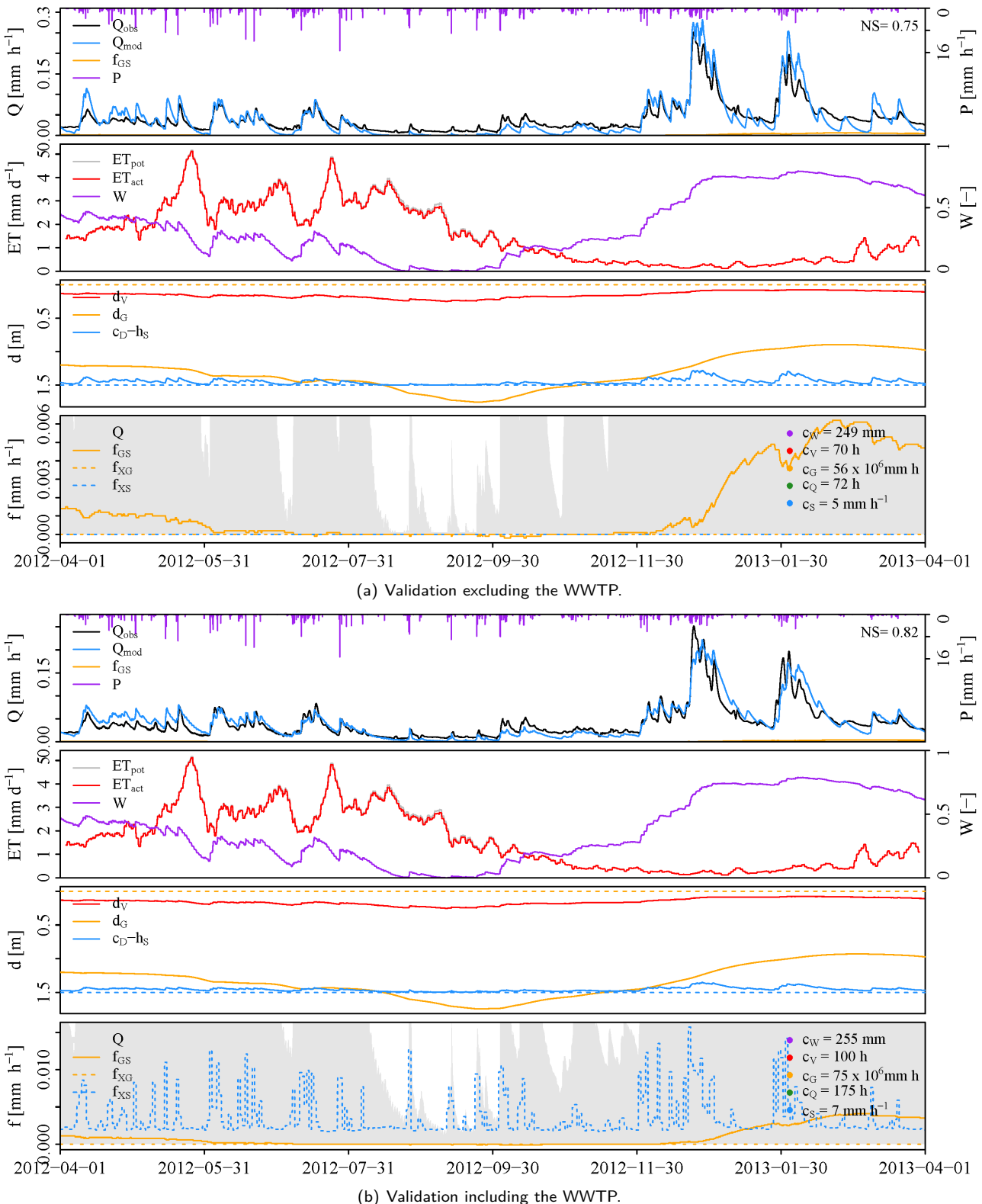


Figure B.26: Validation of the selected parameter set for catchment 0024 on the hydrological year 2012–2013.

## B.2 Validation catchment 0072

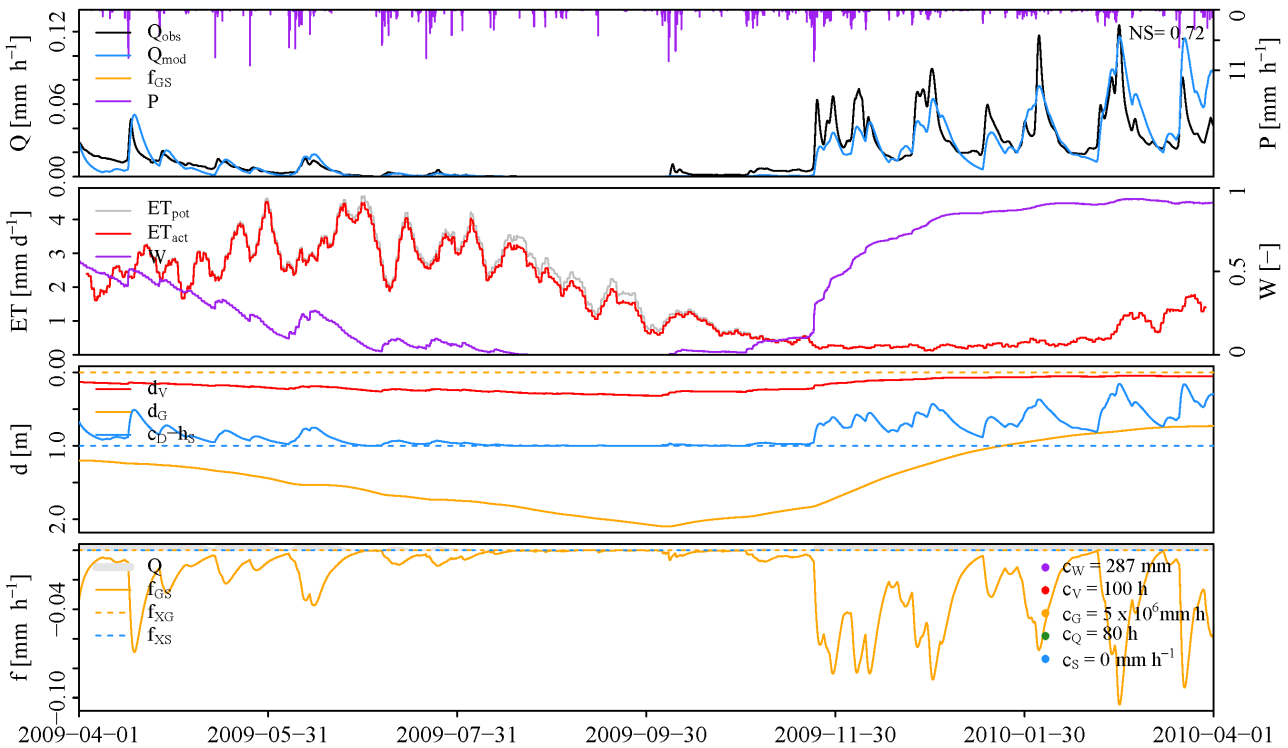


Figure B.27: Validation of the selected parameter set for catchment 0072 on the hydrological year 2009–2010.

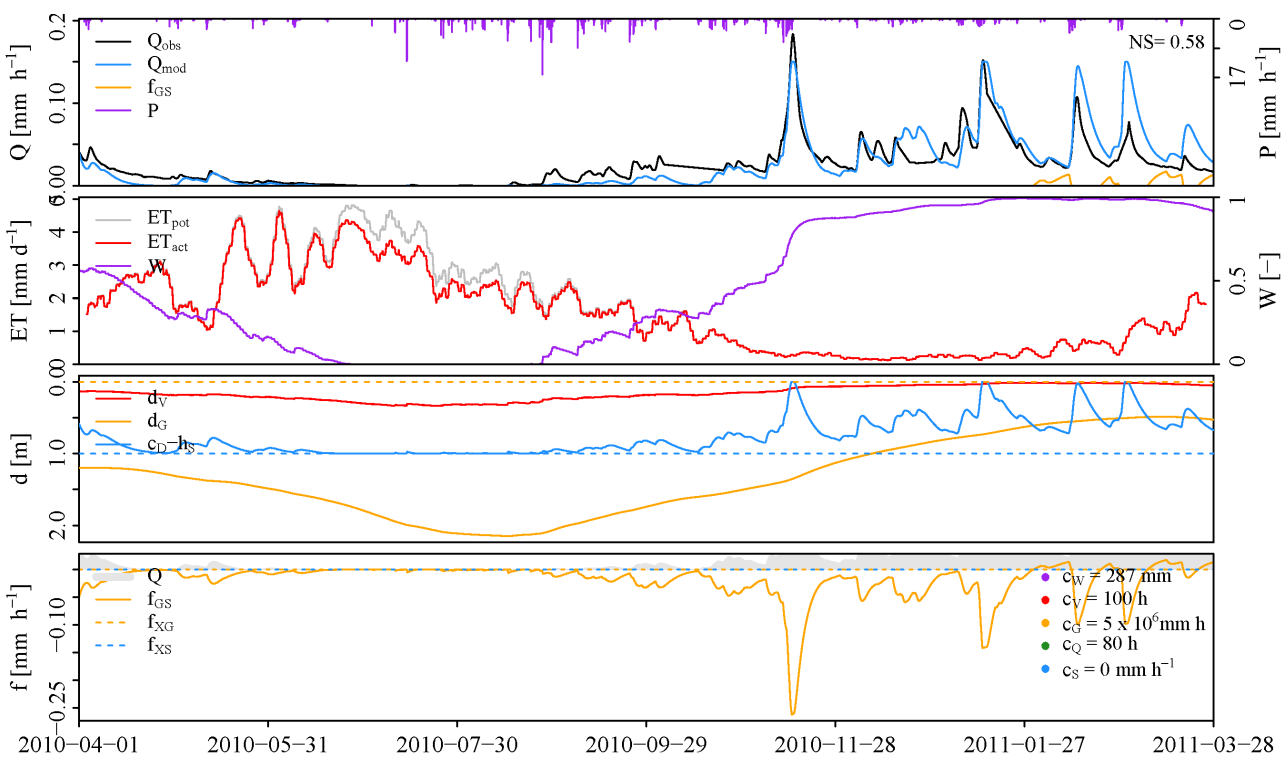


Figure B.28: Validation of the selected parameter set for catchment 0072 on the hydrological year 2010–2011.

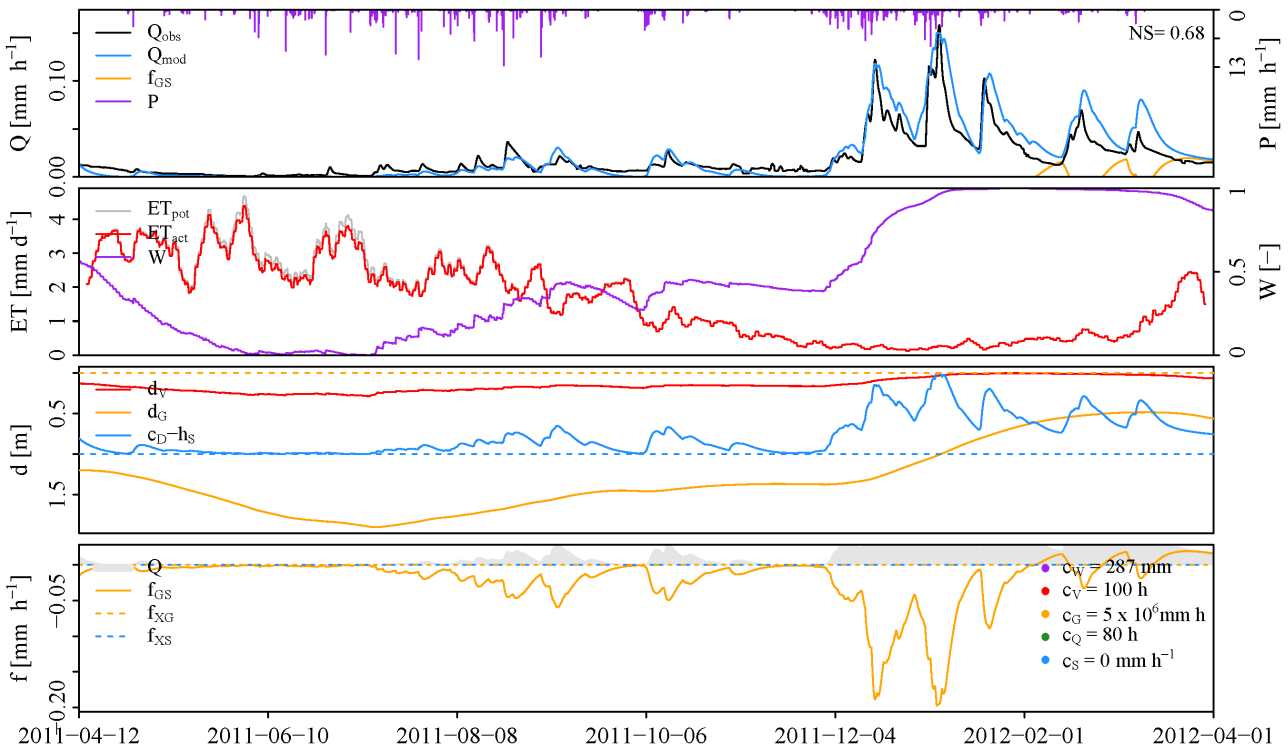


Figure B.29: Validation of the selected parameter set for catchment 0072 on the hydrological year 2011–2012.

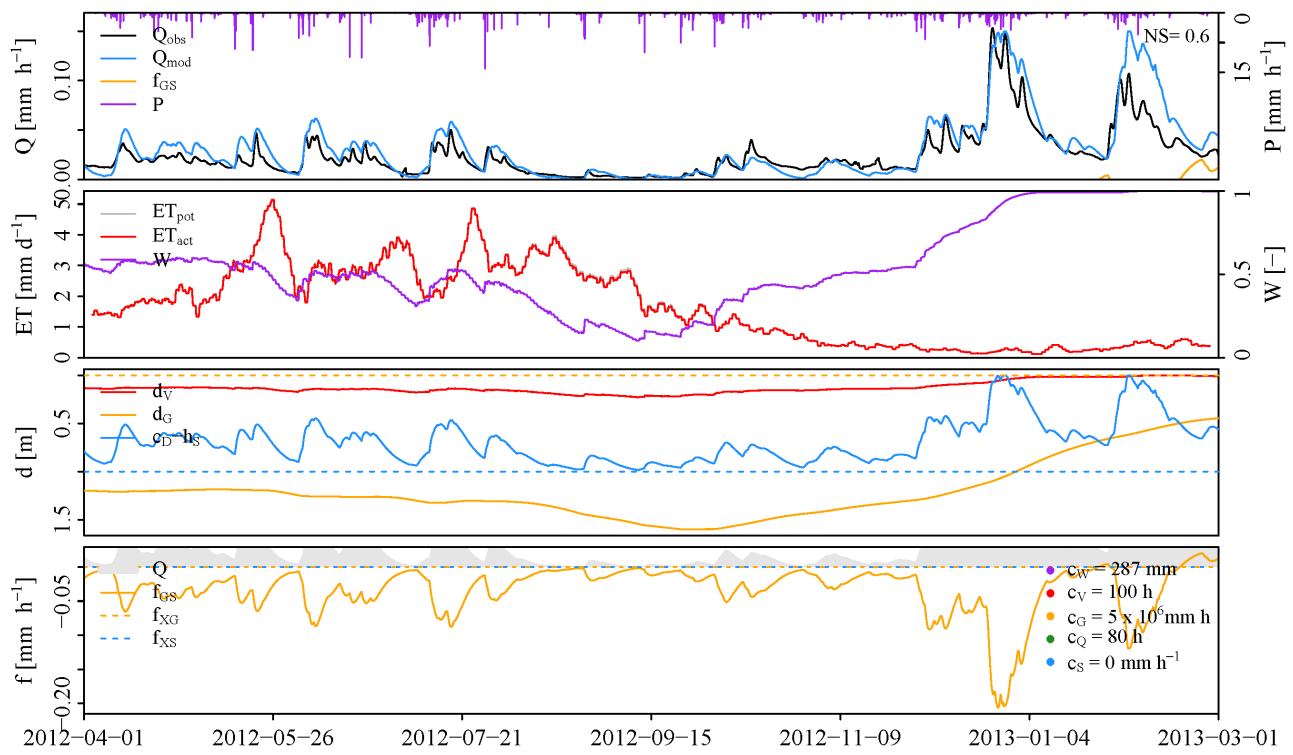


Figure B.30: Validation of the selected parameter set for catchment 0072 on the hydrological year 2012–2013.

### B.3 Validation catchment 0098

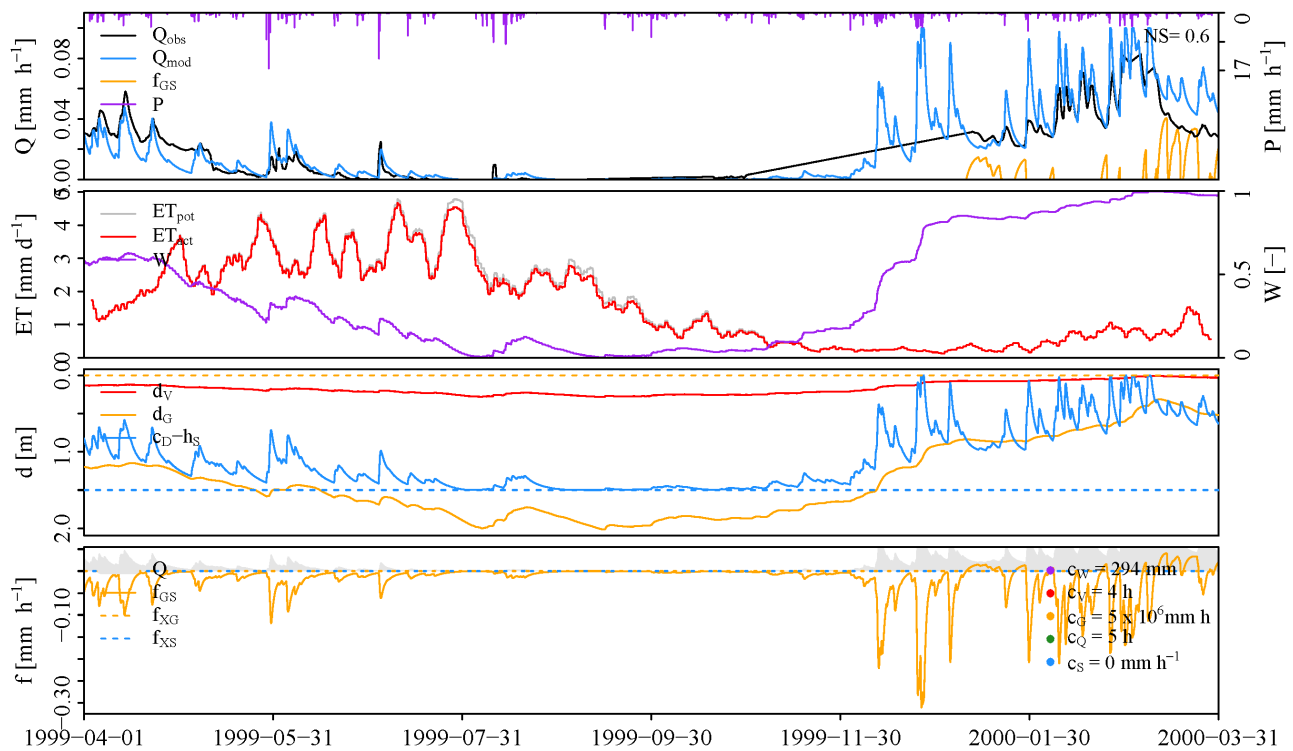


Figure B.31: Validation of the selected parameter set for catchment 0098 on the hydrological year 1999–2000.

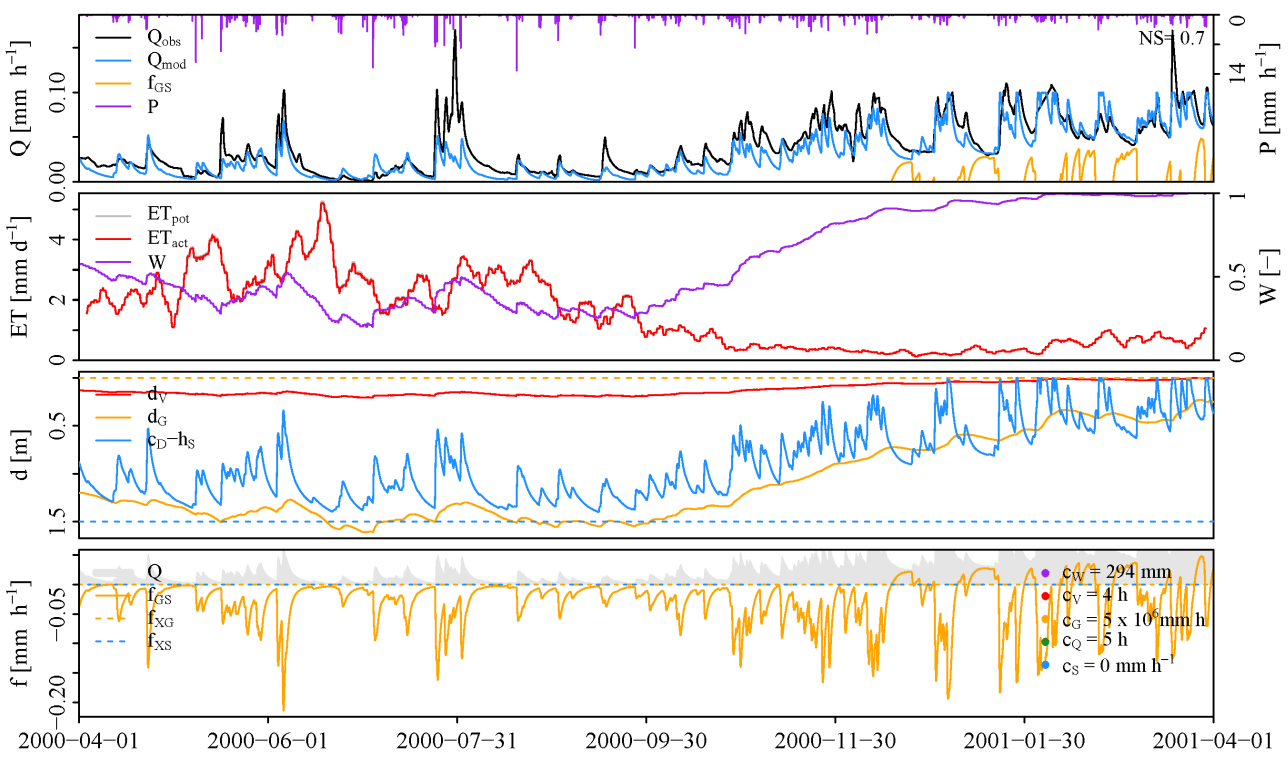


Figure B.32: Validation of the selected parameter set for catchment 0098 on the hydrological year 2000–2001.

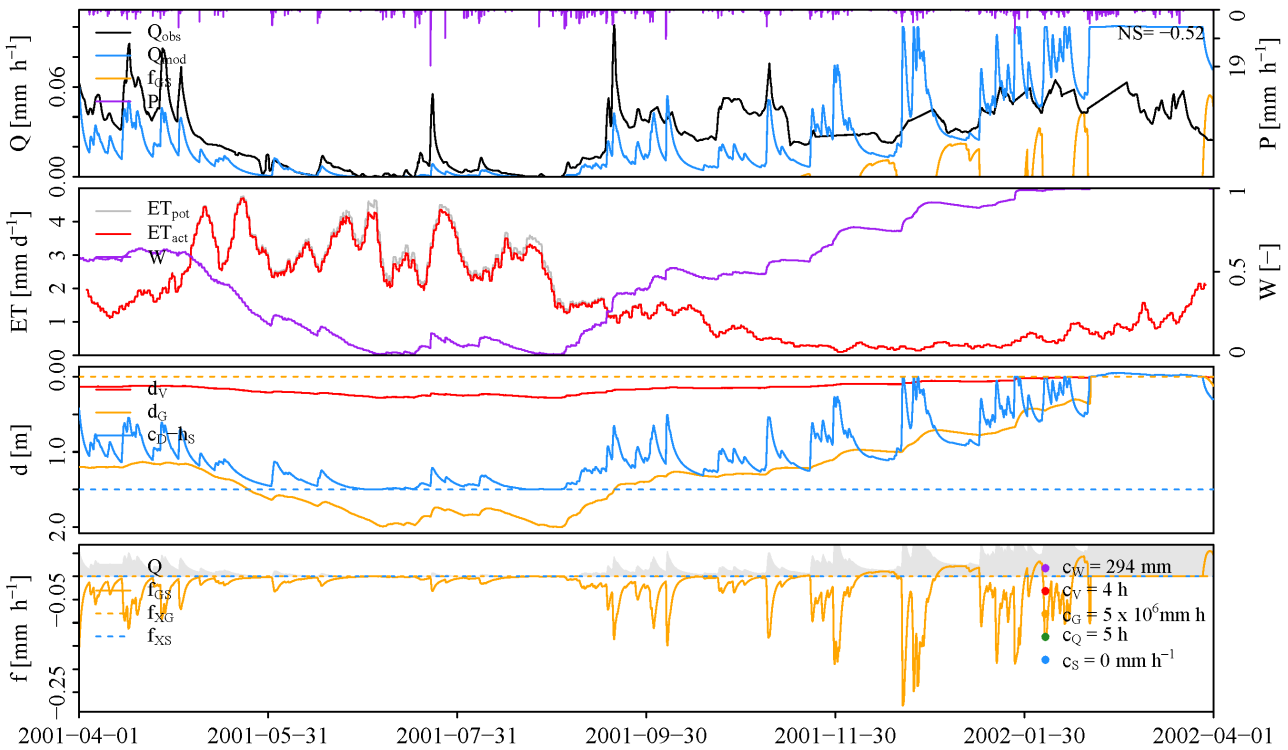


Figure B.33: Validation of the selected parameter set for catchment 0098 on the hydrological year 2001–2002.

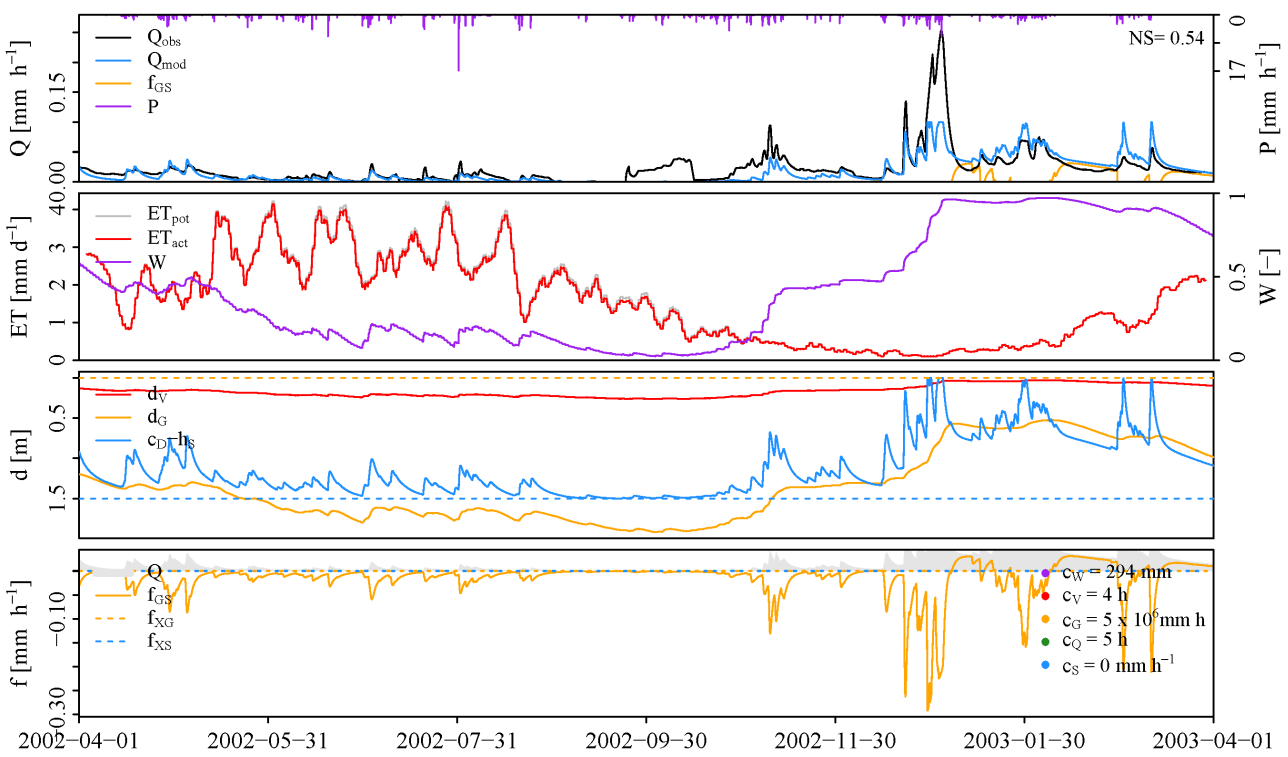


Figure B.34: Validation of the selected parameter set for catchment 0098 on the hydrological year 2002–2003.

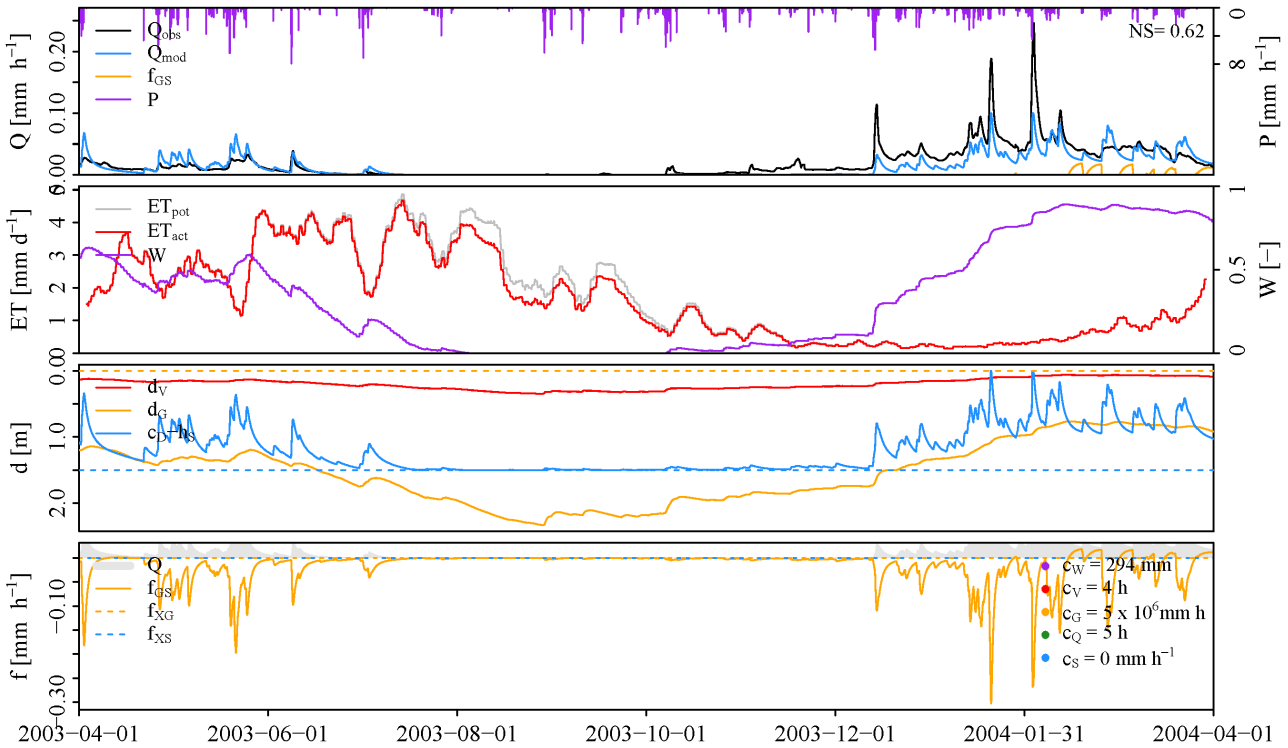


Figure B.35: Validation of the selected parameter set for catchment 0098 on the hydrological year 2003–2004.

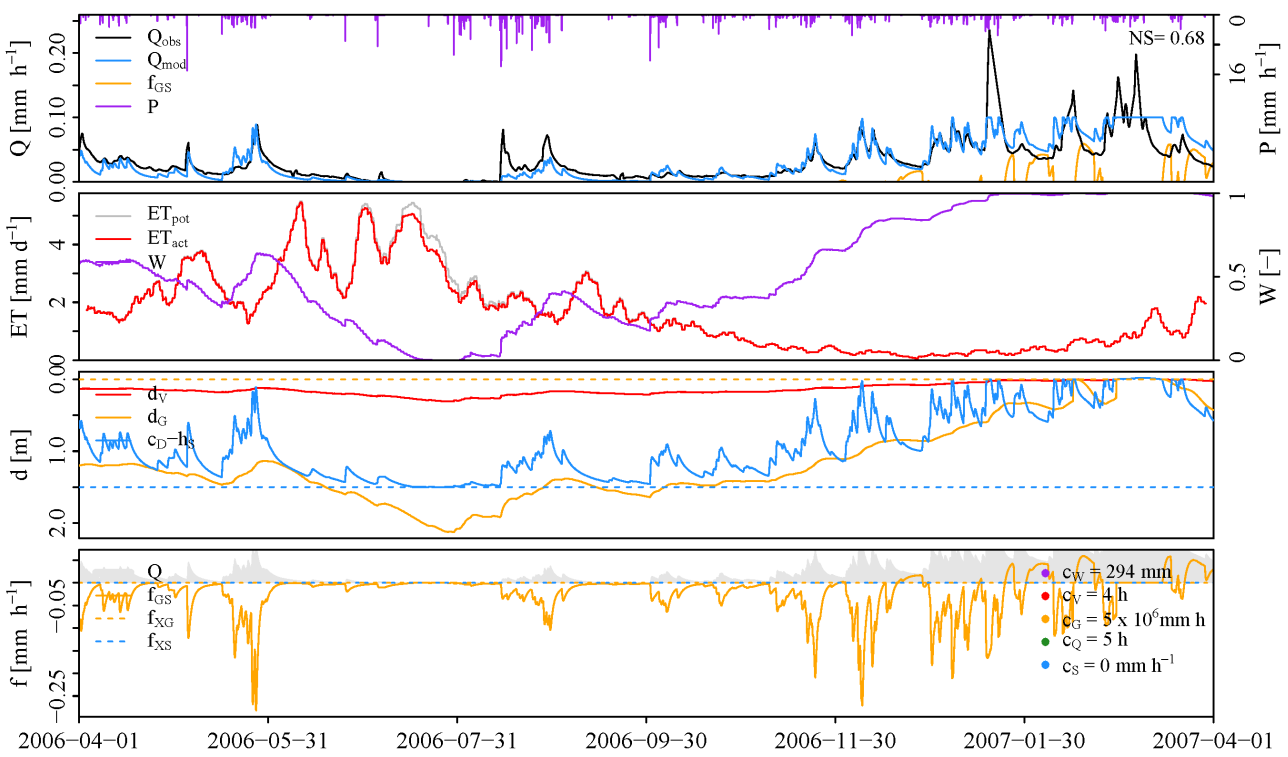


Figure B.36: Validation of the selected parameter set for catchment 0098 on the hydrological year 2006–2007.

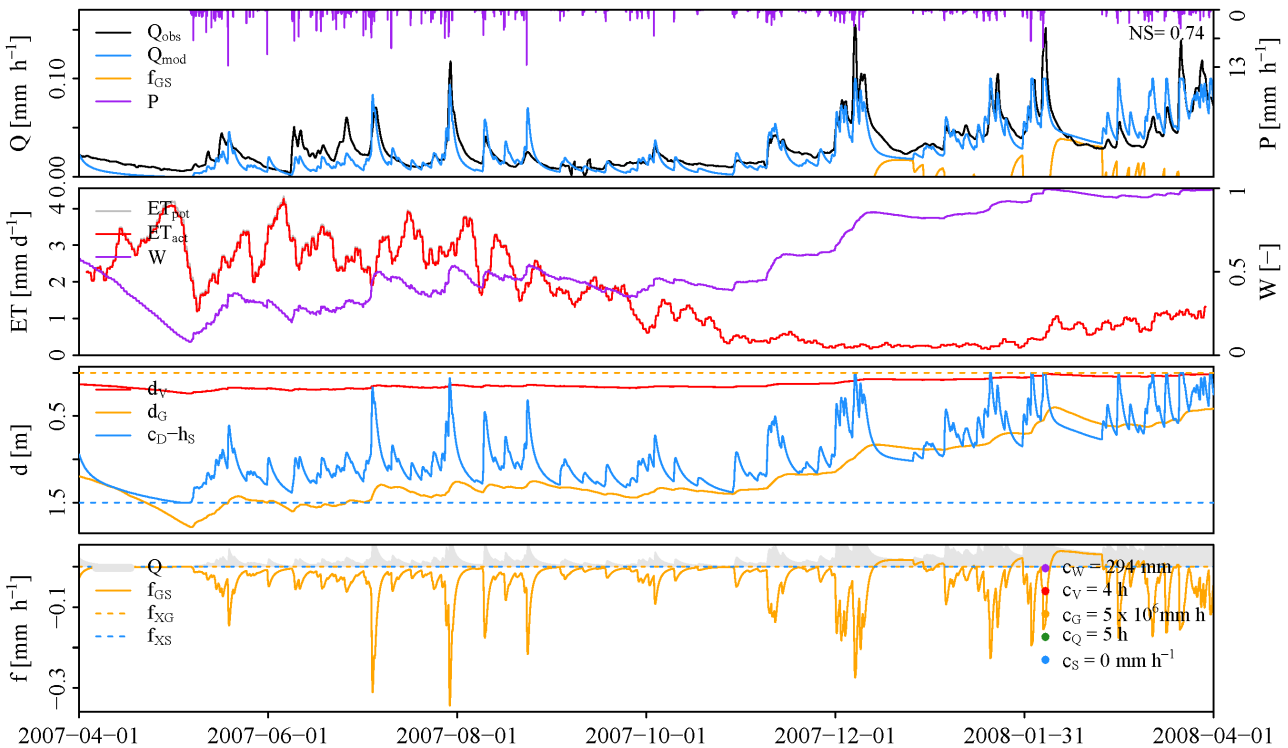


Figure B.37: Validation of the selected parameter set for catchment 0098 on the hydrological year 2007–2008.

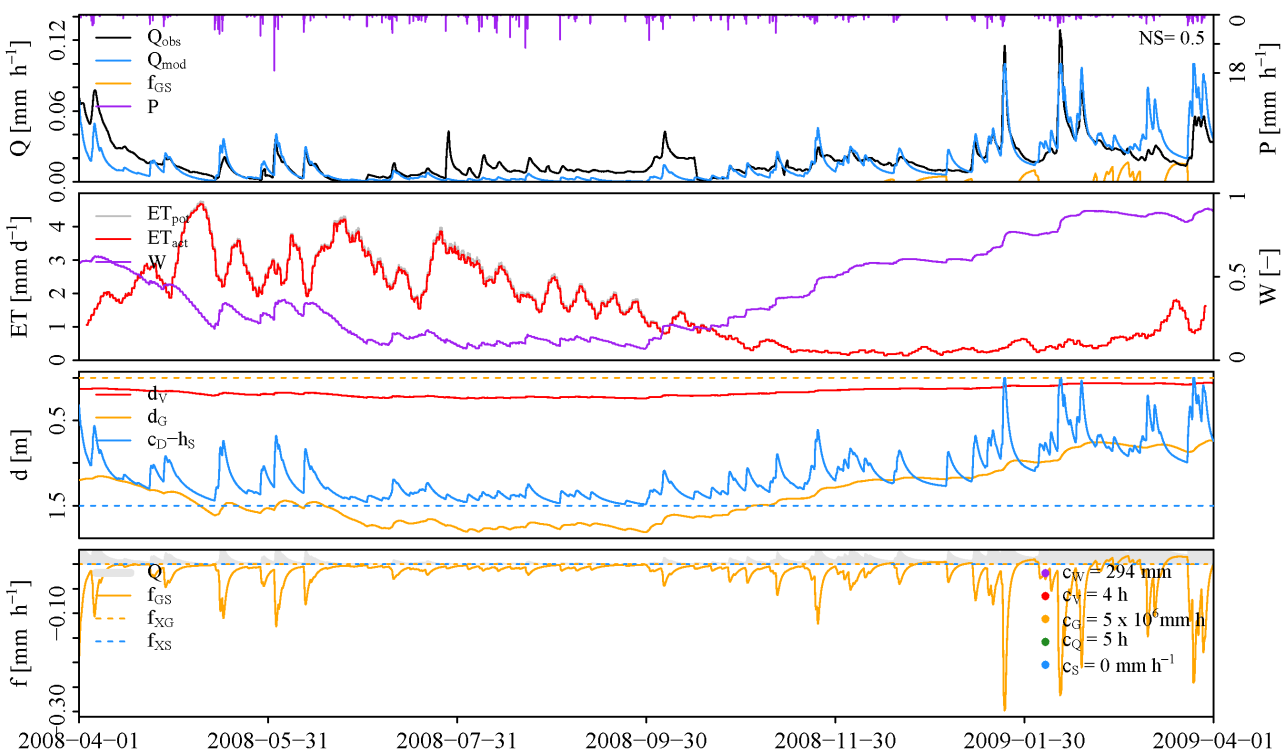


Figure B.38: Validation of the selected parameter set for catchment 0098 on the hydrological year 2008–2009.

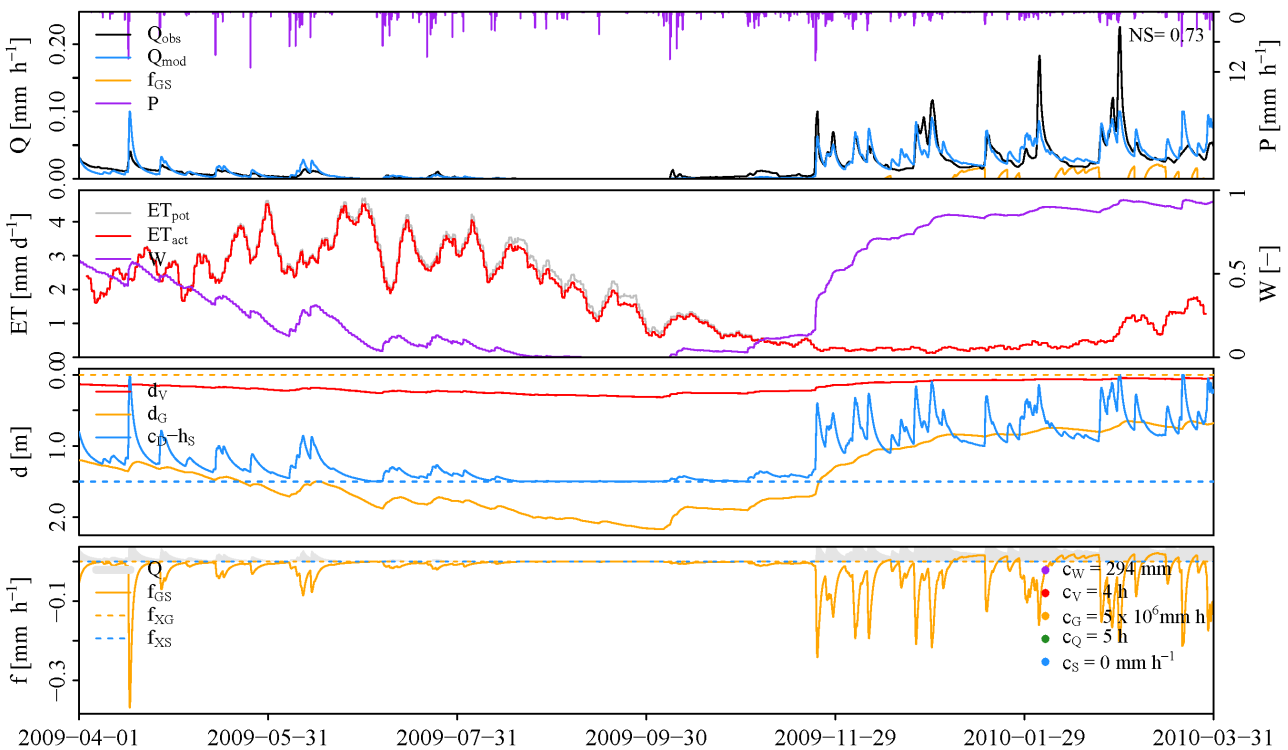


Figure B.39: Validation of the selected parameter set for catchment 0098 on the hydrological year 2009–2010.

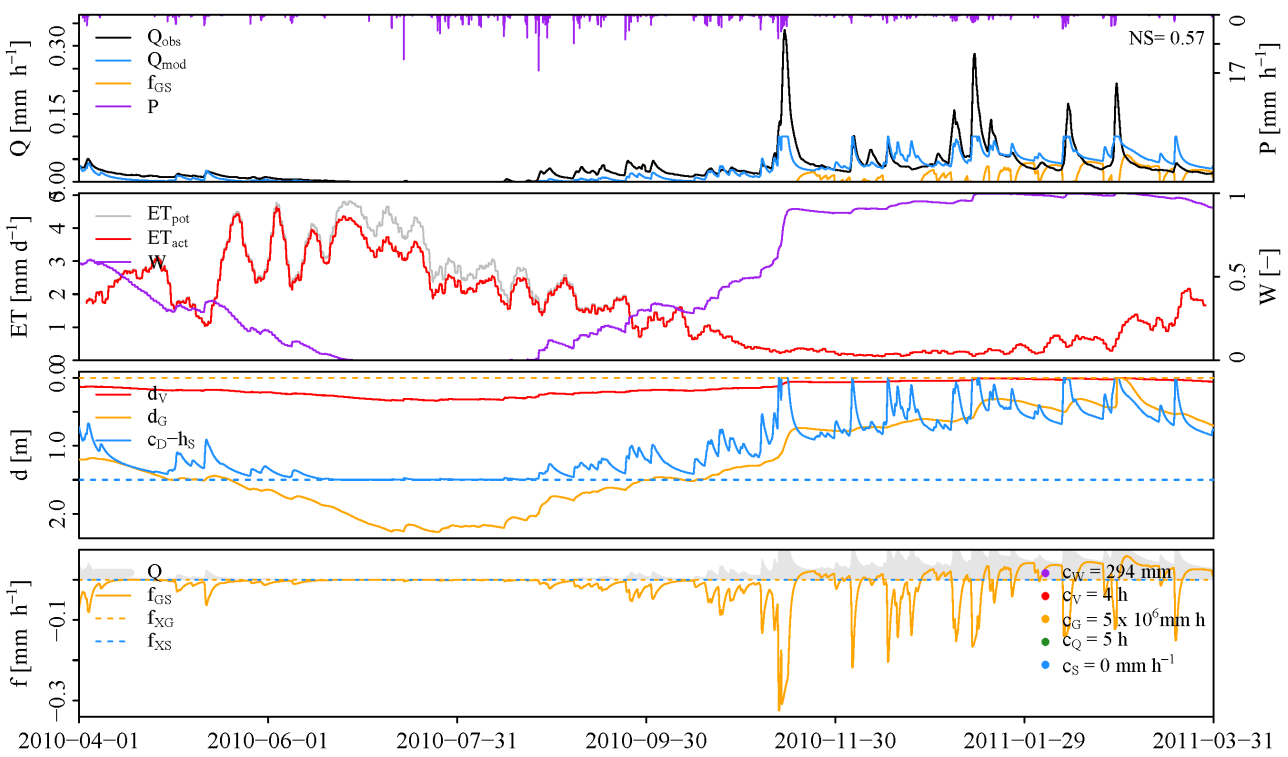


Figure B.40: Validation of the selected parameter set for catchment 0098 on the hydrological year 2010–2011.

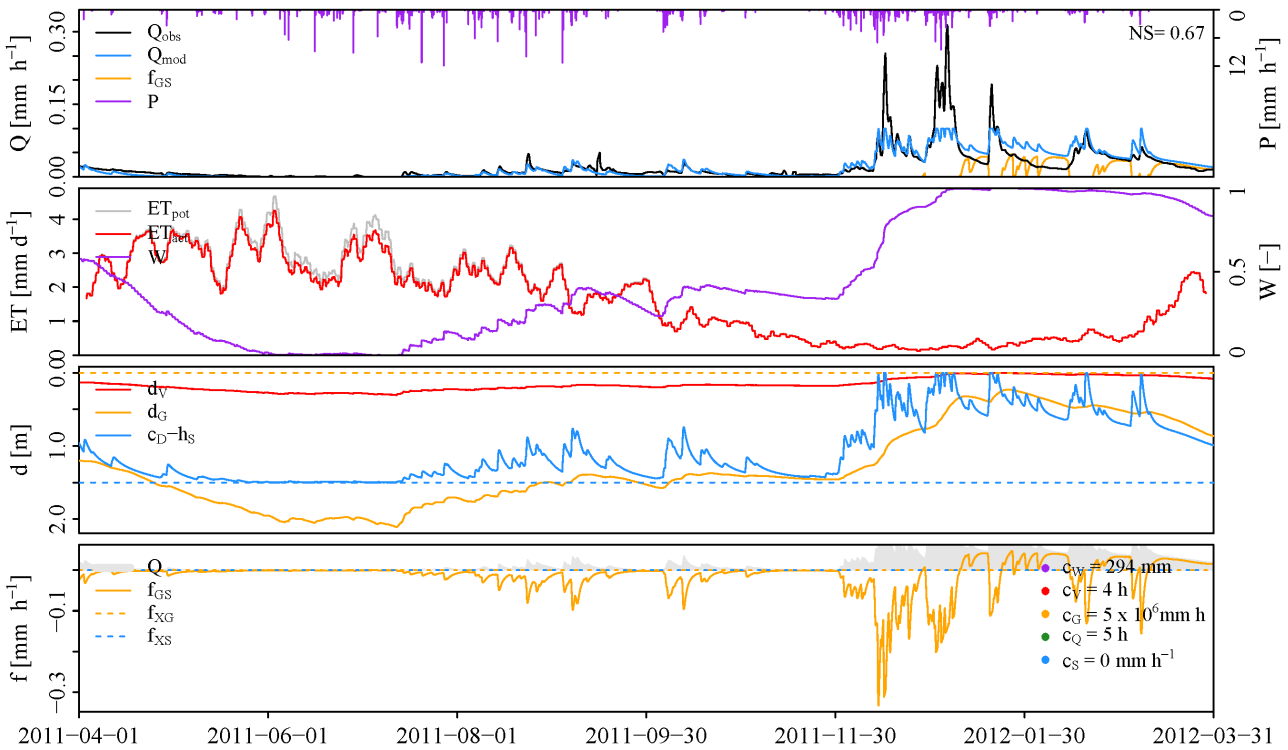


Figure B.41: Validation of the selected parameter set for catchment 0098 on the hydrological year 2011–2012.

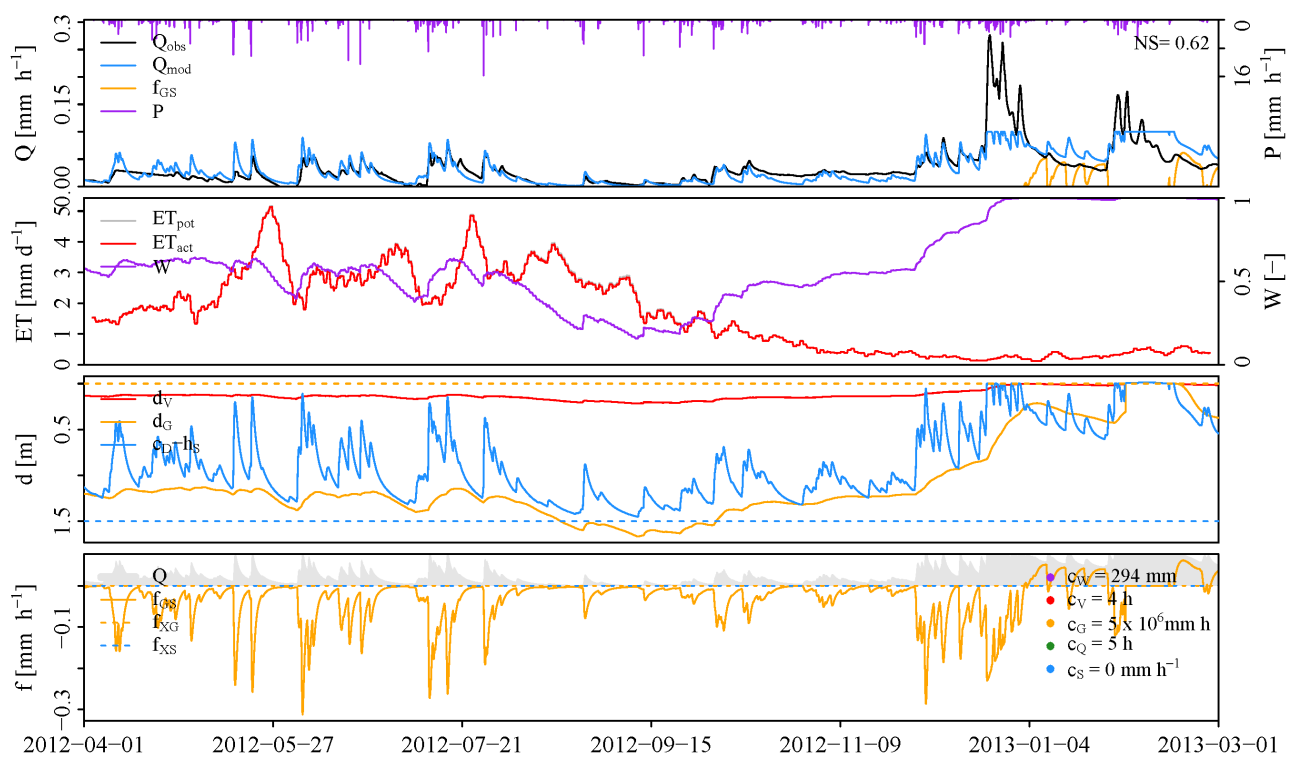


Figure B.42: Validation of the selected parameter set for catchment 0098 on the hydrological year 2012–2013.

## B.4 Validation catchment 0099

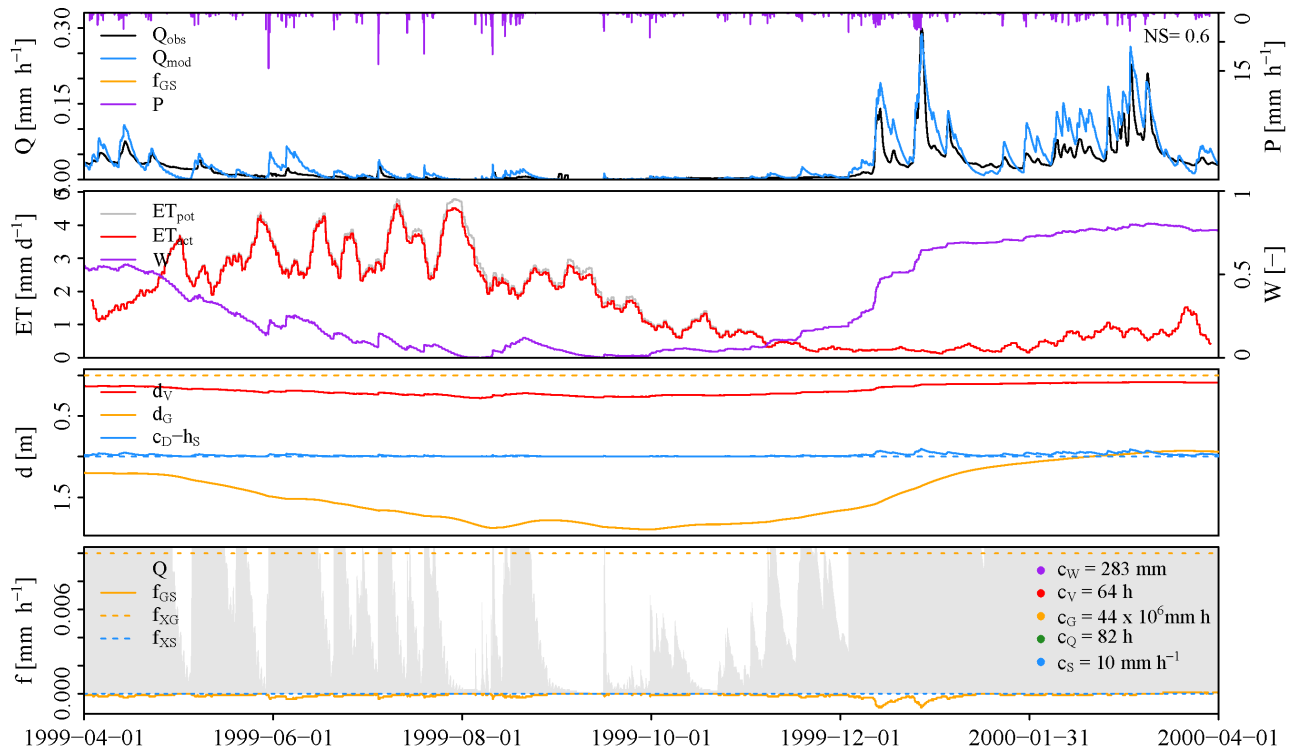


Figure B.43: Validation of the selected parameter set for catchment 0099 on the hydrological year 1999–2000.

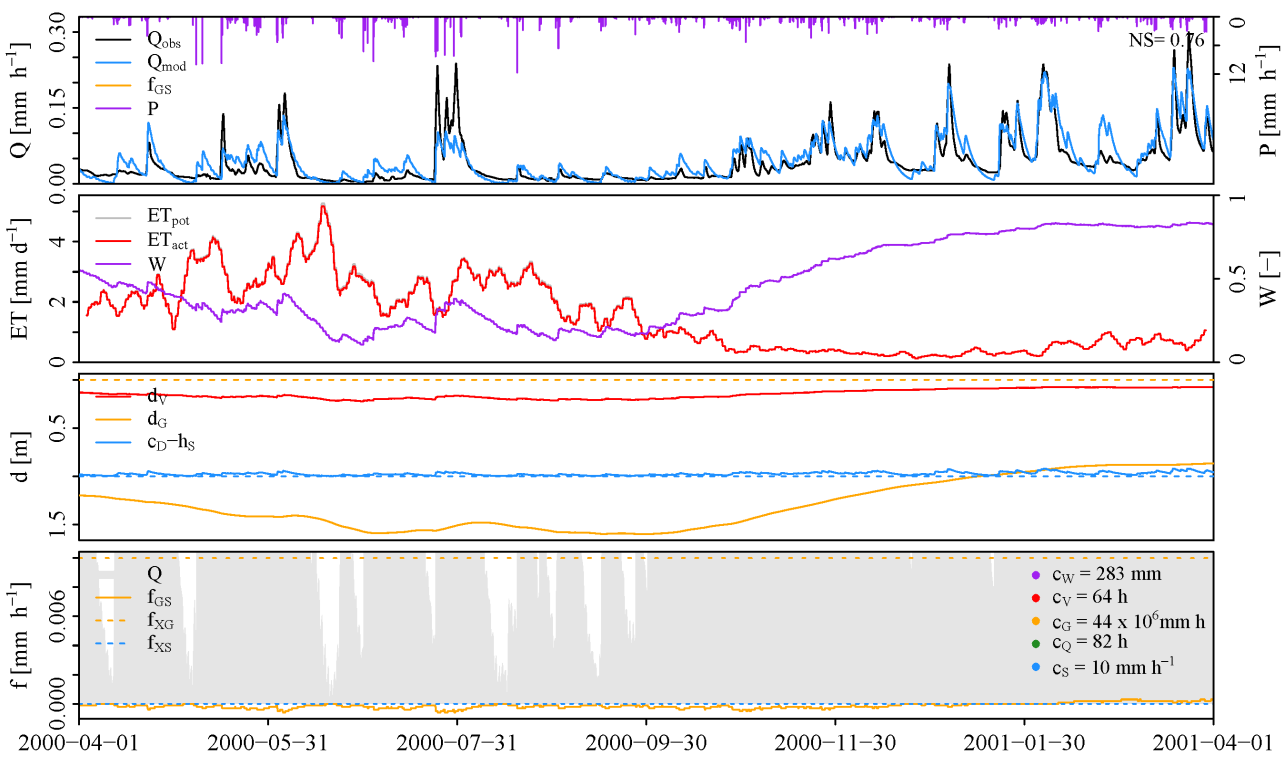


Figure B.44: Validation of the selected parameter set for catchment 0099 on the hydrological year 2000–2001.

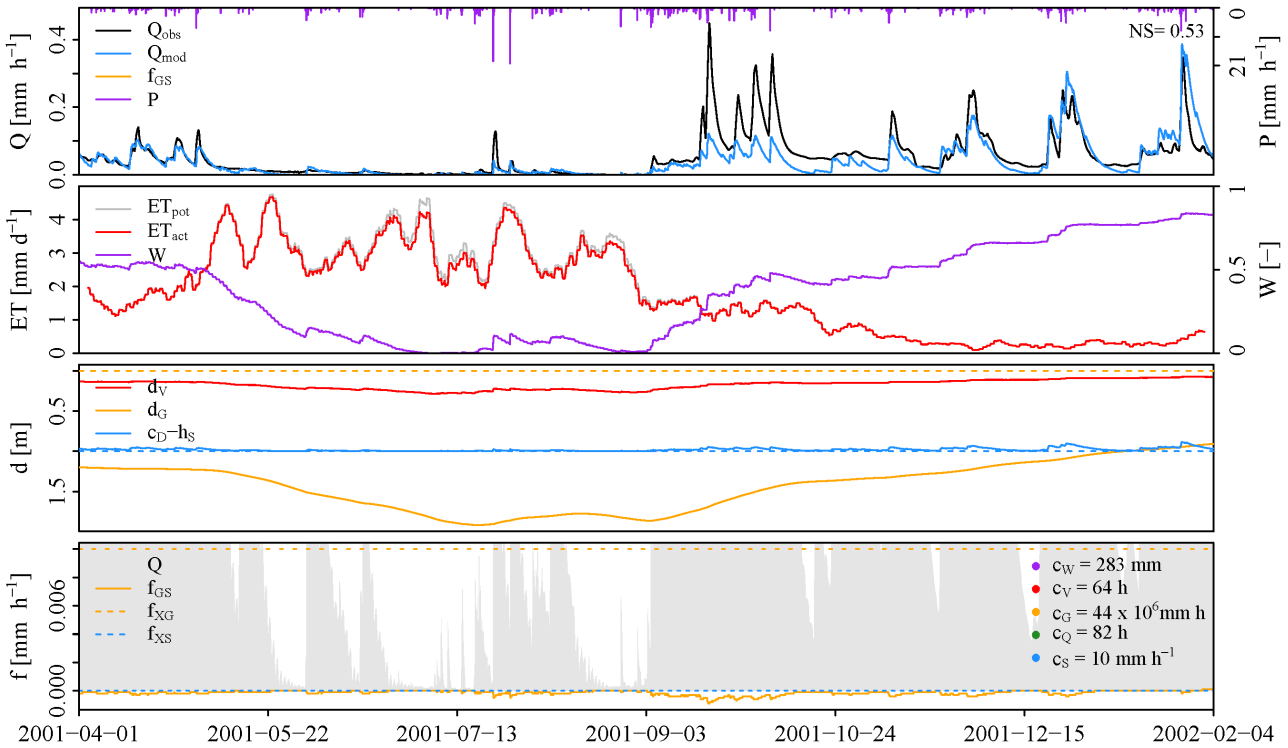


Figure B.45: Validation of the selected parameter set for catchment 0099 on the hydrological year 2001–2002.

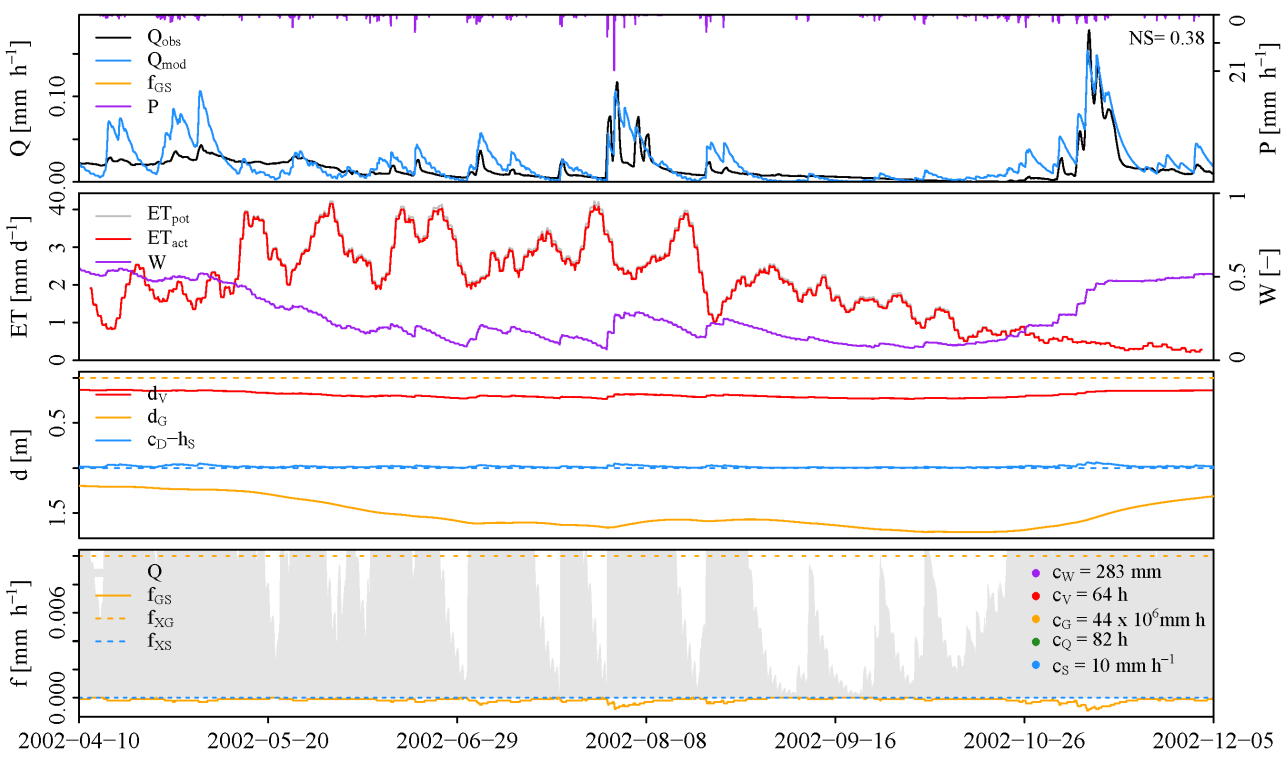


Figure B.46: Validation of the selected parameter set for catchment 0099 on the hydrological year 2002–2003.

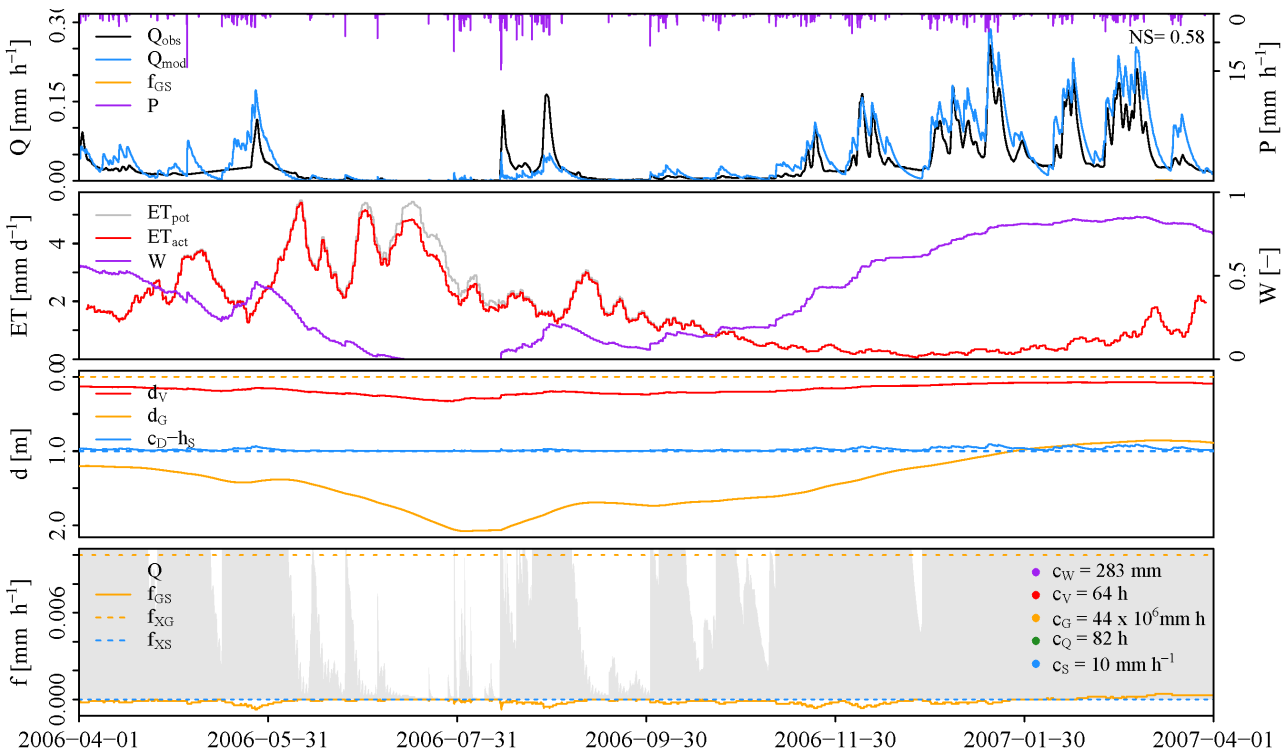


Figure B.47: Validation of the selected parameter set for catchment 0099 on the hydrological year 2006–2007.

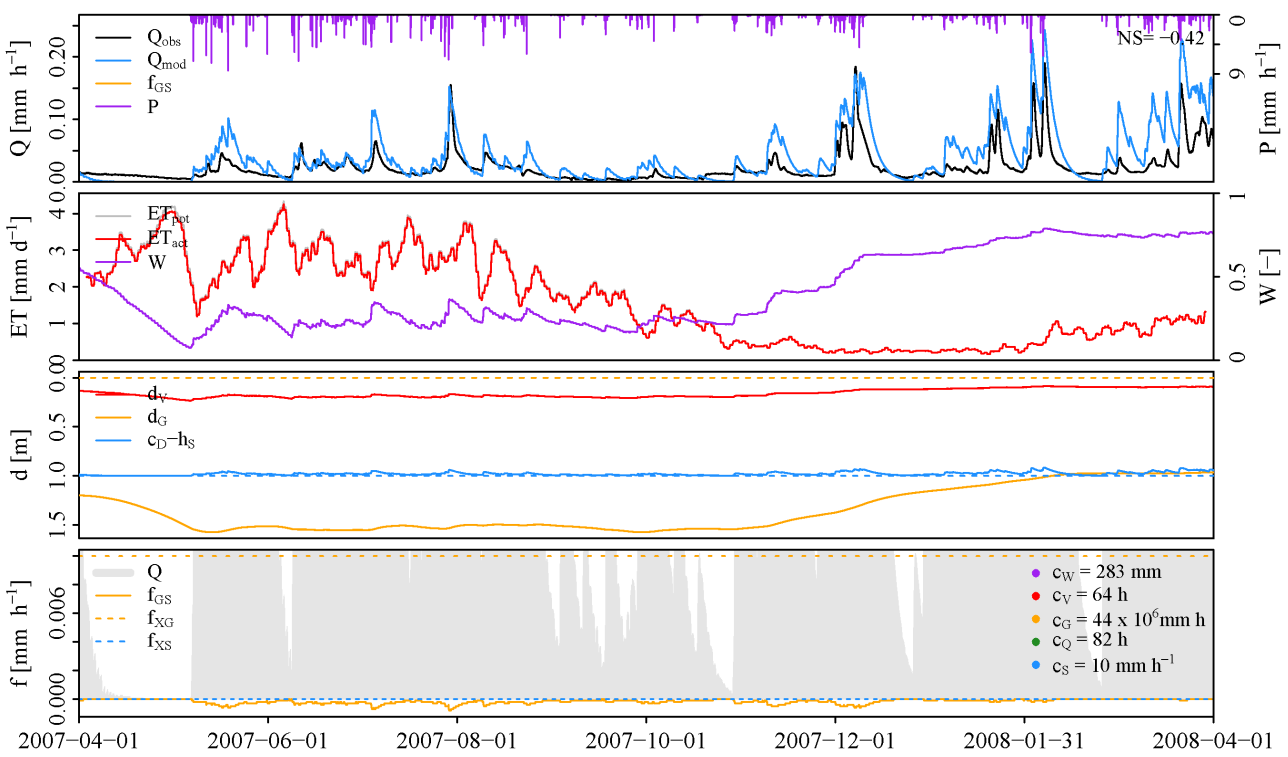


Figure B.48: Validation of the selected parameter set for catchment 0099 on the hydrological year 2007–2008.

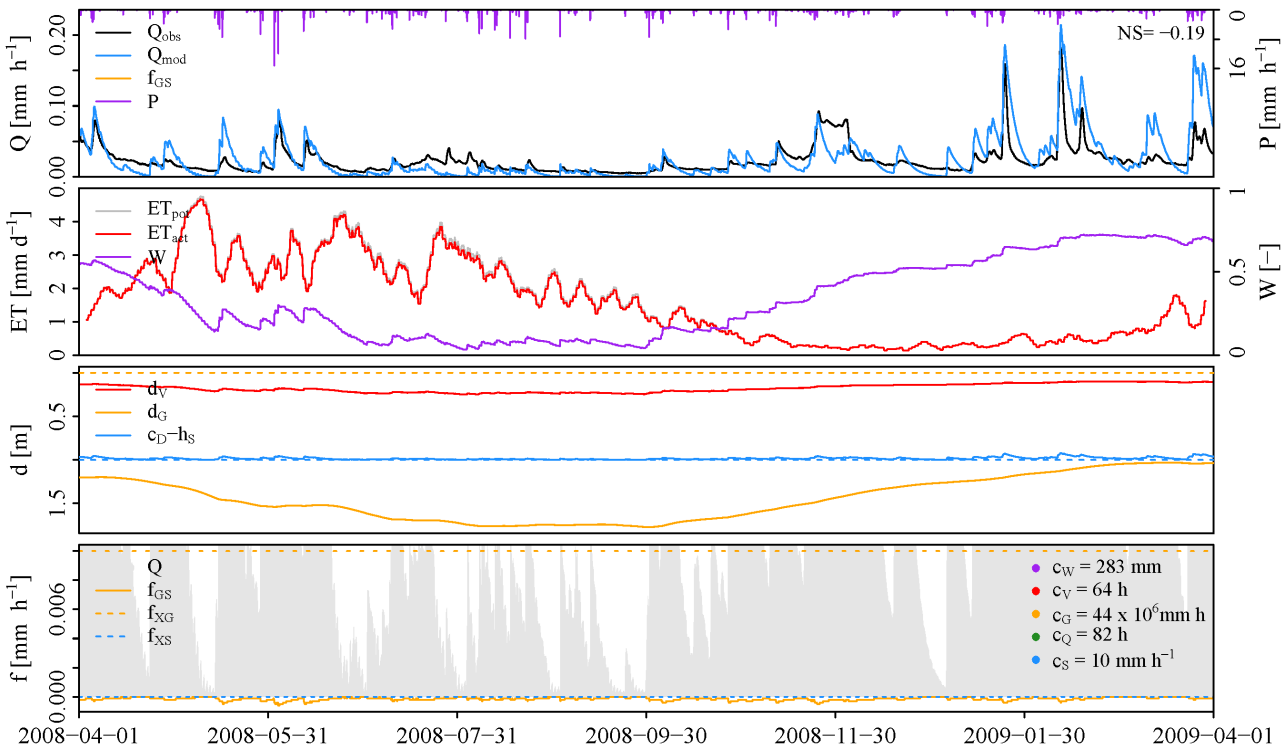


Figure B.49: Validation of the selected parameter set for catchment 0099 on the hydrological year 2008–2009.

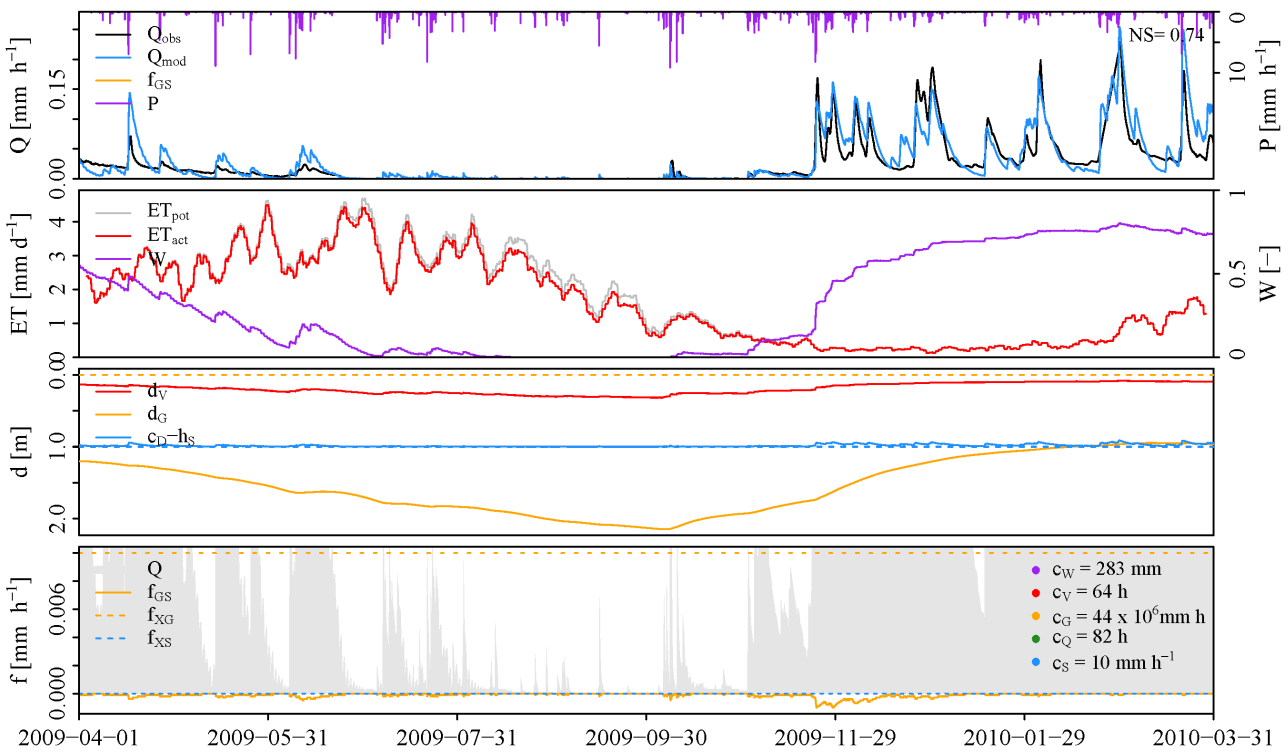


Figure B.50: Validation of the selected parameter set for catchment 0099 on the hydrological year 2009–2010.

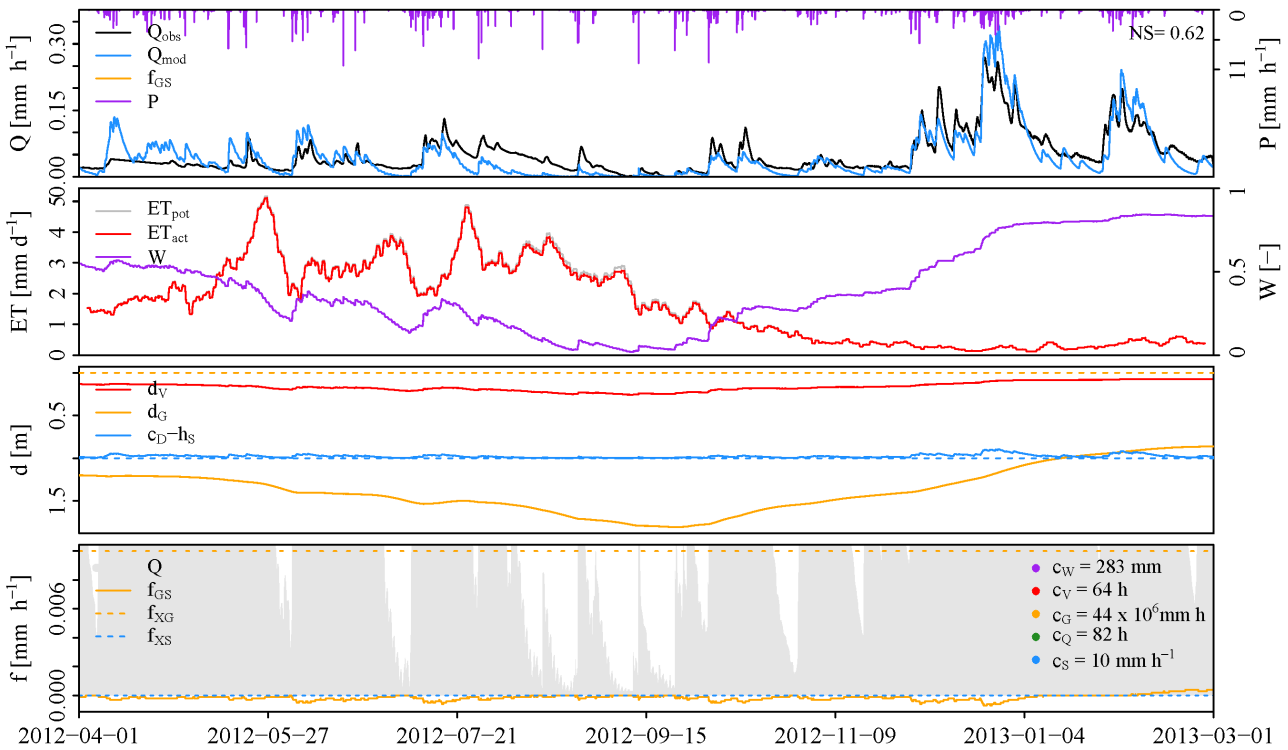
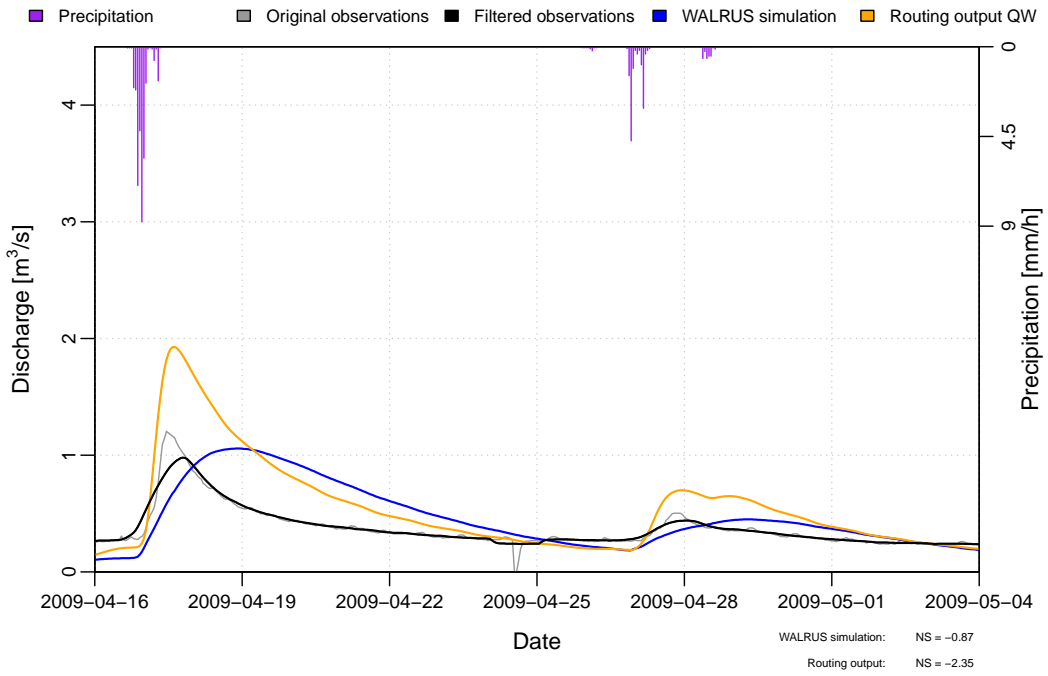


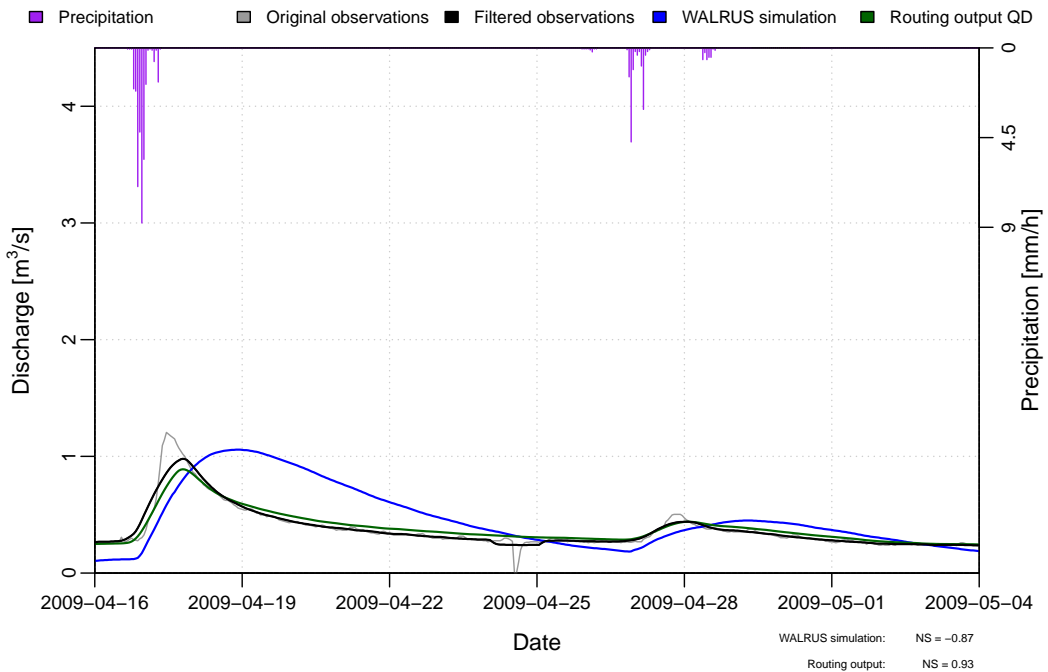
Figure B.51: Validation of the selected parameter set for catchment 0099 on the hydrological year 2012–2013.



# C | Reservoir routing plots

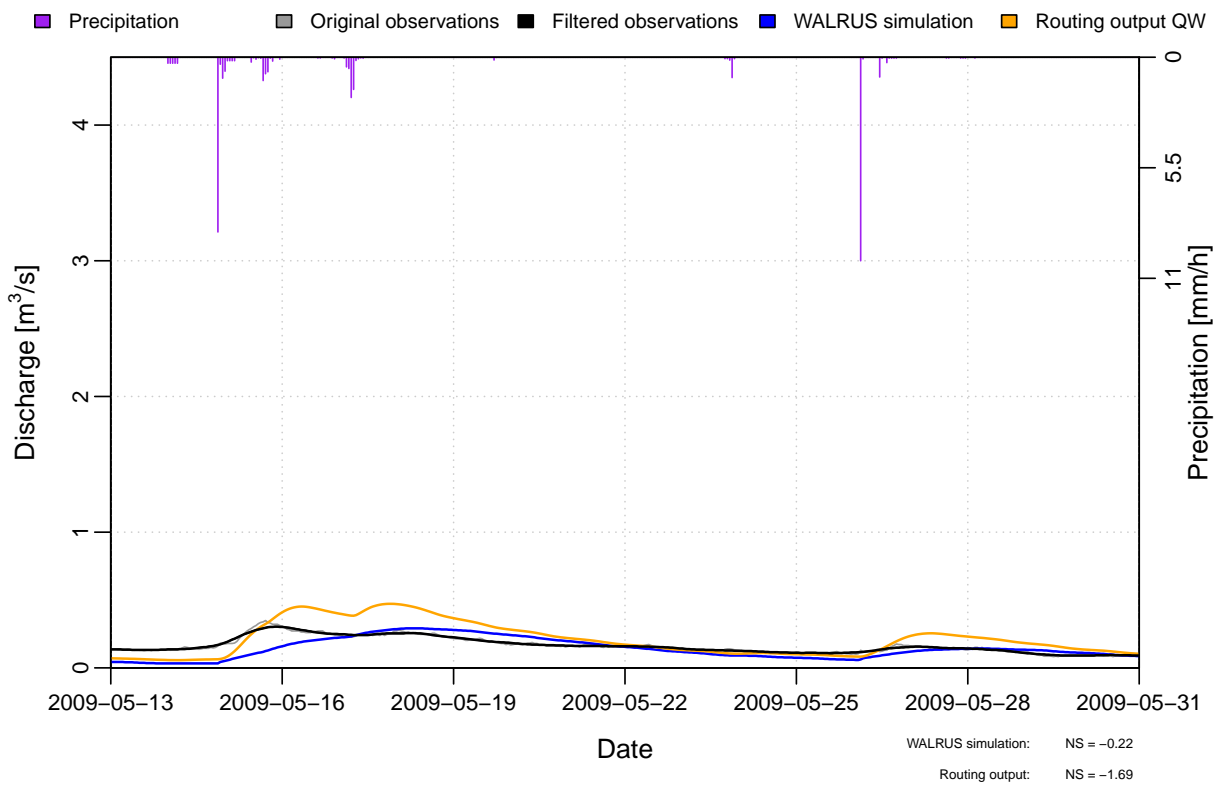


(a) Results of the routing technique using WALRUS output of stations 0098 and 0099.

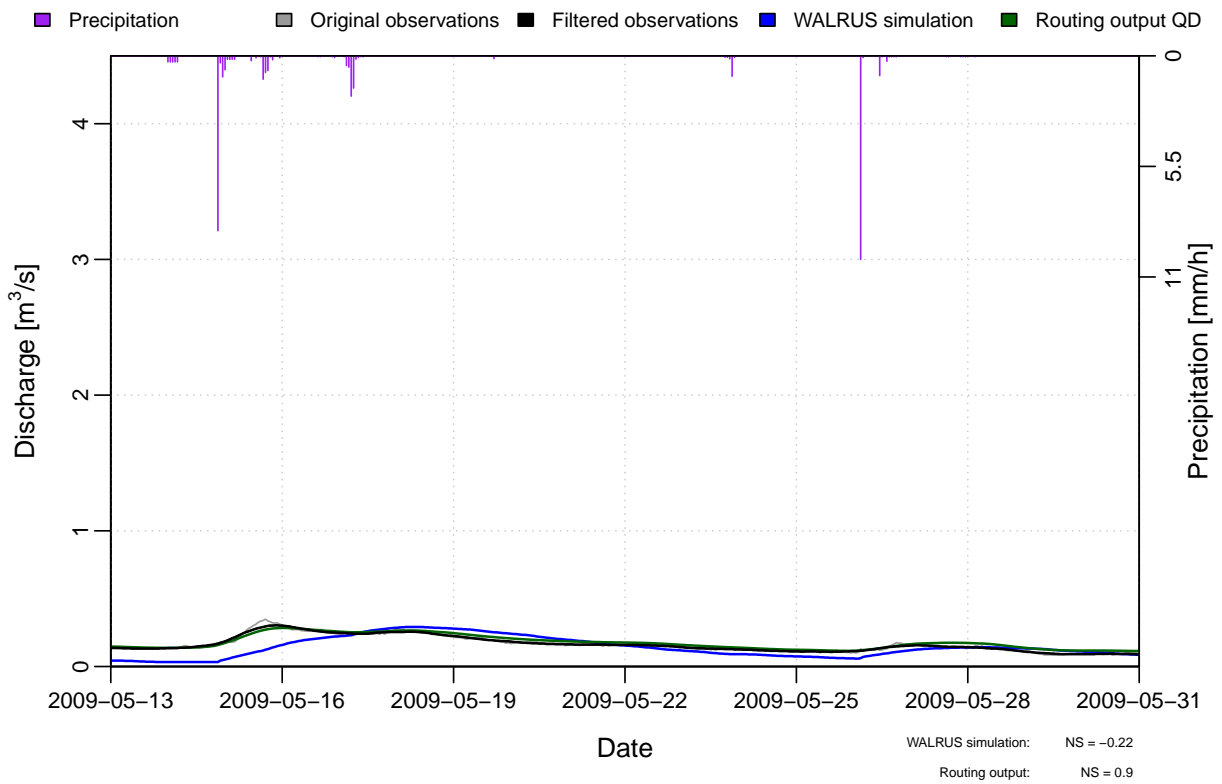


(b) Results of the routing technique using observed discharges of stations 0098 and 0099.

Figure C.1: Routing results for the hydrological year 2009–2010, zoomed in on a 18 days period (1).

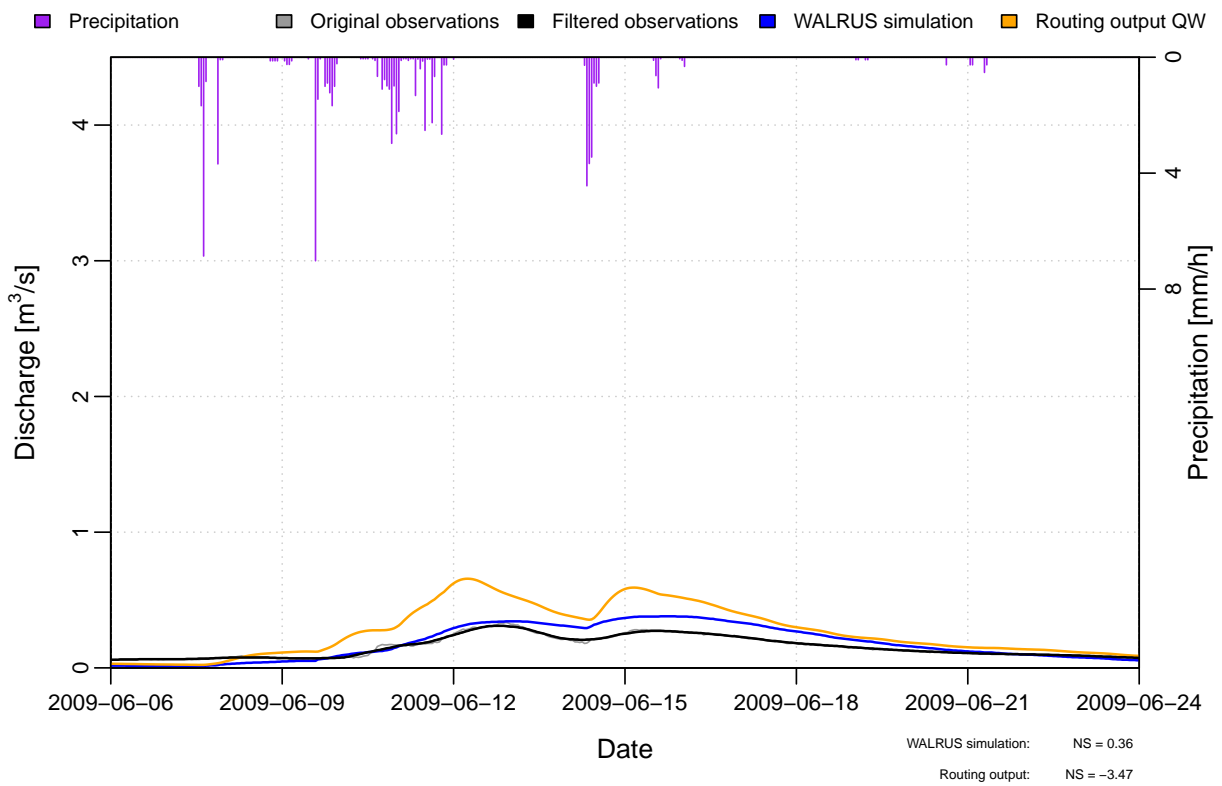


(a) Results of the routing technique using WALRUS output of stations 0098 and 0099.

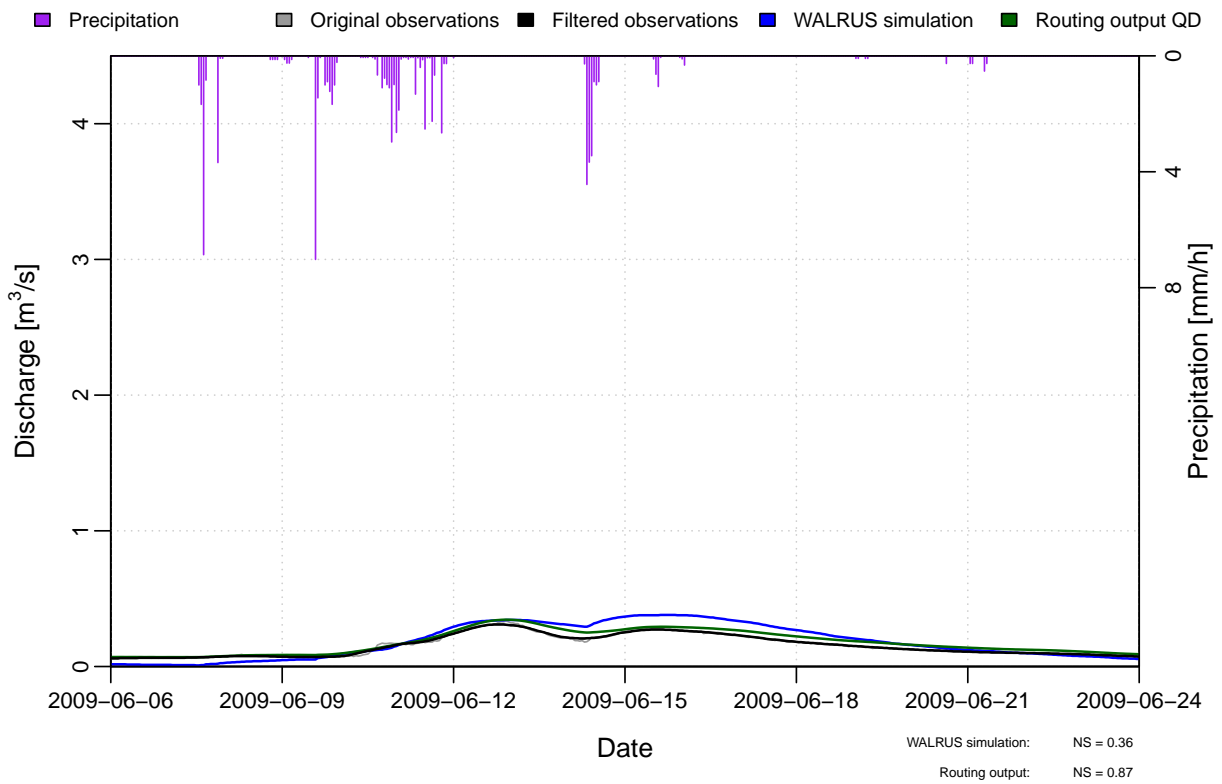


(b) Results of the routing technique using observed discharges of stations 0098 and 0099.

Figure C.2: Routing results for the hydrological year 2009–2010, zoomed in on a 18 days period (2).

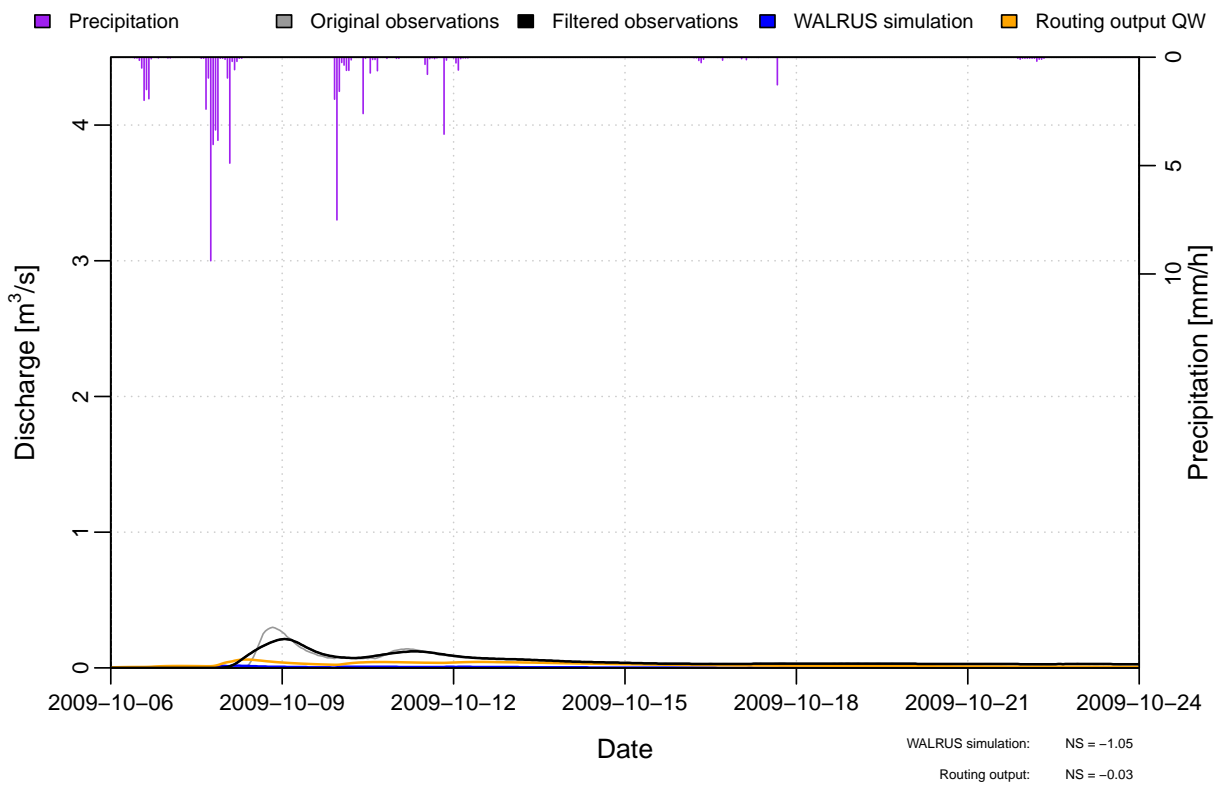


(a) Results of the routing technique using WALRUS output of stations 0098 and 0099.

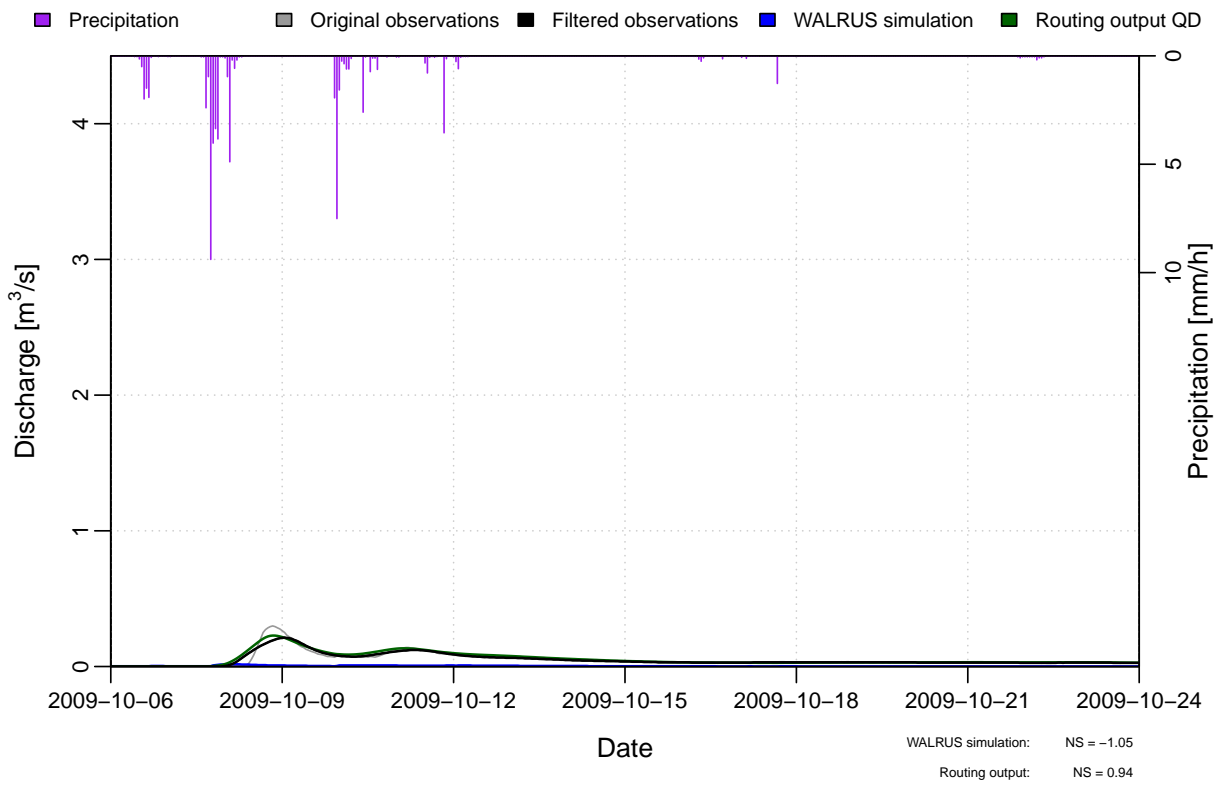


(b) Results of the routing technique using observed discharges of stations 0098 and 0099.

Figure C.3: Routing results for the hydrological year 2009–2010, zoomed in on a 18 days period (3).

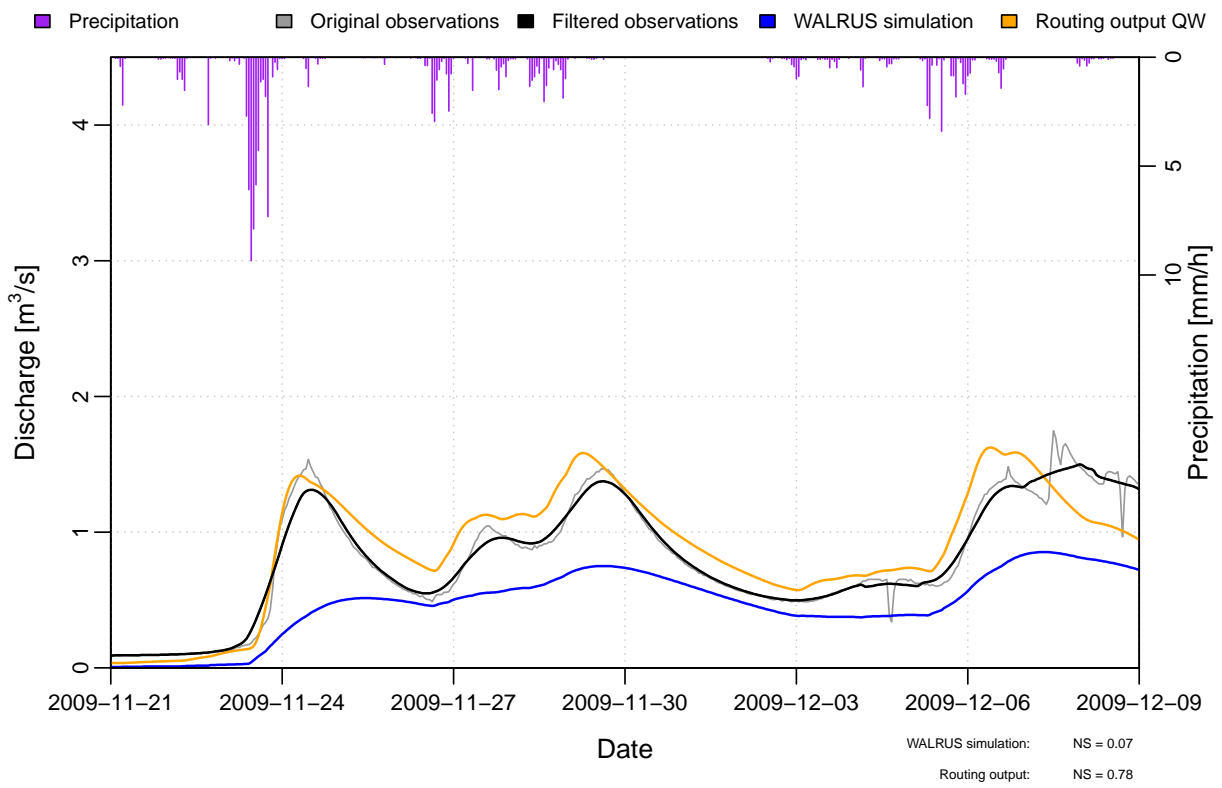


(a) Results of the routing technique using WALRUS output of stations 0098 and 0099.

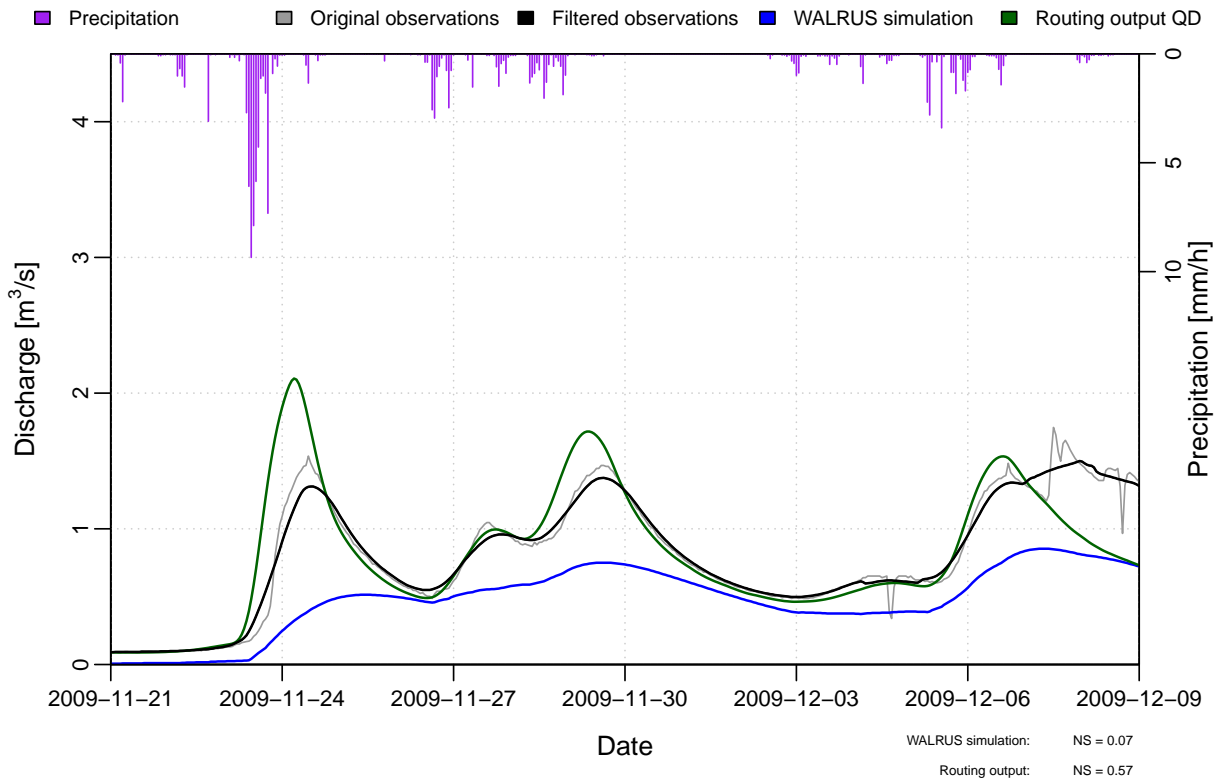


(b) Results of the routing technique using observed discharges of stations 0098 and 0099.

Figure C.4: Routing results for the hydrological year 2009–2010, zoomed in on a 18 days period (4).

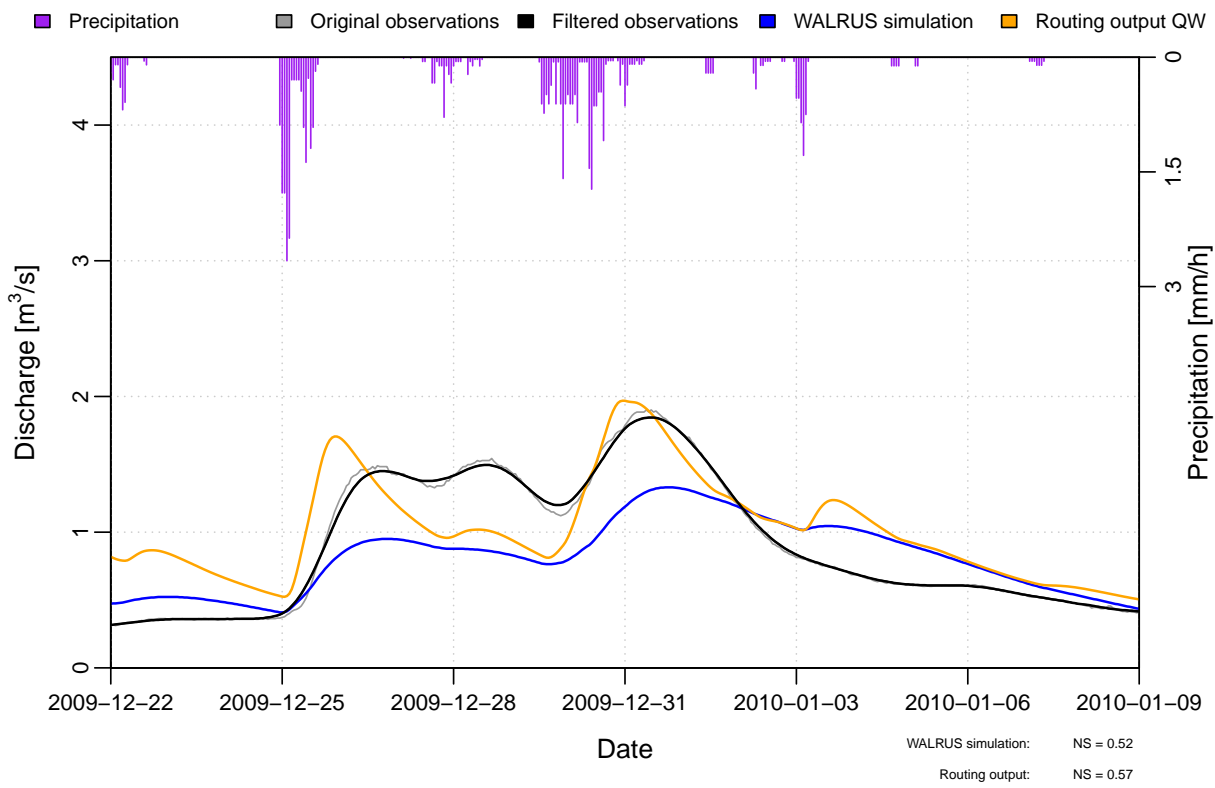


(a) Results of the routing technique using WALRUS output of stations 0098 and 0099.

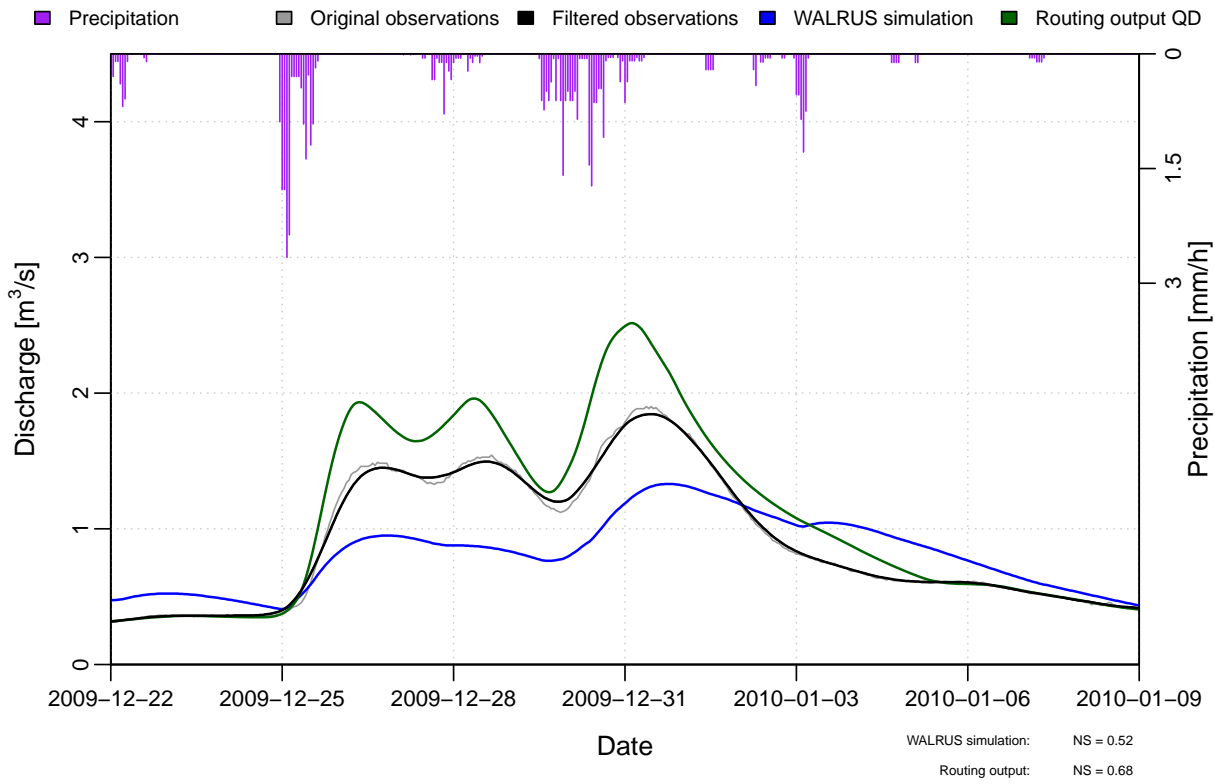


(b) Results of the routing technique using observed discharges of stations 0098 and 0099.

Figure C.5: Routing results for the hydrological year 2009–2010, zoomed in on a 18 days period (5).

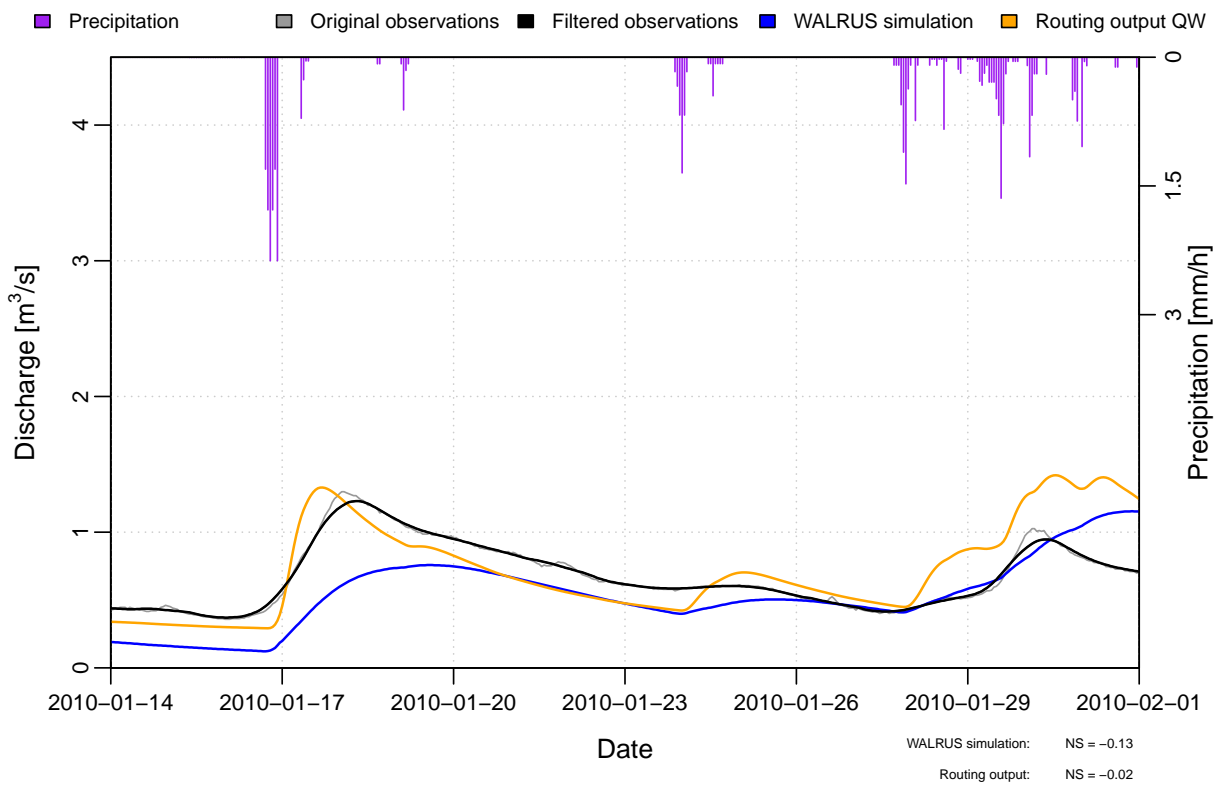


(a) Results of the routing technique using WALRUS output of stations 0098 and 0099.

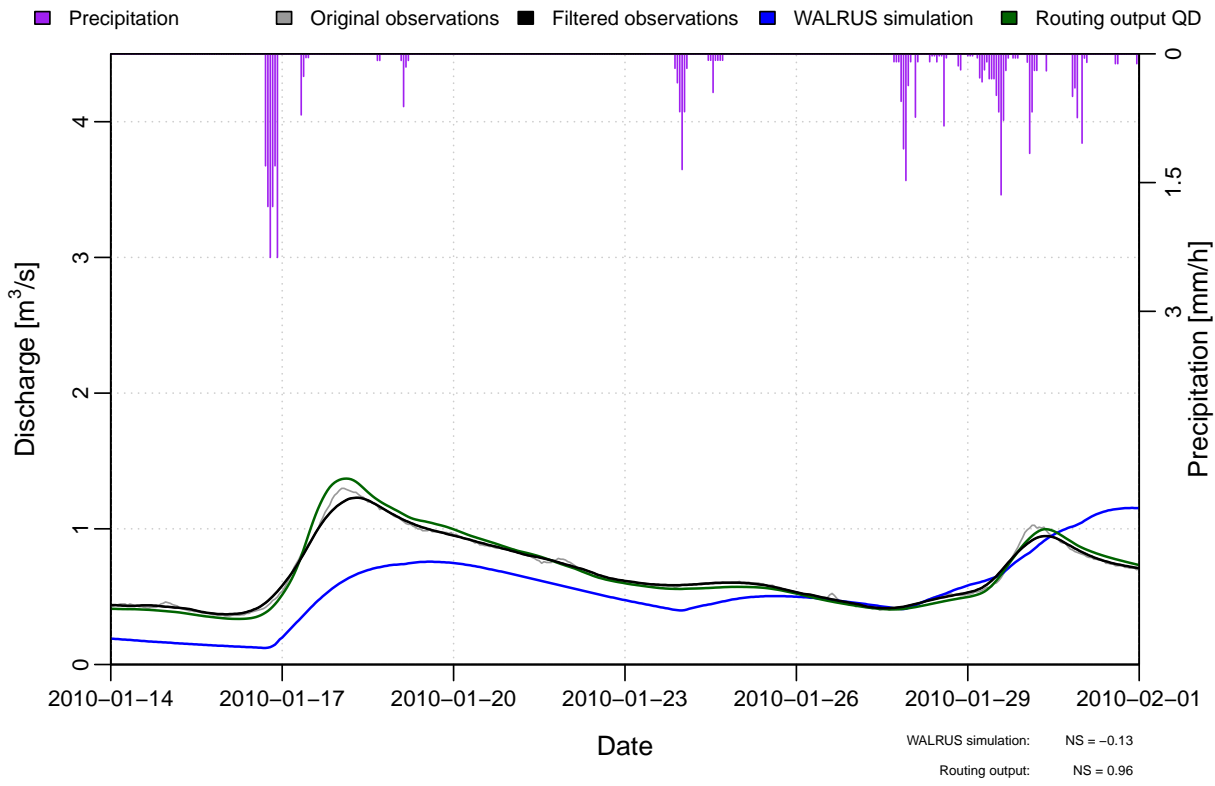


(b) Results of the routing technique using observed discharges of stations 0098 and 0099.

Figure C.6: Routing results for the hydrological year 2009–2010, zoomed in on a 18 days period (6).

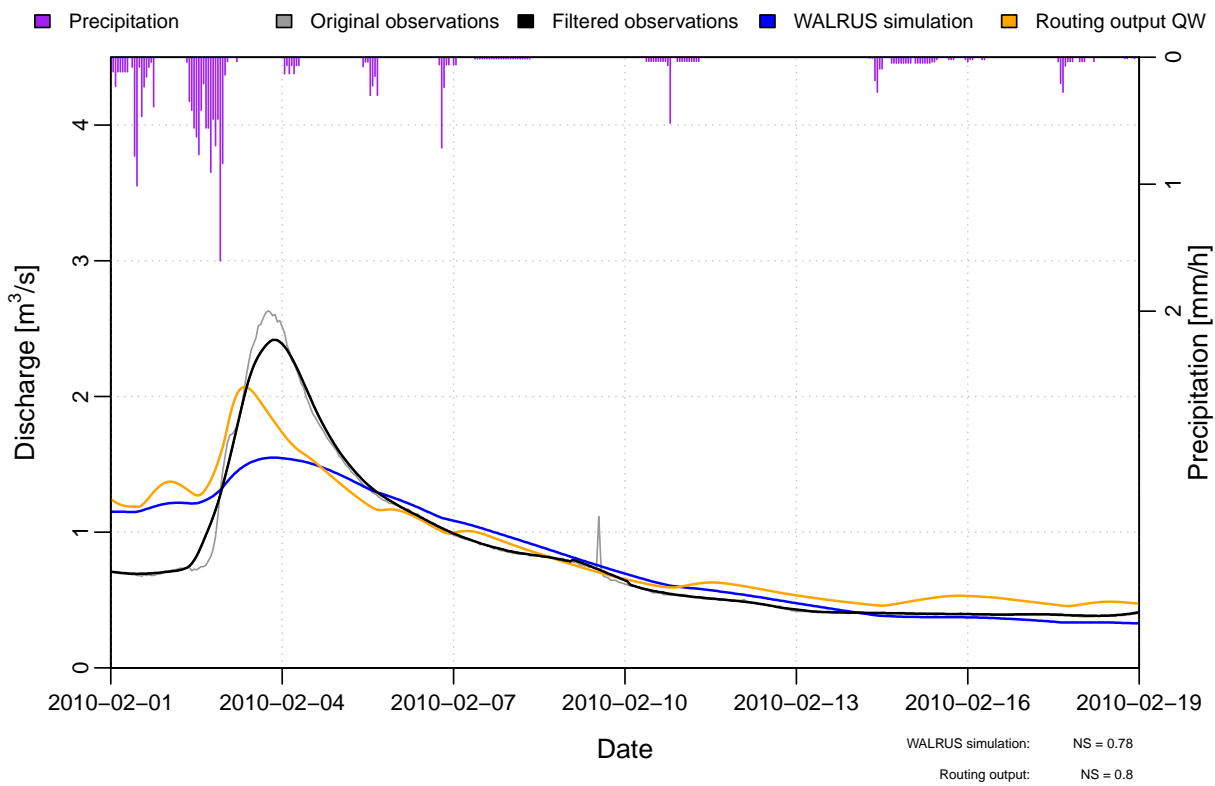


(a) Results of the routing technique using WALRUS output of stations 0098 and 0099.

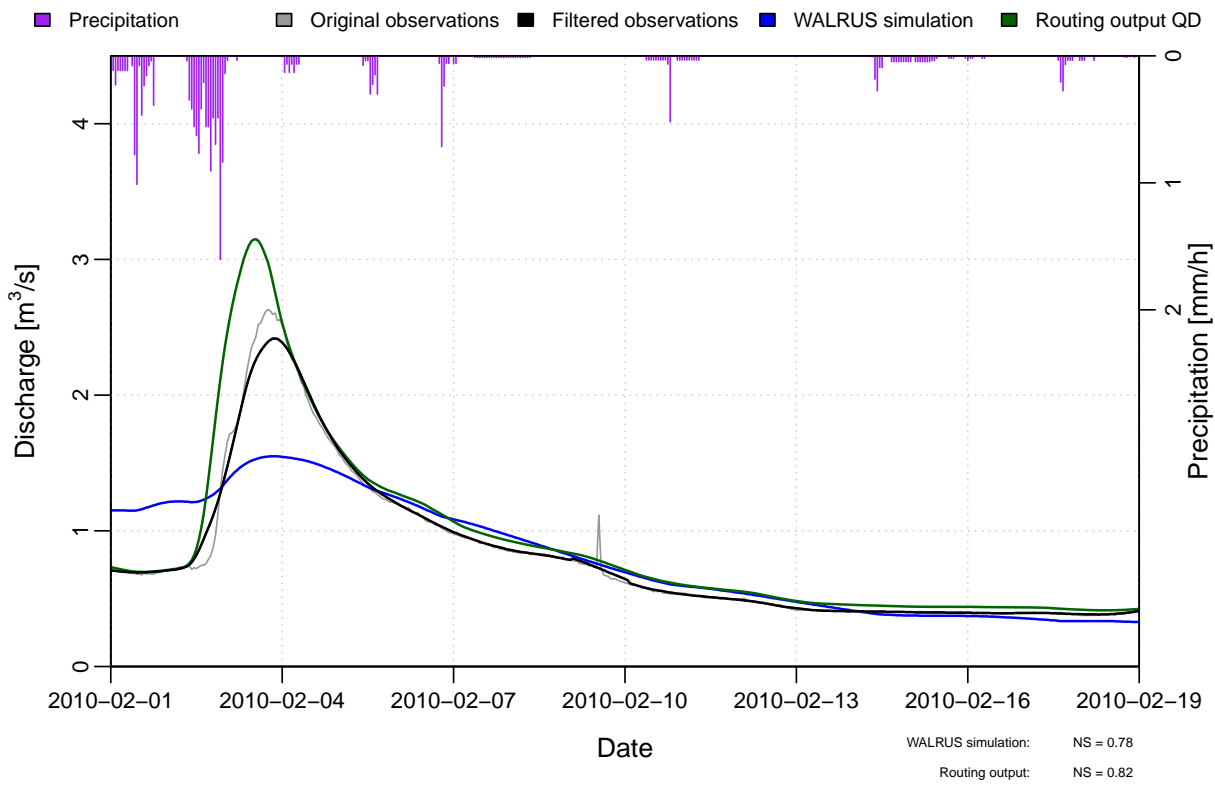


(b) Results of the routing technique using observed discharges of stations 0098 and 0099.

Figure C.7: Routing results for the hydrological year 2009–2010, zoomed in on a 18 days period (7).

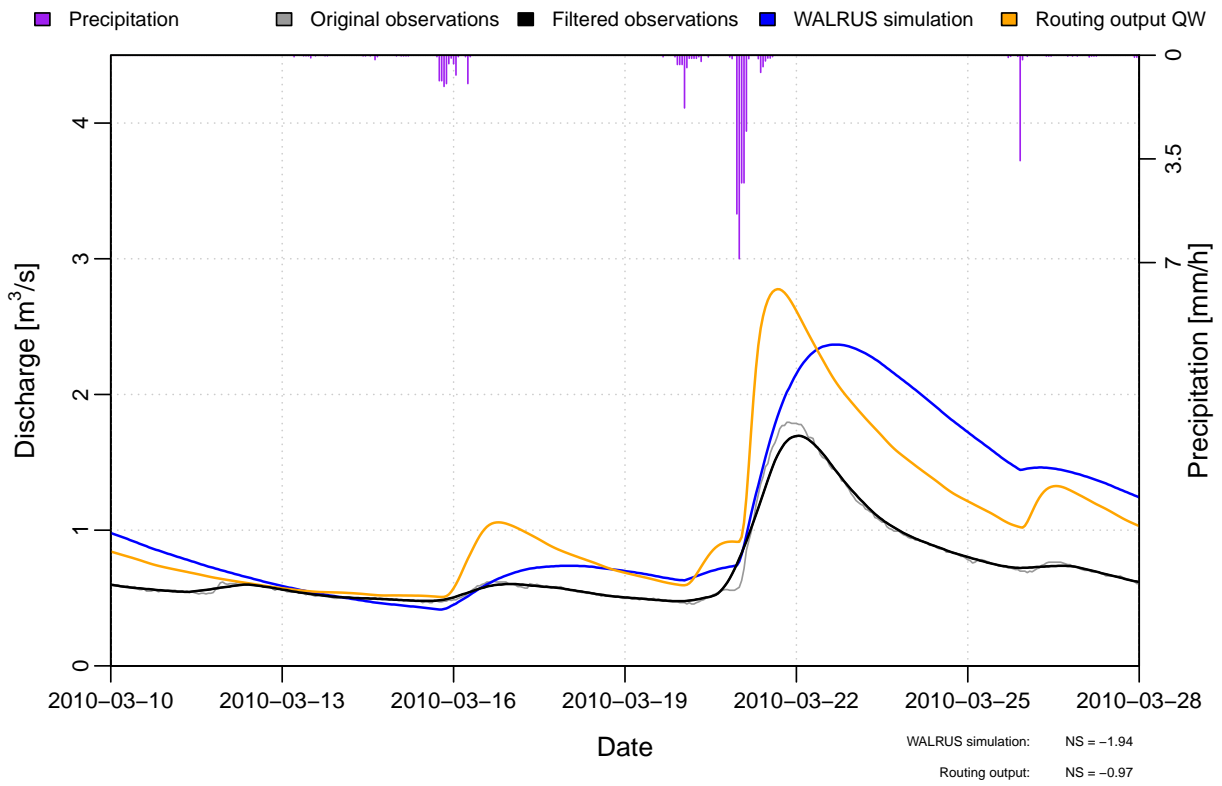


(a) Results of the routing technique using WALRUS output of stations 0098 and 0099.

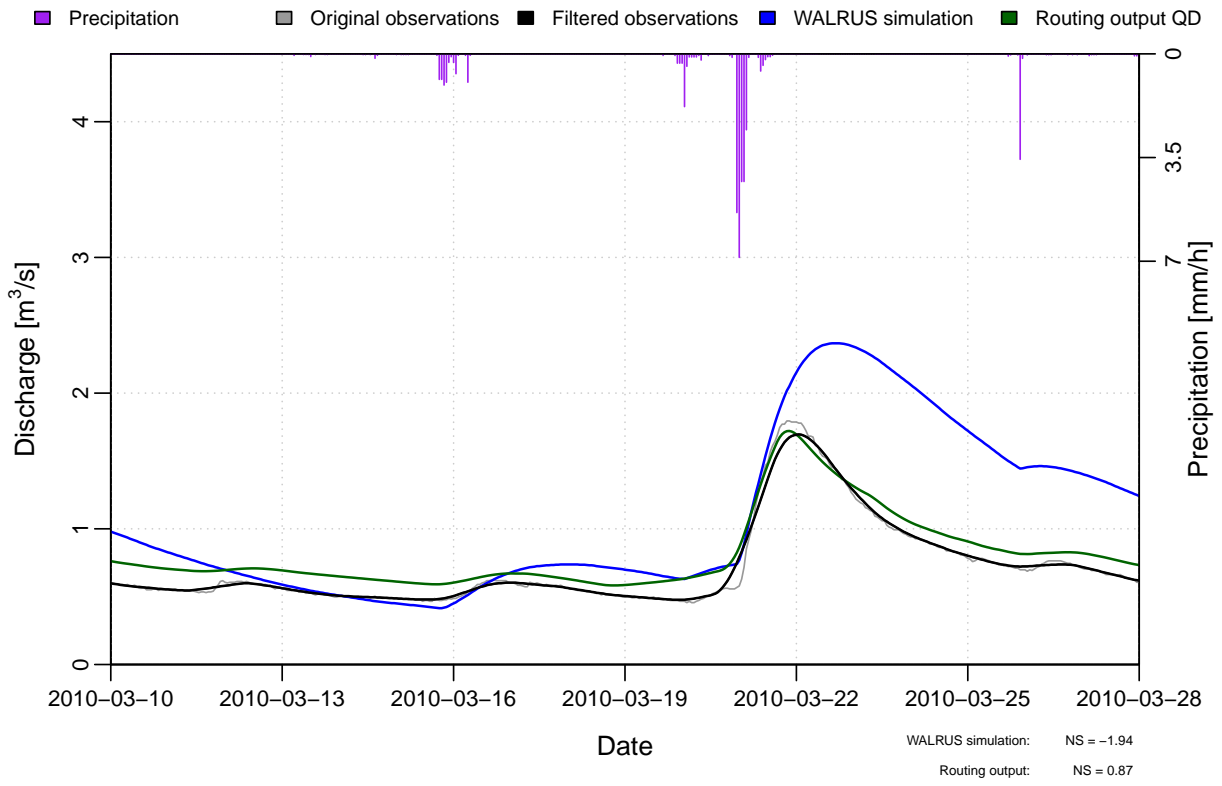


(b) Results of the routing technique using observed discharges of stations 0098 and 0099.

Figure C.8: Routing results for the hydrological year 2009–2010, zoomed in on a 18 days period (8).

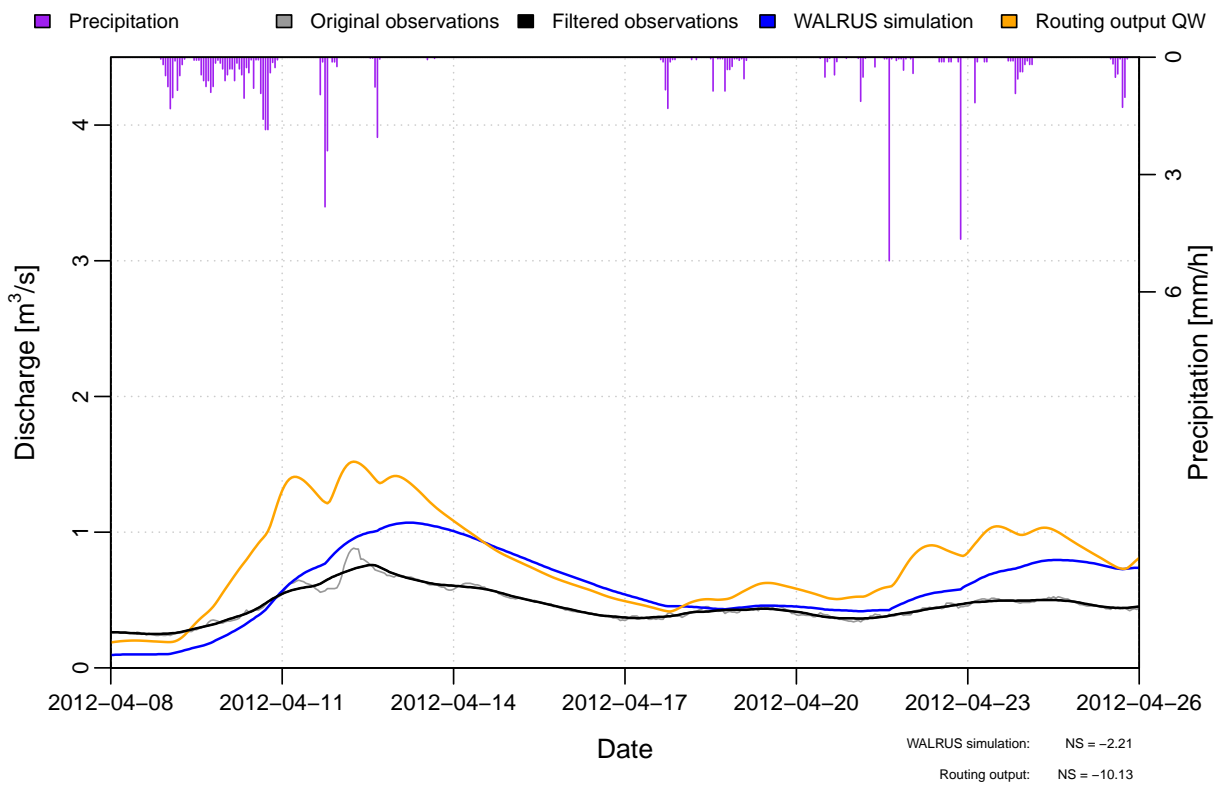


(a) Results of the routing technique using WALRUS output of stations 0098 and 0099.

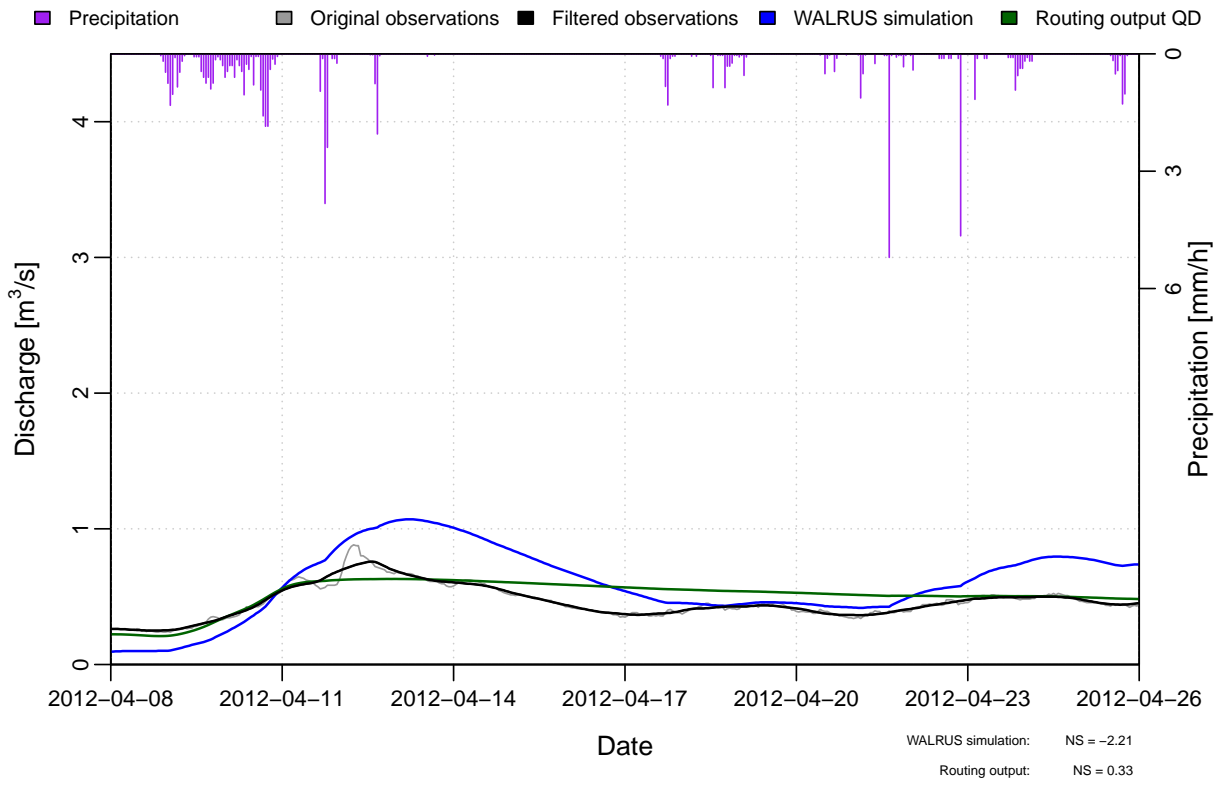


(b) Results of the routing technique using observed discharges of stations 0098 and 0099.

Figure C.9: Routing results for the hydrological year 2009–2010, zoomed in on a 18 days period (9).

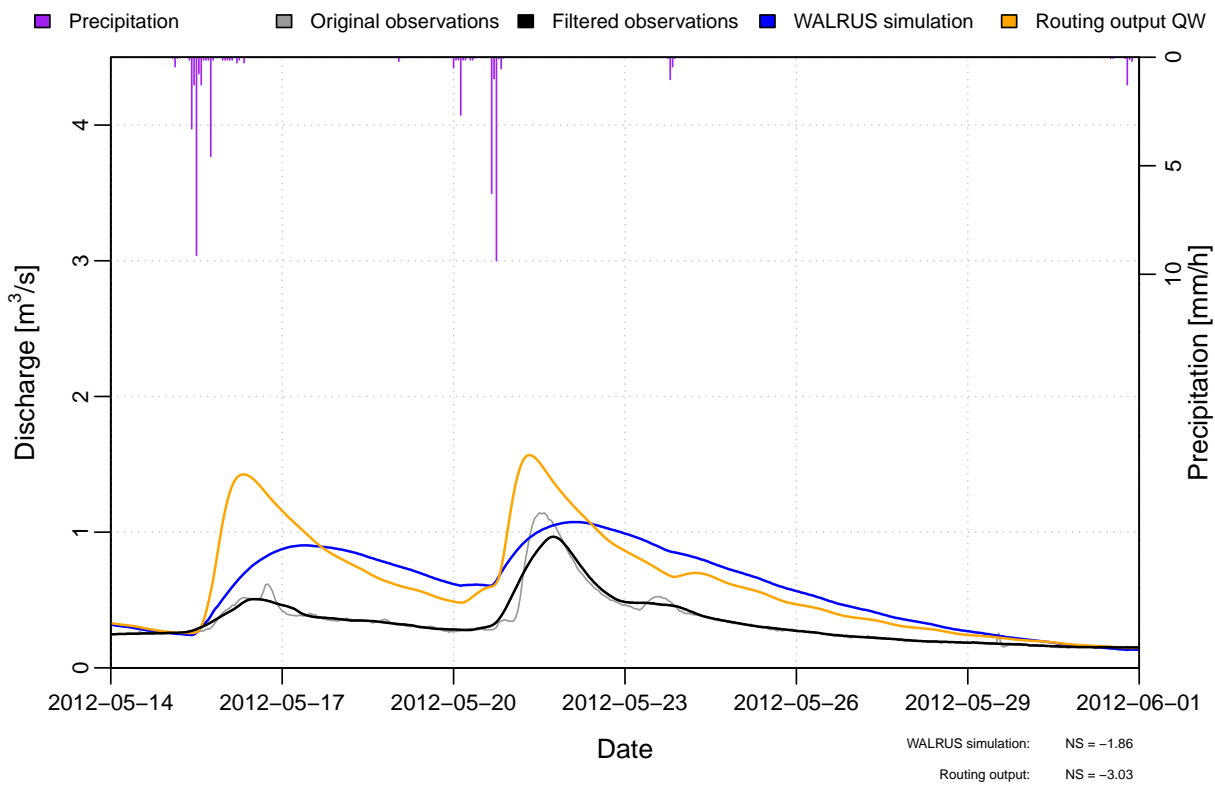


(a) Results of the routing technique using WALRUS output of stations 0098 and 0099.

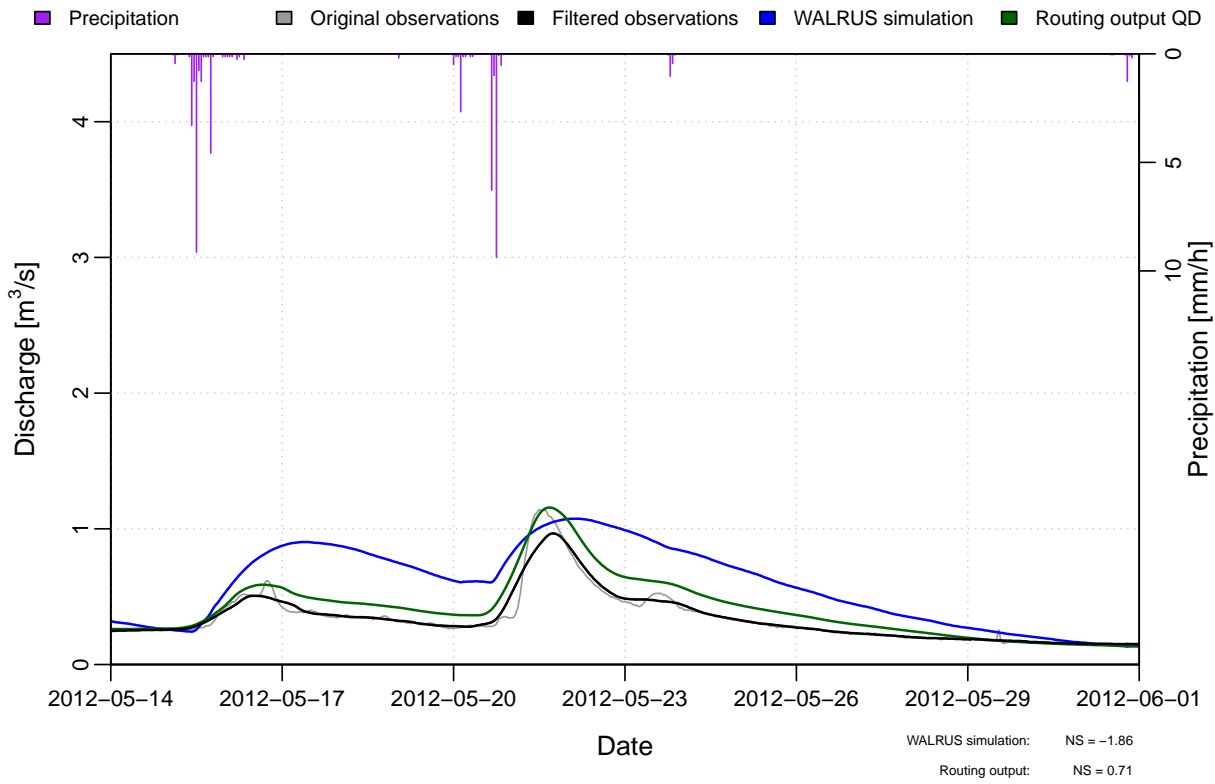


(b) Results of the routing technique using observed discharges of stations 0098 and 0099.

Figure C.10: Routing results for the hydrological year 2012–2013, zoomed in on a 18 days period (1).

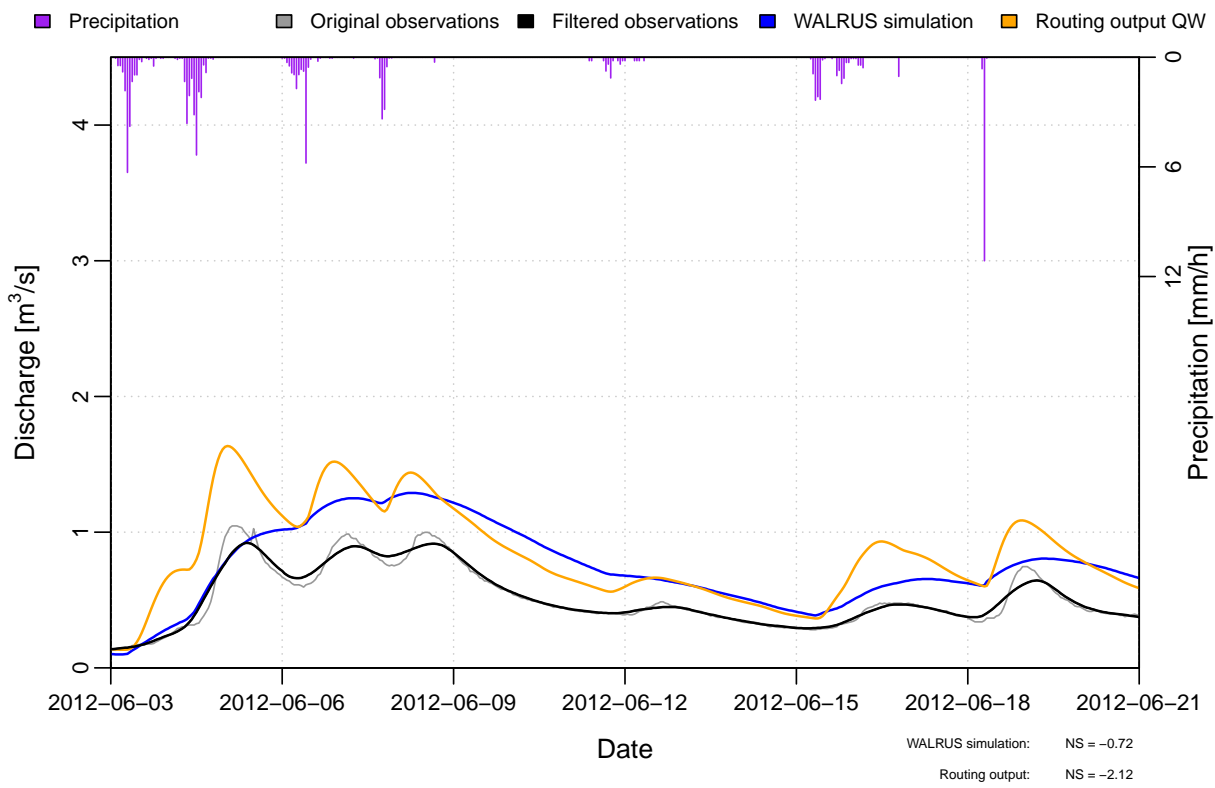


(a) Results of the routing technique using WALRUS output of stations 0098 and 0099.

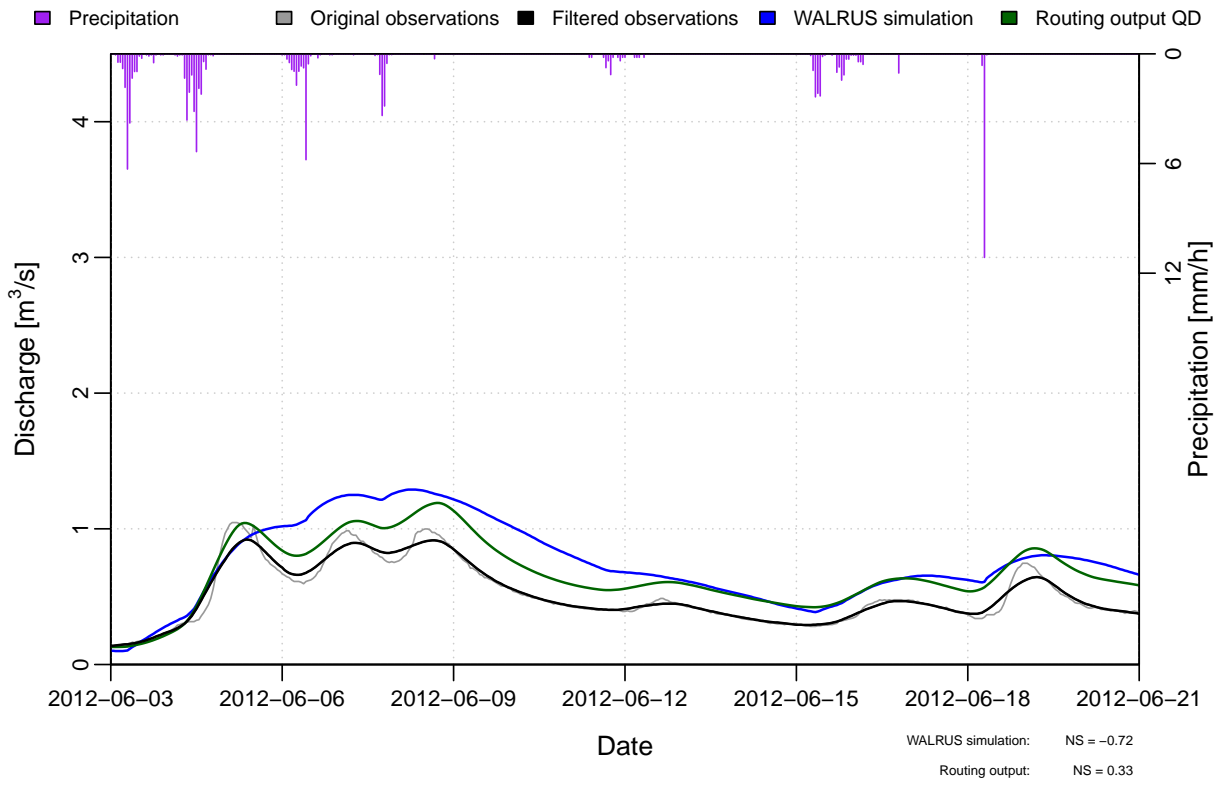


(b) Results of the routing technique using observed discharges of stations 0098 and 0099.

Figure C.11: Routing results for the hydrological year 2012–2013, zoomed in on a 18 days period (2).

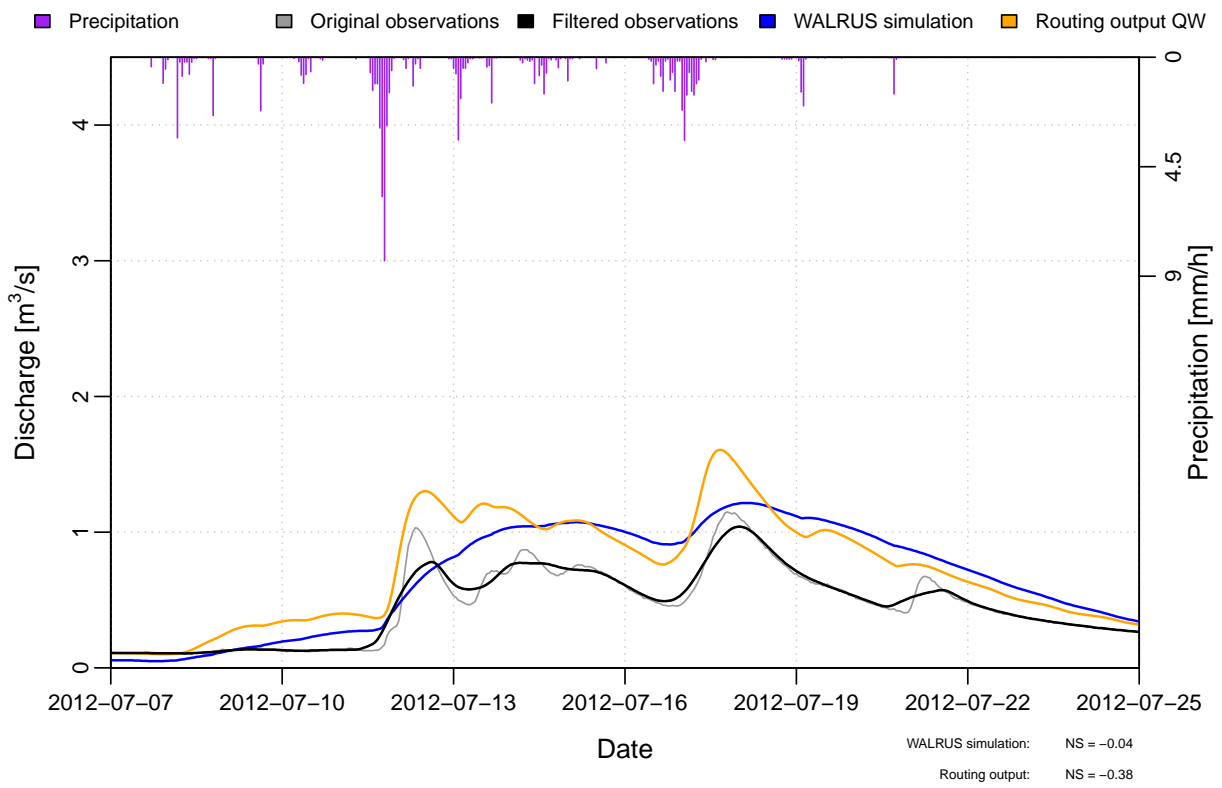


(a) Results of the routing technique using WALRUS output of stations 0098 and 0099.

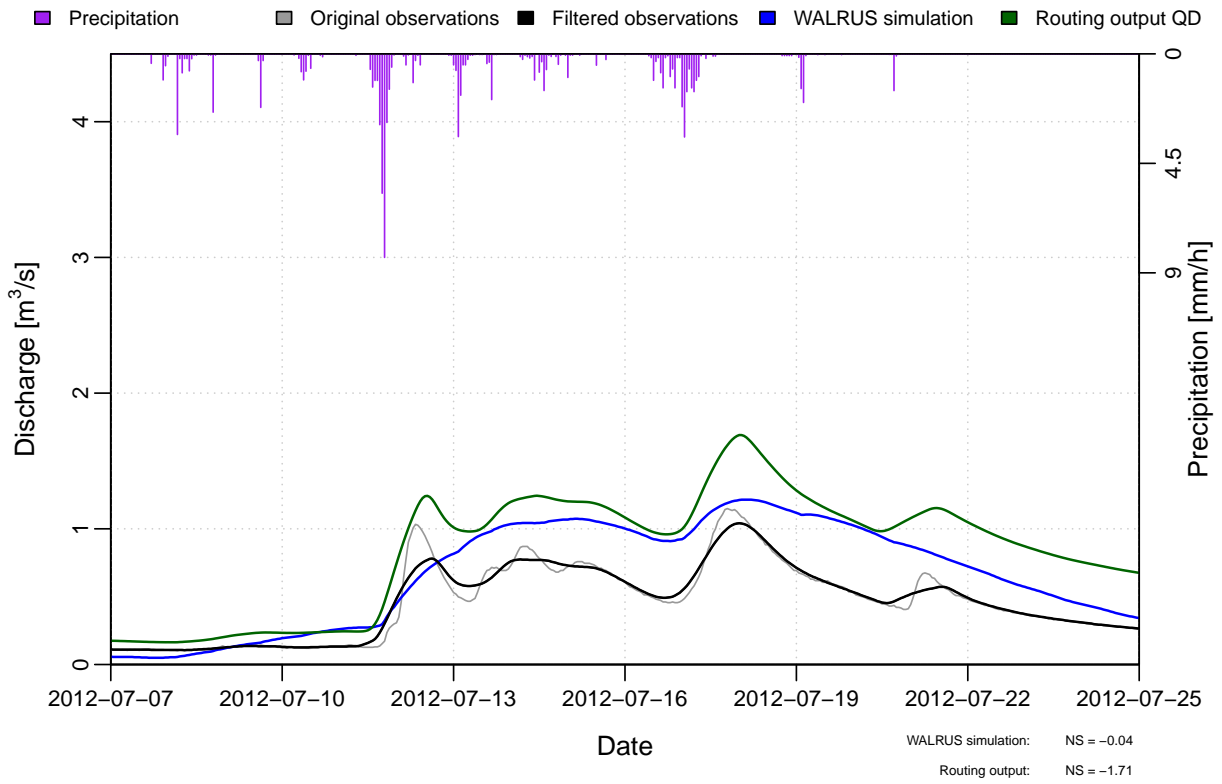


(b) Results of the routing technique using observed discharges of stations 0098 and 0099.

Figure C.12: Routing results for the hydrological year 2012–2013, zoomed in on a 18 days period (3).



(a) Results of the routing technique using WALRUS output of stations 0098 and 0099.



(b) Results of the routing technique using observed discharges of stations 0098 and 0099.

Figure C.13: Routing results for the hydrological year 2012–2013, zoomed in on a 18 days period (4).

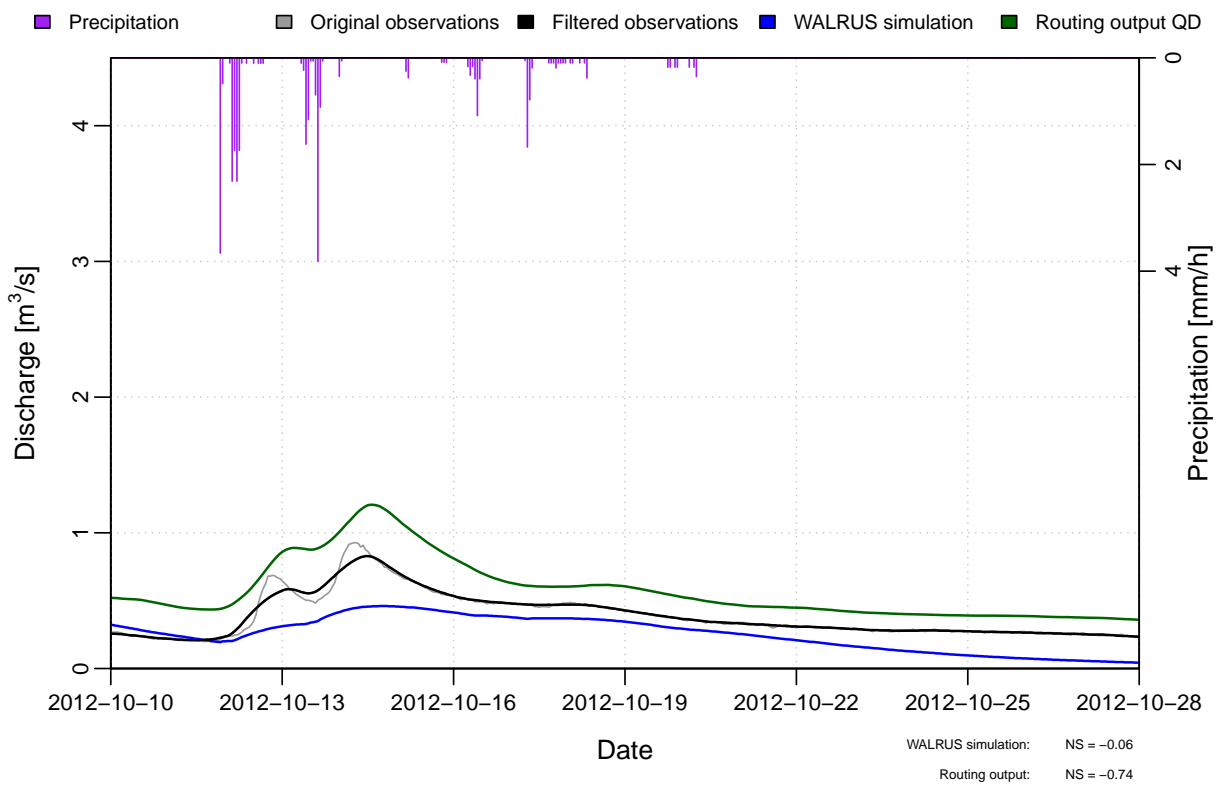
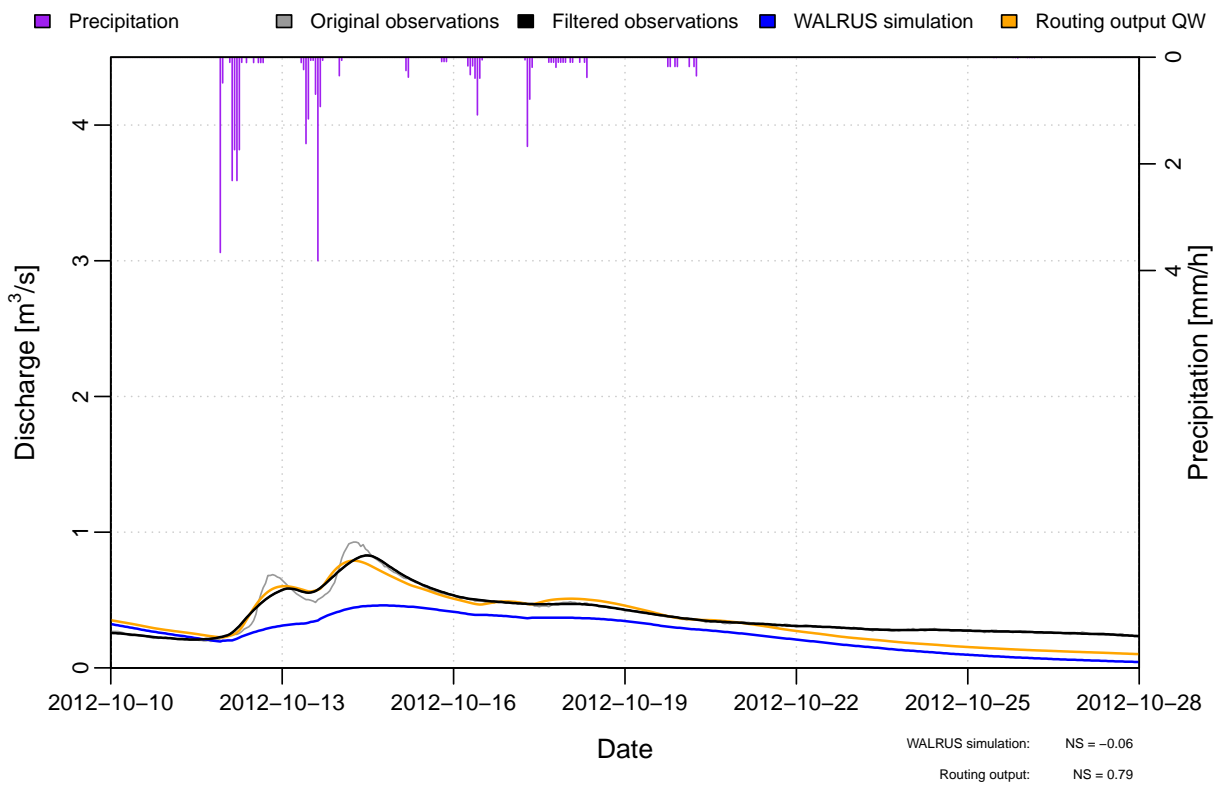
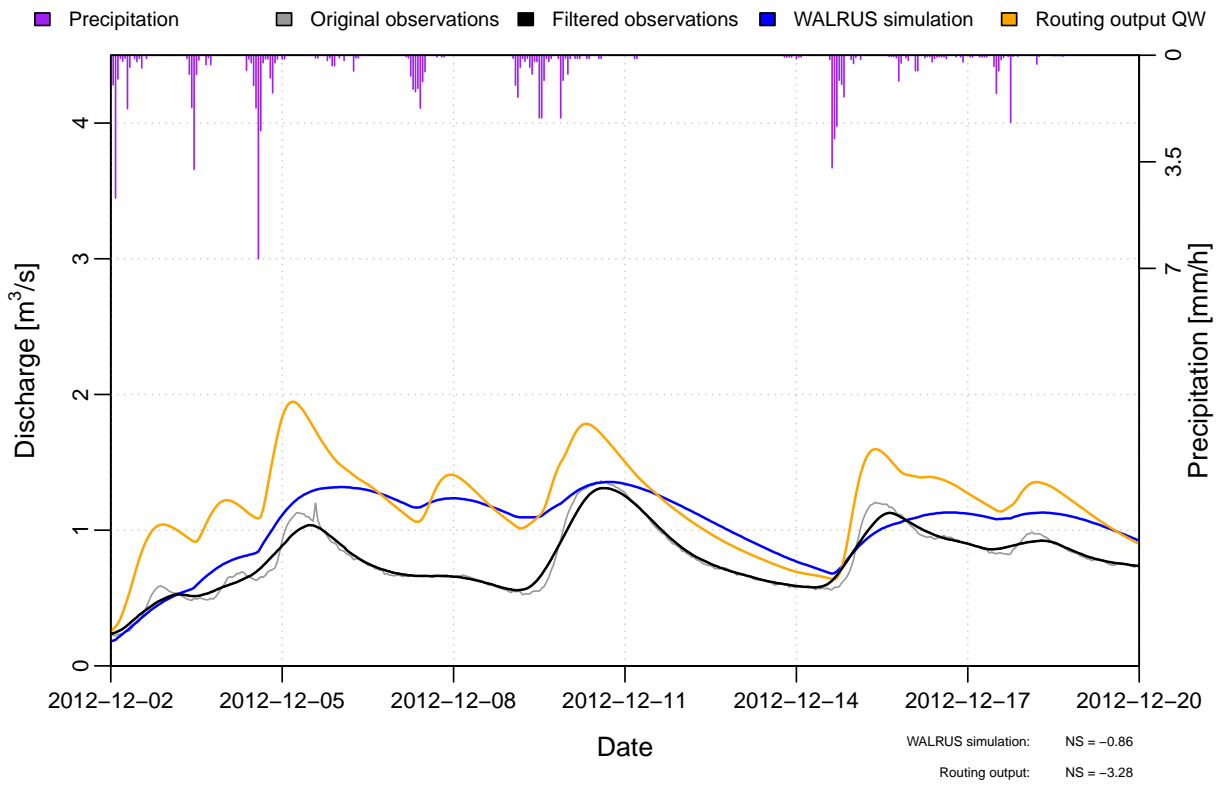
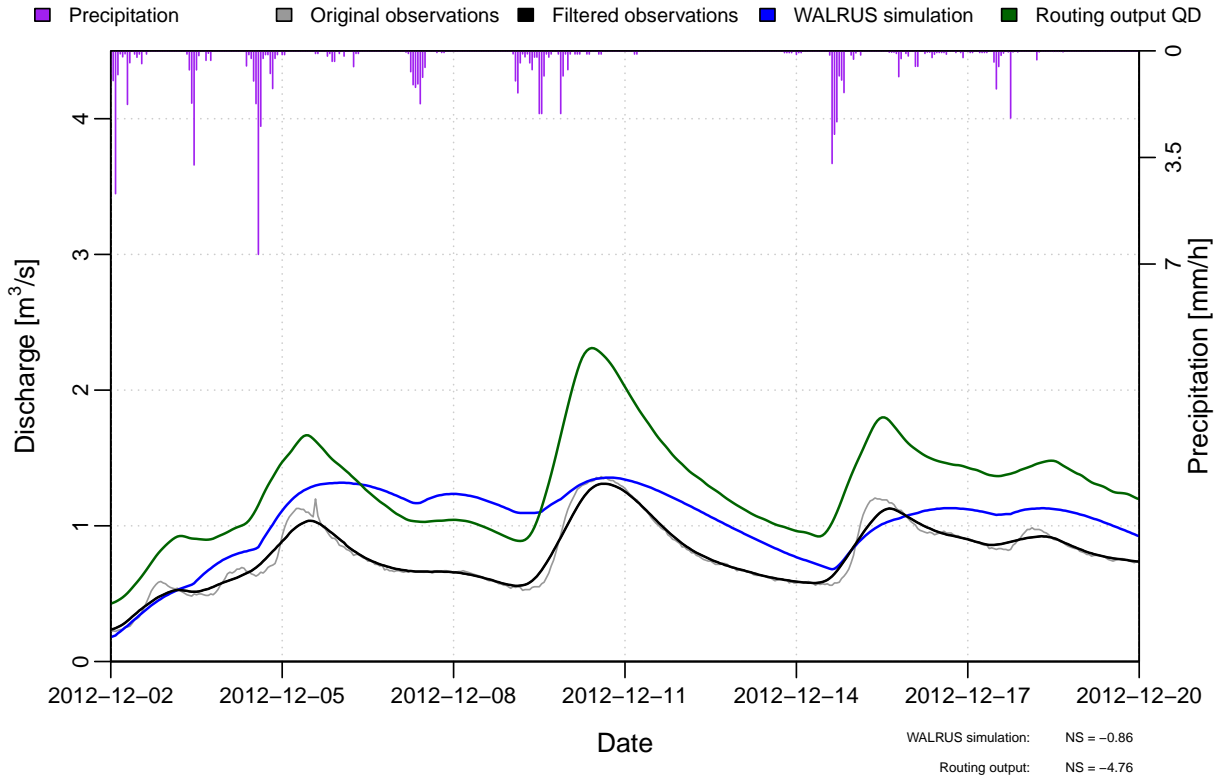


Figure C.14: Routing results for the hydrological year 2012–2013, zoomed in on a 18 days period (5).

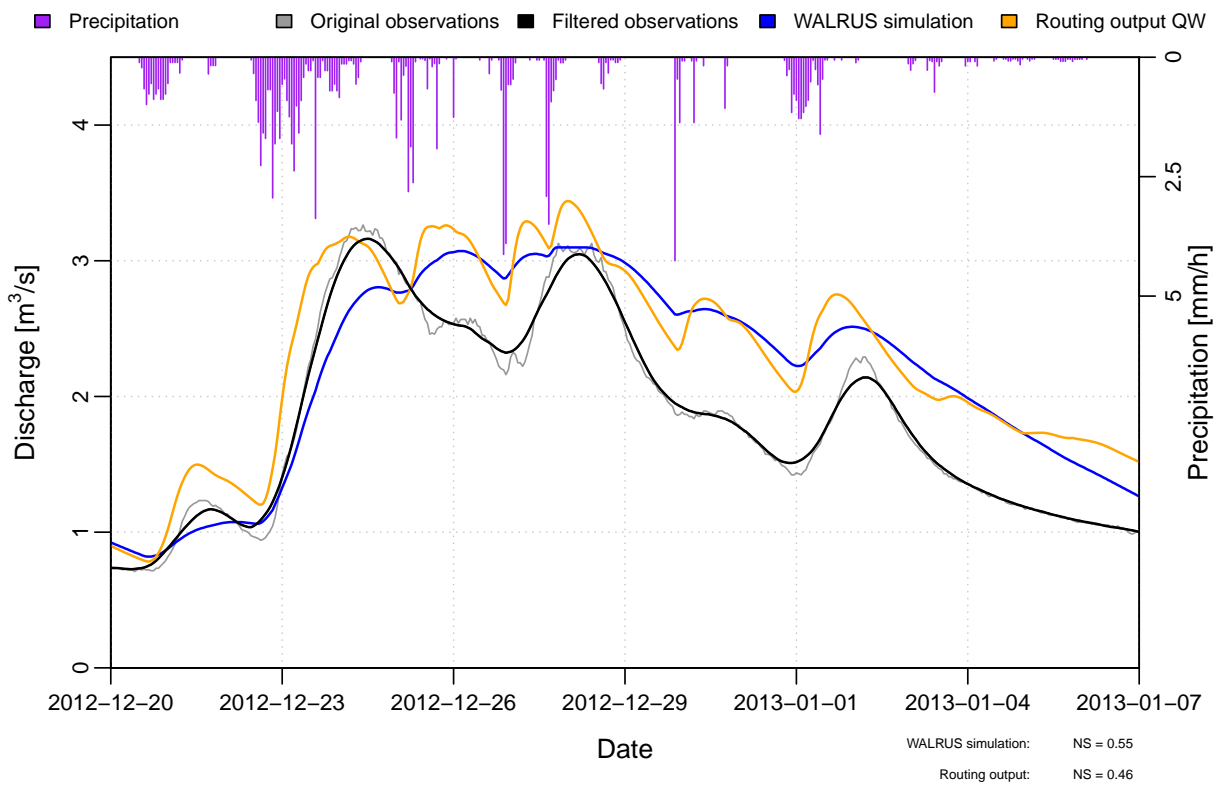


(a) Results of the routing technique using WALRUS output of stations 0098 and 0099.

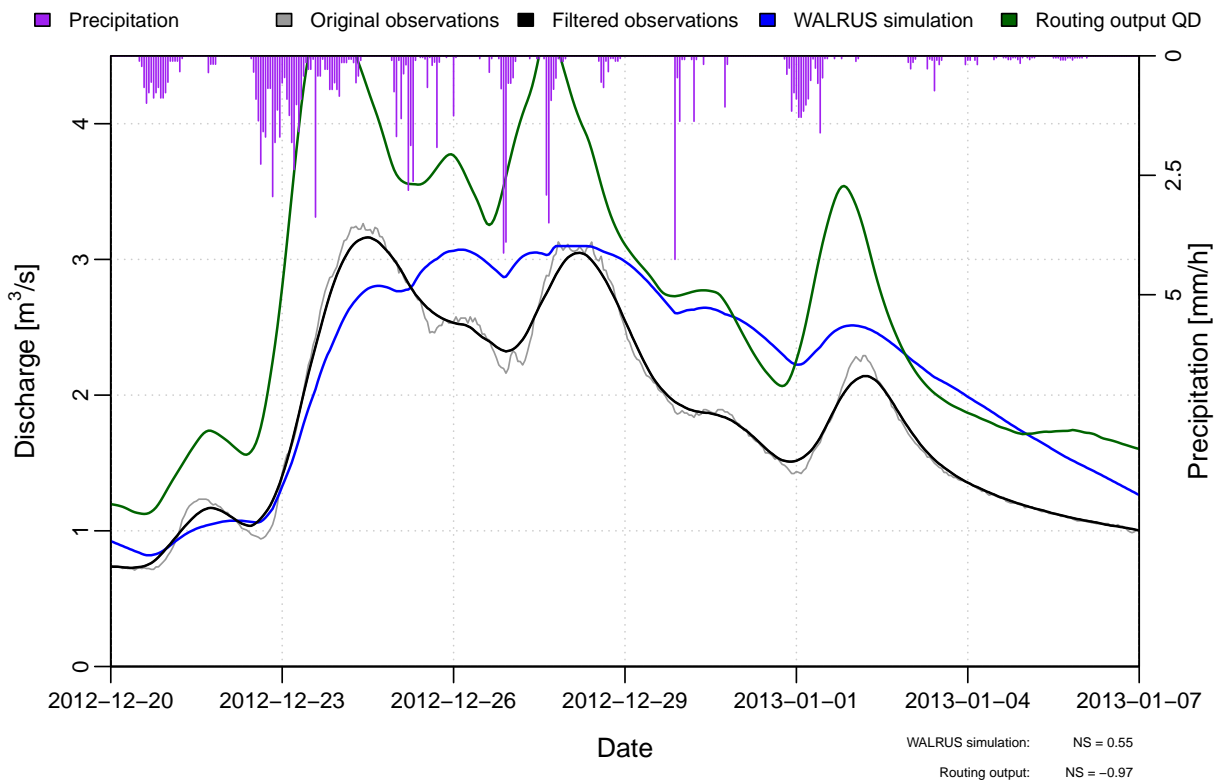


(b) Results of the routing technique using observed discharges of stations 0098 and 0099.

Figure C.15: Routing results for the hydrological year 2012–2013, zoomed in on a 18 days period (6).

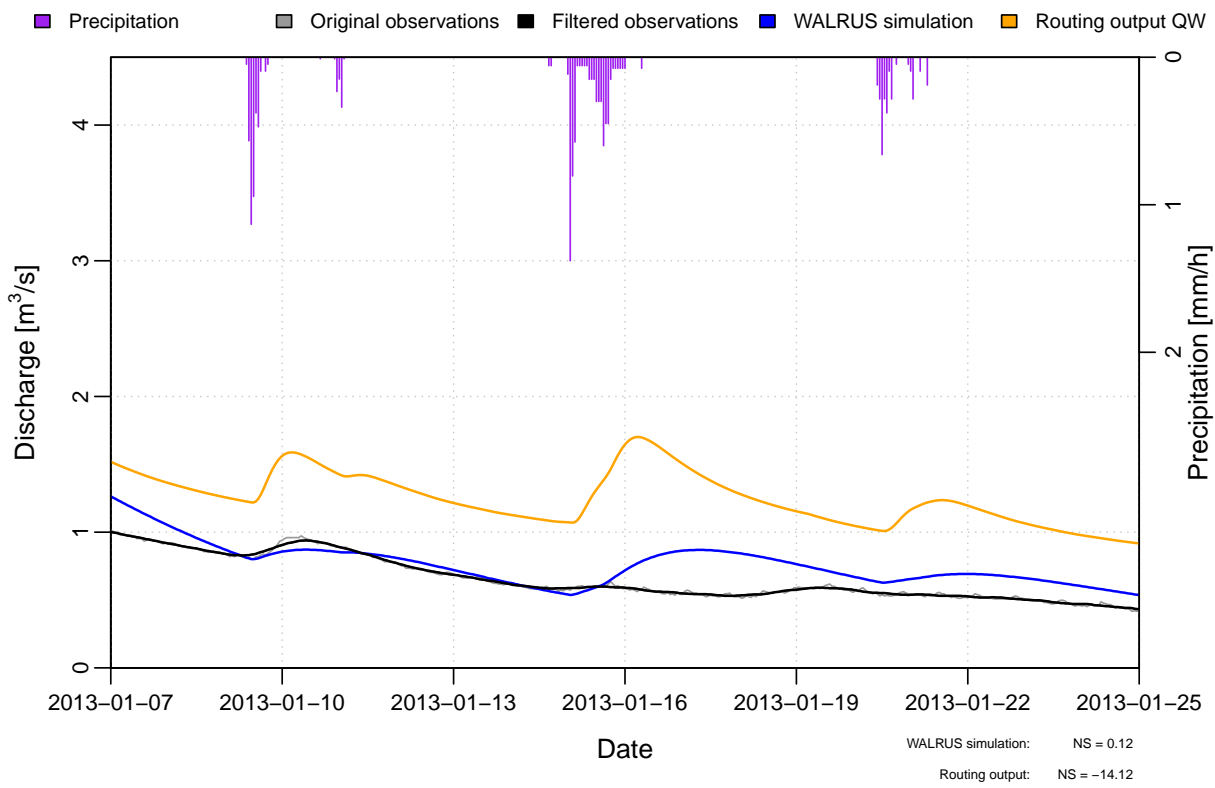


(a) Results of the routing technique using WALRUS output of stations 0098 and 0099.

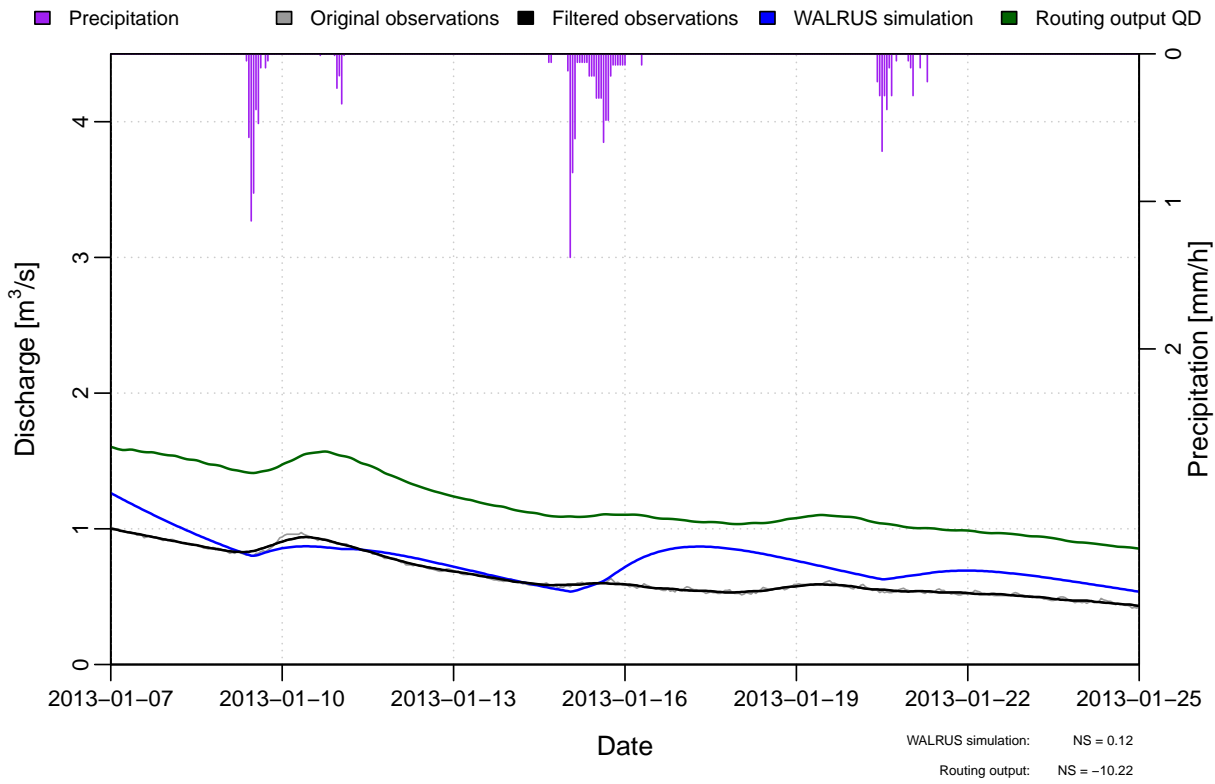


(b) Results of the routing technique using observed discharges of stations 0098 and 0099.

Figure C.16: Routing results for the hydrological year 2012–2013, zoomed in on a 18 days period (7).

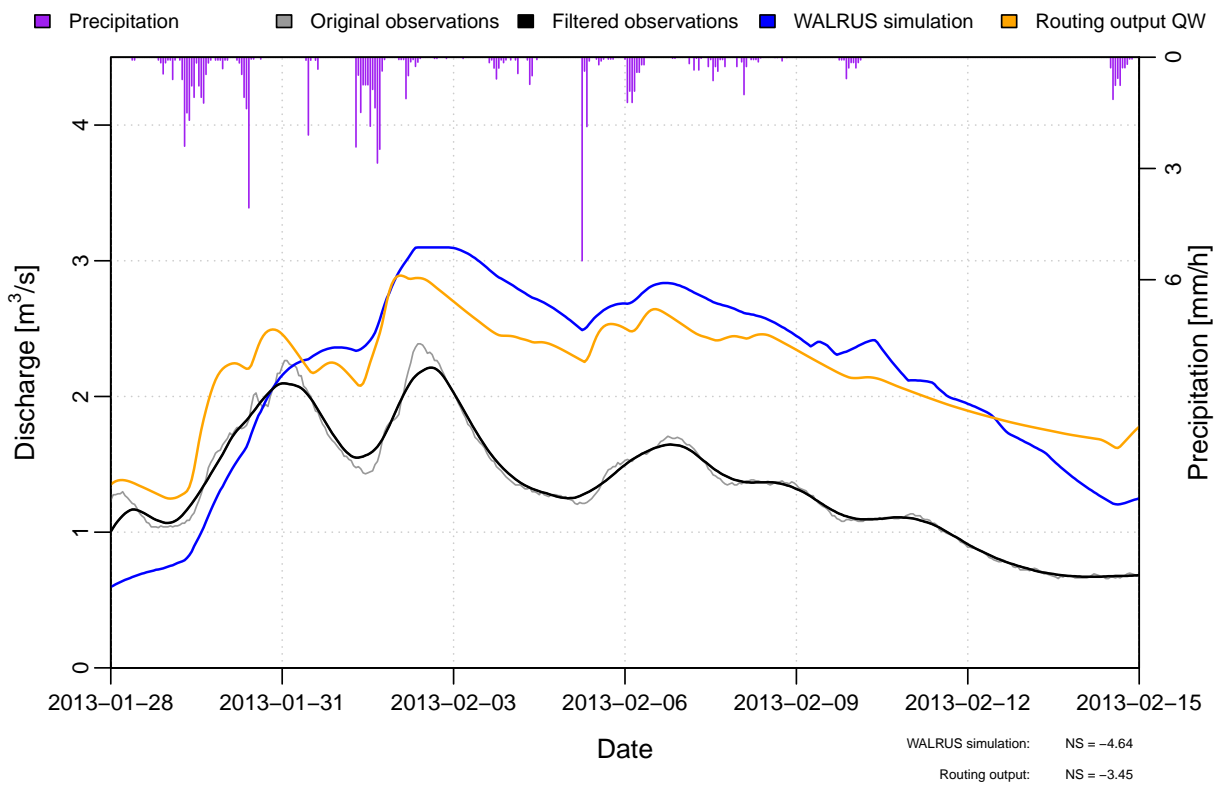


(a) Results of the routing technique using WALRUS output of stations 0098 and 0099.

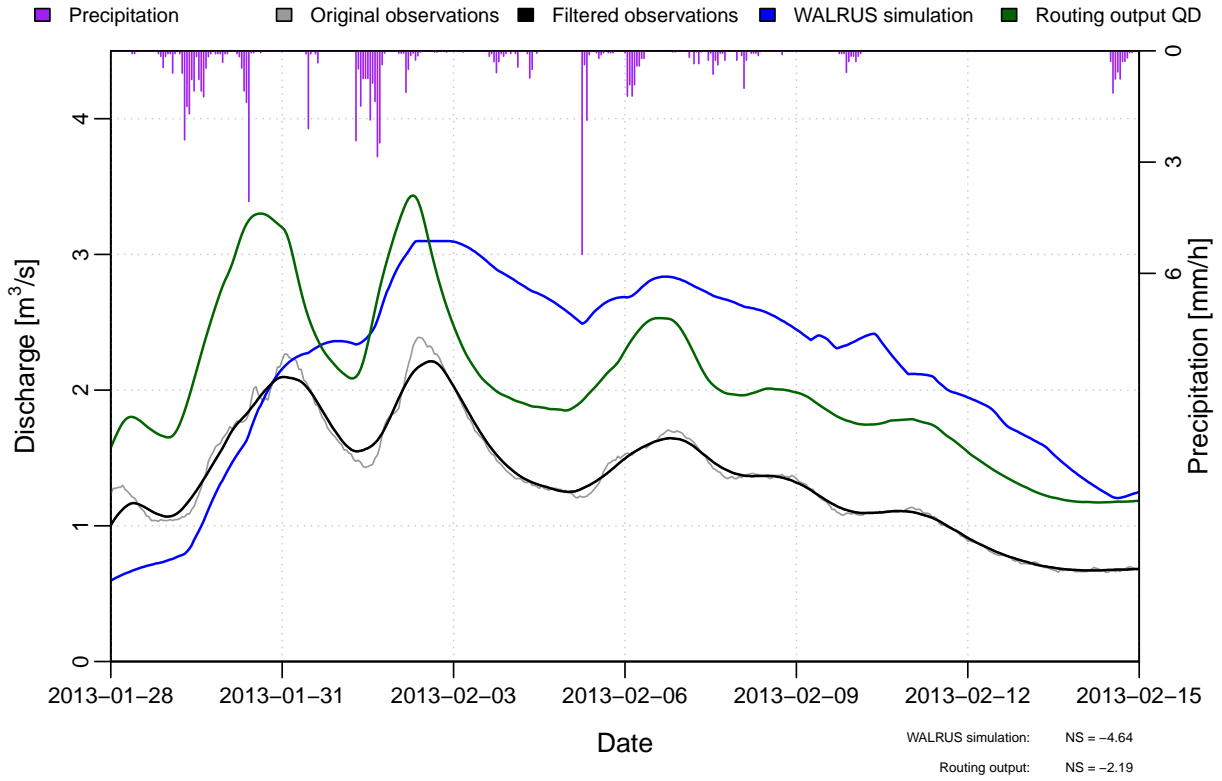


(b) Results of the routing technique using observed discharges of stations 0098 and 0099.

Figure C.17: Routing results for the hydrological year 2012–2013, zoomed in on a 18 days period (8).



(a) Results of the routing technique using WALRUS output of stations 0098 and 0099.



(b) Results of the routing technique using observed discharges of stations 0098 and 0099.

Figure C.18: Routing results for the hydrological year 2012–2013, zoomed in on a 18 days period (9).

# D | WALRUS versus Wageningen Model

Table D.1: Overview of the water balance ( $Bal$ ) which is based on precipitation ( $P$ ), evapotranspiration ( $ET_{pot}$ ) and discharge ( $Q$ ) of the output of WALRUS and the Wageningen Model for the complete catchment. Nash-Sutcliffe efficiencies (NS) are also shown.

| Year | Start date | End date   | Days<br>[d] | Missing<br>[%] | Observed    |                    |             |               | WALRUS      |               |           | Wageningen Model |               |           |
|------|------------|------------|-------------|----------------|-------------|--------------------|-------------|---------------|-------------|---------------|-----------|------------------|---------------|-----------|
|      |            |            |             |                | $P$<br>[mm] | $ET_{pot}$<br>[mm] | $Q$<br>[mm] | $Bal$<br>[mm] | $Q$<br>[mm] | $Bal$<br>[mm] | NS<br>[-] | $Q$<br>[mm]      | $Bal$<br>[mm] | NS<br>[-] |
| 1987 | 1987040101 | 1988033123 | 366         | 0.0            | 1047        | 511                | 590         | -54           | 484         | 52            | 0.88      | 509              | 27            | 0.56      |
| 1991 | 1991040101 | 1992033123 | 366         | 0.0            | 717         | 547                | 215         | -45           | 171         | -1            | 0.62      | 144              | 26            | 0.53      |
| 1994 | 1994040101 | 1995033123 | 365         | 0.0            | 1042        | 586                | 480         | -24           | 439         | 17            | 0.91      | 495              | -39           | 0.62      |
| 1995 | 1995040101 | 1996033123 | 366         | 0.0            | 507         | 591                | 166         | -250          | 49          | -133          | 0.20      | 110              | -194          | 0.37      |
| 1997 | 1997040101 | 1998033123 | 365         | 0.0            | 720         | 596                | 218         | -94           | 141         | -17           | 0.62      | 202              | -78           | 0.26      |
| 1999 | 1999040101 | 2000033123 | 366         | 0.0            | 869         | 601                | 301         | -33           | 257         | 11            | 0.81      | 320              | -52           | 0.74      |
| 2002 | 2002040101 | 2003033123 | 365         | 0.0            | 755         | 584                | 264         | -93           | 201         | -30           | 0.86      | 266              | -95           | 0.63      |
| 2003 | 2003040101 | 2004033123 | 366         | 0.0            | 785         | 642                | 189         | -46           | 183         | -40           | 0.68      | 115              | 28            | 0.62      |
| 2004 | 2004040101 | 2005033123 | 365         | 44.1           | 825         | 584                | 287         | -46           | 228         | 13            | 0.63      | 171              | 70            | 0.59      |
| 2005 | 2005040101 | 2006033123 | 365         | 3.1            | 822         | 604                | 248         | -30           | 204         | 14            | 0.72      | 222              | -4            | 0.19      |
| 2006 | 2006040101 | 2007033123 | 365         | 9.0            | 974         | 618                | 361         | -5            | 356         | 0             | 0.75      | 277              | 79            | 0.72      |

Table D.2: Overview of the water balance ( $Bal$ ) which is based on precipitation ( $P$ ), evapotranspiration ( $ET_{pot}$ ) and discharge ( $Q$ ) of the output of WALRUS and the Wageningen Model for subcatchment 0098. Nash-Sutcliffe efficiencies (NS) are also shown.

| Year | Start date | End date   | Days<br>[d] | Missing<br>[%] | Observed    |                    |             |               | WALRUS      |               |           | Wageningen Model |               |           |
|------|------------|------------|-------------|----------------|-------------|--------------------|-------------|---------------|-------------|---------------|-----------|------------------|---------------|-----------|
|      |            |            |             |                | $P$<br>[mm] | $ET_{pot}$<br>[mm] | $Q$<br>[mm] | $Bal$<br>[mm] | $Q$<br>[mm] | $Bal$<br>[mm] | NS<br>[-] | $Q$<br>[mm]      | $Bal$<br>[mm] | NS<br>[-] |
| 1999 | 1999040101 | 2000033104 | 365         | 32.2           | 854         | 600                | 151         | 103           | 169         | 85            | 0.60      | 272              | -18           | -1.53     |
| 2000 | 2000040106 | 2001033123 | 365         | 2.0            | 945         | 552                | 337         | 56            | 269         | 124           | 0.70      | 303              | 90            | -0.09     |
| 2001 | 2001040101 | 2002033123 | 365         | 11.6           | 971         | 609                | 259         | 103           | 258         | 104           | -0.52     | 405              | -43           | -4.26     |
| 2002 | 2002040101 | 2003033123 | 365         | 0.2            | 751         | 584                | 188         | -21           | 148         | 19            | 0.54      | 215              | -48           | 0.63      |
| 2003 | 2003040101 | 2004033123 | 366         | 0.0            | 767         | 642                | 162         | -37           | 120         | 5             | 0.62      | 92               | 33            | 0.53      |
| 2006 | 2006040101 | 2007033123 | 365         | 1.1            | 975         | 618                | 277         | 80            | 266         | 91            | 0.68      | 240              | 117           | 0.71      |

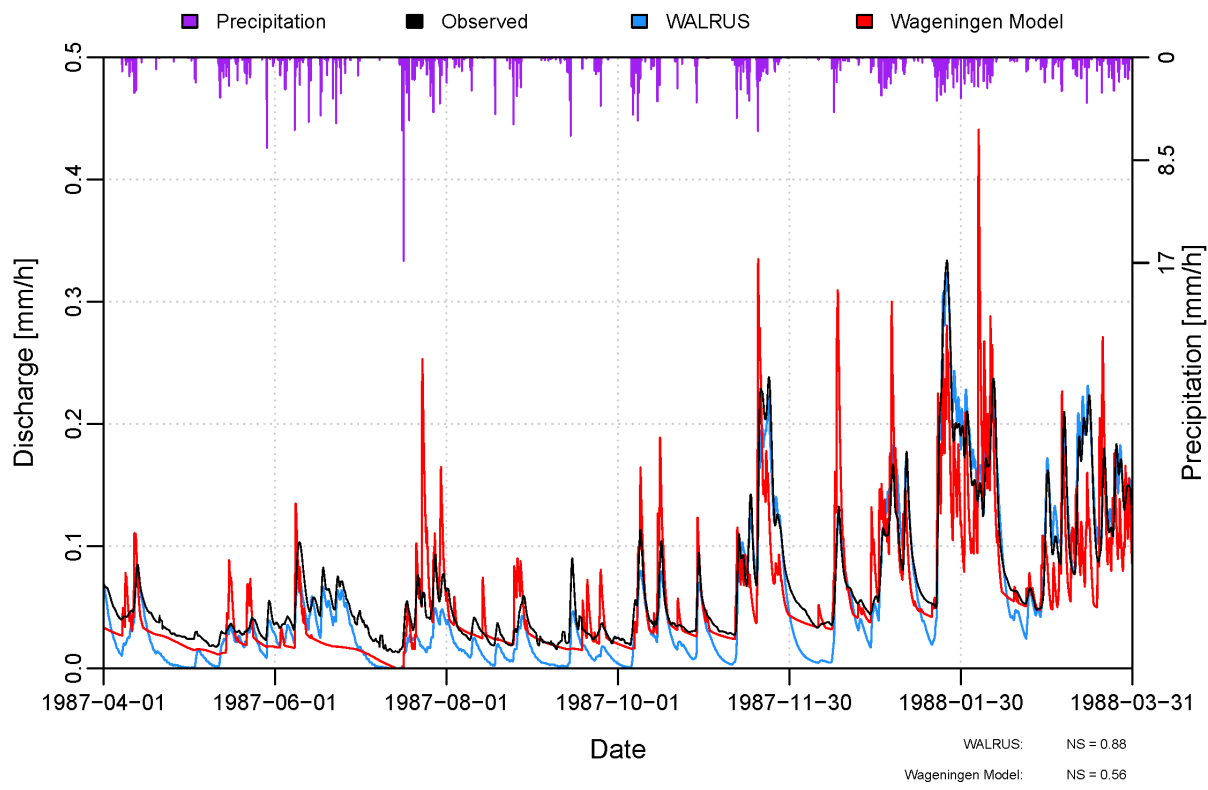


Figure D.1: Simulation of catchment 0024 for the hydrological year 1987–1988.

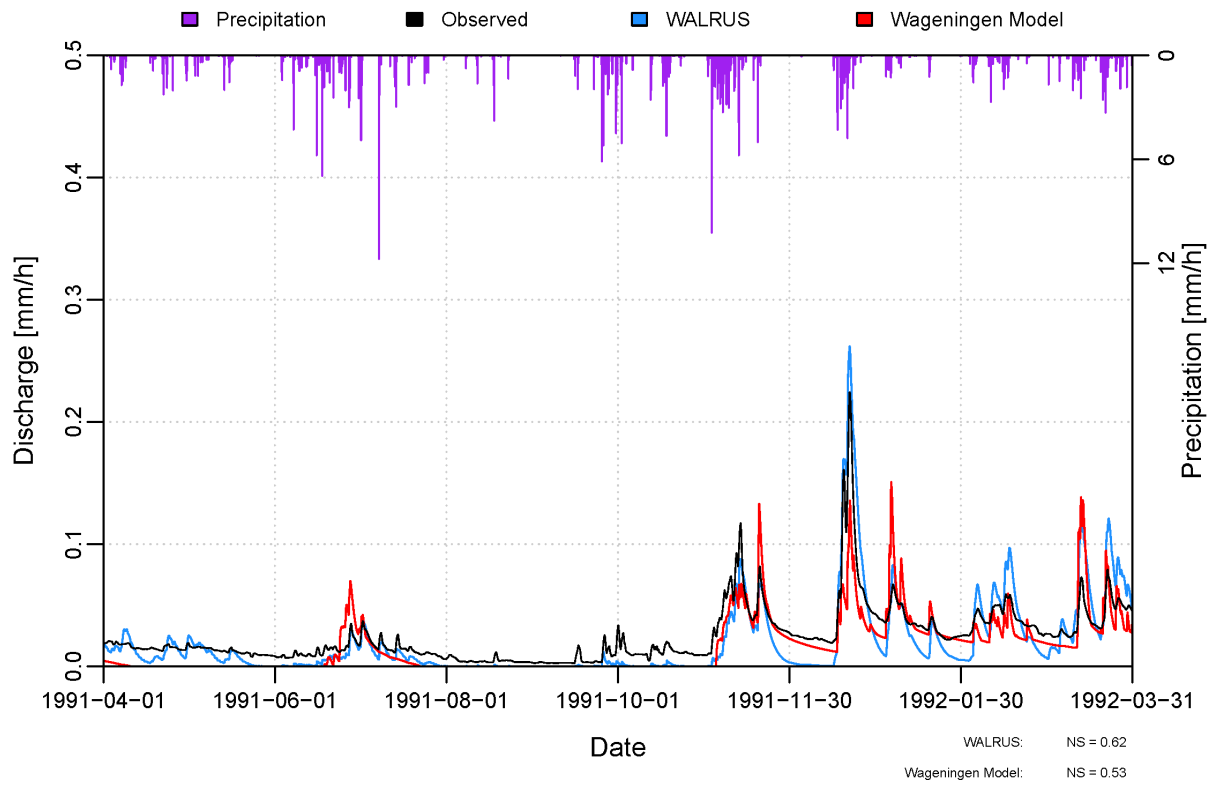


Figure D.2: Simulation of catchment 0024 for the hydrological year 1991–1992.

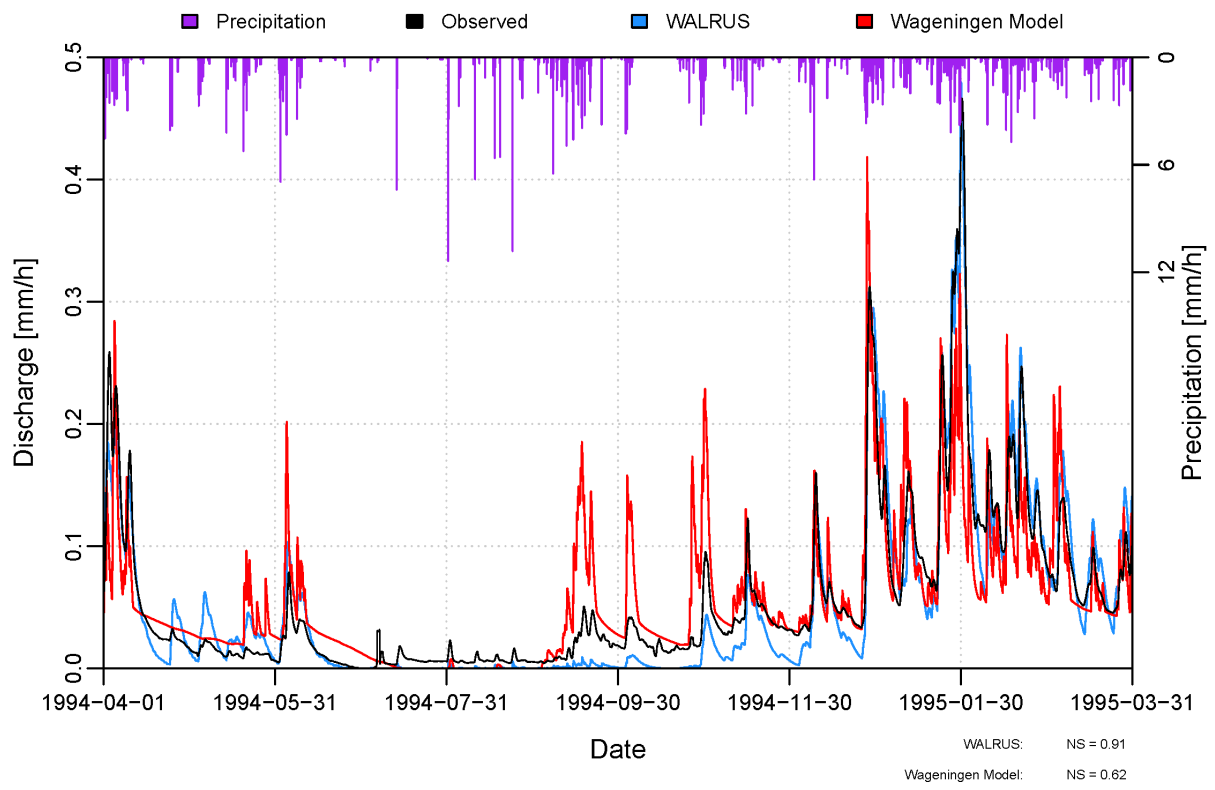


Figure D.3: Simulation of catchment 0024 for the hydrological year 1994–1995.

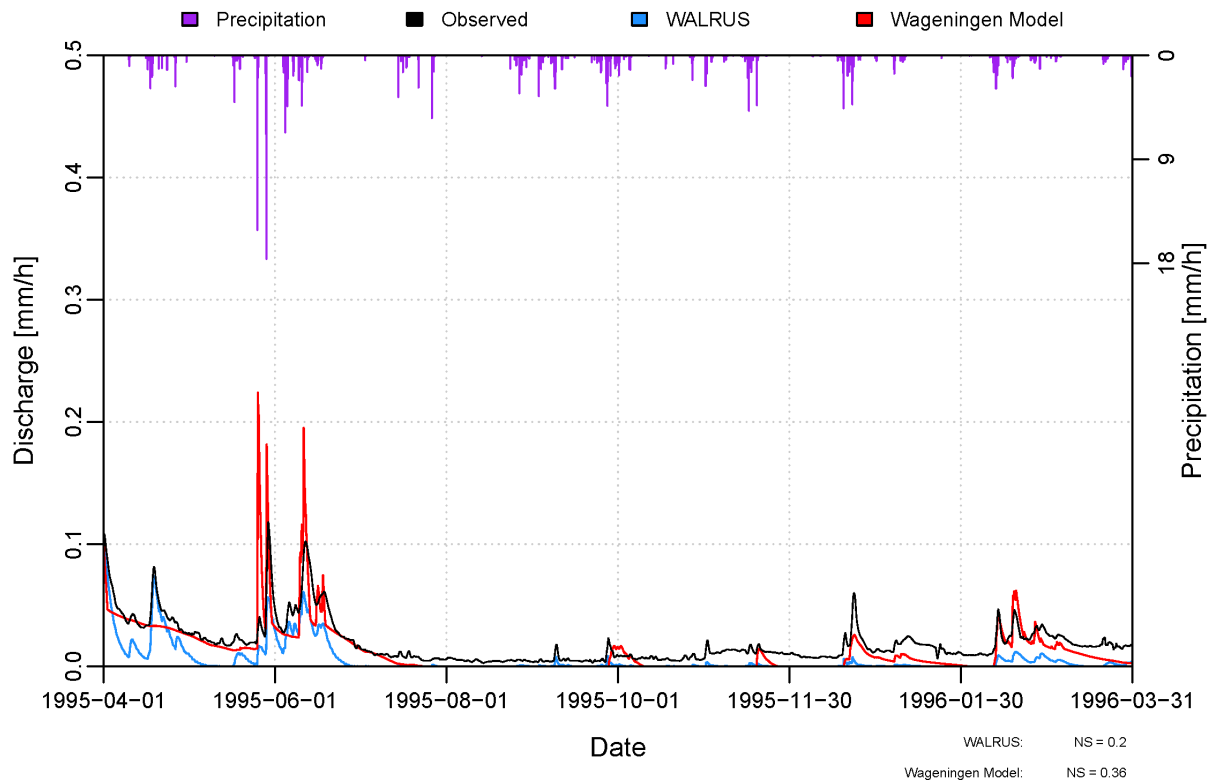


Figure D.4: Simulation of catchment 0024 for the hydrological year 1995–1996.

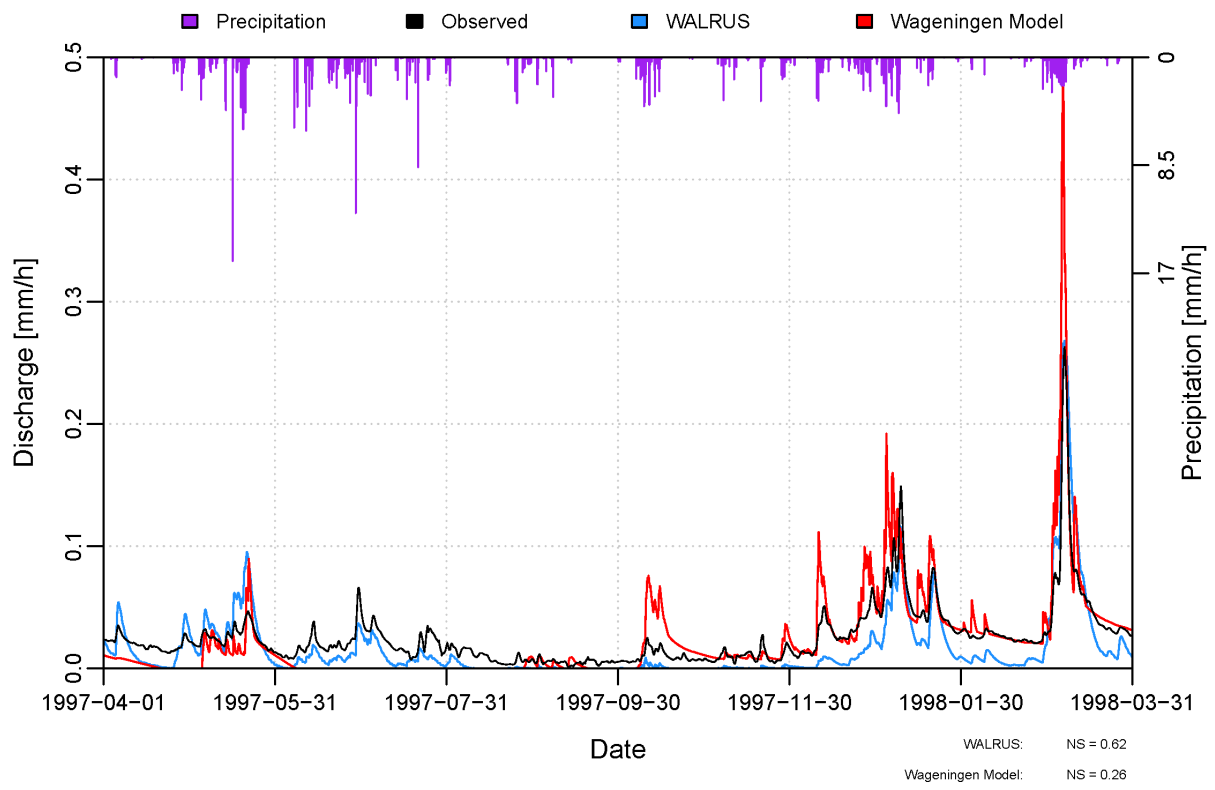


Figure D.5: Simulation of catchment 0024 for the hydrological year 1997–1998.

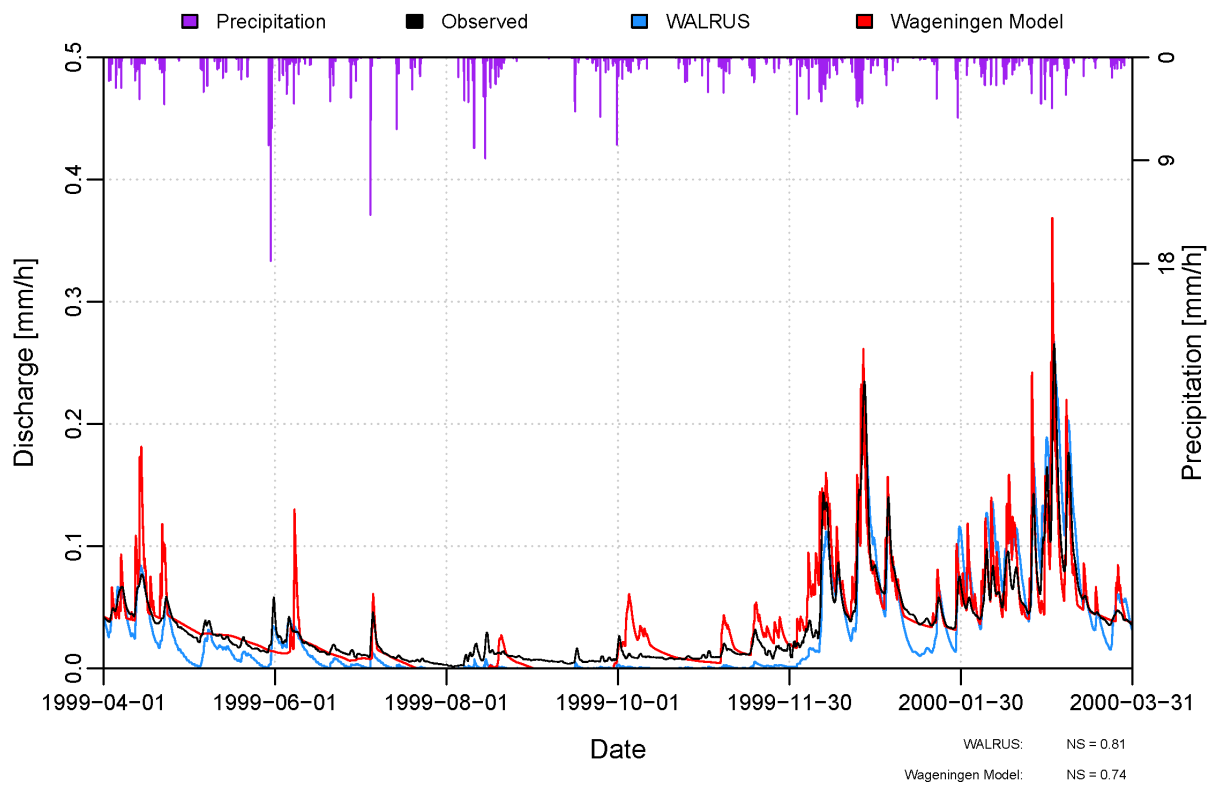


Figure D.6: Simulation of catchment 0024 for the hydrological year 1999–2000.

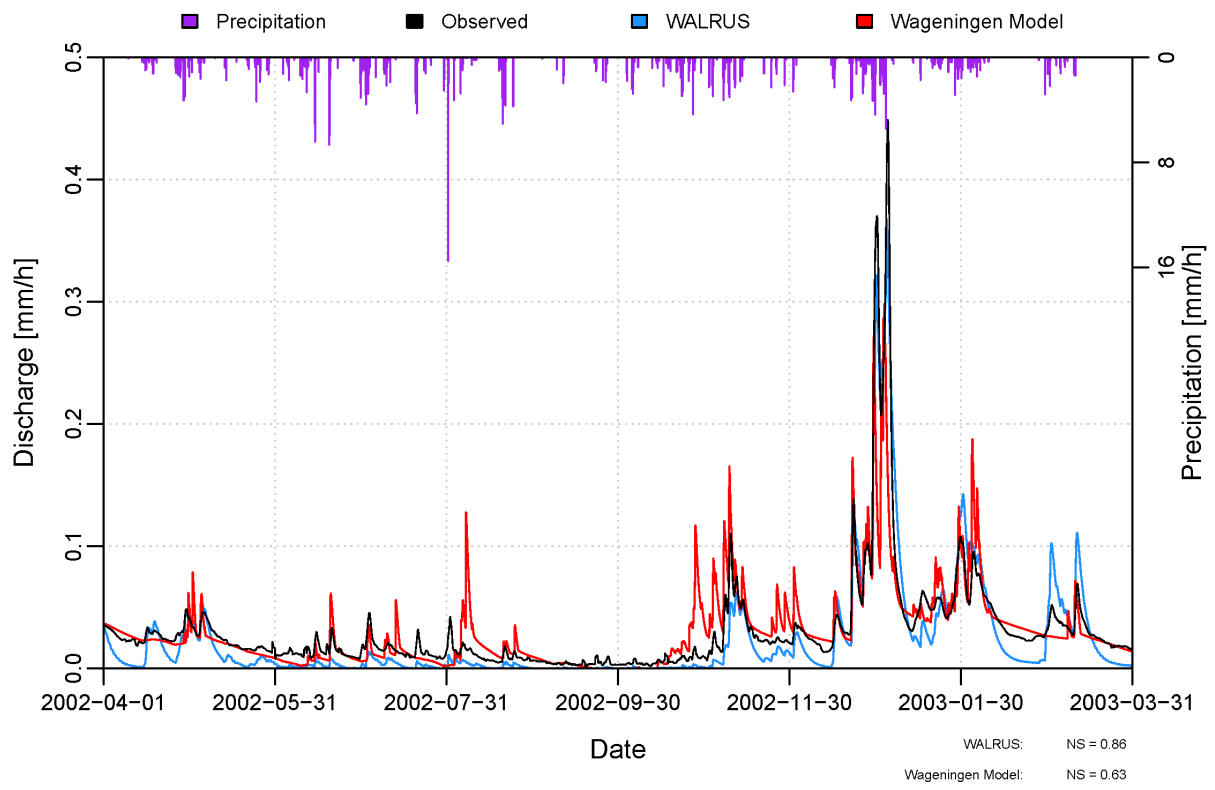


Figure D.7: Simulation of catchment 0024 for the hydrological year 2002–2003.

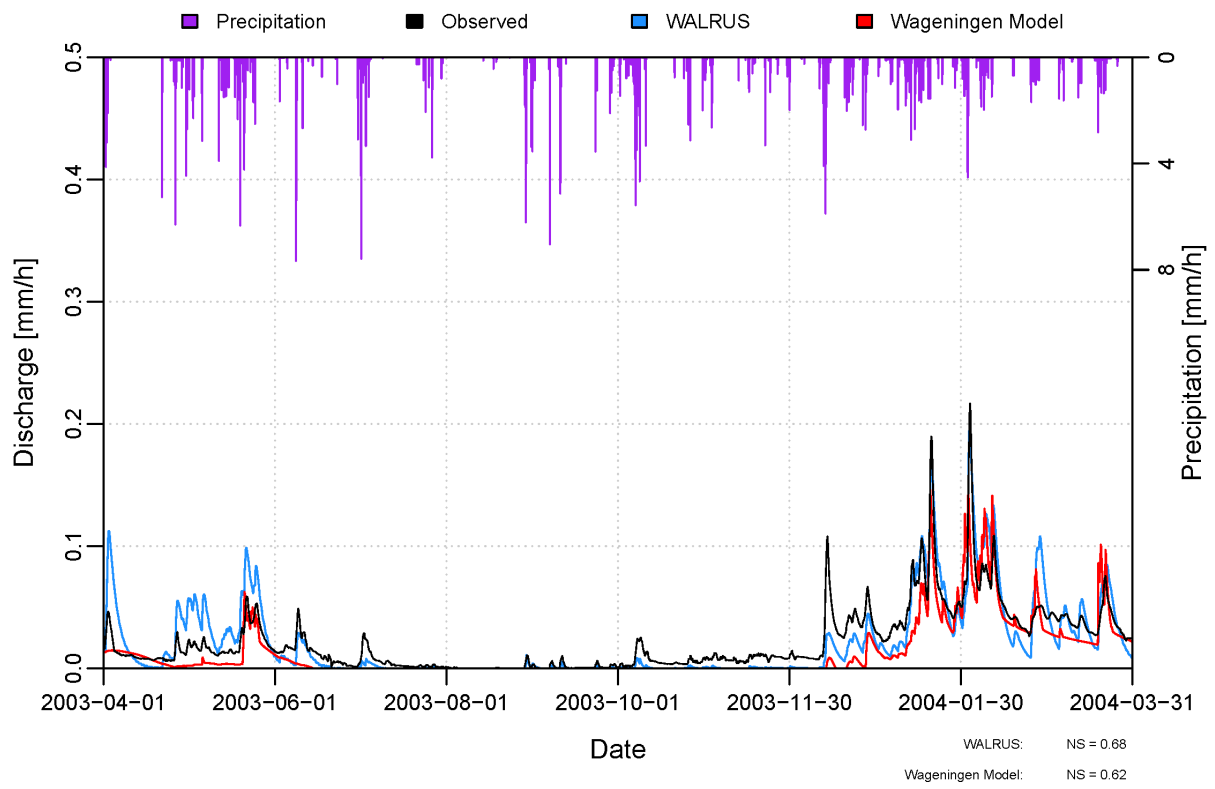


Figure D.8: Simulation of catchment 0024 for the hydrological year 2003–2004.

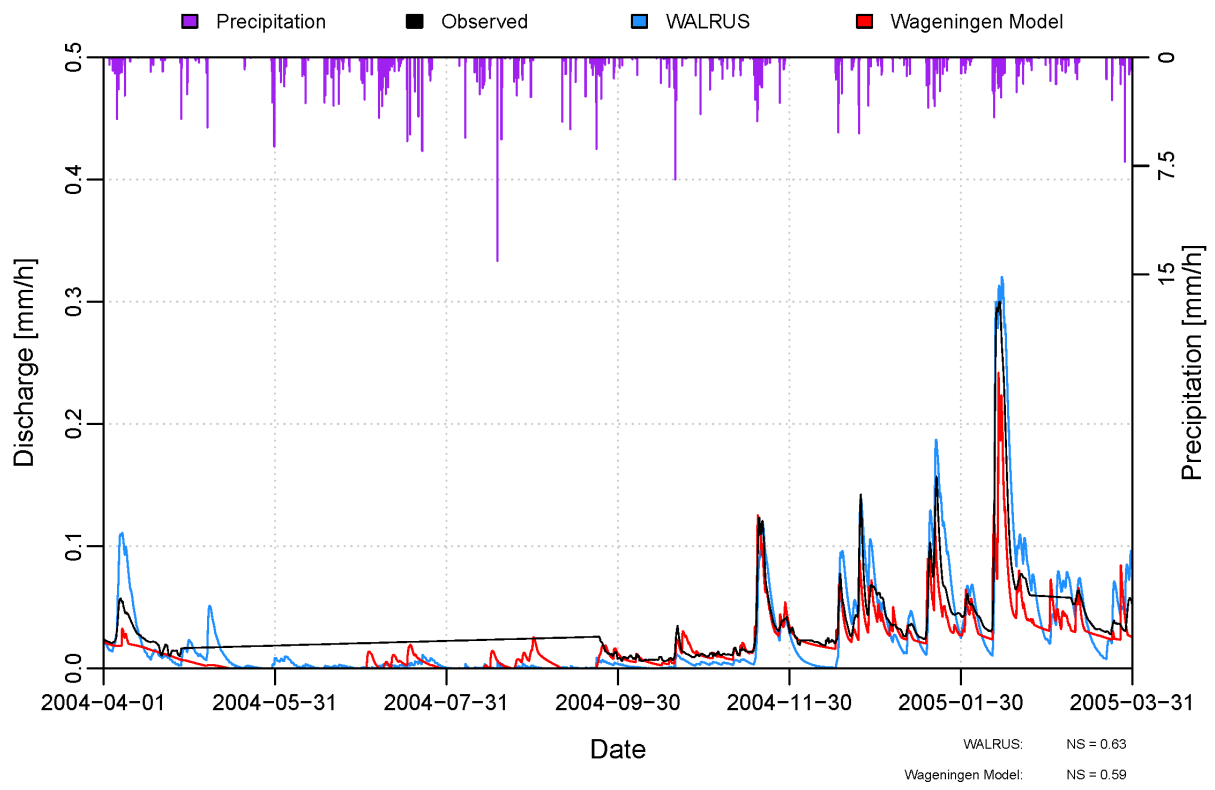


Figure D.9: Simulation of catchment 0024 for the hydrological year 2004–2005.

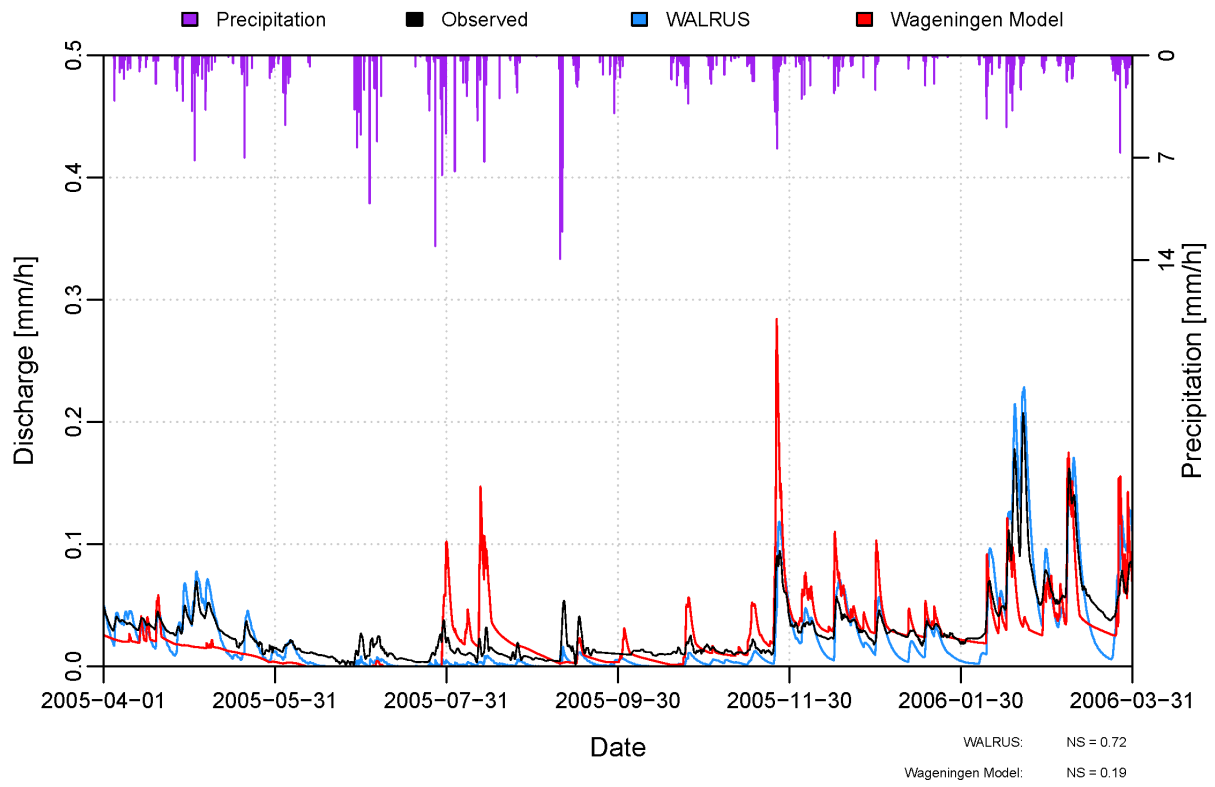


Figure D.10: Simulation of catchment 0024 for the hydrological year 2005–2006.

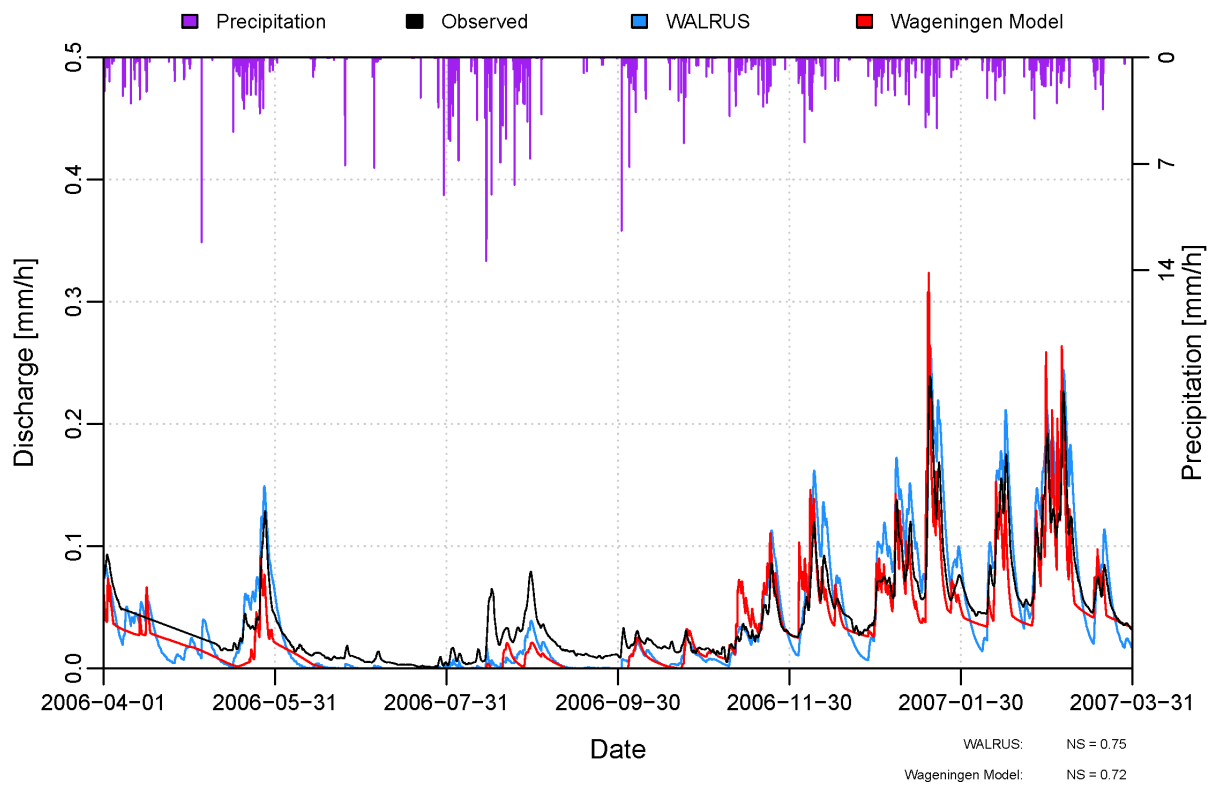


Figure D.11: Simulation of catchment 0024 for the hydrological year 2006–2007.

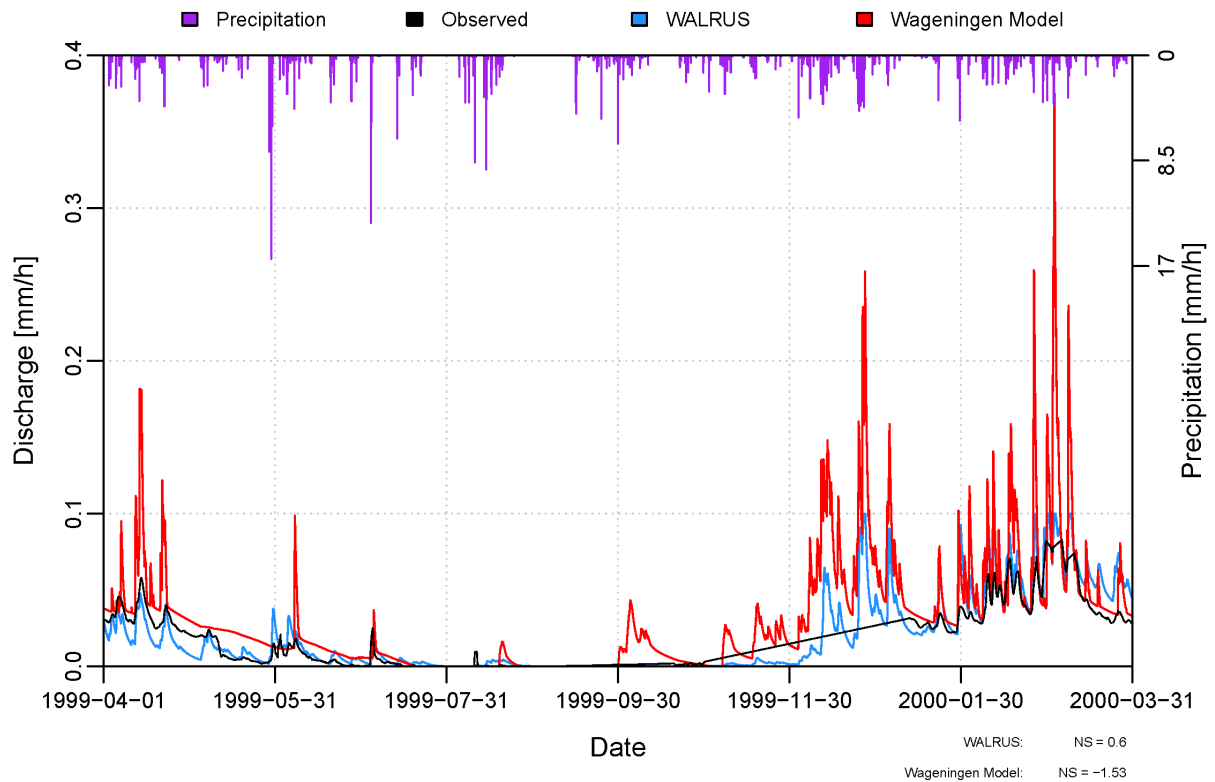


Figure D.12: Simulation of catchment 0098 for the hydrological year 1999–2000.

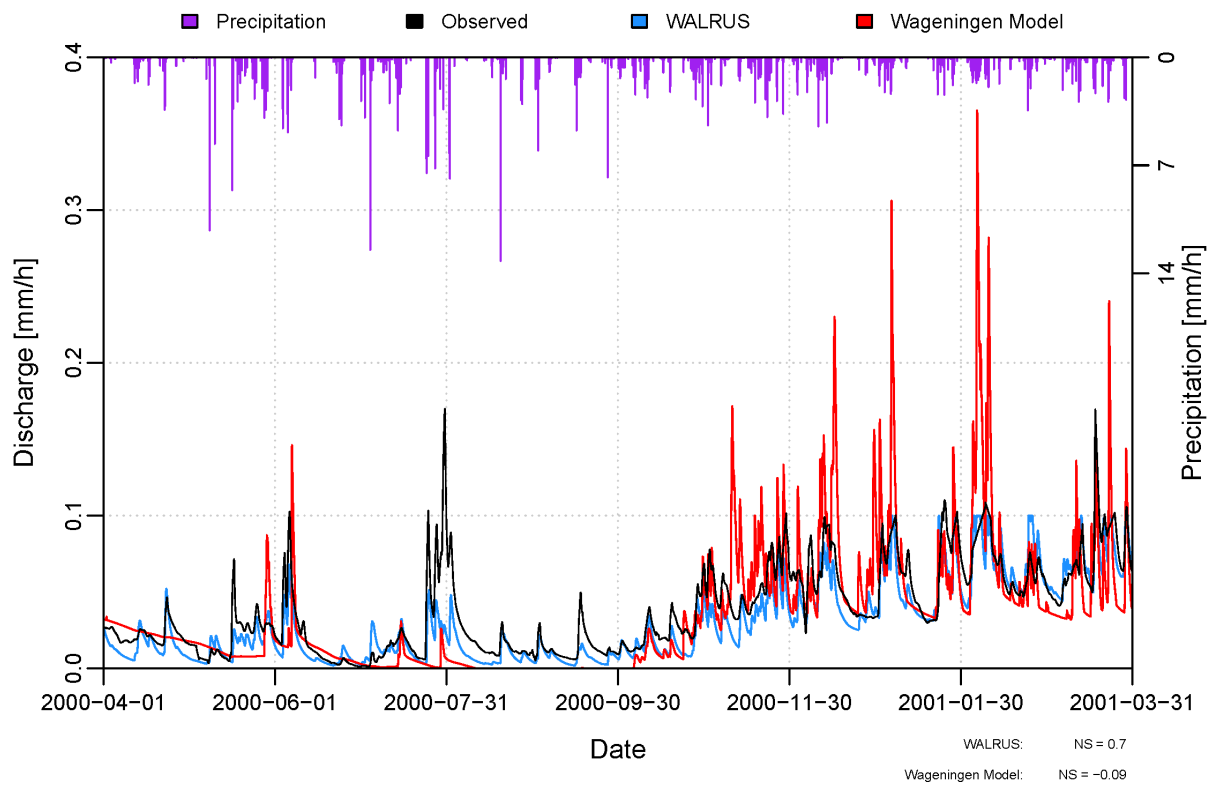


Figure D.13: Simulation of catchment 0098 for the hydrological year 2000–2001.

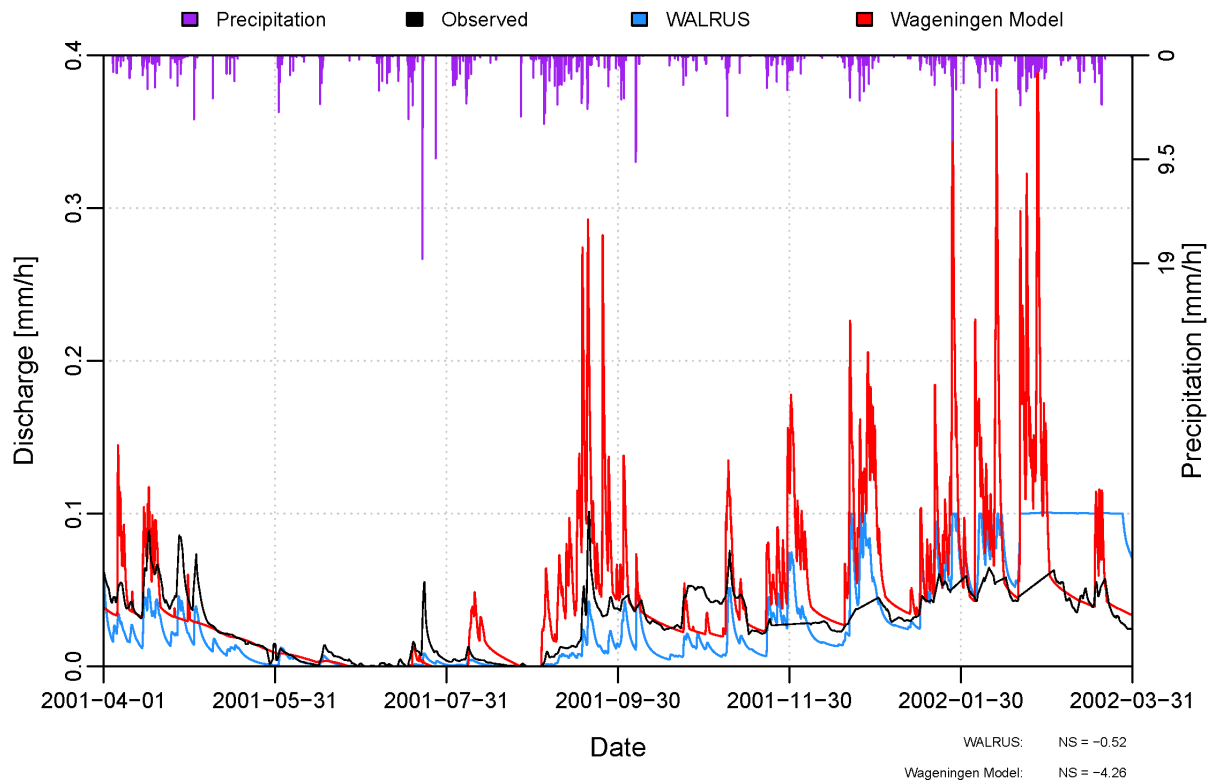


Figure D.14: Simulation of catchment 0098 for the hydrological year 2001–2002.

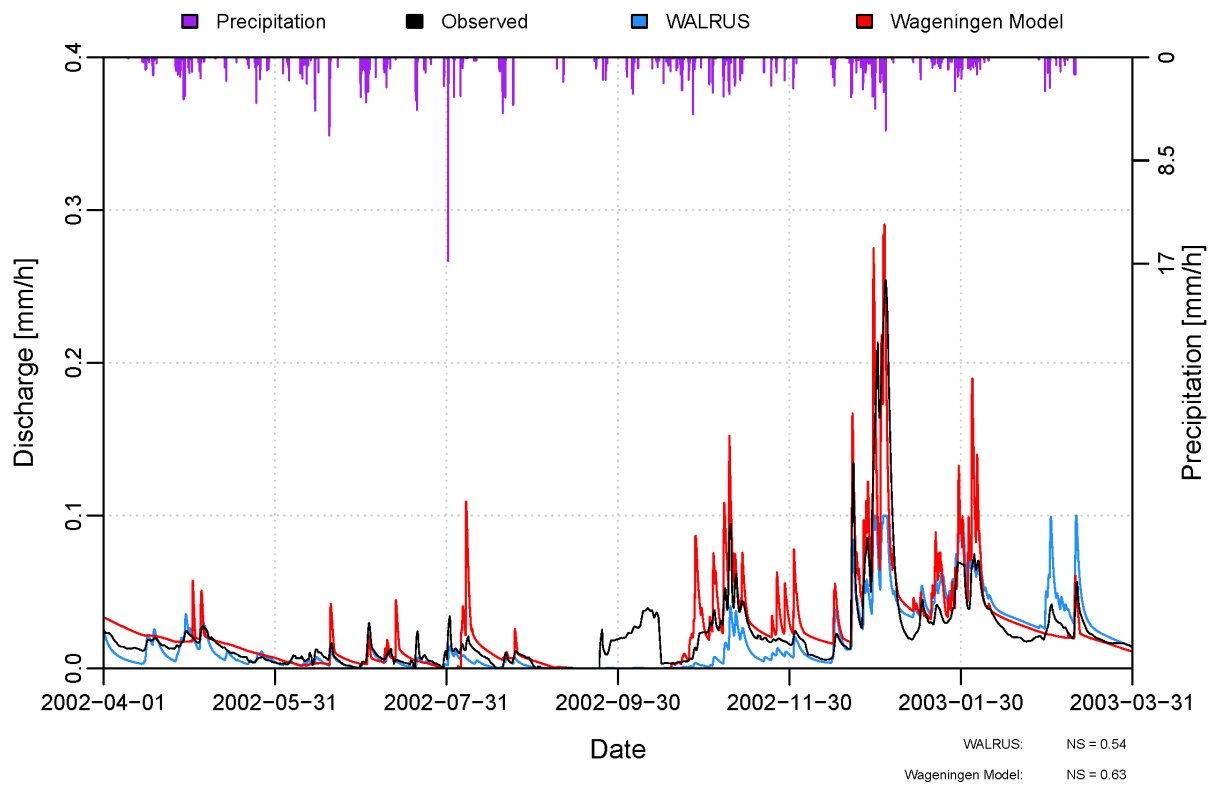


Figure D.15: Simulation of catchment 0098 for the hydrological year 2002–2003.

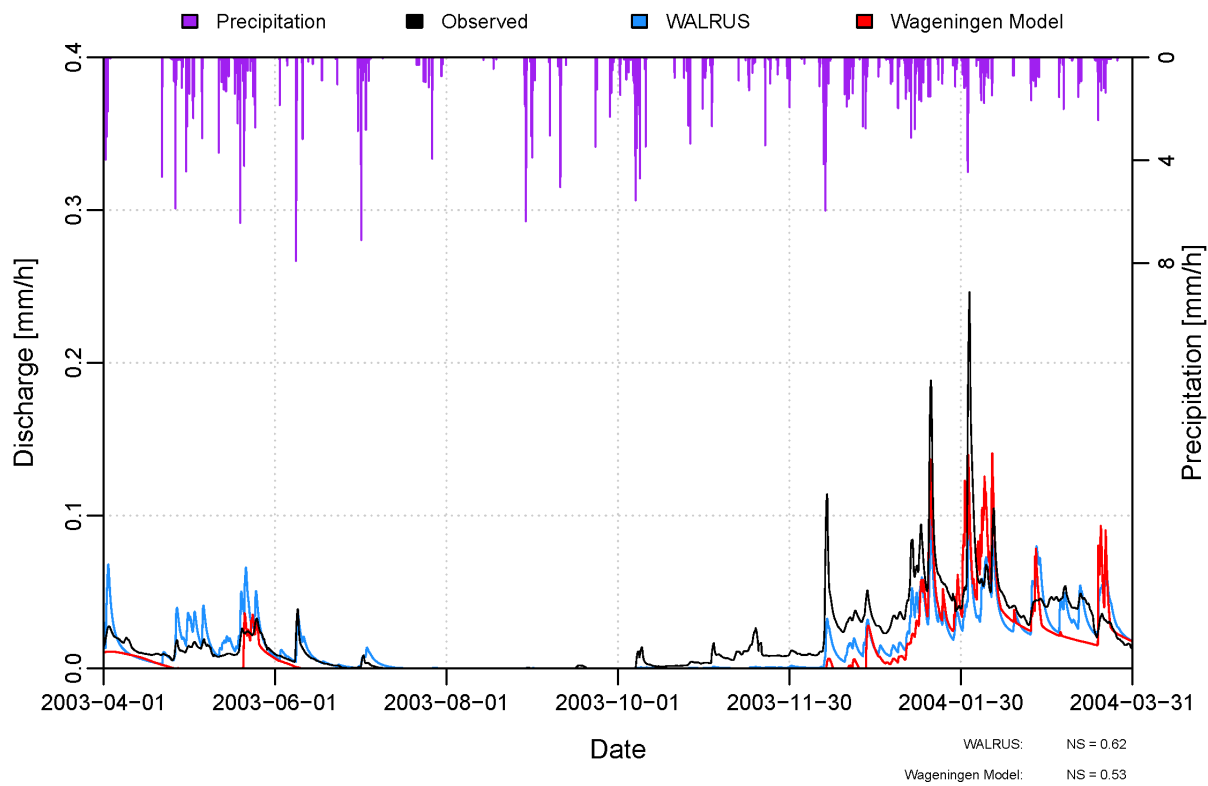


Figure D.16: Simulation of catchment 0098 for the hydrological year 2003–2004.

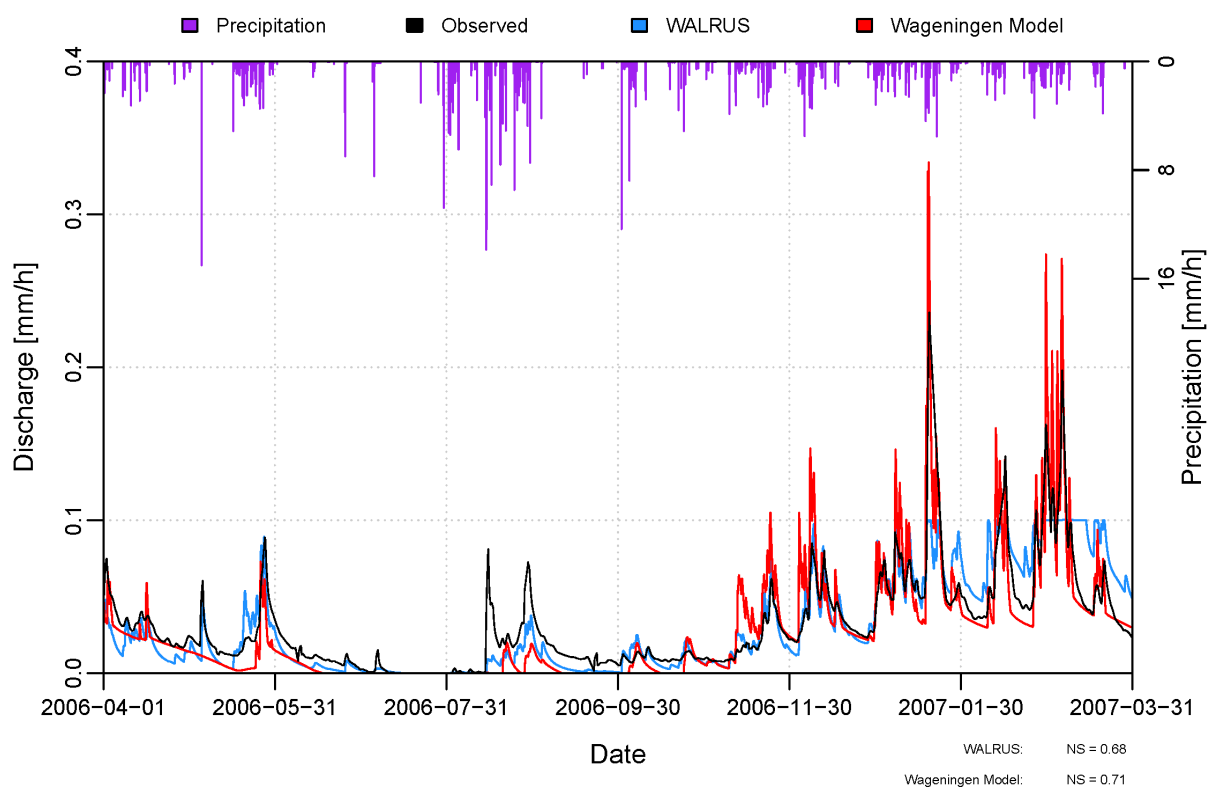


Figure D.17: Simulation of catchment 0098 for the hydrological year 2006–2007.